NASA CONTRACTOR REPORT

NASA CR-1
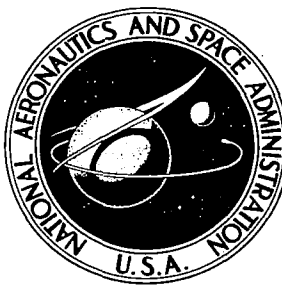
LUNAR ORBITER V
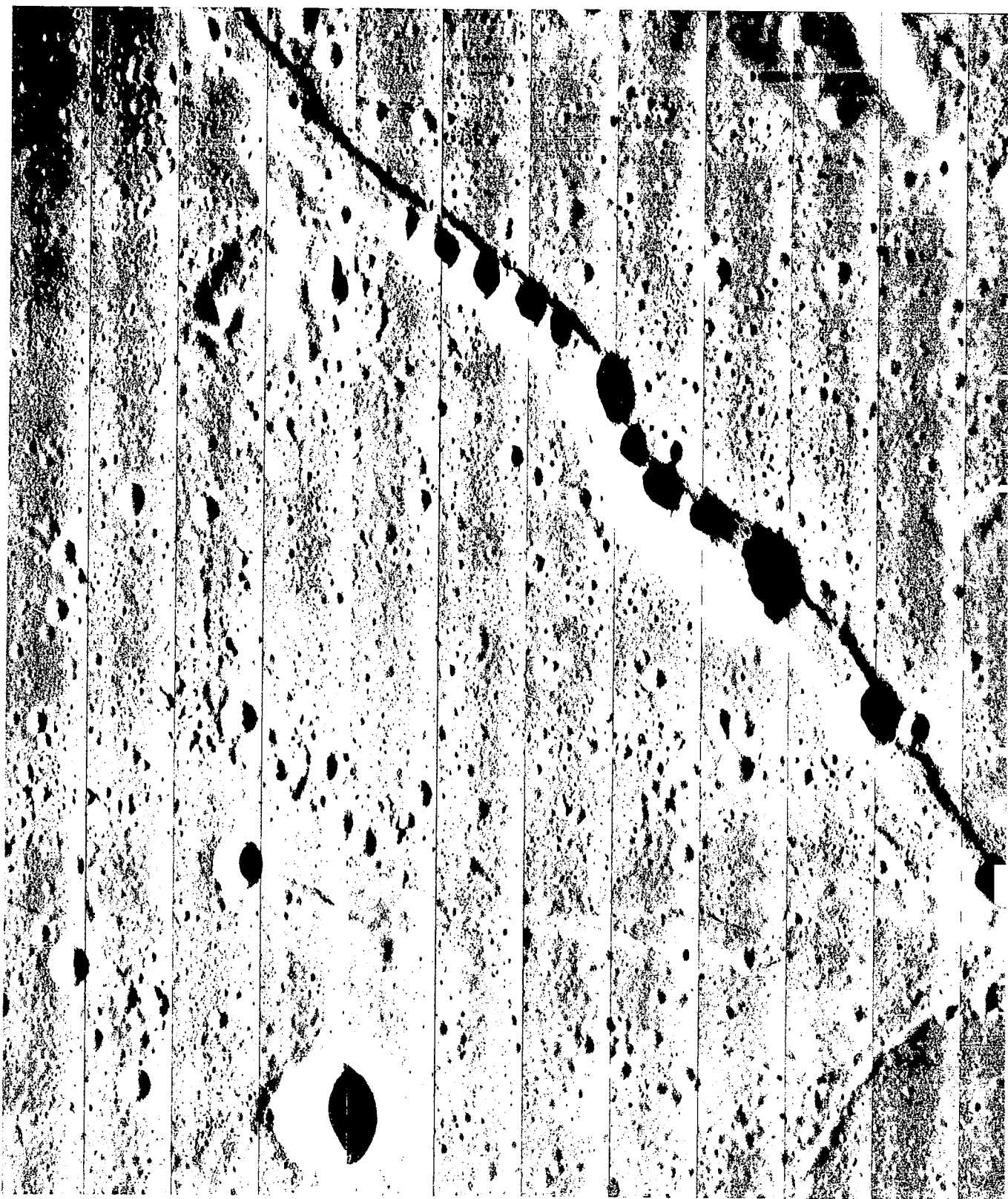
Photographic Mission Summary

Prepared by
THE BOEING COMPANY
Seattle, Wash.
for Langley Research Center

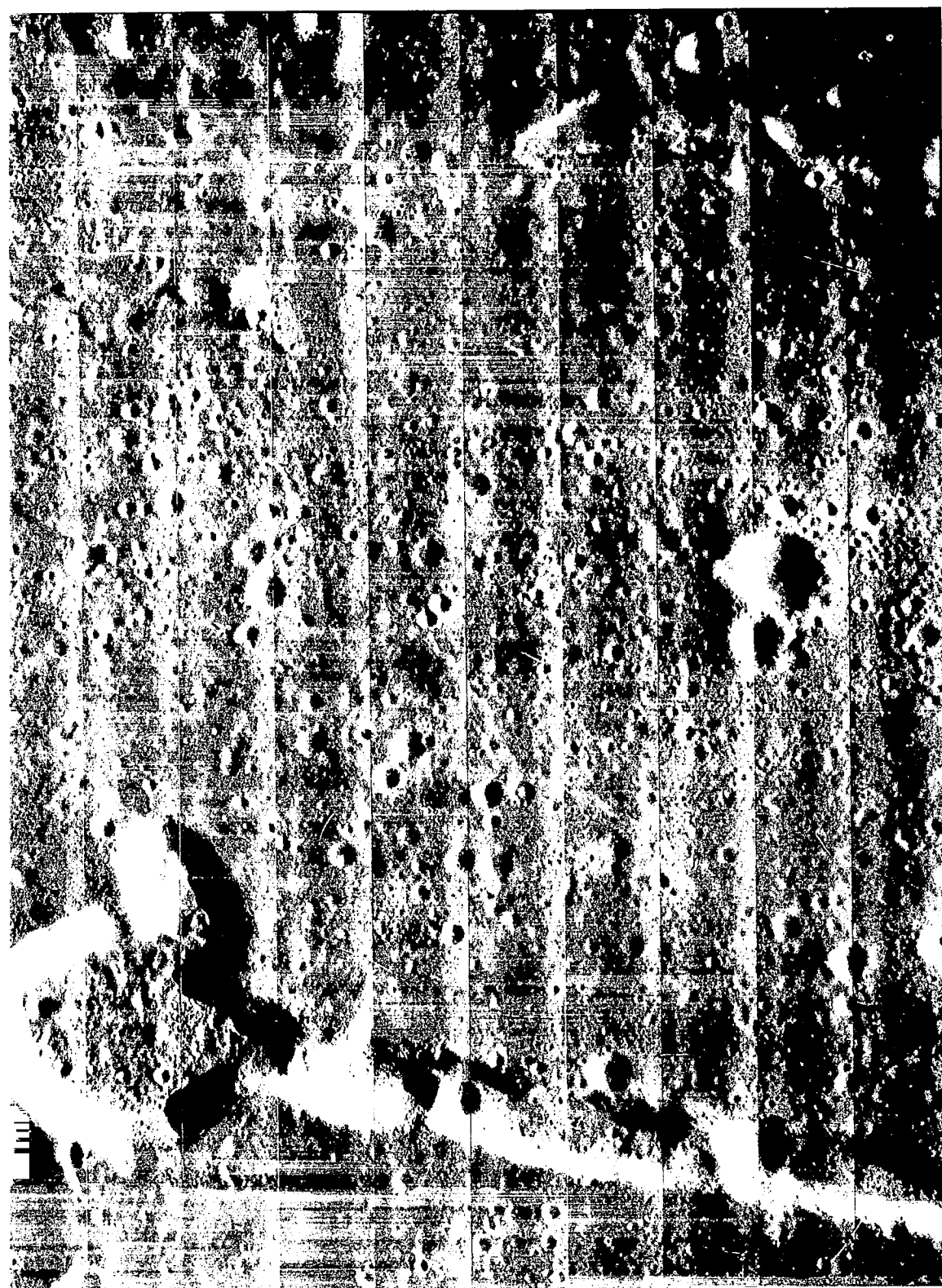NATIONAL AERONAUTICS AND SPACE ADMINISTRATION • WASHINGTON, D. C. • JULY 1968

Hyginus Rille
Photo taken by NASA-Boeing Lunar Orbiter V, August 14, 1967, 03:02:56 GMT from a distance of 65 miles.

LUNAR ORBITER V

Photographic Mission Summary

Issued by Originator as Boeing Document D2-100755-1 (Vol. I)

Contents

Figures

Tables

Illustrations

Wide-Angle Frame 102, Site V-25
Centered on the Alpine Valley.
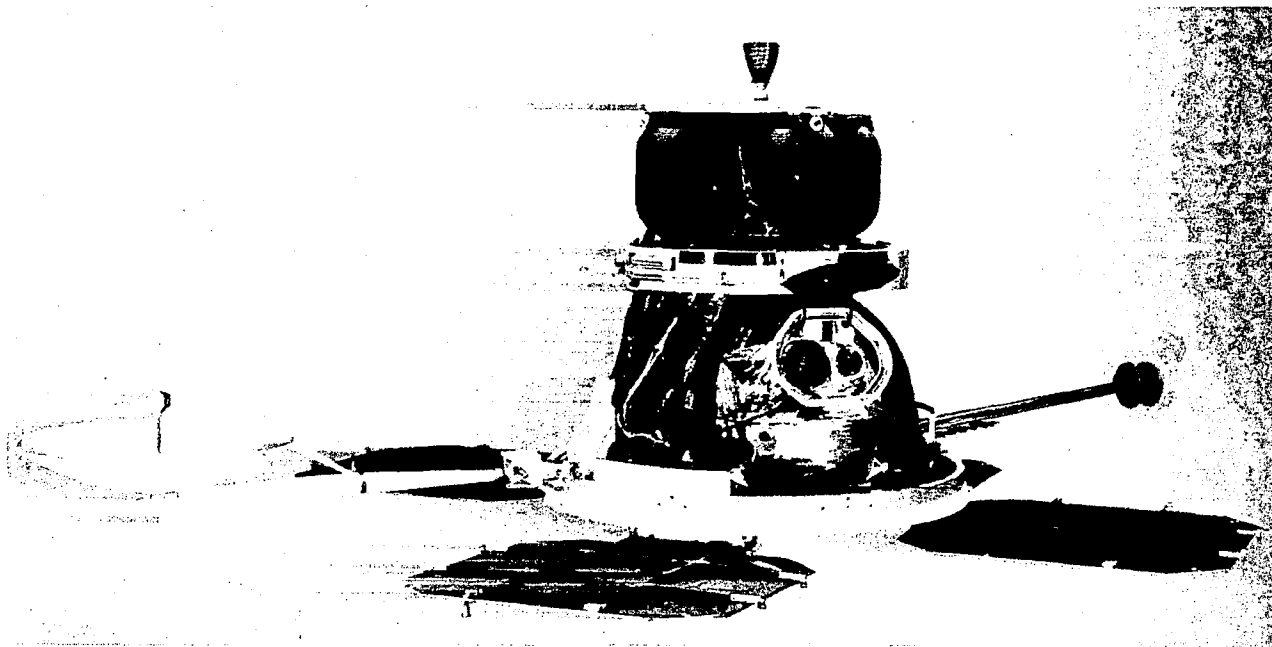
LUNAR ORBITER V

PHOTOGRAPHIC MISSION SUMMARY

The last of five Lunar Orbiter spacecraft was successfully launched from Launch Complex 13 at the Air Force Eastern Test Range by an Atlas-Agena launch vehicle at 22:33 GMT on August 1, 1967. Tracking data from the Cape Kennedy and Grand Bahama tracking stations were used to control and guide the launch vehicle during Atlas powered flight. The Agena-spacecraft combination was boosted to the proper coast ellipse by the Atlas booster prior to separation. Final maneuvering and acceleration to the velocity required to maintain the 100-nautical-mile-altitude Earth orbit were controlled by the preset on-board Agena computer. In addition, the Agena computer determined the maneuver and engine-burn period required to inject the spacecraft on the cislunar trajectory about 33 minutes after launch. Tracking data from the downrange stations and the Johannesburg, South Africa station were used to monitor the boost trajectory.

Deployment of the solar panels and spacecraft antennas was initiated by stored program com-

mands shortly after spacecraft separation and before acquisition by the Deep Space Network tracking stations. Significant events during the cislunar trajectory included the star map and Canopus acquisition sequences and the single midcourse trajectory correction. Unlike previous missions, all trajectory changes and orbit transfers included the requirement that Primary Site V-8a be photographed with 5 degrees of cross-track tilt during Orbit 26.

Lunar injection occurred 90.25 hours after launch with a velocity change of 643 meters per second. The initial orbit parameters were: apolune, 6,028 kilometers; perilune, 195 kilometers; orbit inclination, 85 degrees; and orbit period, 8.5 hours. At apolune of the fourth orbit, a velocity change of 15.97 meters per second reduced the intermediate orbit perilune to the desired initial value of 100 kilometers. A second orbit transfer, initiated by a 233.66 meter-per-second velocity change, was made at perilune of Orbit 10 to place the spacecraft in the desired final elliptical orbit. This maneuver reduced

the apolune altitude to 1,499 kilometers. All other orbit parameters (except orbit period) were unchanged during these Hohmann-type orbit changes.

Mission photography was initiated in the second orbit to obtain the farside coverage beyond the western limb. Eighteen dual-frame exposures of four sites and one filmset exposure were taken from the initial ellipse. Farside photography was continued in the 5.5 orbits of the intermediate ellipse by taking six single-frame exposures. An additional photo was taken in Orbit 8 of a near full-Earth and centered approximately 60 miles west of the southern tip of India. In the final ellipse 13 additional single-frame exposures were taken to complete the areal coverage of the farside.

Primary-site photography of the nearside was initiated in Orbit 15 at 20:58 GMT on August 9. A total of 174 exposures were taken in 50 sequences during 69 orbits. Photo sites included candidate Apollo landing sites, Apollo Applications Program sites, Surveyor landing sites, and scientifically interesting sites with potential interest as specified areas or features of scientific interest at widely distributed areas. Many of these sites were photographed with single-frame exposures. With the exception of the addition of the Earth photo site and some relocations of photo sites during the mission, the photo mission was accomplished according to pre-mission plans.

Examination of the photos showed that all photo objectives were accomplished. Farside coverage, when added to the results of Missions I through IV, provided nearly complete coverage of the hemisphere. Photo quality was extremely good and the resolution of nearside telephoto photos ranged from 2 to 7 meters depending on the spacecraft altitude and slant range. Apollo landing site photography from this mission completed the NASA requirement of vertical, oblique, and convergent telephoto stereo coverage for each of the selected sites.

The spacecraft recorded one micrometeoroid impact on the detectors mounted on the periphery of the tank deck; no apparent effect was indicated in the performance data. Radiation dosage during the 27-day photo mission was extremely low.

All mission objectives were completely accomplished. This mission terminates the Lunar Orbiter program, which in five successful flights has provided data for the selection of eight candidate Apollo landing sites and provided detailed photography of virtually the entire lunar surface at resolutions at least an order of magnitude better than that obtainable from Earth-based observations.
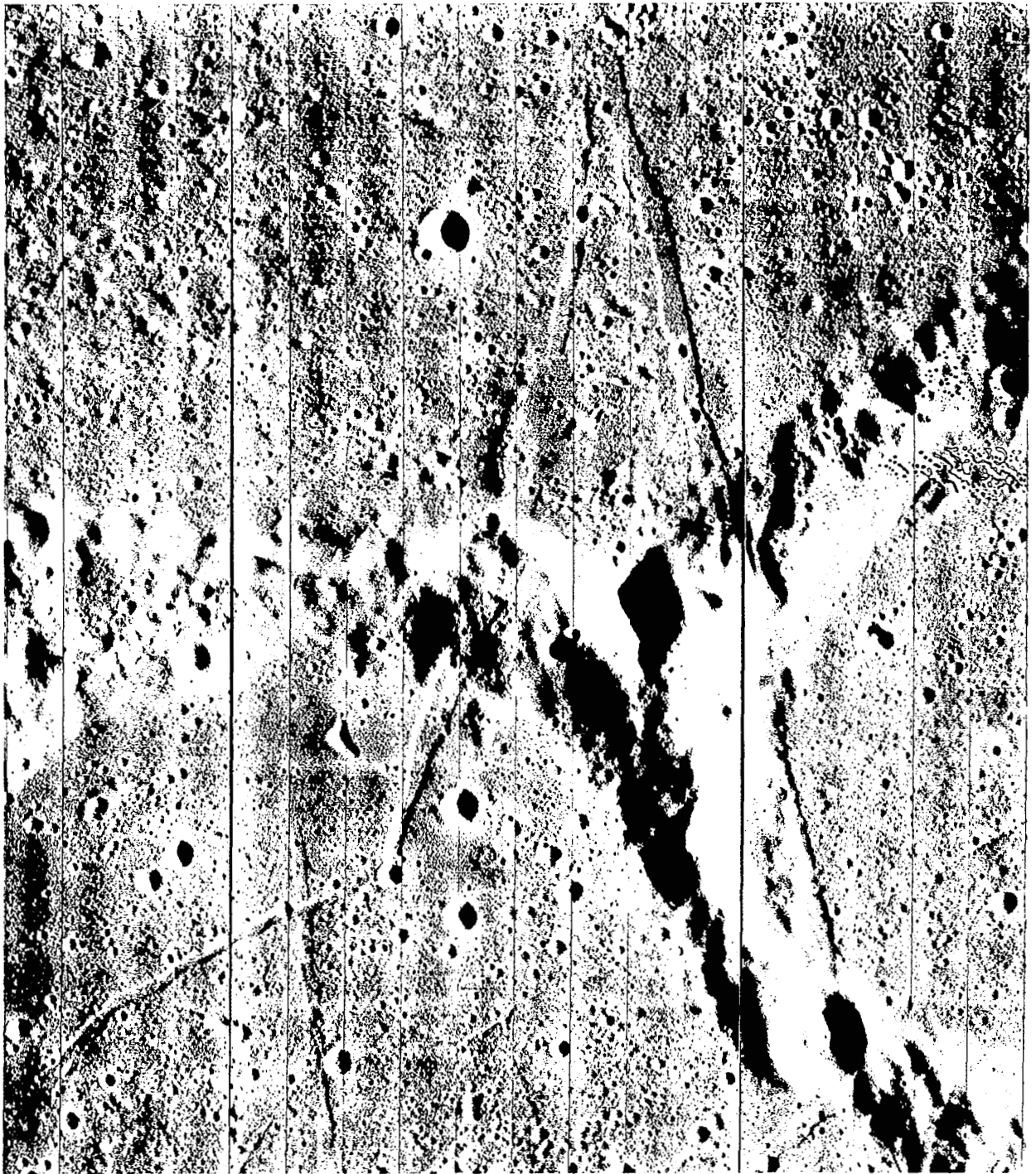
Wide-Angle Frame 138, Site V-34
Centered on the crater Fra Mauro

1.0 Introduction

The Lunar Orbiter program was formalized by Contract NAS1-3800 on May 7, 1964, as one of the lunar and planetary programs directed by the NASA headquarters Office of Space Sciences and Applications. The program is managed by the Langley Research Center, Hampton, Virginia, with The Boeing Company as the prime contractor. Lunar Orbiter is the third in a succession of unmanned missions to photograph the Moon and to provide lunar environmental data to support the Apollo manned lunar landing mission.

1.1 PROGRAM DESCRIPTION

The primary task of the Lunar Orbiter program was to obtain, from lunar orbit, detailed photographic information of various lunar areas to assess their suitability as landing sites for Apollo and Surveyor spacecraft. The landing site aspects of this task were essentially completed during the first three flights.

Site-search missions of potential areas in southern and northern latitude bands within the established Apollo zone of interest ($\pm 5°$ latitude and $\pm 45°$ longitude) were examined by the Lunar Orbiter I and II missions, respectively. Twelve of these sites were rephotographed by a comprehensive integration of vertical, oblique, and forward wide-angle stereo and convergent telephoto stereo photography by the site-confirmation mission of Lunar Orbiter III. Eight candidate sites for early Apollo missions were selected from the data obtained by these three missions. It is anticipated that three sites will be chosen from this set of eight candidates for the first Apollo landing on the Moon. In addition, secondary-site photography provided extensive coverage of the farside of the Moon and many areas of scientific interest on the nearside of the Moon.

These results enabled the lunar exploration program to concentrate, for the last two flights of the Lunar Orbiter program, on the basic scientific interests of broadening the knowledge of the Moon. Representatives of the scientific community collaborating in the program were near-unanimous in agreeing that the remainder of the program should consist of:
- Surveying the entire lunar surface at a resolution significantly better than that obtainable from Earth.
- Examining in detail various surface geological processes identified from this survey.

The photographic results of such a broad survey would be useful not only for identifying interesting targets for the next mission, but would stand for many years as the prime source of data on lunar surface features.

Lunar Orbiter IV provided photographic coverage of over 99% of the nearside lunar surface at resolutions at least an order of magnitude better than Earth-based observations. Approximately 50% of the initially selected Mission V sites were altered on the basis of Mission IV photography to improve the scientific data recovery.

Mission V was to provide additional photography of specific candidate Apollo landing sites to complete the NASA photo requirements for each site. In addition, specific areas and features were to be photographed to provide the data necessary for scientific investigations and the overall understanding of the Moon as an entity.

1.2 PROGRAM MANAGEMENT

Successful accomplishment of Lunar Orbiter program objectives requires the integrated and cooperative efforts of government agencies, private contractors, numerous subcontractors, and the worldwide data collection system of the NASA Deep Space Network. The functional relationship and responsibilities of these organizations are shown in Figure 1-1.

As the prime contractor, Boeing is responsible to the Lunar Orbiter Project Office of the NASA-Langley Research Center for the overall project management and implementation of the complete operating system. Boeing is also responsible for the establishment -- with and through
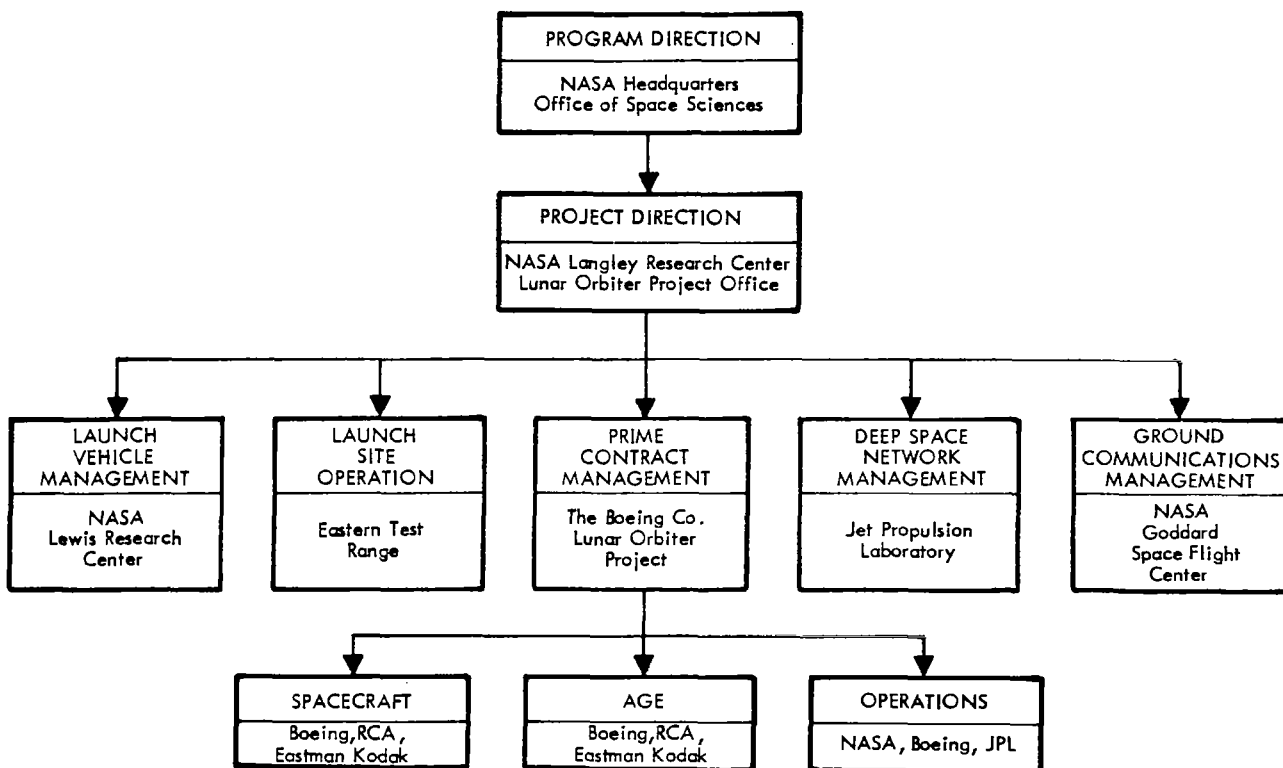
Figure 1-1: Lunar Orbiter Project Organization

the NASA-Langley Research Center -- of effective working relationships with all participating government agencies.

The NASA Lewis Research Center supports the Lunar Orbiter program by providing the Atlas-Agena launch vehicle and associated services that are necessary to: (1) ensure compatibility of the spacecraft with the launch vehicle; and (2) launch and boost the spacecraft into the proper cislunar trajectory.

The Air Force Eastern Test Range (AFETR) provides facilities, equipment, and support required to test, check out, assemble, launch, and track the spacecraft and launch vehicle. The AFETR also controls the Atlas launch vehicle trajectory and monitors Agena performance through cislunar injection, separation, and retrofire to ensure orbital separation. Appropriate instrumentation facilities, communications, and data recorders are provided at downrange and instrumentation ships to ensure the availability

of data for boost trajectory control, acquisition by the Deep Space Station tracking radars, and postmission analysis.

The Deep Space Network (DSN) is managed by the Jet Propulsion Laboratory. This network, consisting of the Space Flight Operations Facility (SFOF) and the Deep Space Stations (DSS), provides two-way communications with the spacecraft, data collection, and data processing. Facilities are provided for operational control which interface with Lunar Orbiter mission-peculiar equipment. Support is also provided in terms of personnel, equipment calibration, and housekeeping services.

Goddard Space Flight Center is the agency responsible for the worldwide network of communication lines necessary to ensure prompt distribution of information between the several tracking stations and the Space Flight Operations Facility during the mission and mission training periods.

1.3 PROGRAM OBJECTIVES

The prime program objective of the Lunar Orbiter was to secure topographic data regarding the lunar surface for the purpose of extending our scientific knowledge, and selecting and confirming landing sites for Apollo. To accomplish the objective, high-resolution photographic data covering specified areas on the lunar surface and moderate-resolution photographic data coverage of extensive areas were necessary.

Other objectives were to secure information concerning the size and shape of the Moon, the properties of its gravitational field, and lunar environmental data.

Landing sites are desired at a number of locations to fulfill the exploration and scientific objectives of the Apollo program and to provide an adequate launch window. The topography of an Apollo landing site must be smooth enough for an Apollo landing module (LM) landing and the approach terrain must be reasonably level to allow satisfactory LM landing radar performance. The surface resolution requirement to enable selection of suitable sites for Apollo landings is approximately 1 meter.

Selection of the photo sites for Lunar Orbiter missions is primarily based on Apollo constraints and preferences as modified to reflect the knowledge gained by preceding missions. As Apollo photo requirements are fulfilled, secondary scientific requirements are used in selecting photo sites.

Completion of the initial primary photographic objectives in the minimum of three missions permitted concentration on the scientific goals during the remaining two flights. Upon the near-unanimous recommendation of the numerous scientists supporting the program, additional primary objectives were defined to broaden the scientific knowledge required to understand the Moon as an entity by:
- Surveying the entire lunar surface at a resolution significantly better than that obtainable from Earth;
- Examining in detail various surface geological processes identified from this survey.

Lunar Orbiter IV provided coverage of more than 99% of the nearside of the Moon at resolutions about 10 times better than obtainable from Earth-based observations. The photographic results of Mission IV were used for identifying interesting targets for Mission V. Lunar Orbiters I through IV provided photo coverage of approximately 60% of the farside and identified those areas to be covered during Mission V.

The selenodetic and environmental mission data objectives require no special instrumentation. Tracking data obtained throughout the mission produce the basic data required to satisfy the selenodetic objectives. Micrometeoroid detectors mounted on the periphery of the spacecraft and radiation detectors mounted internally monitor the lunar environmental data on each flight for transmission to the Earth stations.

1.3.1 Mission V Objectives

The specific objectives for Mission V were defined by NASA as follows:

"Prime Objective
- To obtain from lunar orbit photography of selected scientifically interesting areas on the front and far sides of the Moon, and supplemental photography of candidate Apollo sites.

Secondary Objectives
- To provide precision trajectory information for use in improving the definition of the lunar gravitational field.
- To provide measurements of the micrometeoroid flux and radiation dose in the lunar environment, primarily for spacecraft performance analysis.
- To provide a spacecraft which can be tracked in lunar orbit by the MSFN stations for the purpose of exercising and evaluating the tracking network and Apollo Orbit Determination Program."

The prime objective was divided by NASA into five tasks, namely:
- "Provide additional photography for Apollo.

7

- Provide broad-survey photography of un-photographed areas on the farside.
- Provide photography of scientifically interesting Surveyor sites.
- Provide photography of scientifically interesting "landable" areas for the Apollo Application Program (AAP).
- Provide photography of scientifically interesting areas."

Figure 1-2 illustrates the point locations of the nearside sites photographed in Mission V. Table 1-1 provides a list of all nearside sites for Mission V, along with the orbit on which the site was photographed, the latitude and longitude of the site, the site name, and the number of frames.

The farside areas to be photographed during Mission V consisted of a 45-degree longitudinal band just beyond the western limb and areas located between 30 and 60°N latitude, and a small centrally located area between 35 and 60°S latitude.

A minimum launch window of 3 days was required for Mission V, with a controlled-crash capability. As for all prior Lunar Orbiter missions, the plan for flight beyond the nominal photographic mission (extended mission) included as long a lifetime as possible. It also incorporated the constraint of the operational capability for a controlled terminal maneuver for impact on the nearside within the Apollo zone.

Maximum possible priority readout during the photographic phase was required with telephoto frames generally considered as having higher priority than wide-angle frames.

1.4 MISSION DESIGN
The Lunar Orbiter mission was designed to use the full capabilities of the spacecraft and its photo subsystem to ensure the maximum probability of success of the photographic mis-

sion. In addition, the mission design considered all requirements for placing the spacecraft over the mission target(s) in the proper attitude, altitude, and within the established lighting limitations to achieve quality photography. Launch vehicle, spacecraft, and photographic considerations were integrated into the design effort to optimize the trajectory and sequence of events to satisfy mission photographic objectives.

Selection of the trajectory was based on numerous operational conditions which must be satisfied, such as:
- Transit time (Earth to Moon) of approximately 90 hours.
- Midcourse maneuver to adjust the cislunar trajectory for launch vehicle dispersion and facilitate injection into near-polar orbit.
- Initial lunar orbit apolune altitude approximately 6,000 kilometers, perilune altitude 200 kilometers, period 8.5 hours.
- Intermediate lunar orbit apolune altitude approximately 6,000 kilometers, perilune altitude 100 kilometers, period 8.38 hours.
- Final lunar orbit apolune altitude of 1,500 kilometers, perilune altitude of 100 kilometers, and orbit period of 3.2 hours.
- A plane change of approximately 13.79 degrees at lunar injection to achieve the required near-polar orbit.
- Orbit inclination of approximately 85 degrees.
- Ascending-node photography on nearside for Canopus acquisition.
- Perilune near lunar equator for equal north-south resolution.
- Posigrade orbit for two-station visibility of injection.
- Sun illumination band.

Trajectory and orbit data used for mission design were based on computations using various lunar models with Earth effects. The data used were the output of the following computer programs:
- Translunar Search;
- Translunar Orbit Description;
- Lunar Orbit Description.
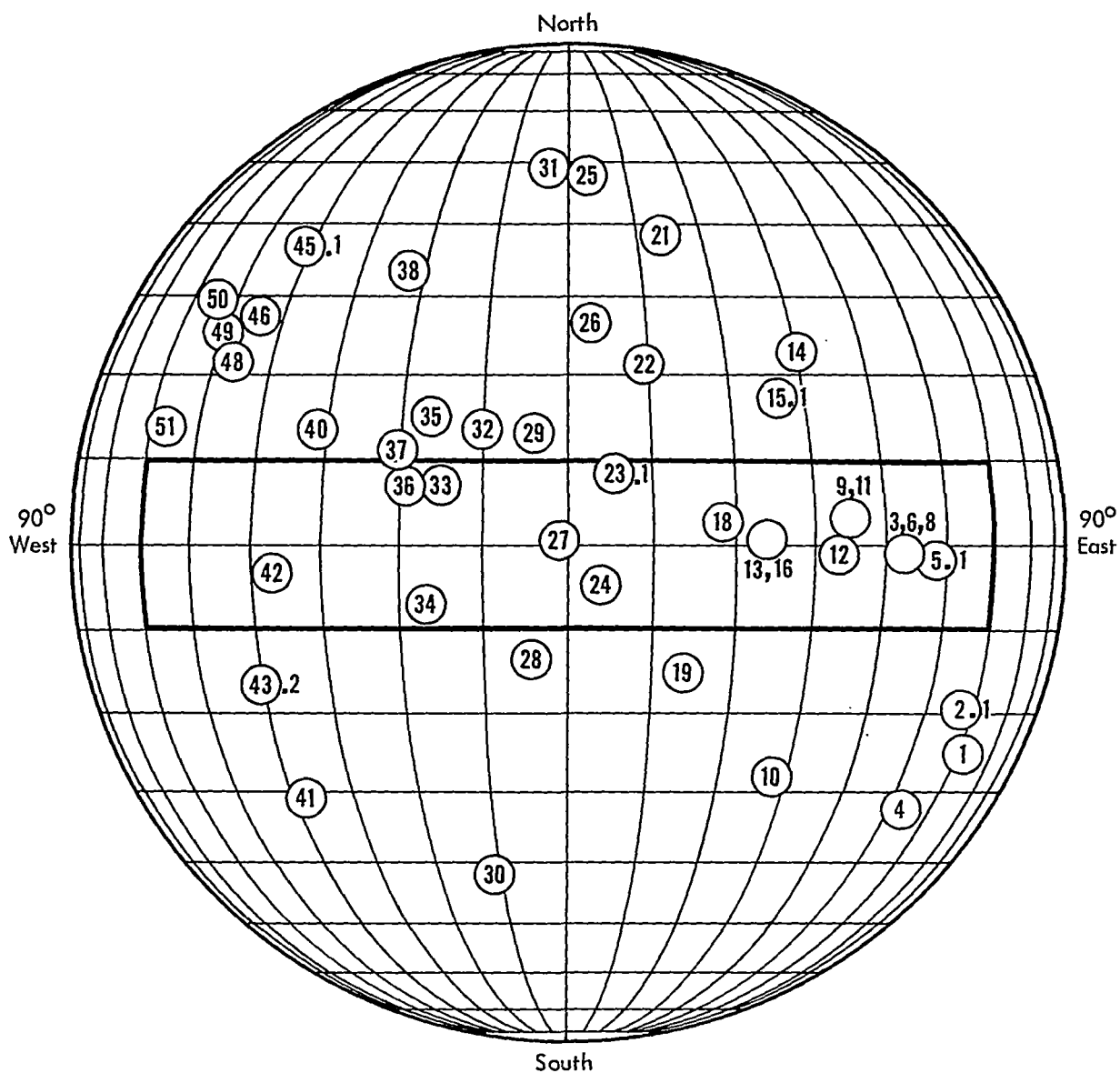
Figure 1-2: Photo Site Location — Nearside

Table 1-1: Mission V Photographic Site Location -- Nearside

Site No.	Orbit No.	Latitude	Longitude	Name	Coverage*	Notes*
V-1	15	25° 10' S	60° 40' E	Petavius	F4	NV
V-2.1	17	19° 25' S	57° 05' E	Petavius B	1	NV
V-3.1	19	1° 00' S	42° 56' E	IP-1	1	WO (to include zero phase point)
		(1° 00' S	42° 30' E	Camera axis intercept)		
V-4	20	31° 50' S	51° 50' E	Stevinus A	1	NV
V-5.1	21	2° 10' S	47° 16' E	Messier	1	CO (look west perpendicular to orbit)
V-6	23	1° 00' S	42° 56' E	IP-1	1	WO
		(1° 00' S	44° 24' E	Camera axis intercept)		
V-8a	26⎫	1° 00' S	42° 56' E	IP-1	F4	CTS
V-8b	27⎭				F4	
V-9.1	28	2° 40' N	34° 45.6'E	IIP-2	1	WO
V-10	30	28° 00' S	27° 45' E	Altai Scarp	1	CO (look southwest)
V-11a	31⎫	2° 40' N	34° 14' E	IIP-2	F4	CTS
V-11b	32⎭				F4	
V-12	33	0° 26' S	32° 43' E	Censorinus	1	NV
V-13	34	0° 45' N	23° 51' E	IIP-6	1	WO
		(0° 45' N	25° 13.8'E	Camera axis intercept)		
V-14	35	22° 12' N	29° 20' E	Littrow	F4	NV
V-15.1	36	17° 12' N	26° 20' E	Dawes	1	NV
V-16a	37⎫	0° 45' N	23° 51' E	IIP-6	F4	CTS
V-16b	38⎭				F4	
V-18	41	2° 42' N	18° 00' E	Dionysius	F4	NV
V-19	42	14° 50' S	14° 00' E	Abulfeda	1	NV
V-21	45	38° 30' N	13° 30' E	South of Alexander	F4	NV
V-22	46	21° 00' N	9° 20' E	Sulpicius Gallas rilles	F4	NV
V-23.2	47	8° 03' N	6° 0' E	Hyginus rilles	F4	NV

*Abbreviations defined on last page of table.

Table 1-1 (Continued)						
Site No.	Orbit No.	Latitude	Longitude	Name	Coverage*	Notes*
V-24	48	4° 45' S	4° 05' E	Hipparchus	F4	NV
V-25	49	48° 55' N (48° 06' N	3° 00' E 1° 00' E	Alpine Valley Camera axis intercept)	1	CO (look southwest with telephoto frame parallel to valley) V/H OFF
V-26.1	50	25° 52' N	3° 00' E	Hadley rille	S4	NV
V-27a V-27b	51} 52}	0° 25' N	1° 06' W	IIP-8	F4 F4	CTS
V-28	53	13° 40' S	4° 10' W	Alphonsus	F4	NV
V-29	54	12° 50' N	4° 00' W	Rima Bode II	F4	NV
V-30	55	41° 45' S	11° 30' W	Tycho	F4	NV
V-31	56	49° 30' N	2° 40' W	Sinuous rille east of Plato	F4	NV
V-32	57	13° 25' N	10° 35' W	Eratosthenes	S4	NV
V-33	59	6° 25' N	14° 45' W	Area of Copernicus CD	1	NV
V-34	60	7° 12' S	16° 45' W	Crater Fra Mauro	F4	NV
V-35	61	14° 40' N	16° 15' W	Copernicus secondaries	S4	NV
V-36	62	6° 52' N	18° 15' W	Copernicus H	F4	NV
V-37	63	10° 25' N	20° 18' W	Copernicus	F8	NV
V-38	65	32° 40' N	22° 00' W	Imbrium flows	F4	NV
V-40	69	13° 10' N	30° 55' W	Tobias Mayer dome	F4	NV
V-41	70	30° 25' S	37° 25' W	Vitello	1	NV
V-42a V-42b	71} 72}	3° 30' S (3° 30' S	36° 11' W 36° 31' W	IIIP-11 Camera axis intercept V-42b)	F4 F4	CTS
V-43.2	73	16° 52' S	40° 00' W	Gassendi	S4	NV

11

Table 1-1 (Continued)

Site No.	Orbit No.	Latitude	Longitude	Name	Coverage*	Notes*
V-45.1	76	35° 55' N	41° 30' W	Jura domes	F4	NV
V-46	77	27° 15' N	43° 38' W	Harbinger Mts.	F8	NV
V-48	79	23° 15' N	47° 25' W	Aristarchus	F8	NV
V-49	80	25° 09' N	49° 30' W	Cobra Head	F4	NV
V-50	82	28° 00' N	52° 45' W	Aristarchus Plateau	F4	NV
V-51	83	13° 45' N	56° 00' W	Marius Hills	F8	NV

Legend

F . . . . Fast		WO . . . . . . Westerly oblique	
S . . . . Slow		CO . . . . Conventional oblique	
NV . . . . Near vertical		CTS . . . . . . Convergent telephoto stereo	

Table 1-2 tabulates launch window characteristics for the August launch periods. The nominal sequence of events presented in the mission event sequence and time-line analysis was based on a launch time approximately 1.9 hours into the first launch window.

The trajectories required to accomplish the photographic objectives during these launch periods were documented in the form of:
- Targeting specifications for the booster contractor;
- Tabulated trajectory data;

- Tracking and telemetry coverage plan;
- Station view periods;
- Acquisition analyses;
- Preflight predictions;
- Mission error analysis;
- Nominal mission studies;
- Alternate mission studies;
- Photo coverage analyses.

The set of orbit parameters that provided the required coverage of the photo sites determined the sequence and timing of events to obtain the desired photo coverage. Other factors that af-

Table 1-2: Launch Window Summary

Launch Date (GMT)	Launch Start	Window End	(GMT) Duration	Launch Azimuth (deg) Start	End
August 1, 1967	20:09	24:00	3.85 hours	90.0	114.0
2-3 "	21:56	01:28	3.53 hours	90.0	114.0
3-4 "	23:40	02:56	3.27 hours	90.0	114.0

fected photo subsystem sequences included such operational or spacecraft performance constraints as:

- Start readout no sooner than 10 minutes after earthrise to ensure adequate time for spacecraft acquisition and photo subsystem video adjustments;
- Interval of 5 minutes between end of processing and the start of readout;
- Interval of 2 minutes between end of readout and the start of processing to turn off readout and activate processor;
- Advance one frame at least every 8 hours to avoid film set;
- After initiating processing of nearside photography, process at least two frames every 4 hours to reduce Bimat dryout;
- Read out as many frames as possible between photo passes to support the near-real-time mission operation and control functions.

The nominal planned sequence of photographic events from injection into lunar orbit to the completion of film processing and "Bimat cut" command (Orbit 83) is shown in Figure 1-3. The ordinate covers the period of one complete orbit (8 hours, 30 minutes, 30 seconds; 8 hours, 23 minutes, 30 seconds; and 3 hours, 11 minutes, 15 seconds for each of the three elliptical orbits) and the abscissa covers successive orbits. The left chart covers the photo sequences of the first two elliptical orbits during the first 10 orbits of the Moon. Time progresses from the bottom to top and the top of any orbit is identical to the bottom of the next orbit. The periods of Earth and Canopus occultation are shown. The bar charts at the top represent the approximate viewing periods of the three primary Deep Space Stations. The figure also shows when the photos are taken with respect to time from orbit apolune as well as the time allotted for film processing and priority readout.

Figure 1-4 shows spacecraft exposure number and photo site number of each photo and shows the planned sequence of photography. The shaded portions indicate the wide-angle frames planned to be read out in priority mode.

1.5 FLIGHT VEHICLE DESCRIPTION

The Lunar Orbiter spacecraft is accelerated to injection velocity and placed on the cislunar trajectory by the Atlas-Agena launch vehicle.

Spacecraft Description — The 380-kilogram (853-pound) Lunar Orbiter spacecraft is 2.08 meters (6.83 feet) high, spans 5.21 meters (17.1 feet) from the tip of the rotatable high-gain dish antenna to the tip of the low-gain antenna, and measures 3.76 meters (12.4 feet) across the solar panels. Figure 1-5 shows the spacecraft in the flight configuration with all elements fully deployed (the mylar thermal barrier is not shown). Major components are attached to the largest of three deck structures which are interconnected by a tubular truss network. Thermal control is maintained by controlling emission of internal energy and absorption of solar energy through the use of a special paint and mirrors covering the bottom side of the deck structure. The entire spacecraft periphery above the large equipment-mounting deck is covered with a highly reflective aluminum-coated mylar shroud, providing an adiabatic thermal barrier. The tank deck is designed to withstand radiant energy from the velocity control engine to minimize heat losses in addition to its structural functions. Three-axis stabilization is provided by using the Sun and Canopus as spatial references, and by a three-axis inertial system when the vehicle is required to operate off celestial references, during maneuvers, or when the Sun and/or Canopus are occulted by the Moon.

The spacecraft subsystems (as shown in the block diagram of Figure 1-6) have been tailored around a highly versatile "photo laboratory" containing two cameras, a film supply, film processor, a processing web supply, an optical electronic readout system, an image motion compensation system (to prevent image smear induced by spacecraft velocity), and the control electronics necessary to program the photographic sequences and other operations within the photo subsystem. Operational flexibility of this photo subsystem includes the capability to adjust key system parameters (e.g., number of frames per sequence, time interval between frames, shutter speed, line-scan tube focus) by remote control from the ground.

13
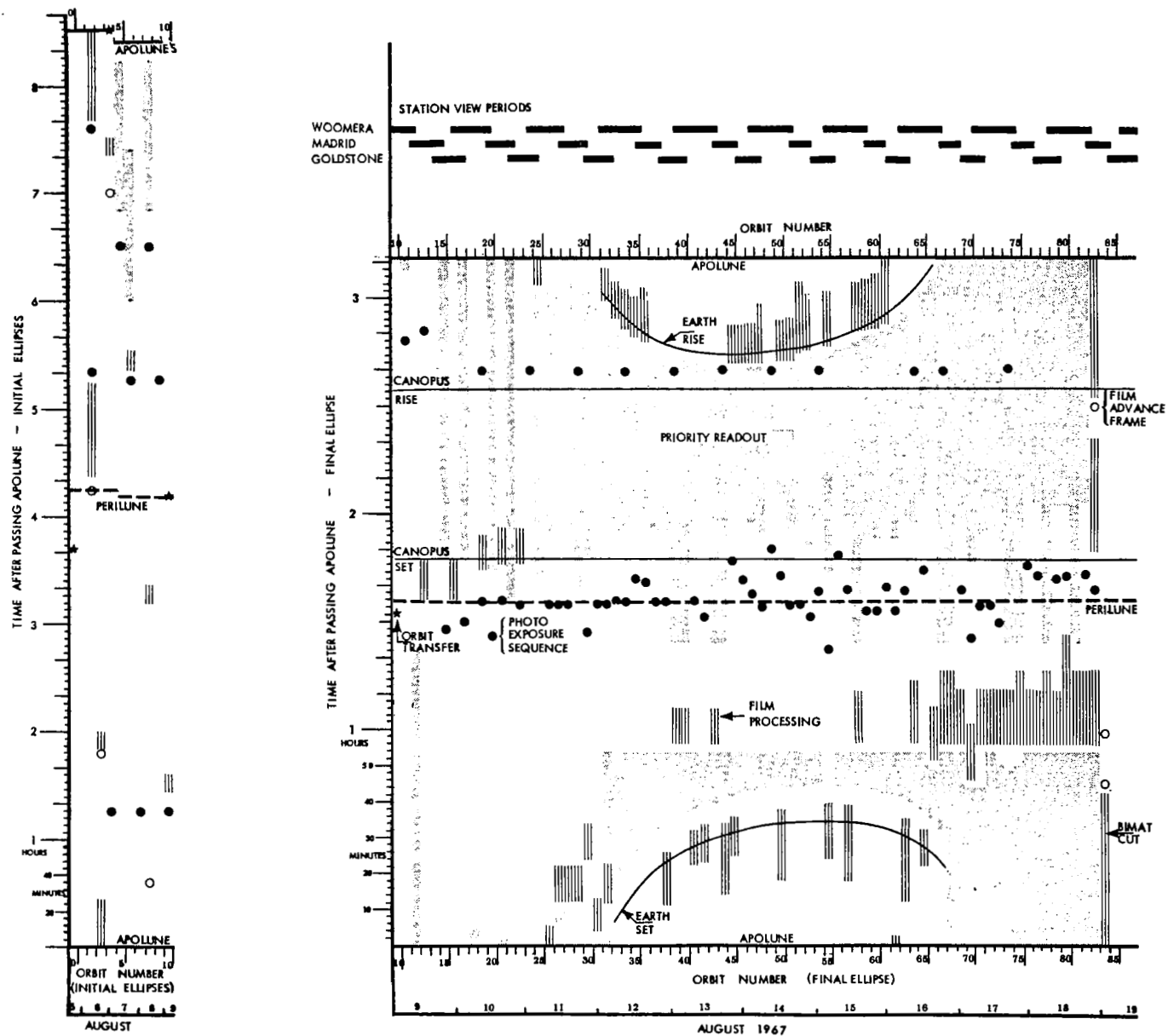
Figure 1-3: Planned Photo Period Sequence of Events

14

Figure 1-4: Exposure Sequences and Priority Readouts

Figure 1-5: Lunar Orbiter Spacecraft
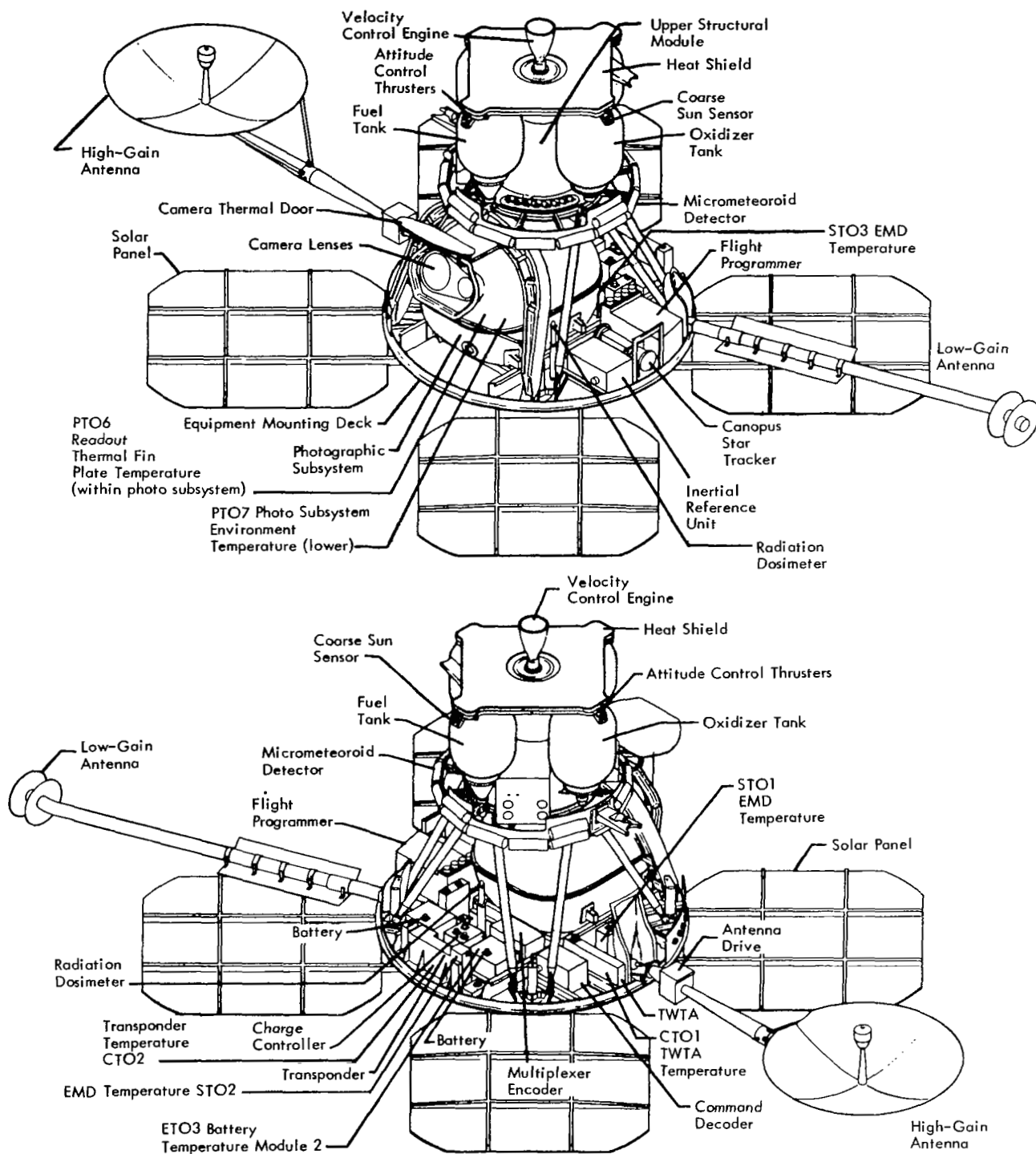
Note: Shown with Thermal Barrier Removed

16
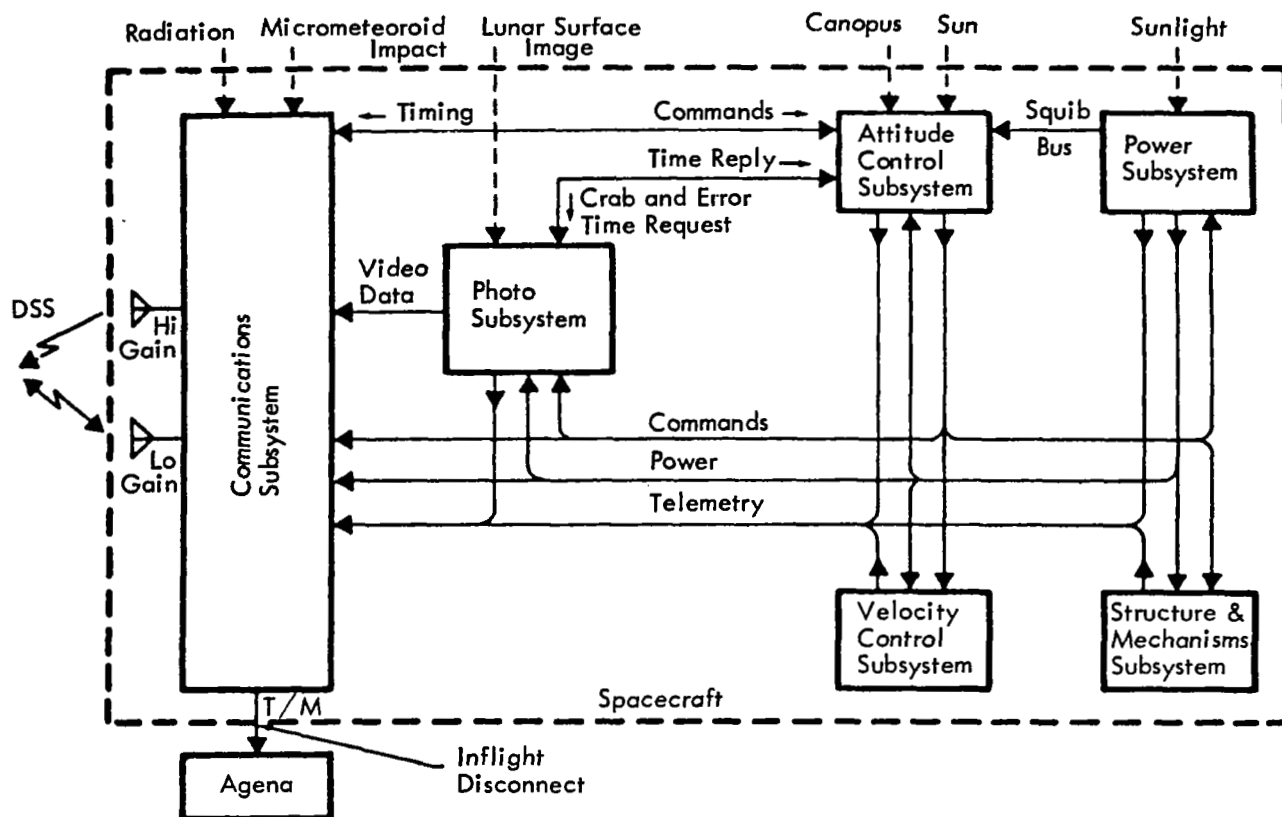
Figure 1-6: Lunar Orbiter Block Diagram

The influence of constraints and requirements peculiar to successful operation in lunar orbit are apparent in the specific design selected.

- A three-axis stabilized vehicle and control system were selected to accommodate the precise pointing accuracies required for photography and for accurate spacecraft velocity-vector corrections during midcourse, lunar orbit injection, and orbit-transfer maneuvers.

- The spacecraft is occulted by the Moon during each orbit, with predictable loss of communication from Earth. Since spacecraft operations must continue behind the Moon, an on-board command system with a 128-word memory was provided to support up to 16 hours of automatic operation. It can be interrupted at virtually any time during radio communication to vary the stored sequences or introduce real-time commands. The selected programmer design is a digital data processing system containing register, precision clock, and comparators, to permit combining 65 spacecraft control functions into programming sequences best suited to spacecraft operations required during any phase of the mission.

- The communications system high-gain antenna was provided with a $\pm$ 360-degree rotation capability about the boom axis to accommodate pointing errors introduced by the Moon's rotation about the Earth.

- Two radiation detectors were provided to indicate the radiation dosage levels in the critical unexposed film storage areas. One detector measured the exposure "seen" by the unexposed film remaining in the shielded supply spool. The second detector measured the integrated radiation exposure seen by undeveloped film in the camera storage looper. The data from these detectors allow the selection of alternate mission plans in the event of solar flare activity.

The overall operation of taking the lunar pictures, processing the film, and reading out and

17

transmitting the photo video data within the spacecraft is shown in schematic form in Figure 1-7. In addition, the photo reconstruction process at the Deep Space Stations; the 35-mm GRE film copying process at Eastman Kodak, Rochester, New York; and the manual reassembly by NASA and Army Map Service are also shown.

A detailed description of the spacecraft is provided in NASA Report CR 782, *Lunar Orbiter I Photographic Mission Summary — Final Report.* Changes incorporated on Lunar Orbiters II, III, and IV are defined in NASA Reports CR 883, CR (*) and CR (*) — *Lunar Orbiters II, III and IV Photographic Mission Summary — Final Reports,* respectively. Certain other changes peculiar to Mission V to accommodate spacecraft objectives are listed below.

● Modified the light baffles on the 80- and 610-mm lens and the upper shell.

● Deleted readout-looper-full logic.
● Changed the shroud between the V/H sensor and back of mirror from aluminum to cloth to reduce mirror vibration.
● Provided electrical rather than mechanical adjustment of the 610-mm-shutter slit servo damper.
● Added 72 additional 1-inch-square solar reflectors under the TWTA and photo subsystem.
● Installed sun shade on back of the load resistor panel.
● Painted areas of solar panels to reduce glint to star tracker.
● Installed different thermal coating coupons and monitoring telemetry sensors to continue the thermal paint degradation studies.
● Installed "camera thermal door closed" position indicator and associated telemetry.
● Increased the charge controller maximum rate of charge from 1.0 to 1.4 amps.
● Added a d.c. voltage boost regulator to en-
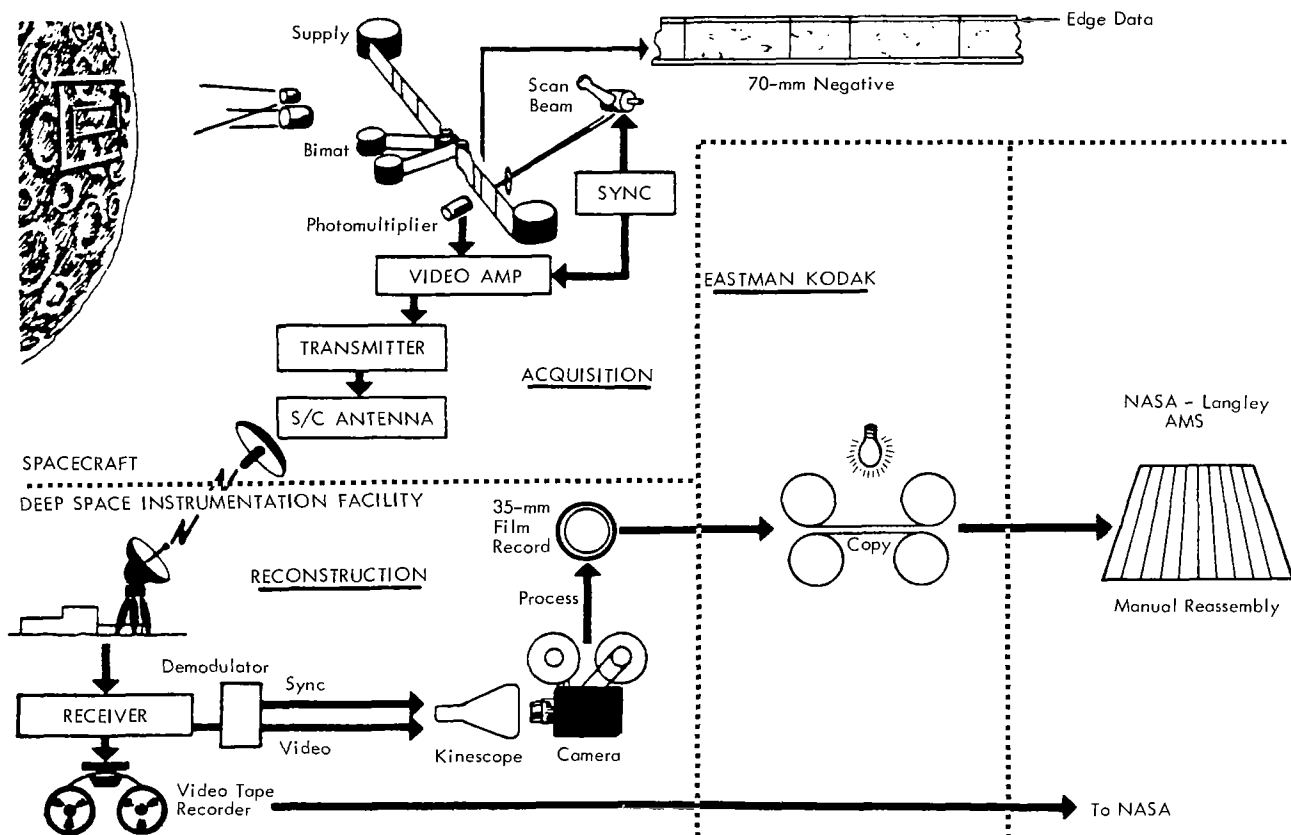
Figure 1-7: Photographic Data Acquisition, Reconstruction, and Assembly

*To be published.

18

sure adequate voltage to photo subsystem during off-Sun attitude required for photography of this mission.

Launch Vehicle — The Atlas-Agena combination is a two-and-a-half-stage vehicle as illustrated in Figure 1-8.

Two interconnected subsystems are used for Atlas guidance and control — the flight control (autopilot) and radio guidance subsystems. Basic units of the flight control subsystem are the flight programmer, gyro package, servo control electronics, and hydraulic controller. The main ground elements of the radio guidance subsystem are the monopulse X-band position radar, continuous-wave X-band doppler radar (used to measure velocity), and a Burroughs computer. The airborne unit is a General Electric Mod III-G guidance package which includes a rate beacon, pulse command beacon, and decoder. The radio guidance subsystem interfaces with the flight control (autopilot) subsystem to complete the entire guidance and control loop. All engines of the SLV-3 Atlas are ignited and stabilized prior to launch commitment.

The upper stage, an Agena space booster, includes the spacecraft adapter and is adapted for use in the Lunar Orbiter mission by inclusion of optional and "program-peculiar" equipment. Trajectory and guidance control is maintained by a preset on-board computer. The Agena engine is ignited twice: first to accelerate the Agena-Lunar Orbiter combination to the velocity required to achieve a circular Earth orbit, and second to accelerate the spacecraft to the required injection velocity for the cislunar trajectory.

The Agena Type V telemetry system includes an E-slot VHF antenna, a 10-watt transmitter, and individual voltage-controlled oscillators for IRIG standard channels 5 through 18 and channel F. Channels 12 and 13 are used to transmit spacecraft vibrational data during the launch phase. Channel F contains the complete spacecraft telemetry bit stream during the launch phase.
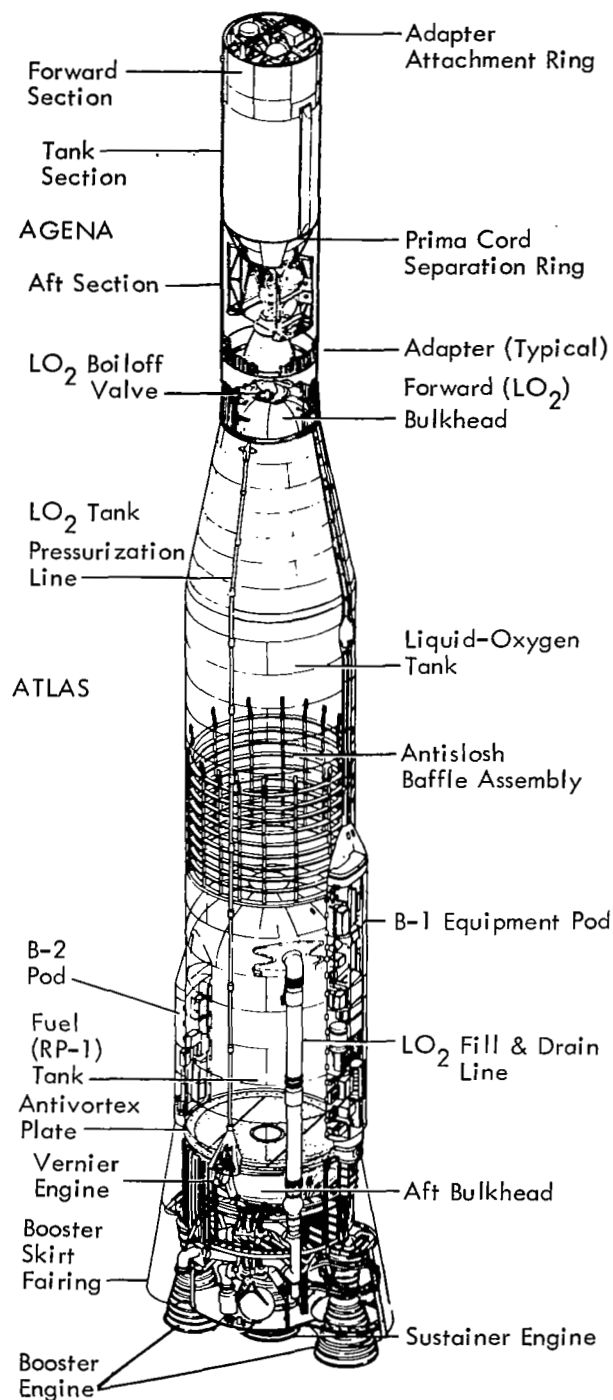
Figure 1-8: Launch Vehicle

19
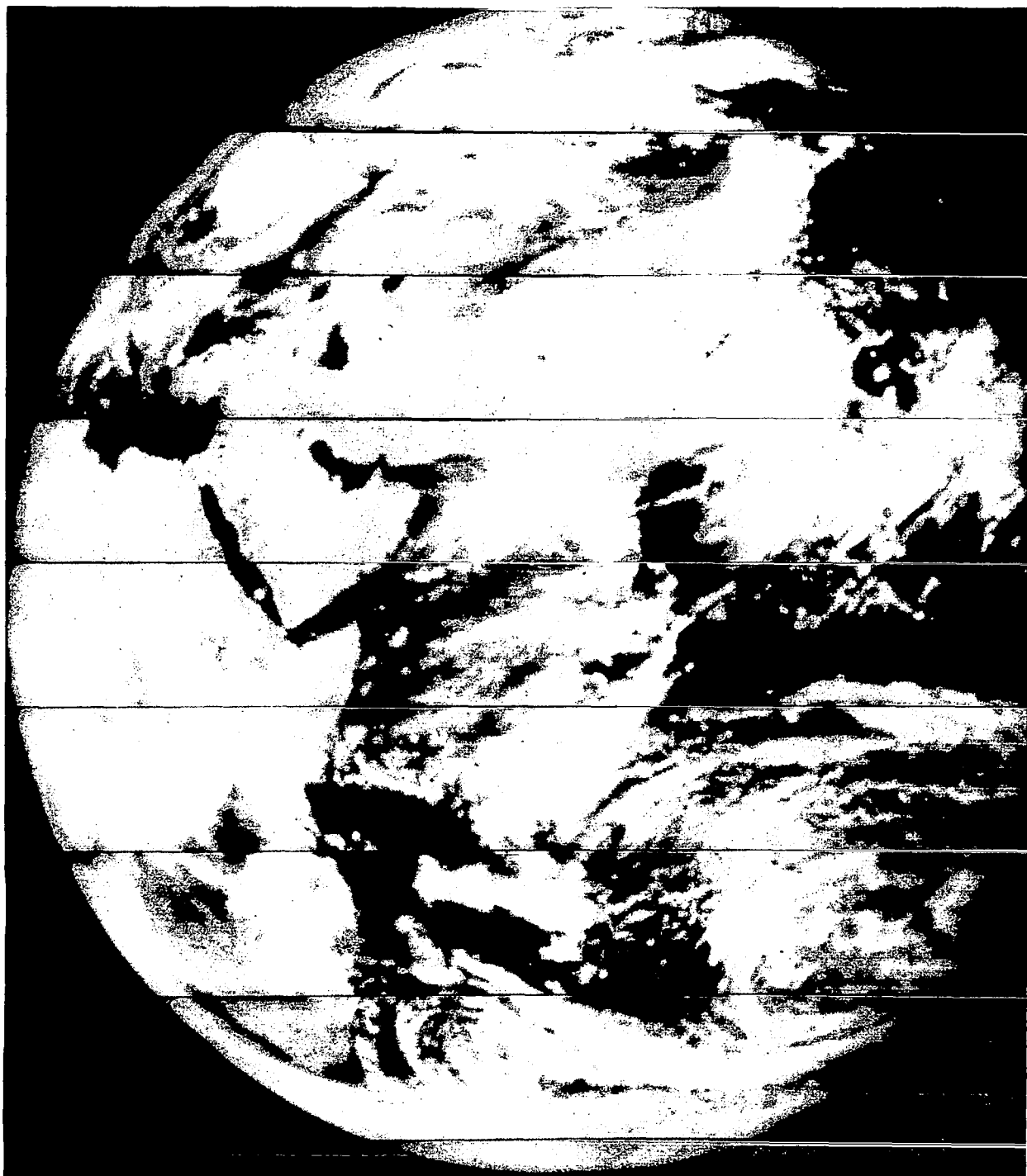
Telephoto Frame 27, Site VA-9

The Earth — centered approximately 60 miles west of southern tip of India.

2.0 Launch Preparation and Operations

Lunar Orbiter V mission preparation started with arrival of the spacecraft at ETR, where it was assembled, tested, and readied for launch. The Atlas-Agena boost vehicle and the Lunar Orbiter spacecraft each received quality acceptance tests at the individual contractor's plant prior to delivery to the AFETR. Early planning included dissemination of information to the launch agency for proper programming of the Atlas-Agena system for the projected launch days. Activities at AFETR of the Atlas, Agena, and Lunar Orbiter spacecraft were integrated so that all systems were properly checked out to support the scheduled launch date. Lunar illumination requirements, Earth-Moon geometry, and Sun-Moon relationships required that these plans be geared to use the available launch windows.

Control of the launch was delegated to the Lewis Research Center, supported by the down-range stations and appropriate instrumentation ships located in the Atlantic and Indian Oceans. Upon acquisition of the spacecraft by the Deep Space Network tracking stations, control of the Lunar Orbiter mission was passed from the AFETR to the Space Flight Operations Facility at Pasadena, California.

The following sections summarize the activities and performance prior to acquisition by the Deep Space Network.

2.1 LAUNCH VEHICLE PREPARATION

The Lunar Orbiter V launch vehicle consisted of the Atlas SLV-3, Serial Number 5805, and the Agena-D, Serial Number 6634, boosters. Significant prelaunch events in launch vehicle preparation are shown in Table 2-1.

Table 2-1: Launch Vehicle Preparation Summary

Date	Event
5-27-67	Atlas and Agena arrived at ETR
6-6-67	Atlas 5805 erected on Complex 13
6-23-67	Lunar Orbiter E spacecraft arrived
6-28-67	Atlas fuel and LOX tanking test
7-7-67	Atlas B-FACT conducted
7-19-67	Atlas/Agena mated at Complex 13
7-20-67	Second B-FACT conducted
7-24-67	J-FACT conducted
7-25-67	Agena/spacecraft mated
7-28-67	Simulated launch test
8-1-67	Launch

Upon arrival at AFETR, the launch vehicle was prepared for launch as summarized in Figure 2-1. This figure shows the test and checkout functions performed in buildup of the integrated flight vehicle.

During normal test and checkout procedures, no major problems occurred on the Atlas which could have delayed the launch. However, several leaking valves were replaced as were three defective transducers. On the Agena, however, due to the need for replacement of fuel seals, the decision was made to replace the entire engine assembly with an engine incorporating the higher clearance bearings, new fuel secondary seal, and the preferred gears.

During the several flight acceptance tests performed, the following vehicle discrepancies were observed and corrected.
- The U-clamp holding the Atlas sustainer yaw telemetry transducer was broken, giving a constant output.
- An Agena RSC battery failed.

2.2 SPACECRAFT PREPARATION
Lunar Orbiter E arrived at Cape Kennedy on March 10, 1967, to be prepared as a backup spacecraft for Mission IV. The spacecraft was tested at Hangar S and at the explosive safe area. During the deactivation of this spacecraft after the May launch of Mission IV, out-of-tolerance leaks were discovered in the bladders of the oxidizer tanks. The spacecraft was then shipped to Seattle by air-conditioned van for replacement of the bladders.

On June 23, 1967, the spacecraft arrived back at Cape Kennedy for retest in accordance with preflight test requirements documentation. Modifications were made to the spacecraft due to the substantially different type of mission planned for Mission V. No significant discrepancies were disclosed by the retests.

The spacecraft was moved to the explosive safe area on July 13, 1967, for final testing, installation of ordnance, loading of the photo subsystem, fueling, and final weight and balance checks.

2.3 LAUNCH COUNTDOWNS
On July 28, 1967, the simulated launch countdown was conducted in accordance with the planned time sequences, with the Atlas, Agena, and spacecraft participating. Following the simulated launch, Atlas airborne command destruct receivers were changed at the request of the Eastern Test Range. All other flight systems functioned properly, although the spacecraft power turn-on was delayed due to ground equipment problems. The multipath problem, previously encountered during checkout of the spacecraft while setting up the photo system for optimum video, was once again experienced at T-315 minutes. A successful method for verification of photo subsystem operation was devised by going to high power on the TWTA with readout from the spacecraft van. The delays incurred were made up and no holds were called.

The launch countdown began on schedule on August 1, 1967. During the count the Agena velocity meter was replaced which, together with adverse weather conditions, caused a total unscheduled hold time of 2 hours and 24 minutes. An rf multipath problem was encountered during the photo subsystem video readout tests but was handled so as to cause minimum lost time. The high-power signal transmitted via the high-gain antenna was also reflected by spacecraft and ground system structures, thereby degrading the video signal recorded at the Cape Kennedy (DSS-71) station. By T-215 minutes the spacecraft had caught up with the countdown clock. At T-118 the air conditioning for the vehicle failed. Portable units were used and, by T-94, the air conditioning was again ready to support the launch activities.

During the weather hold at T-90 minutes, due to severe thunderstorms in the launch area, the spacecraft and photo subsystem were placed in as safe a standby mode as possible so they were the least susceptible to transients that might have been caused by lightning.

From T-90 minutes to T-0, the countdown was nominal. Liftoff occurred at 22:33:00.352 GMT, 30 minutes after the scheduled launch time, in light rain.

ATLAS

HANGAR J
1. RECEIVING AND INSPECTION
2. PROPELLANT UTILIZATION SYSTEM CHECKOUT AND CALIBRATION
3. PROGRAMMER EVALUATION
4. GYRO TEST
5. EVALUATION OF FILTER SERVO CAN

AGENA

HANGAR E
1. RECEIVING & INSPECTION
2. VEHICLE BUS RESISTANCE CHECK
3. HORIZON SENSOR ALIGNMENT AND HEAD PRESSURE TEST
4. BEACON SYSTEM VALIDATION TEST
5. VEHICLE INSTRUMENTATION CALIB
6. DESTRUCT SYSTEM TEST
7. TELEMETRY SYSTEM VALIDATION
8. GUIDANCE SYSTEM VALIDATION AND FINAL ADJ.
9. GUIDANCE FLIGHT CONTROL SYSTEM PREFLIGHT CHECKS
10. PROPULSION SYSTEM LEAK AND FUNCTIONAL TESTS AND ENGINE SERVICING
11. VEHICLE WEIGHT DETERMINATION

TRANSPORTER

TRANSPORTER WITH SHROUD & ADAPTER

SPACECRAFT

ESA
1. RECEIVING AND INSPECTION
2. SUBSYSTEM VALIDATION CHECKS & COMBINED SYSTEMS RUN
3. EQUIPMENT INSTALLATIONS
4. MATE S/C & ADAPTER, INSTALL THERMAL BARRIER AND SHROUD

SPACECRAFT

HANGAR S
1. RECEIVING, INSPECTION & AIRWASH
2. SUBSYSTEM TESTS & OPTICAL ALIGNMENT
3. SYSTEMS & VERIFICATION TESTS

ATLAS

ERECT VEHICLE
1. PROPULSION SYSTEM LEAK & FUNCTIONAL CK ENGINE ALIGNMENT
2. PROPELLANT UTILIZATION SYSTEM LEAK CK
3. TELEMETRY SYSTEM LOCKHOUSE COMPATIBILITY AND FUNCTIONAL TESTS
4. RELEASE SEQUENCE TEST
5. MISSILE ELECTRICAL BLOCKHOUSE COMPATIBILITY TEST
6. RANGE SAFETY COMMAND SYSTEM CHECKOUT
7. MODE IIIG BLOCKHOUSE & AIRBORNE GUIDANCE CK
8. GUIDANCE COMMAND TEST
9. AUTOPILOT SQUIB CIRCUITRY CK
10. INTEGRATED LAUNCH CONTROL TEST
11. BOOSTER TANKING TEST
12. BOOSTER FLIGHT ACCEPTANCE COMPOSITE TEST
13. MATE BOOSTER ADAPTER

AGENA
1. MATING PROCEDURE
2. PYROTECHNIC INSTALLATION
3. PROPULSION SYSTEM PRESSURE TEST AND INSPECTION
4. ELECTRICAL SYSTEM/AGE COMPATIBILITY TESTS
5. GUIDANCE SYSTEM/AGE COMPATIBILITY TESTS
6. TELEMETER & BEACON RF FUNCTIONAL TESTS

SPACECRAFT
1. ENCAPSULATED S/C MATING PROCEDURE
2. SPACECRAFT AGE COMPATIBILITY TESTS (BLOCKHOUSE COMPATIBILITY CHECKS) RF READOUT

ATLAS/AGENA/ SPACECRAFT
1. COMBINED VEHICLE RF INTERFERENCE TEST
2. JOINT FLIGHT ACCEPTANCE COMPOSITE TEST
3. SIMULATED LAUNCH

ATLAS
1. COMPLEX MECHANICAL PRECOUNT OPERATIONS
2. PROPULSION PRECOUNT OPERATIONS
3. AIRBORNE HYDRAULIC PRECOUNT OPERATIONS
4. AUTOPILOT PRECOUNT OPERATIONS
5. AIRBORNE RF TELEMETRY PRECOUNT OPERATIONS
6. COMPLEX ELECTRICAL PRECOUNT OPERATIONS
7. BATTERY INSTALLATION & CHECKS

AGENA
1. PROPELLANT PRESSURE SYSTEM CHECKS
2. BATTERY CHARGING
3. DESTRUCT SYSTEM VALIDATION
4. FUSISTOR CONTINUITY AND RESISTANCE CHECKS
5. PYRO FIT AND INSTALL. CHECKS

SPACECRAFT
PRECOUNT OPERATIONS

LAUNCH COUNTDOWN

LAUNCH COMPLEX TESTS

MISSILE ASSEMBLY BUILDING TESTS

Figure 2-1: Launch Operations Flow Chart

A simplified countdown sequence for the spacecraft and supporting functions is shown in Figure 2-2.

2.4 LAUNCH PHASE

The launch phase covers performance of the Lunar Orbiter E flight vehicle from liftoff through spacecraft separation from the Agena and subsequent acquisition of the spacecraft by the Deep Space Network.

2.4.1 Launch Vehicle Performance

Analysis of vehicle performance, trajectory, and guidance data indicated that all launch vehicle objectives were satisfactorily accomplished. Atlas objectives were to:

- Place the upper stage in the proper coast ellipse as defined by the trajectory and guidance equations;
- Initiate upper-stage separation;
- Start the Agena primary timer;
- Relay the jettison spacecraft shroud command;
- Start the secondary timer commands of the launch vehicle.

Agena objectives were to:

- Inject the spacecraft into a lunar-coincident transfer trajectory within prescribed orbit dispersions;
- Perform Agena attitude and retro maneuvers after separation to ensure noninterference with spacecraft performance.

All of these objectives were accomplished and the launch vehicle performance was well within the prescribed parameters.

Table 2-2 provides a summary of planned and actual significant events during the ascent trajectory. All times are referenced to a liftoff time of 22:33:00.352 GMT on August 1, 1967.

Atlas Performance -- All Atlas SLV-3 (Serial Number 5805) systems performed satisfactorily and a satisfactory ascent trajectory was attained. Vehicle acceleration reached peak values of 6.0 and 3.2 g at booster and sustainer engine cutoffs, respectively. Telemetered data and performance calculations indicated 1,497 pounds of liquid oxygen and 882 pounds of fuel re-
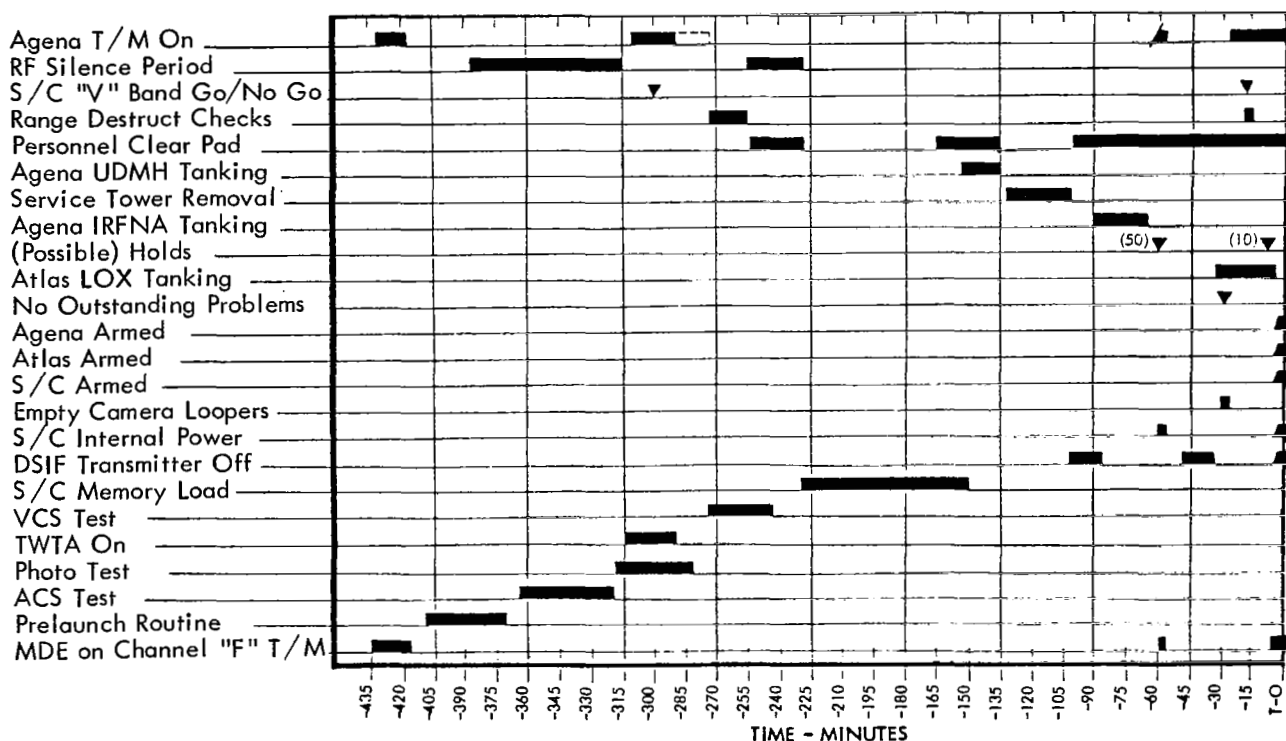
Figure 2-2: Master Countdown Time Sequence

24

Table 2-2: Sequence of Significant Flight Events

Event	Nominal Times	Actual Flight Times (sec)
Liftoff 22:33:00.352 GMT		—0—
Booster engine cutoff (BECO)	128.9	128.6
Booster engine staging	131.9	131.7
Start Agena aux. restart timer	271.85	272.4
Sustainer engine cutoff (SECO)	287.9	288.6
Start Agena primary timer	291.8	296.3 (1)
Vernier engine cutoff (VECO)	308.1	307.9
Uncage gyros	308.1	307.9
Jettison horizon sensor fairings	308.1	307.9
Fire shroud ejection squibs	310.5	310.3
Fire Atlas/Agena separation squibs	312.5	312.4
Initiate Agena first burn sequence	364.8	369.3
Steady-state thrust 90% Pc	365.95	370.45
Agena first-burn cutoff (VM)*	517.6	523.58
Stop primary D-Timer		651.5
Restart primary D-Timer		1,865.4
Initiate Agena second-burn sequence		1,879.4

Event	Nominal Times	Actual Flight Times (sec)
Steady-state thrust 90% Pc	1,880.0	1,880.11
Agena second-burn cutoff (VM)**	1,966.55	1,967.6
Fire ejection squibs (spacecraft)	2,132.85	2,133.42
Initiate yaw maneuver	2,135.85	2,136.39
Stop yaw maneuver	2,195.85	2,196.27
Initiate retro fire	2,732.85	2,733.5
Retro rocket burnout	2,748.85	2,750.5

* First-burn duration   153.13 secs
** Second-burn duration   87.5 secs
     Total burn time   240.63 secs

(1) Primary D-Timer started
     four seconds late.

mained at sustainer engine cutoff. This was equivalent to 8.05 seconds of additional engine burn time.

Launch vehicle stability was maintained throughout all phases of powered flight by the Atlas flight control system. All staging and separation operations and response to guidance steering and discrete commands were satisfactory. The transients and oscillations associated with the staging sequence were normal. Gyro data indicated a highly stable vehicle during vernier phase. Residual rates and displacements at vernier engine cutoff (VECO) were zero. Postflight evaluation of ground and telemetered vehicle-borne data indicated that both the Mod III-A ground station and the Mod III-G airborne-guidance equipment performed satisfactorily. The launch vehicle was acquired as planned and good track was maintained in both the track and rate subsystems until well beyond SLV-3/Agena separation. The following insertion parameters and computed values for the semimajor and semiminor axes of the boost vehicle coast ellipse were obtained from data at VECO plus 2 seconds, through standard computational processes.

Parameter	Computed Value	
Semimajor axis	14,511,901 ft	
Semiminor axis	12,708,669 ft	
Velocity magnitude	18,534	ft/sec
Velocity to be gained	+ 0.51	ft/sec
Filtered yaw velocity	+ 2.07	ft/sec
Filtered altitude rate minus desired altitude rate	−11.73	ft/sec

Agena Performance -- The Agena-D (Serial Number 6634) performed satisfactorily subsequent to separation from the Atlas and placed the spacecraft on the desired cislunar trajectory.

The primary sequence timer was started 4.6 seconds later than nominal; therefore, all the timer-controlled functions were proportionately late. Engine performance calculations, based on telemetered data, showed the average combustion chamber pressure was 511.0 psig and that 16,219 pounds of thrust were developed during the first burn period. The average turbine speed was measured at 25,040 rpm. Based on a computed total flow rate of 55.59 pounds per second, the specific impulse was calculated to be 291.8 lb-sec per pound. The first-burn duration (from 90% chamber pressure to velocity-meter-initiated engine shutdown) was 153.05 seconds, 1.4 seconds longer than predicted. The second-burn duration, as determined from data retransmitted from Pretoria, was 87.0 seconds, 0.5 second longer than the predicted nominal.

Velocity meter performance during the first burn was satisfactory and the telemetry continued to monitor the accelerometer output through loss of signal at Antigua. There were no changes in the last 98 seconds of Antigua data; this indicated a near-zero null torque variation.

Programmed pitch and roll maneuvers during the Atlas booster operation were sensed by the caged Agena gyros. Small disturbances were also noted at booster engine cutoff. Sustainer engine cutoff, vernier engine cutoff, and Atlas-Agena separation were extremely smooth.

During the flight, the shroud separation monitor indicated premature Agena/shroud separation. This apparently was a failure of the telemetry monitor point, since shroud separation at the proper time was confirmed through spacecraft measurements.

The Agena performed well through loss of signal, as indicated by telemetry received at Building AE. The time of second-burn ignition was nominal, indicating the restart timer functioned normally. Orbit determination by the Deep Space Instrumentation Facility (DSIF) showed the uncorrected spacecraft trajectory passing the trailing edge of the Moon on August 5, 1967, 18:28:43.06 GMT ($\overline{B}\cdot\overline{T}$ 6,918 km and $\overline{B}\cdot\overline{R}$ 3,467 km). After placing the spacecraft on this extremely accurate trajectory, the Agena performed a successful retro maneuver which caused the vehicle to miss the Moon by 25,317

kilometers at its closest approach. The Agena vehicle is in a long-lifetime Earth orbit with apogee/perigee altitudes of 369,831/9,380 kilometers, respectively, and a period of approximately 10 days.

Spacecraft Performance — Spacecraft performance during the period from liftoff to acquisition by the Deep Space Network was satisfactory. There was no performance data obtained to provide the time of antenna deployment or solar panel deployment. When two-way lock with the spacecraft was acquired by DSS-41 at 23:23:17 GMT, these events had taken place.

2.5 DATA ACQUISITION

Earth track of the Lunar Orbiter V mission is shown in Figure 2-3. Significant events and planned coverage of the AFETR facilities are shown on this trajectory plot.

The AFETR preliminary test report showed the data coverage presented in the following tables. A list of electronic tracking coverage from all stations is contained in Table 2-3, together with the type of tracking operation employed for each period. Telemetry data recording is summarized in Table 2-4 by recording station and downlink frequency.

Lunar Orbiter telemetry data were recorded via Channel F of the Agena link and also via the spacecraft telemetry system. Prior to spacecraft separation, the spacecraft transmissions (2,298.3 MHz) were made with the antenna in the stowed position.

Weather conditions during the launch operation were favorable. Upper wind shears were within acceptable limits. At liftoff the following surface conditions were recorded:

- Temperature   75°F
- Relative humidity   94%
- Visibility   10 miles with light rain
- Dew point   73°F
- Surface winds   4 knots at 180°
- Clouds   overcast with 10/10 cloud cover
- Pressure (sea level) 30.010 inches of mercury
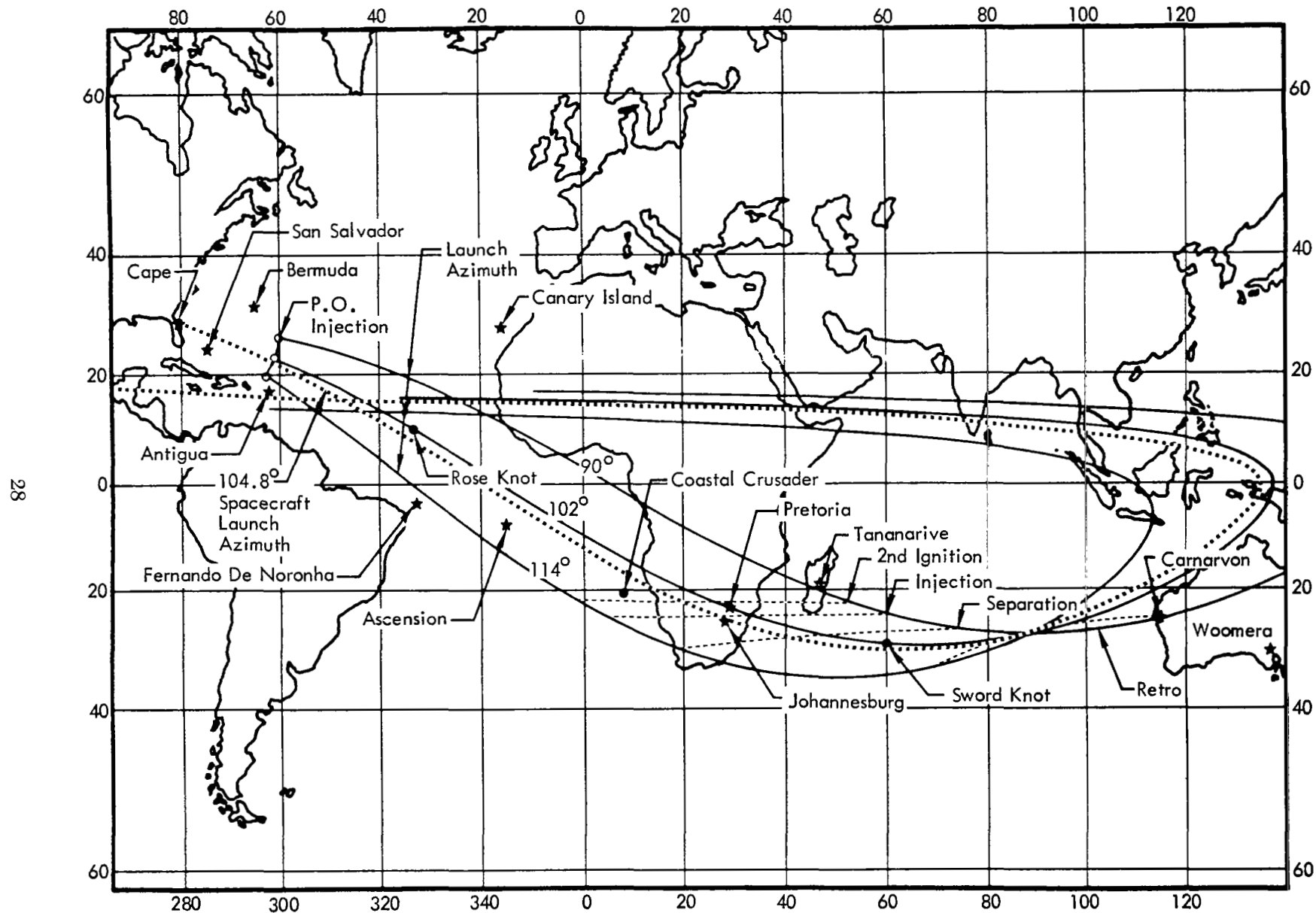
Figure 2-3: Ground Track for August 1, 1967

Table 2-3: Electronic Tracking Coverage

Location	Radar No.	Period of Coverage (sec) From	To	Mode (a) of Operation	Location	Radar No.	Period of Coverage (sec) From	.To	Mode (a) of Operation
Radar:							82	197	AB
Patrick	0.18	13	228	AB			197	359	AS
		228	287	AS			363	450	AB
		287	297	AB	Station 3	3.18	85	484	AB
		297	340	AS	Station 91	91.18	376	780	AB
		361	468	AB	Station 12	12.16	1,187	1,570	AB
Station 1	1.1	0	2	TV		12.18	1,187	1,611	AB
		2	48	IR	Station 13	13.16	1,875	2,080	AB
		48	127	AS			2,086	2,413	AB
	1.2	0	4	TV					
		4	49	IR	Special Instrumentation:				
		49	127	AS	Station 1 Tel ELSSE:				
	1.16	9	72	AS	12-110		6	450	F
		72	478	AB	14-110		6	445	P
Station 19	19.18	12	82	AS					

(a) Modes of Operation: AB — Automatic Beacon Track   F — Flight Line   TV — Television
AS — Automatic Skin Track   IR — Infrared Track   P — Program

Table 2-4: Telemetry Coverage

Location	Link (MHz)	Period of Coverage (sec) From	To	Location	Link (MHz)	Period of Coverage (sec) From	To
					2,298.33	320	774
Station 1 Tel II	249.9	−420	410	RIS Victor	244.3	763	1,225
Station 1 Tel IV	244.3	−420	410	Station 12 (Ascension)	244.3	1,109	1,660
	249.9	−420	410		2,298.33	1,168	1,570
	2,298.33	−420	410	RIS Whiskey (Crusader)	244.3	1,561	2,081
Station 3 (Grand Bahama)	244.3	75	524		2,298.33	1,549	1,572
	249.9	75	524	RIS Yankee	244.3	2,101	6,830
	2,298.33	101	466		2,298.33	2,252	7,454
Station 4	249.9	85	525	Station 13 (Pretoria)	244.3	1,840	2,480
Station 91 (Antigua)	244.3	307	833		2,298.33	1,860	2,280
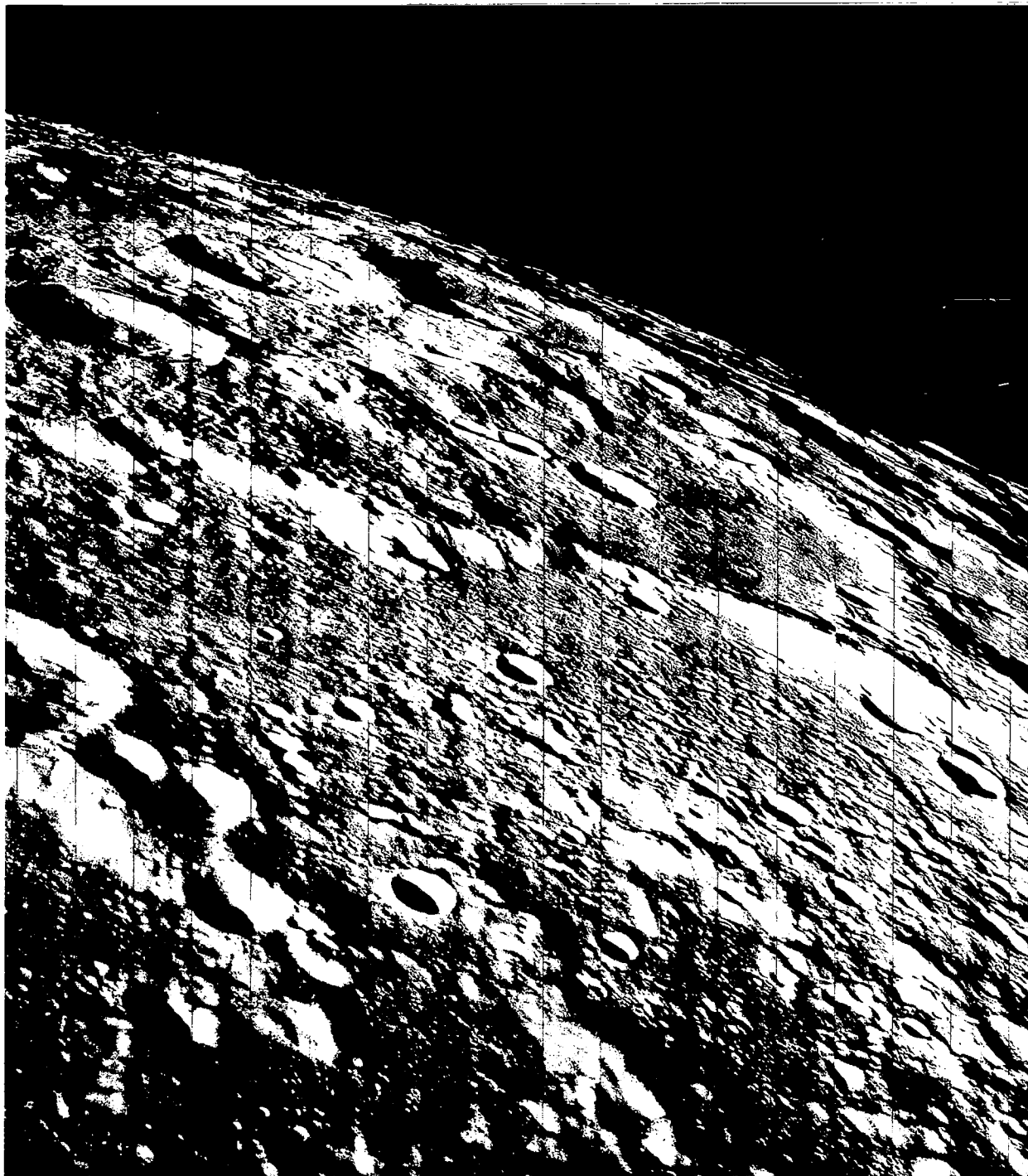
Wide-Angle Frame 54, Site V-10
Centered on the Altai Scarp.

3.0 Mission Operations

Operation and control of Lunar Orbiter V required the integrated services of a large number of specialists stationed at the Space Flight Operations Facility (SFOF) in Pasadena, California, as well as at the worldwide Deep Space Stations. The Langley Research Center exercised management control of the mission through the mission director. Two primary deputies were employed: the first, the launch operations director located at Cape Kennedy; the second, the space flight operations director located at the SFOF in Pasadena.

Launch vehicle and spacecraft performance after liftoff was monitored in the launch mission control center at ETR by the mission director. Telemetry data were used by the launch team and relayed in real time to the SFOF through the Cape Kennedy Deep Space Station. This dissemination of spacecraft performance data to the launch and operations teams enabled efficient and orderly transfer of control from Cape Kennedy to the SFOF.

Mission flight control was centralized at the SFOF for the remainder of the mission. All commands to the spacecraft were coordinated by the spacecraft performance analysis and command (SPAC) and flight path analysis and command (FPAC) team of subsystem specialists and submitted to the space flight operations director for approval prior to being transmitted to the DSIF site for retransmission to the spacecraft.

Operational performance of the spacecraft and the worldwide command, control, and data recovery systems is presented in the following sections.

3.1 MISSION PROFILE

The Lunar Orbiter V space vehicle was successfully launched at 22:33:00.3 GMT on August 1, 1967 from Launch Complex 13 at AFETR. Liftoff occurred 30 minutes after the scheduled time with nearly 1.5 hours remaining in the August 1 launch window. The liftoff trajectory was based on Launch Plan 1K with a flight azimuth of 105.6 degrees.

Figure 3-1 provides a pictorial summary of the 28-day photographic mission of Lunar Orbiter V. The timing of events from countdown initiation through acquisition of the spacecraft by the Woomera Deep Space Station is given with respect to the liftoff time. The remaining mission functions are referenced to Greenwich Mean Time. The small inset diagrams show the location of the photo sites on the nearside as well as the area to be photographed of the farside. With the exception of redefining several photo site locations, the mission was flown as planned and all photos taken were processed and read out. Also shown in Figure 3-1 are the major events during the powered portion of the flight necessary to inject the spacecraft on the cislunar trajectory. The major spacecraft functions required to make it fully operational and oriented to the celestial references to achieve and maintain the desired lunar orbit are shown.

The spacecraft was acquired by the Woomera, Australia Deep Space Station 46 minutes after launch. Initial performance telemetry data verified that the spacecraft antenna and solar panel sequences had been accomplished. The Sun acquisition sequence was completed 4 minutes later. After a gyro drift test was conducted, a star map was completed and Canopus located and verified at 19:00 GMT on August 2. At 31 hours, 27 minutes after launch, a velocity change of 29.76 meters per second (midcourse guidance correction maneuver) was commanded and initiated.

Injection into the initial lunar ellipse occurred 90 hours, 15 minutes after launch by a velocity reduction of 643 meters per second. The initial orbit parameters were apolune, 6,028 kilometers; perilune, 195 kilometers; and orbit inclination, 85 degrees. Photography was initiated in the second orbit to obtain the specified coverage of the farside areas. At apolune of Orbit 4 (08:28 GMT August 7), a velocity change of 15.97 meters per second reduced the perilune to the desired initial value of 100 kilometers. The remaining orbit parameters were essentially unchanged. Photography of farside areas
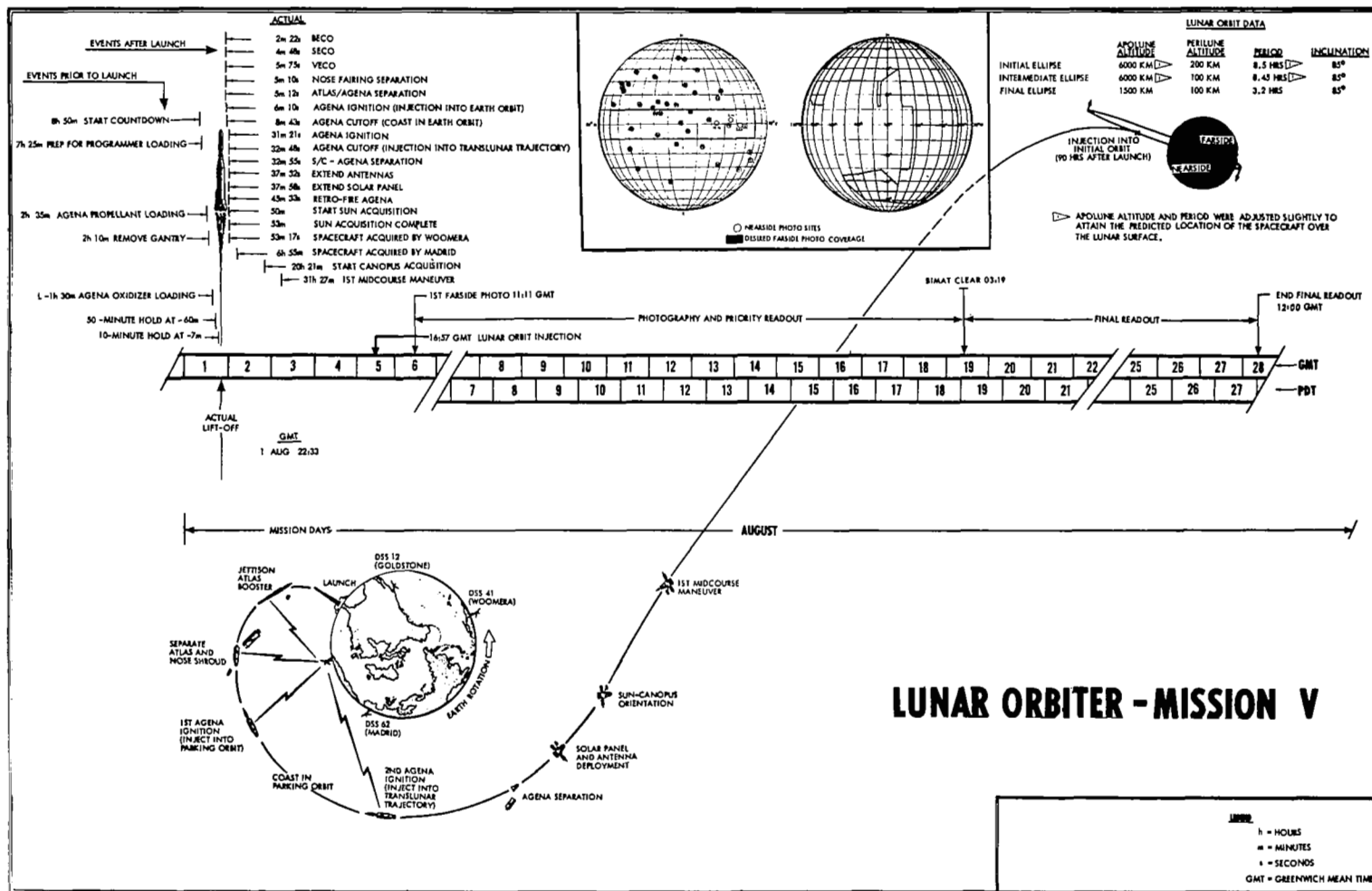
Figure 3-1: Lunar Orbiter V Flight Profile

was continued in the intermediate-ellipse orbit, including the photo of the near-full Earth.

A second orbit transfer maneuver was performed at perilune of Orbit 10 (05:08 GMT on August 9) to place the spacecraft in the final ellipse. This maneuver reduced the apolune from 6,083 to 1,499 kilometers as desired. As in the previous orbit transfer, the remaining orbit parameters (except orbit period) remained essentially unchanged. Photography of farside photo sites continued during each orbit. Nearside photography was initiated during Orbit 15.

During the 74 orbits in the final ellipse, 41 nearside and 13 farside photo sites were photographed during 63 separate sequences.

Unlike previous missions, many of the primary sites on the nearside were photographed as single-frame exposures. Photography of these sites was accomplished by using near-vertical, conventional oblique, westerly oblique, and convergent telephoto stereo methods. A total of 213 dual-frame exposures was taken between 11:22 GMT August 6 and 21:40 GMT August 18. Between photo sequences the priority readout mode was employed to recover a greater percentage of the photos than on Missions I, II, and III. Approximately 5 minutes prior to execution of the "Bimat cut" command, a "Bimat clear" indication was received in the telemetry performance data, indicating that all of the Bimat had been moved through the processor. As a result, the last two wide-angle exposures of an eight-frame sequence were affected. The last exposure was not processed and the next to the last was degraded. All other photos were completely processed.

Final readout was initiated at 04:30 GMT on August 19, starting with Wide-Angle Exposure 216. Readout progressed in a nearly continuous manner without any problems. Combining the priority and final readout phases resulted in reading out (at least once) all of the photo data obtained by 01:10 GMT August 26. Final readout continued until 05:38 GMT, August 27 when readout of the first exposure was completed.

One micrometeoroid hit was recorded during

the mission on August 9 and there was no detectable effect or damage to spacecraft systems. The radiation dosage encountered by Lunar Orbiter V was low, as shown by the final readings of 1.5 rads at the cassette detector and 1.0 rad at the camera looper. Spacecraft thermal control required the spacecraft to be flown off the sunline for long periods to offset the degrading effects of the continual solar illumination on the protective paint applied to the outer face of the equipment mounting deck. These factors upset the thermal balance of the entire spacecraft by significantly increasing the amount of heat energy reaching the spacecraft.

3.2 SPACECRAFT PERFORMANCE
The performance of Lunar Orbiter V has been evaluated with respect to the program and the specific mission objectives. Accordingly, the performance of each subsystem is discussed in the following paragraphs and contains a brief functional description.

To place the photo subsystem in the proper location and attitude at the right time to obtain the desired photographs, the Lunar Orbiter was required to:

- Perform a midcourse, injection, and two orbit transfer maneuvers so that the spacecraft would pass over a specified point during Orbit 26.
- Be injected into a selected orbit about the Moon whose size, shape, and center of gravity and mass are not precisely known.
- Perform critical attitude maneuvers and precise velocity reductions to achieve the specified initial, intermediate, and final elliptical orbits.
- Accomplish a precise attitude maneuver prior to photographing each specified site and actuate the cameras at precisely the commanded time (approximately 200-meter position error at perilune for each 0.1-second error).
- Provide adequate electrical power for photo subsystem operation during periods when the solar panels were not illuminated by the Sun.
- Continue to operate in an unknown radiation environment and in an unknown density of micrometeoroids over an extended time.

- Provide the tracking and doppler signals required to determine orbit parameters and compute the photographic mission maneuvers.

Failure to satisfy any of these conditions could jeopardize successful accomplishment of the Lunar Orbiter V mission. How well these critical tasks were accomplished is shown in Table 3-1, which is indicative of the control accuracy accomplished by the attitude and velocity control subsystems.

During the 90-hour cislunar trajectory and the 145 lunar orbits, the spacecraft satisfactorily accomplished the many sequences of events and multi-axis maneuvers required to establish the three lunar orbits, photograph the specified areas on the near and far sides of the Moon, and transmit the photo video, tracking, and performance data to the Deep Space Stations. Each of the specified Apollo landing, and the scientifically interesting, sites (including those of potential interest to Apollo Applications program and Surveyor program) and farside photo sites were photographed as planned. In addition, one film-set frame was redefined to obtain a photograph of the almost completely illuminated Earth. All of these photographs, except the last wide-angle exposure, were reconstructed during the mission.

3.2.1 Photo Subsystem Performance

Photo subsystem performance was satisfactory during the photographic mission. A short roll of Bimat resulted in the failure to completely process the last two wide-angle exposures. The film leader parted during the final stages of winding the film on the supply spool after completion of final readout, thereby preventing any additional photo readouts during the extended mission. Although there were intermittent dropouts of the video data, they appeared as a thin white line in the reconstructed framelet and obscured very little significant data.

The Lunar Orbiter photo subsystem simultaneously exposes two pictures at a time, processes the film, and converts the information contained on the film to an electrical signal for transmission to Earth. The complete system,

Function	Desired Trajectory	Actual Trajectory	Velocity Change (meters per second) Desired	Actual
Cislunar Midcourse	Aim Point 5,712 km	Aim Point 5,707 km	29.76	29.75
Lunar Orbit Injection	Perilune 202 km	195 km	643.04	643.04
	Apolune 6,050 km	6,028 km		
	Inclination 85.05 deg	85.01 deg		
Intermediate Orbit Transfer	Perilune 101 km	100 km	15.97	15.97
	Apolune 6,066 km	6,066 km		
	Inclination 84.62 deg	84.61 deg		
Final Orbit Transfer	Perilune 99 km	99 km	233.67	233.66
	Apolune 1,502 km	1,499 km		
	Inclination 84.76 deg	84.76 deg		

Table 3-1: Trajectory Change Summary

shown schematically in Figure 3-2, is contained in a pressurized temperature-controlled container.

The camera system features a dual-lens (telephoto and wide-angle) optical system that simultaneously produces two images on the 70-mm SO-243 film. Both lenses operate at a fixed aperture of f/5.6 with controllable shutter speeds of 0.04, 0.02, and 0.01 second. A 0.19 neutral-density filter is added to the 80-mm (wide angle) lens to nearly equalize light transmission characteristics of the two lens systems.

A double-curtained focal-plane shutter is used with the telephoto lens and a between-the-lens shutter is used with the wide-angle lens. Volume

limitations within the photo system container necessitated the use of a mirror in the optical path of the 610-mm lens. This mirror caused reversal of all telephoto images on the spacecraft film (along the long axis of the 610-mm lens format) with respect to the wide-angle system.

An auxiliary optical system, which operates through the telephoto lens, samples the lunar terrain image and determines a velocity-to-height (V/H) ratio. This output controls the linear movement of each camera platen to compensate for image motion at the film plane (IMC). The V/H ratio also controls the spacing of shutter operations to provide the commanded overlap. Camera exposure time for each frame is exposed on the film in binary code by 20 timing lights.

The latent-image (exposed) film is developed, fixed, and dried by the processor-dryer. Processing is accomplished by temporarily laminating the emulsion side of the Bimat film against the SO-243 film emulsion as the film travels around the processor drum.

Photographic data are converted by the readout system into an electrical form that can be transmitted to the ground receiving station. Scanning the film with a 6.5-micron-diameter high-intensity beam of light produces variations in transmitted light intensity proportional to the changes in film density. A photomultiplier tube converts these variations to an analog electrical voltage, and the readout system electronics adds timing and synchronization pulses, forming the composite video signal shown in Figure 3-3. Thus, it is possible to transmit continuous variations in film tone or density rather than the discrete steps associated with a digital system. The electrical signals are fed to a video amplifier and passed to the modulation selector; transmission is via a transponder, traveling-wave-tube amplifier (TWTA), and high-gain antenna.

Evaluation of the mission photographs showed that the performance of the camera and processor were normal during the photo mission. Processing defects, characteristic of the intermittent processing mode employed, were evident in many of the photographs. A total of 213 dual-
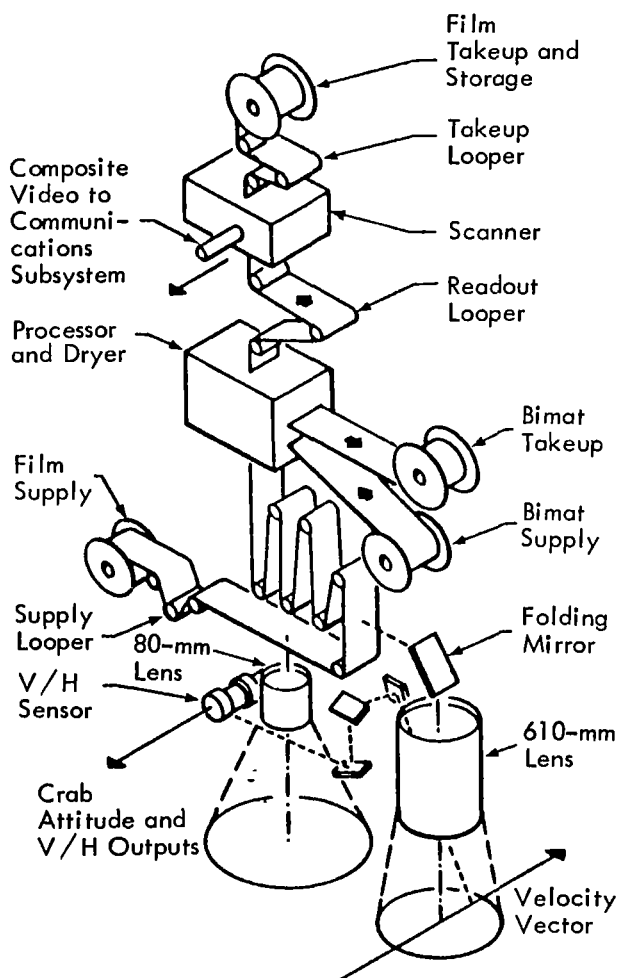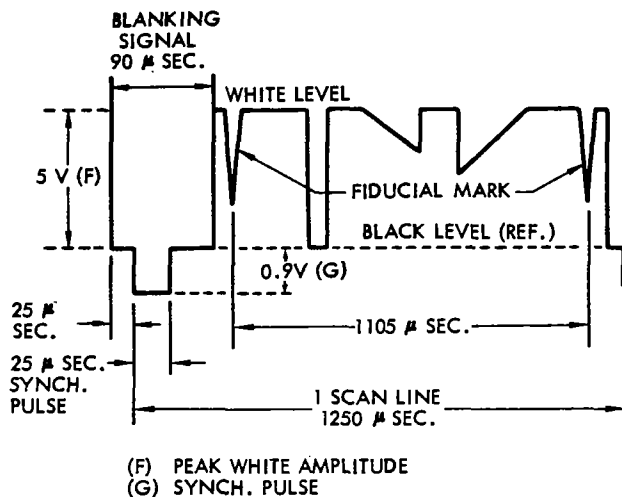

Figure 3-2: Photo Subsystem

BLANKING
SIGNAL
90 μ SEC.

WHITE LEVEL

5 V (F)

FIDUCIAL MARK

BLACK LEVEL (REF.)

0.9V (G)

25 μ
SEC.

1105 μ SEC.

25 μ SEC.
SYNCH.
PULSE

1 SCAN LINE
1250 μ SEC.

(F) PEAK WHITE AMPLITUDE
(G) SYNCH. PULSE

Figure 3-3: Video Signal Waveform

frame exposures were taken in a single frame, four- or eight-frame fast sequences, or four-frame slow-mode sequences during 82 orbits. With the exception of the last wide-angle exposure, all of these photographs were processed and read out during the mission.

Photography was initiated during the second lunar orbit approximately 18.5 hours after lunar injection. Priority readout was started during Orbit 5 after the first orbit transfer had occurred. A total of 86 priority readouts was completed during the photo taking portion of the mission, which varied in duration from 5 minutes to 2.97 hours. Approximately 43 minutes are required to read out a successive wide-angle and telephoto frame. There were 61 final readout sequences required to cover all of the Mission V photographs. The longest readout sequence contained four successive frames.

At irregular intervals during the priority and final readouts, the video data was not present on from three to six successive scan lines, although the synchronizing pulses were present. Immediately following each video dropout, an additional three to four successive scan lines showed a gradual return to the normal levels. Each dropout appeared as a thin white line (0.003 to 0.006 inch wide) on the GRE film and, therefore, obscured very little of the photo data.

Subsequent investigation revealed that the most probable cause of the loss of video data was the intermittent loss of voltage (1 kv) to the line-scan tube in the optical-mechanical scanner system which blanked the electron beam and reduced the video output to zero. The slow buildup to normal was found to be characteristic of the removal of a short from the power supply output terminals for the screen grid. The short may have been produced by a momentary breakdown in a capacitor, a self-healing breakdown in the potting surrounding the terminals of the power supply, or a similar breakdown in the lead to the screen grid of the line-scan tube. Limitations of telemetry sampling preclude establishing the exact cause of the irregularity. Even though several video dropouts effecting six to ten scan lines each occurred intermittently in some framelets, the amount of data lost was not significant when compared to the 17,000 scan lines required to produce each framelet. Late in the final readout the number of dropouts in some framelets increased. These same framelets were also read out in the priority readout mode with few or no dropouts. Therefore, no data were actually lost.

An operational decision was made to delay the Bimat-cut sequence until photo data from Sites V-48 and V-49 were read out in the priority mode. Therefore, the "Bimat cut" command was rescheduled for execution during Orbit 85. Approximately 5 minutes before the command was programmed to occur, a "Bimat clear" signal was evident in the telemetry data. This early exhaustion of the Bimat indicated that the supply roll was about 5 feet shorter than expected. Examination of the last photos processed showed the characteristic knurled pattern from the Bimat supply core in the shape of the end of the Bimat web. The short Bimat roll resulted in the failure to process the last wide-angle exposure and the next to last wide-angle exposure was degraded by the knurled core impressions into the Bimat web. These two exposures were part of an eight-frame fast-mode sequence, and represented a loss of about 7% of the wide-angle site coverage and the degradation of an additional 7%. There was no effect on the telephoto coverage of the site. All other photos were properly processed.

Performance of the photo video chain was better than any previous mission as indicated by the few adjustments of the video output gain required. There were no changes in the gain setting after Readout Sequence 006. The white level remained constant at 5 volts (with the exception of the Bimat dryout areas produced by the planned interruption of processing). Even in these areas, the drop was less than experienced on previous missions.

After final readout was completed, it was required to wind the film on the supply spool so that only the film leader would be threaded in the camera. This was done to avoid film set and also enable further readout, if desired during the extended mission. Before this rewind had been completed, the performance telemetry data showed that the leader had broken in or near the readout gate or approximately 7 feet from the splice. All attempts to move the film through the photo subsystem to the takeup spool failed, thus confirming that the leader had torn. All photo subsystem operations were then terminated.

As an overall evaluation, the photo subsystem of Lunar Orbiter V produced the best quality photographs of the five flight systems and only one out of the 426 photographs taken was not recovered.

3.2.2 Power Subsystem Performance

Power subsystem performance was satisfactory in all respects during the entire mission. The booster regulator, installed for this mission, maintained the nominal voltage to the photo subsystem at 30.5 volts, even when the solar panels were oriented at greater than 90 degrees to the sunline. Battery power was required prior to solar panel deployment; during the mid-course, injection, and orbit transfer maneuvers; and during some photo maneuvers. At all other times the electrical power was supplied directly from the solar panels.

All electrical power required and used by the spacecraft is generated by the solar cells mounted on the four solar panels. Solar energy is converted into electrical energy to supply spacecraft loads, power subsystem losses, and charge

the hermetically sealed nickel-cadmium battery. The subsystem is shown schematically in Figure 3-4. The shunt regulator dissipates excess electrical energy through heat dissipation elements while limiting the output of the solar array to a maximum of 31 volts. Auxiliary regulators provide closely regulated 20-volt d.c. outputs for the temperature sensors and the telemetry converter. A booster regulator was incorporated into the Lunar Orbiter V power subsystem to ensure proper voltages to the photo subsystem during all photo maneuvers, including off-Sun operation (photography on all previous missions required on-Sun operation). Charge controller electronics protect the battery from over-voltage and over-temperature conditions by regulating the charging current to a maximum rate of 1.35 amps. The 12-ampere-hour battery (packaged in two 10-cell modules) provides electrical power at all times when there is insufficient output from the solar array.

Each of the four solar panels has 2,714 individual solar cells mounted in a 12.25-square-foot area. The N-on-P silicon solar cells on each
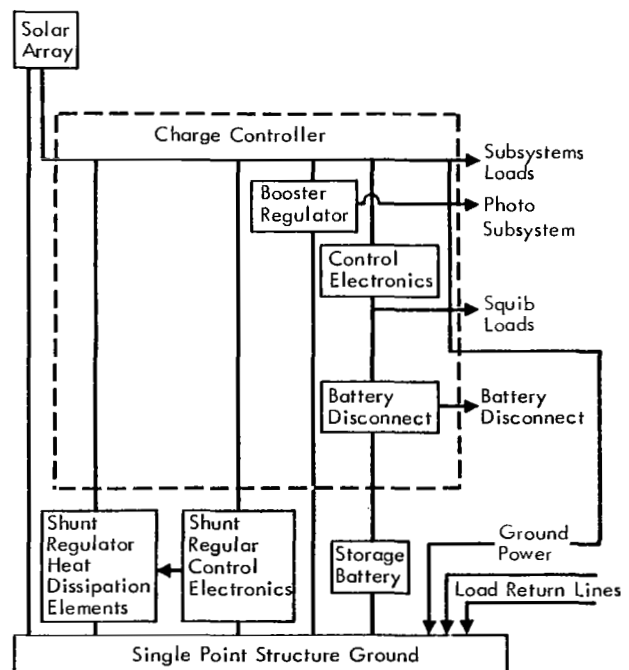

Figure 3-4: Power Subsystem Block Diagram

solar panel are connected into five diode-isolated circuits. Four of these individual circuits are connected in series-parallel combinations to provide the spacecraft power. The fifth circuit consists of ten cells in series and is used as a voltage reference in the charge controller.

All electrical power demands were supplied by the batteries from 6 minutes prior to launch until solar panel deployment approximately 38 minutes after launch. During this time, telemetry data were recorded at Cape Kennedy for 42 minutes. Based on the average discharge current of 4.37 amps, it was estimated that a maximum battery depth of discharge was 25%. The solar panels had been deployed and the battery was charging at the maximum rate of 1.35 amps when telemetry data were initially acquired at Woomera. The solar array output was 12.47 amps at 30.56 volts.

During initial-ellipse photography the spacecraft loads were supplied entirely by the battery and the camera bus voltage was held at 30.52 volts by the booster regulator. This performance confirmed satisfactory operation of the booster regulator on this spacecraft. The charge controller initiated the proper constant voltage charge control in the presence of a cool battery and an increasing battery voltage following the photo maneuvers. Representative spacecraft electrical loads for the various operating modes during the mission are shown in Table 3-2.

Based on the experience gained during the intermediate-ellipse photography, the battery current load was reduced by inhibiting the photo heaters before the photo maneuver to maintain a higher bus voltage. The heaters were again enabled after the solar array was reoriented to the Sun. Satisfactory readout and

Operational Mode	Photo Heaters			Spacecraft Loads (amps)			Power Source
	Inhibited	Solar Eclipse On	Solar Eclipse Off	Min	Nom	Max	
Cislunar	X			3.43	3.62	3.68	Array Supplying Power Battery Charging
Cislunar		X		3.68	4.25	4.49	
TWTA On	X			–	5.29	–	
Engine Burn		X		–	9.01	–	
Photo Standby + TWTA			X	6.68	6.86	7.10	
Processing + TWTA			X	5.96	7.75	8.05	
Readout	X			6.86	6.92	7.10	
Engine Burn		X		8.17	8.59	8.83	Battery Supplying Power
Photo Maneuver + TWTA	X			5.29	5.90	6.02	
Photo Sequence + TWTA	X			5.96	6.02	7.22	

Table 3-2: L.O. V Electrical Loads

film processing were supported at off-Sun angles up to 41 degrees.

As in Mission IV, the spacecraft was constantly illuminated by the Sun and required a partial off-Sun line orientation for temperature control. The spatial geometry was such that the solar intensity increased approximately 1% during the mission and tended to conceal some of the array degradation. Correcting the output data for this solar intensity increase showed a degradation of about 2%, which is compatible with the previous missions.

The booster regulator provided a constant potential of 30.52 ± 0.16 volts to the camera bus throughout the photo mission. Input voltages varied from 24.32 to 30.56 volts.

3.2.3 Communications Subsystem Performance

The communications subsystem was employed in the same manner as during Mission IV and performed satisfactorily in all phases. The ground transmission frequency was offset by increasing the VCO by an average of 330 Hz so that spacecraft response would produce the minimum interference with communications from Lunar Orbiters II and III. All photo video, performance telemetry, and tracking information presented to the communications subsystem was transmitted to the Deep Space Stations with adequate signal strength. The TWTA was turned off only when the possibility of damage to the tube could occur, such as during engine operation and certain off-Sun operations when low bus voltages were predicted.

The Lunar Orbiter communications system is an S-band system capable of providing telemetry and video data, doppler and ranging information, and receiving and decoding command messages and interrogations. Major components of the communications subsystem, shown in Figure 3-5, are the transponder, command decoder, multiplexer encoder, modulation selector, telemetry sensors, traveling-wave-tube amplifier, and two antennas.
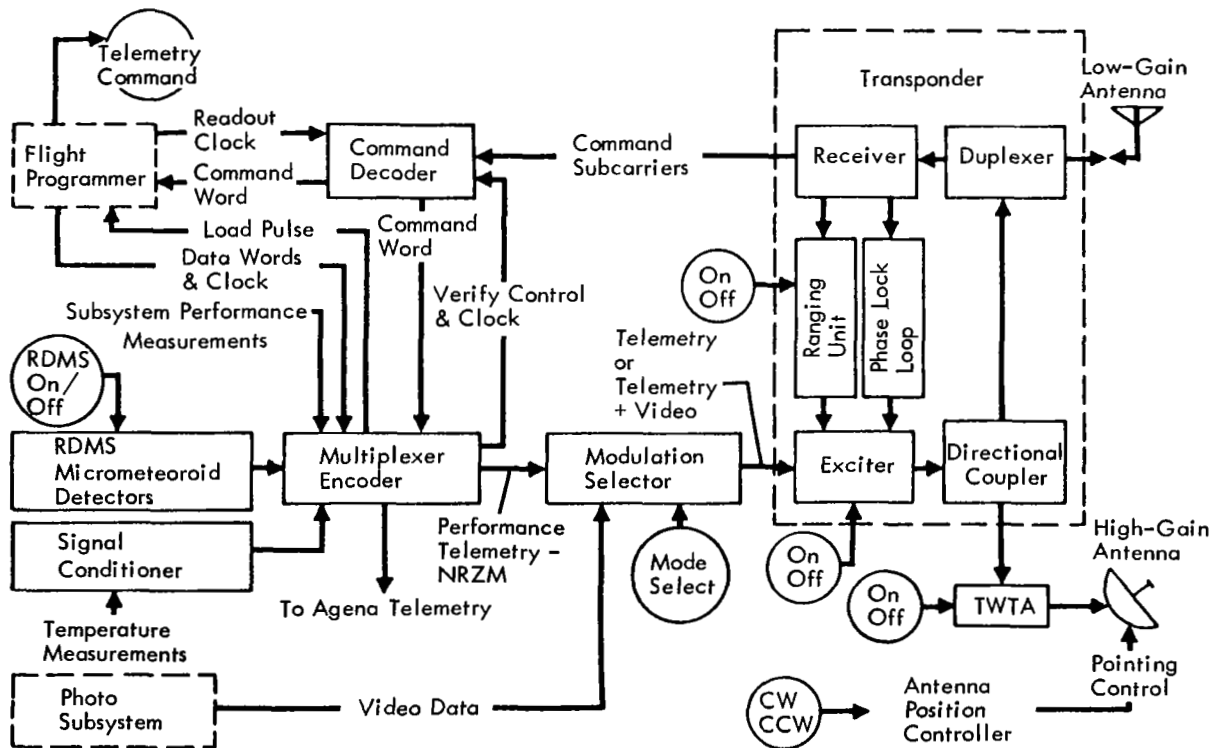

Figure 3-5: Communications Subsystem Block Diagram

The transponder consists of an automatic phase tracking receiver with a nominal receiving frequency of 2,116.38 MHz, narrow-and wide-band phase detectors, a phase modulator, and a 0.5-watt transmitter with a nominal frequency of 2,298.33 MHz. In the two-way phase-lock mode the transmitted frequency is coherently locked to the received frequency in the ratio of 240 to 221.

The command decoder is the command data interface between the transponder receiver and the flight programmer. To verify that the digital commands have been properly decoded, the decoded command is temporarily stored in a shift register, and retransmitted to the DSIF by the telemetry system. After validating proper command decoding, appropriate signals are transmitted to the spacecraft to shift the stored command into the flight programmer for execution at the proper time. The command decoder also contains the unique binary address of the spacecraft.

The PCM multiplexer encoder is the central device that puts performance telemetry data into the desired format for transmission. Seventy-seven analog inputs are sequentially sampled at one sample per frame, and one analog channel is sampled at eight times per frame. The output of these 85 data samples is converted from analog to digital form. The multiplexer also combines the 20-bit flight programmer words, the 133 one-bit discretes, and the four-bit spacecraft identification code into nine-bit serial output words.

The modulation selector mixes the photo video information and the 50-bit-per-second performance telemetry information for input to the transponder for transmission. The selector receives control signals from the flight programmer to operate in one of the modes listed below.

The telemetry system samples the output of sensors within the various spacecraft subsystems. Normal telemetry data channels include such information as temperatures, pressures, voltages, currents, and error signals. Special instrumentation includes 20 micrometeoroid detectors located on the tank deck periphery. Radiation dosage measurement, in the form of two scintillation counter dosimeters and the associated logic, are mounted in the photo subsystem area.

The traveling-wave-tube amplifier (TWTA) consists of a traveling-wave tube, a bandpass filter, and the required power supplies. This equipment, used only to transmit the wide-band video data and telemetry during photo readout (Mode 2), has a minimum power output of 10 watts. All of the necessary controls and sequencing for warmup of the traveling-wave tube are self-contained.

The spacecraft employs two antennas, a high-gain antenna that provides a strongly directional pattern and a low-gain antenna that is omni-directional. The low-gain antenna is a biconical-discone slot-fed antenna mounted at the end of an 82-inch boom. The high-gain antenna is a

Mode	Data Type	Antenna Employed
1	Ranging and performance telemetry	Low Gain
2	Photo video and performance telemetry	High Gain
3	Performance telemetry	Low Gain

(A Mode 4 exists which is implemented by selecting the normal Mode 2 modulation but exercising the Mode 3 transmission method when no video input data are available. The selection of this particular mode increases the available power in the down-link carrier.)

36-inch parabolic reflector that provides at least 20.5 db of gain within ± 5 degrees of the antenna axis. The radiated output is right-hand circularly polarized. The antenna dish is mounted on a boom and is rotatable in 1-degree increments about the boom axis to permit adjustments for variations in the relative positions of the Sun, Moon, and Earth.

Spacecraft transmissions via the Agena transmission link were received until 35.52 minutes after launch. The first S-band transmissions from the spacecraft were received at Johannesburg (DSS-51) 1.21 minutes after cislunar injection and prior to the antenna deployment. Woomera (DSS-41) acquired the spacecraft 46 minutes after launch at a signal strength of −131 dbm on the S-band acquisition aid antenna. Two-way lock was established 5 minutes later. Communication Mode 4 was initiated by stored program command at 45 minutes after launch and turned off by a real-time command 44 minutes later.

The overall performance of the communications subsystem in the low-power, high-power command, and ranging modes was satisfactory. The traveling-wave-tube amplifier (TWTA) was turned on and off six times during the photo mission for a total operating time of 469.6 hours. Signal levels recorded during video transmission varied from −90.6 to −98.9 dbm, which corresponds to a video margin of 6.9 db above and 1.4 db below the nominal link design.

During the cislunar flight, two high-gain-antenna maps were obtained during the 360-degree roll star mapping maneuver. These antenna maps agreed within 2 degrees with the roll position determined from the attitude control subsystem data.

As in Mission IV, the transponder receiving frequency was shifted by increasing the VCO setting an average value of 330 Hz to avoid interference with Lunar Orbiters II and III. During the cislunar phase, the transponder frequency was adjusted to the best lock frequency, and the static phase error was effectively 0 degree. Station handovers were accomplished in a routine manner using the offset frequency

in all but one case. In this instance the uplink was dropped during handover. The ground transmitter frequency was reset to the predicted best lock frequency and acquisition was readily completed. Following acquisition the frequency was readjusted to the operating offset frequency.

There were no problems encountered in the operation of the component operation and no data was lost by the communications subsystem.

3.2.4 Attitude Control Subsystem Performance
Performance of the attitude control subsystem was within operating specifications for the many tasks required and accomplishing the 472 attitude maneuvers. Because of the continued solar illumination, the spacecraft was pitched from 30 to 54 degrees away from the sunline about two thirds of the mission to maintain temperature control. Control procedures developed during previous missions were used to an advantage in controlling the spacecraft activities during this extremely complex photo mission.

Execution of all spacecraft events and maneuvers is controlled by or through the attitude control subsystem, Figure 3-6, to precisely position the spacecraft for picture taking, velocity changes, or orbit transfers.

The basic operating modes are:
Celestial Hold -- The basic references in this mode are the Sun and Canopus; the gyro systems operate as rate sensors. This mode was planned for use during normal cruise operations and as the initial conditions for all commanded attitude changes. (In practice, Canopus was used as a reference only and the roll axis was maintained in inertial hold.)

Inertial Hold -- The basic references in this mode are the three gyros operating as attitude-angle sensors. This mode was used during all attitude and velocity change maneuvers.

Maneuver Mode -- In this mode the spacecraft acquires the commanded angular rate about a single axis. The remaining two gyros are held in the inertial hold mode.

41

Closed-Loop Electronics

Velocity Mode Select

Deadband Change

Slew Plus

$+1/2°$/ sec
$-1/2°$/ sec

Slew Minus

Two-Step Gain
K = 1 or 10

Switching Amplifier

Thrust Vector Control Electronics

Thrust Vector Control Actuator (Pitch & Yaw)

One-Shot

Valve Driver

Plus Jet

One-Shot

Valve Driver

Minus Jet

Spacecraft Dynamics

$\dfrac{1}{4}\dfrac{(4S+1)}{(0.1S+1)}$

Position
4 v/o
Rate
4 v/o/sec

Inertial Reference Unit

Rate

Rate

Gyro Mode Select

Sun Sensor Select

Switch Yaw Control

Fine Sun Sensor *

Coarse Sun Sensor *

Photo Subsystem V/H Crab Angle **

Sun Occulted

Solar Detector

*Sun Sensor Replaced by Star Tracker in Roll
**Yaw Only

Figure 3-6: Altitude Control Subsystem Functional Block Diagram

Engine On, Inertial Hold -- This mode is similar to the previously defined inertial hold mode except that the pitch and yaw error signals during the velocity change are also used to control the engine actuators.

Limit Cycling -- The spacecraft is commanded to maintain a position within ± 0.2 degree for all photographic and velocity control maneuvers

or whenever commanded. (The normal deadband is ± 2 degrees.)

The on-board digital programmer directs the spacecraft activities by either stored program command or real-time command. The unit provides spacecraft time, performs computations and comparisons, and controls 120 spacecraft functions through real-time, stored, and

42

automatic program modes. The information stored in the 128-word memory is completely accessible at all times through appropriate programming instructions.

The inertial reference unit maintains the spacecraft attitude. Three gyros provide appropriate rate or angular deviation information to maintain proper attitude and position control. A linear accelerometer provides velocity change information in increments of 0.1 foot per second to the flight programmer during any firing of the velocity control engine.

Sun sensors are located in five positions about the spacecraft to provide spherical coverage and ensure Sun acquisition and lock-on and the resulting alignment of the solar panels. Error signals are generated whenever angular deviation from the spacecraft sunline exists. A celestial reference line for the spacecraft roll axis is established by identifying the celestial body that the star tracker acquires, locks on, and tracks. Under normal conditions the star, Canopus, is used for this purpose; however, any known celestial body of suitable brightness and within the tracker's field of view as the spacecraft is rotated about the roll axis can be used to satisfy this function.

The closed-loop electronics provides the switching and electronic controls for the reaction control thrusters and positioning of the velocity control engine actuators. Attitude maneuver and control are maintained by the controlled ejection of nitrogen gas through the cold-gas thrusters mounted on the periphery of the engine deck. During a velocity control maneuver, gimbaling of the velocity control engine is used to maintain stable orientation of the spacecraft.

Multi-axis spacecraft maneuvers were required to support the four velocity change maneuvers and to orient the spacecraft for the 75 photo sequences. Three-axis maneuvers were executed to support velocity changes and perilune photography while two-axis maneuvers were used for apolune photos. During the 27-day photo mission, 472 single-axis maneuvers were executed to support all operational functions. To compensate for the additional heat resulting from continual solar illumination of the near-

polar orbit, the spacecraft was pitched from 30 to 54 degrees away from the sunline to maintain thermal control. Table 3-3 identifies the maneuvers performed for each function. The operational requirement to conserve nitrogen gas for use in the extended mission and the low gyro drift rates were combined to reduce the maneuvers required. In several instances the reverse photo and thermal pitch-off maneuvers were combined into one maneuver. During the mission there were 91 Sun acquisitions, of which all but two were accomplished in the narrow deadband attitude control mode.

Table 3-3: Maneuver Summary

	Planned Total	Actual			
		Roll	Pitch	Yaw	Total
Velocity change	16	8	8	0	16
Photography	402	147	155	93	395
Attitude update	43	11	10	6	27
Thermal pitch-off	62	0	23	0	23
Star Map and Others	9	6	4	1	11
Total	532	172	200	100	472

Canopus tracker operation was significantly restricted by the continuous solar illumination and was operated only in the open-loop mode. Spacecraft roll position control was maintained by using the same procedures employed on previous missions. Once or twice in each orbit the Canopus tracker was turned on with the star in the field of view and the tracking error signal monitored via the telemeter system. The subsystem analyst used this data to maintain and update the spacecraft roll position history throughout the mission. During the cislunar trajectory the star mapping voltage showed that the stars Canopus and Acrux (α Crucis) and the planet Mars were detected. The tracker was cycled on and off 198 times, of which seven were required by glint effects, for a total operating time of 34 hours, 10 minutes.

The inertial reference unit, containing the Sperry SYG-1000 gyros, exhibited low and stable drift rates which contributed to the efficient utilization of nitrogen gas and the ease of maintaining attitude control during periods of three-axis inertial hold. Drift rate tests were performed during the cislunar trajectory. Results of the three-axis tests are shown in Table 3-4.

Table 3-4: Gyro Drift Rates

Axis	Drift Rate (degrees per hour)	
	8/2/67	8/3/67
Roll	0.045	0.038
Pitch	0.078	0.094
Yaw	0.093	0.090

Maneuver accuracy tests were made during a positive and negative roll maneuver of 360 degrees. The maneuver error, consisting of both gyro and flight programmer errors, was −0.065% and −0.029% for the positive and negative roll test, respectively, and are both well within the mission tolerance of $\pm$ 0.32%.

Closed-loop electronics operation was satisfactory in selecting the proper switching to support the flight programmer output commands to the inertial reference unit, sun sensors, Canopus star tracker, sensor outputs, and vehicle dynamics. Data indicated that the one-shot multivibrators, controlling operation of the cold-gas thrusters, were operating between 11 and 14 milliseconds duration (nominal value is 11 milliseconds).

Over 17,000 individual thruster operations were performed during the photographic mission. The estimated breakdown is shown in Table 3-5.

Table 3-5: Thruster Operation Summary

Mode	Roll	Pitch	Yaw	Total
Limit Cycle	4,100	5,740	6,150	15,990
Maneuvers	344	491	291	1,126
Total	4,444	6,231	6,441	17,116

Residual spacecraft rates after each engine operation were lower than the predicted maximums for stable limit cycle operation. The lateral movement of the CG, as the propellants were consumed, was low as evidenced by the movement of the velocity control engine actuators. The maximum excursion was 0.21 degree in pitch (during injection) and 0.43 degree in yaw (during midcourse).

All commands received from the command decoder were properly acted upon by the flight programmer. These included 1,703 real-time commands and 2,822 stored program commands. The repetitive execution of stored program routines increased this total by approximately 14,000 individual commands. The total clock error during the mission was +0.66 second, which reflects a drift rate of 1.23 milliseconds per hour.

Sun sensor operation was also satisfactory. As in previous missions, the ability to switch to combinations of coarse and fine sensor significantly aided the spacecraft attitude control monitoring and efficient nitrogen gas usage during off-Sun operation.

3.2.5 Velocity Control Subsystem Performance
Satisfactory operation of the velocity control subsystem was evidenced during the midcourse, injection, and two orbit transfer maneuvers. Engine performance parameters were close to predictions and the orbit parameters achieved were also close to the mission requirements.

The velocity control subsystem provides the velocity change capability required for midcourse correction, lunar orbit injection, and orbit adjustment as required. The spacecraft includes a 100-pound-thrust, gimbaled, liquid-fuel rocket engine. The propulsion system uses a radiation-cooled bipropellant liquid rocket engine that employs nitrogen tetroxide (N_2O_4) as the oxidizer and Aerozine-50 (a 50-50 mixture by weight of hydrazine and unsymmetrical dimethylhydrazine, UDMH) as the fuel. The propellants are expelled from the tanks by pressurized nitrogen acting against teflon expulsion bladders. The propellants are hypergolic and no ignition system is required.

44

The engine is mounted on two-axis gimbals with electrical-mechanical actuators providing thrust directional control during engine operations. A central nitrogen storage tank provides (through separate regulators) the gas required to expel: (1) the propellants in the velocity control system, and (2) the gas for the attitude control thrusters. The nominal gas pressure for Mission V was serviced with 16.80 pounds of nitrogen at 4,100 psi to provide for the maneuvers required during the photo mission. Figure 3-7 identifies subsystem components and shows how they are connected. The specified propellant load provides a nominal velocity change capability of 1,017 meters per second at an oxidizer-to-fuel ratio of 2.0 and a propellant expulsion efficiency of 98%.

Flight performance data obtained during the four engine-burn periods were evaluated and the velocity control engine performance results are summarized in Table 3-6.

The four engine burn periods imported a total of 922.42 meters per second of the calculated
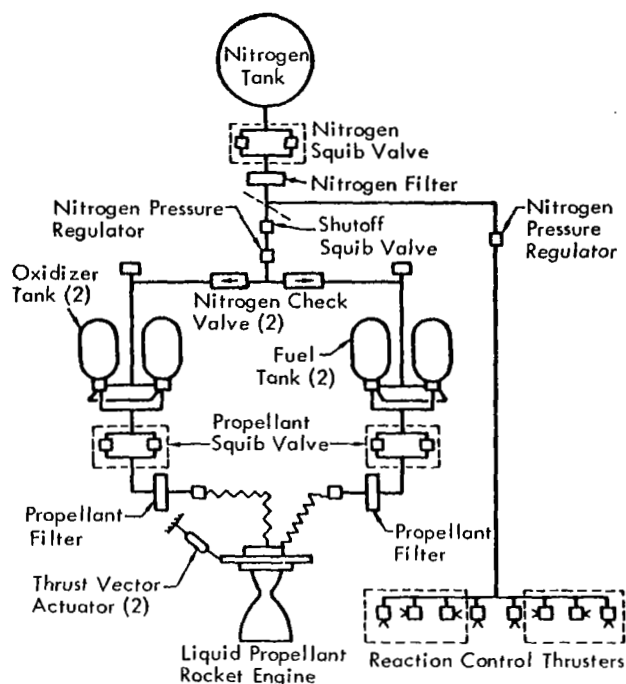
Figure 3-7: Velocity and Reaction Control Subsystem

Table 3-6: Velocity Control Engine Performance				
	Velocity Change (mps)	Burn Time (sec)	Thrust (lb)	Specific Impulse (sec)
Midcourse				
Predict	29.76	26.4 ± 0.08	99	276
Actual	29.75	26.1	99.9	276
Injection				
Predict	643.04	501.1 ± 8.5	99.5	276
Actual	643.04	498.1	100.1	276
Perilune Transfer				
Predict	15.97	10.95±0.6	100	276
Actual	15.97	10.78	101.6	276
Apolune Transfer				
Predict	233.67	151.1 ± 4	101	276
Actual	233.66	152.9	99.9	276

1,000.9±43 meters per second capability. The remaining capability was retained for use as required during the extended mission. During the 498-second burn period of the orbit injection maneuver, the engine valve temperature increased from 68 to 71°F. A maximum value of 109.8°F was reached approximately 53 minutes after the termination.

Activation of the propellant heaters was not required during the mission because the system temperatures were generally in the region of 50 to 75°F.

3.2.6 Structures, Mechanisms, and Integration Elements Performance

All elements of the structure, thermal control, wiring, and mechanisms operated properly during the mission. Lunar Orbiter V encountered more heat from the continual solar illumination and the additional radiated and reflected heat from the lunar surface and the low perilune. The combination of adding mirrors to the equipment mounting deck and pitching the spacecraft off the sunline satisfactorily controlled the spacecraft temperature with no interference with the operational functions.

The Lunar Orbiter spacecraft structure includes three decks and their supporting structure. The equipment mounting deck includes a structural ring around the perimeter of a stiffened plate. Mounted on this deck are the photo subsystem and the majority of the spacecraft electrical components.

The tank deck is a machined ring, v-shaped in cross section, closed out with a flat sheet. Fuel, oxidizer, and nitrogen tanks are mounted on this deck. The 20 micrometeoroid detectors are located on the periphery of the ring. The engine deck is a beam-stiffened plate that supports the velocity control engine, its control actuators, the reaction control thrusters, and the heat shield that protects the propellant tanks during engine operation.

Prior to deployment, the low- and high-gain antennas are positioned and locked along the edges of these three decks. The four solar panels are mounted directly under the equip-

ment mounting deck and in the stowed position are compactly folded into the space below it. Electrically fired squibs unlock the antennas and the solar panels at the appropriate time to permit them to be deployed into the flight attitude.

Spacecraft thermal control was passively maintained. An isolating thermal barrier, highly reflective on both the interior and exterior surfaces, encloses the spacecraft structure, except for the Sun-oriented equipment mounting deck and the insulated heat shield on the engine deck. The objective was to maintain average spacecraft temperature in the thermal barrier within the range of 35 to 85°F. Eighty per cent of Lunar Orbiter V's equipment mounting deck exterior surface was exposed to solar radiation, although the entire deck was painted with a zinc-oxide-pigment, silicone-based paint selected to achieve the desired heat balance. This paint has the properties of high emissivity in the infrared region (for dissipation of spacecraft heat) and low absorption at the wave lengths that contain most of the Sun's emitted heat. Twenty per cent of the equipment mounting deck was covered with a geometrical pattern of mirrors to reflect solar energy and thereby reduce the thermal heat dissipation problem. An additional 72 one-inch-square mirrors were added under the photo subsystem and adjacent to the TWTA where additional heat rejection was required. This was in addition to the 370 mirrors added in a geometric pattern on the equipment mounting deck for Mission IV.

A camera thermal door protects the photo subsystem lenses from heat loss and direct sunlight except during photographic periods. Immediately prior to each photographic sequence, the door was opened to permit photography.

Antenna deployment, solar panel deployment, and actuation of the nitrogen isolation squib valve sequences were initiated after spacecraft separation by stored-program commands. These sequences were verified as completed by the first telemetry frame of data received from the Woomera tracking station.

The mission design indicated that the thermal environment of Mission V was more severe than

previous missions and required additional heat rejection capability. Seventy-two additional mirrors were added under the photo subsystem and adjacent to the TWTA, increasing the density in these areas to 30% and offsetting the increased heat generated by these equipments. The spacecraft was oriented on or near the Sun between photo sites in a single orbit to minimize spacecraft maneuvers and usage of nitrogen gas. This resulted in having to dissipate additional heat energy during the remainder of the mission. Spacecraft temperatures were maintained within the operating limits by pitching the spacecraft off the sunline a predetermined value. The spacecraft was pitched from 30 to 54 degrees away from the Sun for approximately 66% of the mission. This method of temperature control was developed during the Lunar Orbiter I mission and used on each succeeding mission. The basic problem of solar paint degradation stems from a state of the art limitation in the development of an adequate thermal control paint and the inability to accurately reproduce or simulate the true space environment in the Earth-based test facilities.

Seven different paint coating coupons were installed on Missions IV and V to obtain data from which to evaluate the stability of each coating in a deep-space environment.

Special tests were completed during the cislunar trajectory to verify that the camera thermal door operated properly. During the mission, the door was cycled 74 times to support mission photography and three times for test purposes. There was no evidence of any operating irregularities.

3.3 OPERATIONAL PERFORMANCE

Operation and control of the Lunar Orbiter V spacecraft required the integrated services of a large number of specialists stationed at the Space Flight Operations Facility (SFOF) in Pasadena, California, and at the worldwide Deep Space Stations (DSS). Mission advisors and other specialists were assigned from the Lunar Orbiter Project Office, supporting government agencies, Jet Propulsion Laboratory, the Deep Space Stations, and The Boeing Company.

The Langley Research Center exercised management control of the mission through the mission director. Two primary deputies were utilized: the first, the launch operations director located at Cape Kennedy; the second, the space flight operations director located at the SFOF. Once the countdown started, the launch operations director directed the progress of the countdown on the launch pad, while the space flight operations director directed the countdown of the Deep Space Network. From the time that these countdowns were synchronized, all decisions (other than Eastern Test Range safety factors) regarding the countdown were made by the mission director, based on recommendations from the launch operations director and/or the space flight operations director.

After liftoff, launch vehicle and spacecraft performance was monitored in the launch mission control center at ETR by the mission director. Telemetry data were used by the launch team and were relayed in real time to the SFOF through the Cape Kennedy DSS. Dissemination of spacecraft performance and tracking data to the launch team and the operations team enabled efficient and orderly transfer of control from Cape Kennedy to the SFOF.

After the spacecraft was acquired by the Deep Space Network (DSN), flight control was assumed by the space flight operations director. Thereafter, the mission director moved from ETR to the SFOF and continued control of the mission. Control of spacecraft operations was delegated to the space flight operations director.

Control of the mission was centralized at the SFOF for the remainder of the mission. All commands to the spacecraft were coordinated by the spacecraft performance analysis and command (SPAC) and flight path analysis and command (FPAC) team of subsystem specialists and submitted to the space flight operations director for approval prior to being transmitted to the Deep Space Instrumentation Facility (DSIF) site for retransmission to the spacecraft. As a backup capability, each prime DSIF was supplied with a contingency capability (including predetermined commands and process tapes) to permit local assumption of the

basic mission control function in the event of communications failures. On-line interpretation of efforts of all major operational areas was accomplished by the assistant space flight operations director on a 24-hour basis.

Mission V was the most complex mission to date in that the mission profile required operation beyond the initial program requirements and, with few exceptions, each of the 213 photo exposures required individual two- or three-axis spacecraft maneuvers. In addition, the priority readout mode was to be used to recover a significant amount of photo data prior to Bimat cut. Additional temperature and attitude control requirements were generated by the lack of Sun occultation periods.

Mission V required the most demanding photographic assignment and the largest number of photo maneuvers of any mission. Premission planning and the retaining of experienced personnel from previous missions contributed to the orderly and timely completion of programming requirements.

3.3.1 Spacecraft Control

The flight operations team was divided into three groups (designated red, white, and blue) to provide 24-hour coverage of mission operations at the Space Flight Operations Facility. Overlap was scheduled to allow detailed coordination between the on-coming and off-going system analysts. The operations team was essentially unchanged for Mission V. Spacecraft control was maintained throughout the mission by generation, transmission, and verification of commands, and transmission of execute tones from the Earth-based facilities. A total of 4,525 (1703 real time and 2822 stored program) commands was generated and properly executed.

Command preparation was accomplished by three teams of two command programmers each. Scheduling was arranged so that the team attending the preliminary command conference for a core map (plan for locating each command in the spacecraft flight programmer memory) also attend the final command conference as

well as completing all of the command preparation before the handover to the following team.

In general, revised command sequences were available to the command programmers before the final command conference. In a few instances, commands were prepared — based on preliminary conference data — and transmitted, and then updated by Mode 1 commands. Changes to stored program commands were made in Mode 3 to compensate for the roll axis reference or last-minute changes for the camera-on times.

Examination of the priority readout photos early in the mission indicated that the planned camera-on-time bias for V/H sensor "on" and "off" did not obtain the desired coverage. A comparison of photos from priority readout showed a consistent downtrack error. To correct for the indicated displacement, additional bias values were added to the predictions for both types of photography to obtain the desired coverage beginning with Site V-25. Thereafter, the variations of actual and desired coverage were randomly distributed.

Spacecraft roll position control was maintained by the flight control analyst by using the Canopus tracker in the open-loop mode. This method had been used on previous missions because glint light would reach the detector when the spacecraft was illuminated and prevent closed-loop tracking of the star. The roll attitude was determined by orienting the spacecraft so that Canopus was in the tracker field of view. The error signals were then used to compute the actual attitude. Measured gyro drift rates were also used to predict the roll position at any desired time. Prior to photo maneuvers, an attitude update maneuver was made and the accurate attitude determined.

The lack of any spacecraft irregularity during the performance of the photo mission contributed a great deal to satisfactory completion of this complex mission and preparation of numerous computations and commands required for implementation. With only minor exceptions, effected in real time to ensure adherence to the planned flight profile, the mission was

conducted as outlined in the mission plans. An operational decision was made to read out data from Sites V-48 and -49 in the priority readout mode. Therefore, the "Bimat cut" command was rescheduled for Orbit 85 rather than as planned in Orbit 83.

3.3.2 Flight Path Control
The Lunar Orbiter trajectory was controlled during the boost phase and injection into cislunar orbit by a combination of the Atlas guidance and control system at AFETR and the on-board Agena computers. After acquisition by the Deep Space Station at Woomera, Australia, trajectory control was assumed and maintained by the Space Flight Operations Facility in Pasadena, California. During the first 6 hours of the mission following injection, the Deep Space Network performed orbit determination calculations to ensure DSS acquisition. Guidance and trajectory control calculations for controlling mission trajectories were performed by the Lunar Orbiter Operations group.

Lunar Orbiter flight path control is the responsibility of the flight path analysis and command (FPAC) team located at the Space Flight Operations Facility (SFOF) in Pasadena, California. Flight path control by the FPAC team entails execution of the following functions.
- Tracking data analysis — Assessment of tracking data (doppler and range) and preparation of DSS tracking predictions.
- Orbit determination — Editing of raw tracking data and determination of the trajectory that best fits the tracking data.
- Flight path control — Determination of corrective or planned maneuvers based on orbit determination results and nominal flight plan requirements.

FPAC activities during the mission were divided into the following phases.
- Injection through midcourse;
- Midcourse through deboost;
- Initial lunar orbit;
- Intermediate lunar orbit;
- Final lunar orbit.

Each phase is discussed in the following sections.

Injection through Midcourse — The spacecraft was acquired by DSS-51, Johannesburg, South Africa, approximately 1.2 minutes after separation from the Agena vehicle. The 108-degree launch azimuth provided only a 5-minute pass for DSS-51. During this period the spacecraft was tracked for 2.57 minutes and was lost because of excessive angular tracking rates. DSS-41, Wommera, Australia, acquired the spacecraft in one-way lock 46 minutes after launch and transferred to two-way lock 4 minutes later. Flight path control was transferred from the DSN to the Lunar Orbiter Project FPAC personnel 3.45 hours after launch.

Final design of the midcourse maneuver was based on 16 hours, 39 minutes of two-way doppler data from the three primary Deep Space Stations. The range unit residuals from this data were of the order of 60 meters or less and the three-way doppler residuals were constant at the predicted doppler levels.

The midcourse maneuver consisted of a 42.07-degree sunline roll, 29.09-degree pitch, and a velocity change of 29.75 meters per second (engine burn time 26.4 seconds). This maneuver was selected from 12 possible two-axis maneuvers based on:
- Maintaining sun lock as long as possible;
- Minimizing total angular rotation;
- DSS line-of-sight vector not passing through an antenna null.

Mission V maneuver and trajectory changes differed from previous missions in that the mission design included the requirement to photograph an early primary site (Site V-8a) with 5 degrees of crosstrack camera axis tilt during Orbit 26. This requirement, therefore, was included in the design of all trajectory change maneuvers to ensure the desired lunar surface orbit track.

The midcourse execution time of 06:00 GMT August 3, 1967 was selected to satisfy the above requirements as well as to obtain two-station viewing during and after the engine operation. Lunar encounter parameters applicable to the midcourse maneuver are shown in Table 3-7. The pre-midcourse (actual) represents the extra-

Table 3-7: Lunar Encounter Parameters

	Nominal (Predict)	Pre-Midcourse (Actual)	Post-Midcourse (Design)
$\overline{B}\cdot\overline{T}$ km	380	6,888	385
$\overline{B}\cdot\overline{R}$ km	5,700	3,478	5,701
Time of Closest Approach August 5 (GMT)	1,710	1,828	1,710

polation of trajectory attained by Agena to the plane of the Moon. The post-midcourse design indicates the magnitude of error, corrected by the midcourse maneuver, to satisfy all mission trajectory and position requirements.

Although the actual pre-midcourse parameters appear to be significant errors with respect to the targeted aiming point, the errors are well within the 3σ launch vehicle allowable dispersion. A doppler shift of 429.0 Hz was measured, as compared with the predicted change of 429.5 Hz.

Midcourse through Deboost — Cislunar orbiter determination made after the midcourse maneuver was computed using the procedures developed for Mission IV. These included:
- Solving for the state vector only using the doppler and ranging data;
- Solving for the state vector, Earth gravitational constraint, and station locations using an *a priori* covariance matrix and doppler data only.

These procedures were effective in obtaining compatible results and the small dispersion in predictions of "time of closest approach" of 19 seconds for Mission V and 10 seconds for Mission IV. The previous method showed 40- and 30-second dispersion for Missions II and III, respectively.

Using both of the above procedures, 17 orbit determinations were made after the midcourse maneuver. A comparison of the design and best estimate of actual lunar encounter parameters is shown in Table 3-8.

Table 3-8: Summary of Encounter Parameters

Element	Midcourse Design	Actual Best Estimate
$\overline{B}\cdot\overline{T}$ km	350.9	352.2
$\overline{B}\cdot\overline{R}$ km	5,701.0	5,696.0
Time of Closest Approach (seconds after 17:10 GMT, August 6)	17.1	12.6

The lunar injection maneuver design was based on 42 hours of two-way doppler data. The design philosophy was to guide the spacecraft from its approach trajectory into an elliptical orbit satisfying the following parameters.
- Longitude of ascending node;
- Perilune radius;
- Orbit inclination;
- Apolune radius;
- Argument of perilune. ,

In addition, the photo requirements specified that Apollo Site V-8a coverage be obtained in Orbit 26 with 5 degrees of crosstrack tilt, which required the spacecraft to be positioned over a specific point at a particular time in the orbit.

To satisfy this photo requirement, the argument of perilune (ω) and the perilune radius (r_p)

were allowed to vary. Because of the accurately executed midcourse maneuver, a near-nominal design of the initial-ellipse orbit was possible.

Engine ignition for the deboost maneuver was commanded to occur at 16:48:54.4 GMT on August 5. The required spacecraft maneuver to achieve the desired initial orbit was:

Sunline roll	20.24 deg
Pitch	76.91 deg
Δ V	643.04 m/sec
Estimated burn time	498.1 sec

Twelve possible maneuvers were computed to perform the deboost function. The final selection was based on similar criteria employed for the midcourse maneuver.

An alternate photo mission was planned in the event that the deboost maneuver was not accomplished. This included a series of flyby photos pointed toward the center of the Moon. These plans were cancelled when the maneuver was completed.

Initial Ellipse -- The initial ellipse was planned to be terminated at apolune of the fourth orbit. During the nearly 40-hour period, the spacecraft maneuvers required to photograph the four farside photo sites (the fourth site was added during the mission) and the orbit transfer maneuvers were determined and executed.

Orbit determinations and predictions were based on two orbit data arcs of two-way doppler tracking data. The Langley Research Center 7/28B lunar model was used in orbit predictions. (This seventh-order model was derived from an analysis of the Mission IV trajectory data.) Although ranging data was desirable during lunar orbits, operational planning could not allocate time within the complex mission to exercise this function. Orbit determination procedures included:

- Solving for the state vector and tailoring the basic lunar model by solving for the higher order (C32, C33, C42, C43, C44, S32, S33, S42, S43, and S44) harmonics;
- Placing the solution epoch at 190 degrees true anomaly.

A comparison of designed and actual initial orbit parameters is shown in Table 3-9. The first estimate was based on 30 minutes of tracking data; 5.5 hours of data were used to compute the best estimate of the orbit parameters.

Selenographic of Date Coordinate System -- The selenographic of date coordinate system is defined as an orthogonal right-hand coordinate system with the origin at the mass center of the Moon. The X axis is defined by the intersection of the Moon's prime meridian and equatorial planes. The Z axis is the Moon's spin axis. The

Table 3-9: Initial Orbit Parameters

| Orbital Element | Deboost Design | Actual | |
		First Estimate	Best Estimate
Perilune altitude (km)	201.7	195.3	194.5
Apolune altitude (km)	6,050.1	6,059.7	6,028.3
Inclination (deg)*	85.05	85.03	85.01
Longitude of ascending node (deg)*	117.9	117.8	117.8
Argument of perilune*	1.35	1.47	1.55

*Selenographic-of-date Coordinates

Y axis is normal to both the X and Z axes. Using this system, any fixed lunar feature will always have the same coordinates. "Of date" refers to the fact that, in order for this to be true, this coordinate system is rotating in space, and reference to any other celestial object must be tied to a specific date and time.

The near-nominal initial orbit resulted in essentially no error correction considerations in design of the transfer maneuver to satisfy the photo site coverage requirements. An attitude maneuver of −63.10 degrees sunline roll, 71.29 degrees pitch, and a velocity change of 15.97 meters per second (engine burn time 10.95 seconds) was selected for the orbit transfer maneuver. The execution time was commanded at apolune of Orbit 4 (08:43:48.7 GMT, August 7). The ground rules employed for design of the orbit transfer maneuver were:

- Photograph Site V-8a during Orbit 26 with 5 degrees of crosstrack tilt.
- Final ellipse (immediately after the second transfer maneuver) to have an apolune altitude of 1,500 kilometers and a perilune altitude of 100 kilometers.
- Reference target for first transfer is the time and location of the second transfer.
- Second transfer to occur at perilune of Orbit 10 and will adjust apolune altitude only (Hohmann transfer).

- First transfer will occur near apolune between Orbits 4 and 5 and will adjust the ellipse to meet the above conditions.

A backup maneuver was also designed for execution one orbit later in the event that the primary maneuver could not be performed. These maneuvers were designed by targeting to a perilune radius of 1,838.09 kilometers, a 71.41-degree longitude of ascending node, and an orbit inclination of 84.75 degrees.

Intermediate Ellipse -- Doppler tracking data indicated that the transfer maneuver was near nominal as evidenced by the comparison given in Table 3-10.

During the 44-hour duration of the intermediate ellipse, 12 orbit determinations were completed. The results were used to verify orbit parameter accuracy and support design of the photo maneuvers and the transfer maneuver to the final ellipse.

Single-frame photographs were taken of seven sites during six orbits. The film-set frame planned during Orbit 8 (Site A-9 Exposure 27) was redefined during the mission to obtain dual photographs of the Earth. The remaining sites were taken of farside areas. As in the initial ellipse, the photo maneuvers were designed to

Table 3-10: Intermediate-Ellipse Parameters

Orbital Element	Design	Actual	
		First Estimate	Best Estimate
Perilune altitude (km)	101.33	118.9	100.4
Apolune altitude (km)	6,065.64	6,075.2	6,066.8
Inclination (deg)*	84.62	84.66	84.61
Longitude of ascending node (deg)*	95.90	95.91	95.90
Argument of perilune (deg)*	1.32	0.903	1.34

*Selenographic-of-date coordinates

obtain the desired coverage as well as to shade the camera windows, whenever required, with the camera thermal door. The photo maneuver for Site A-6 in Orbit 5 was based on predicted orbit parameters because the design had to be completed before the orbit transfer was initiated. All other maneuvers were based on intermediate-ellipse orbit determinations.

A two-axis maneuver (roll, 166.62 degrees and pitch, 38.49 degrees) was commanded to take the Earth photo at 09:05:00 GMT August 8. Figure 3-8 shows the spatial geometry that existed. The spacecraft was 5,870.8 kilometers above the Moon and 361,740 kilometers from Earth when the photo was taken. The Earth was illuminated from approximately 13.6°W through 135°E longitude.

Design of the transfer maneuver to the final orbit was based on the following:
● Photograph Site V-8a from perilune of Orbit 26 with 5 degrees of crosstrack tilt.
● Final ellipse, immediately after the transfer maneuver, to have an apolune altitude of 1,500 kilometers and a perilune altitude of 100 kilometers.

The accuracy of achieving the intermediate orbit permitted a Hohmann transfer to be used to design the trajectory change. A spacecraft maneuver of −84.02-degree sunline roll, −96.79-degree pitch, and a velocity change of 233.67 meters per second (152.9-second engine burn) was commanded to effect the transfer to the final orbit, beginning at 05:08:32.65 GMT, August 9.

Final Ellipse -- Spacecraft performance and doppler tracking data showed that the final orbit transfer was near nominal. Table 3-11 compares predicted and actual performance for several orbit parameters.

The final-ellipse phase provided a verification of how well the velocity control maneuvers were designed and executed to satisfy the mission requirements to photograph Site V-8a. Table 3-12 shows a comparison of preflight requirements with the predicted and actual performance.

The principal functions accomplished during the final ellipse were to:
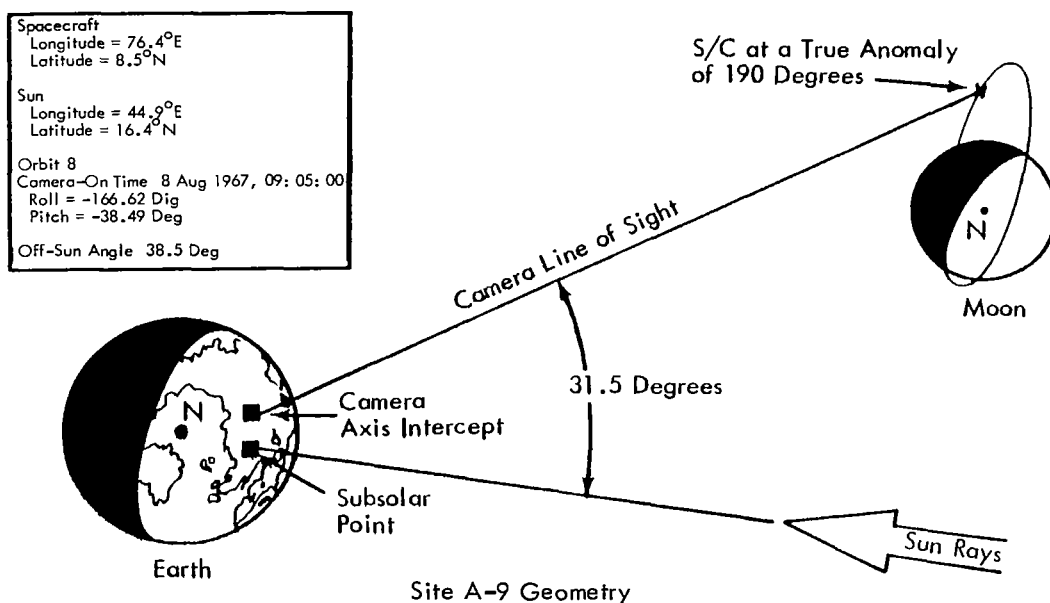● Make a high-quality orbit determination prior to each primary photo event;

Figure 3-8: Earth Photo Spatial Geometry

Table 3-11: Final Transfer Results

Orbital Element	Predicted		Actual		
	Pre-Transfer	Post-Transfer	Transfer Design	First Estimate	Best Estimate
Perilune altitude (km)	99.13	99.11	99.1	98.5	98.9
Apolune altitude (km)	6,082.98	1,501.88	1,501.9	1,499.0	1,499.4
Inclination (deg)*	84.75	84.76	84.76	84.76	84.76
Longitude of ascending node (deg)*	71.40	71.40	71.40	71.39	71.38
Argument of perilune (deg)*	0.90	1.61	1.61	1.80	1.88

*Selenographic-of-date coordinates.

Table 3-12: Orbit 26 Parameters

Element	Preflight Nominal	Pretransfer Prediction	Actual
Epoch (GMT) Aug. 11	08:15:21.0	08:10:13.87	08:08:12.8
Apolune altitude (km)	1,500.41	1,501.32	1,501.61
Perilune altitude (km)	99.51	99.78	97.11
Orbit inclination* (deg)	85.11	85.13	85.00
Longitude of ascending node*(deg)	44.19	43.28	43.27
Argument of Perilune* (deg)	0.07	1.01	1.23
Spacecraft nadir longitude (deg)	43.32	43.36	43.37
Spacecraft nadir latitude*(deg)	0.06	1.01	1.23
Camera axis cross track tilt (deg) to longitude of photo site	5.0	4.62	4.47

*Selenographic-of-date coordinates.

- Design the photo maneuver and compute camera-on times;
- Make trajectory predictions, including station rise and set times.

Flight path control computations were made using a four-orbit data arc (≈ 13 hours). A total of 44 orbit determinations was made during the final ellipse to support the photo requirements. Photo maneuvers were designed to cover the 41 nearside sites during 50 different passes. Spacecraft orientations, on all but one primary site, were controlled so that the short axis of the telephoto photo format was along the direction of motion of the spacecraft and image motion compensation. The exception to this orientation was Site V-25 where the long axis of the telephoto format was oriented parallel to the Alpine Valley and the V/H sensor was turned off.

Photo maneuvers were designed to satisfy the general requirements of one of the following:
- Near vertical — Specified site within one orbit spacing from the spacecraft nadir;
- Conventional oblique — Specified site more than one orbit spacing from the spacecraft nadir;
- Westerly oblique — Specified site from three to seven orbit spacings from the spacecraft nadir;
- Convergent telephoto stereo — Specified site photographed on successive orbits within specified camera axis tilt limitations.

All westerly obliques were taken when the spacecraft was at the same latitude as the specified target. The Alpine Valley photo was taken when the spacecraft was directly over the extension of the valley centerline. All other photos were taken when the distance from the target to the ground trace was a minimum.

Orbit Phase Kepler Elements -- Lunar Orbiter V lunar orbit characteristics are presented in Figures 3-9 through 3-12. These illustrations are time histories of perilune altitude, orbit inclination, argument of perilune, and ascending-node longitude. To show the long-term effects, each parameter covers the injection into

lunar orbit on August 5 to August 23, covering about 125 lunar orbits.

3.4 GROUND SYSTEM PERFORMANCE

The Lunar Orbiter ground system provided the facilities and equipment required to receive, record, and transmit data and commands between the space flight operations facility and the spacecraft. In addition, all facilities necessary to sustain mission operations were provided. This was accomplished through a complex consisting of three primary deep space stations (DSS), the space flight operations facility (SFOF), and the ground communications system (GCS) which provided voice and data communications between all locations. Separate facilities were provided at Eastman Kodak, Rochester, New York and at Langley Research Center, Hampton, Virginia to process, copy, and evaluate the photos and data obtained.

All of these facilities provided the required support during the photographic mission and only minor irregularities were encountered. Each area is separately discussed in the following sections.

3.4.1 Space Flight Operations Facility (SFOF)

The space flight operations facility provided the mission control center, as well as the facilities to process and display data to support operational mission control. The entire system performed very well.

The telemetry processing station and the internal communications system provided telemetry and tracking data from the high-speed data line and teletype lines for use by the SFOF computers and the subsystem analysts in the operations areas. The central computing complex committed to support the program consists of three computer strings, each of which contains an IBM 7094 computer coupled to an IBM 7044 input-output processor through an IBM 1301 disk file memory and a direct data connection (Mode 2). Four computer strings were used to support Mission V for the periods indicated. The "V" computer string was used for the first time to support the Lunar Orbiter program and no problems were encountered.
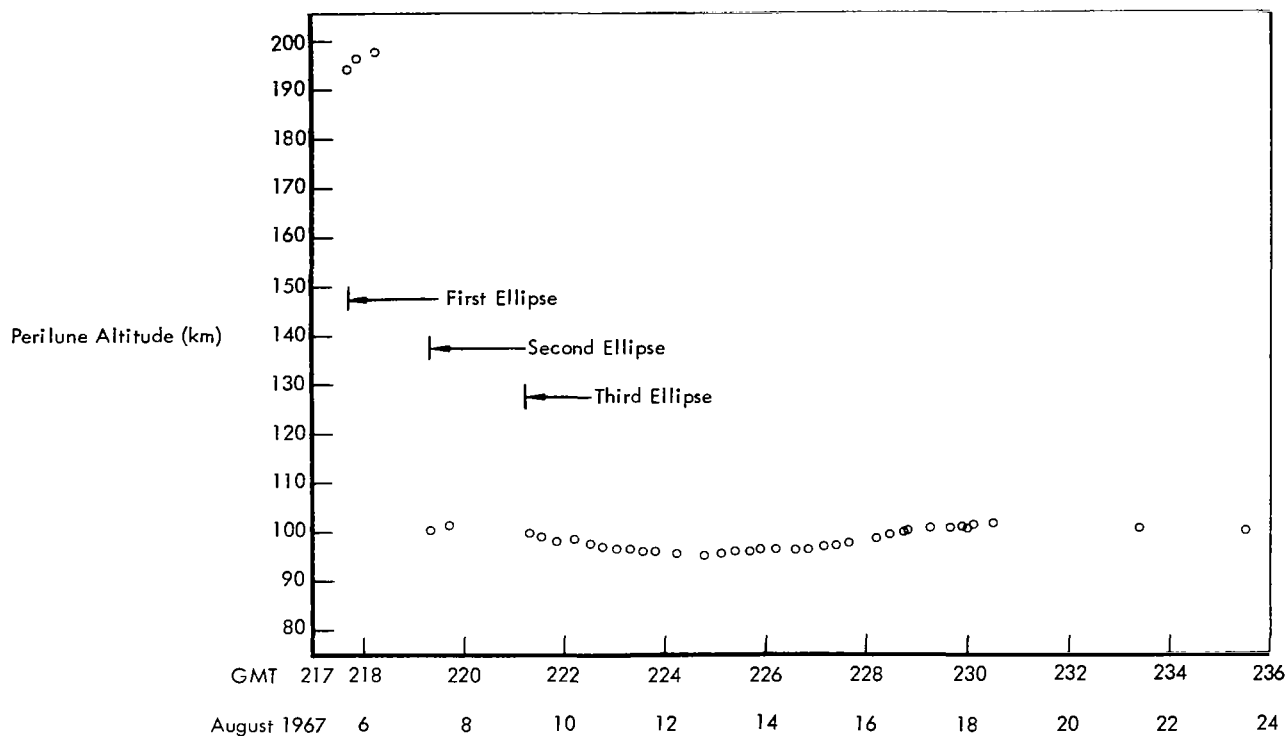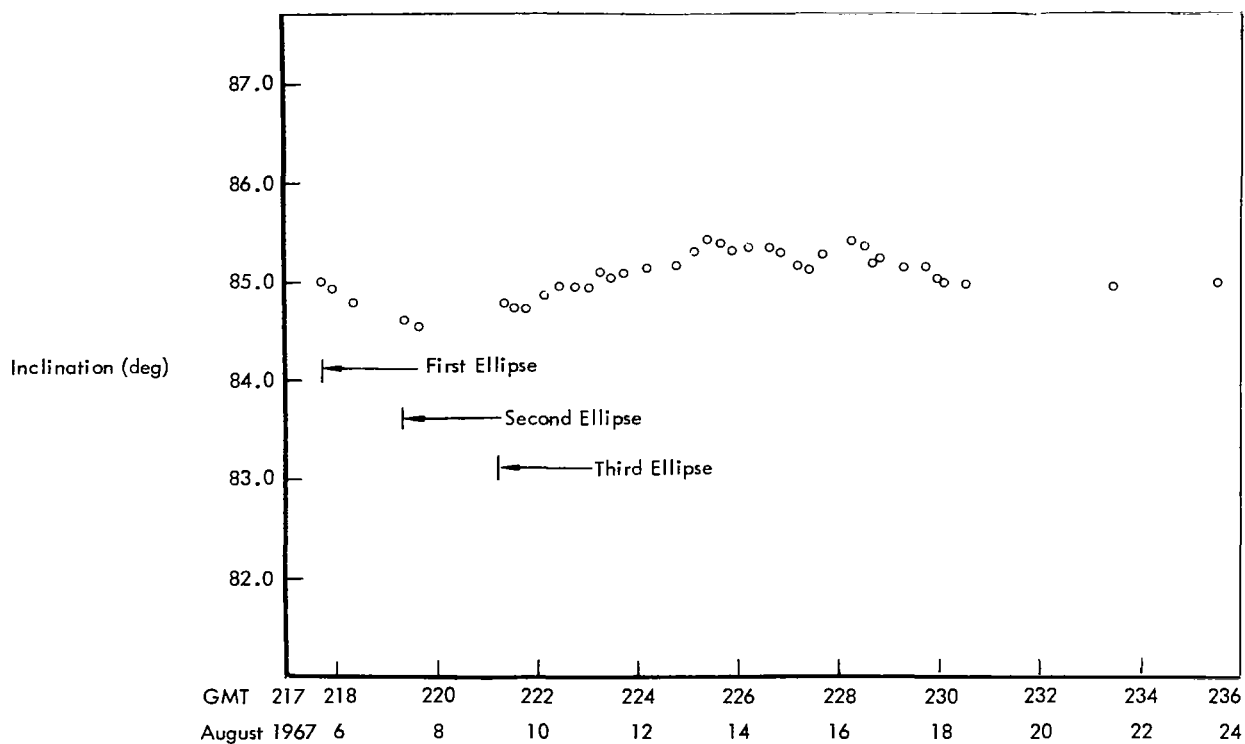
Figure 3-9: Perilune Altitude History
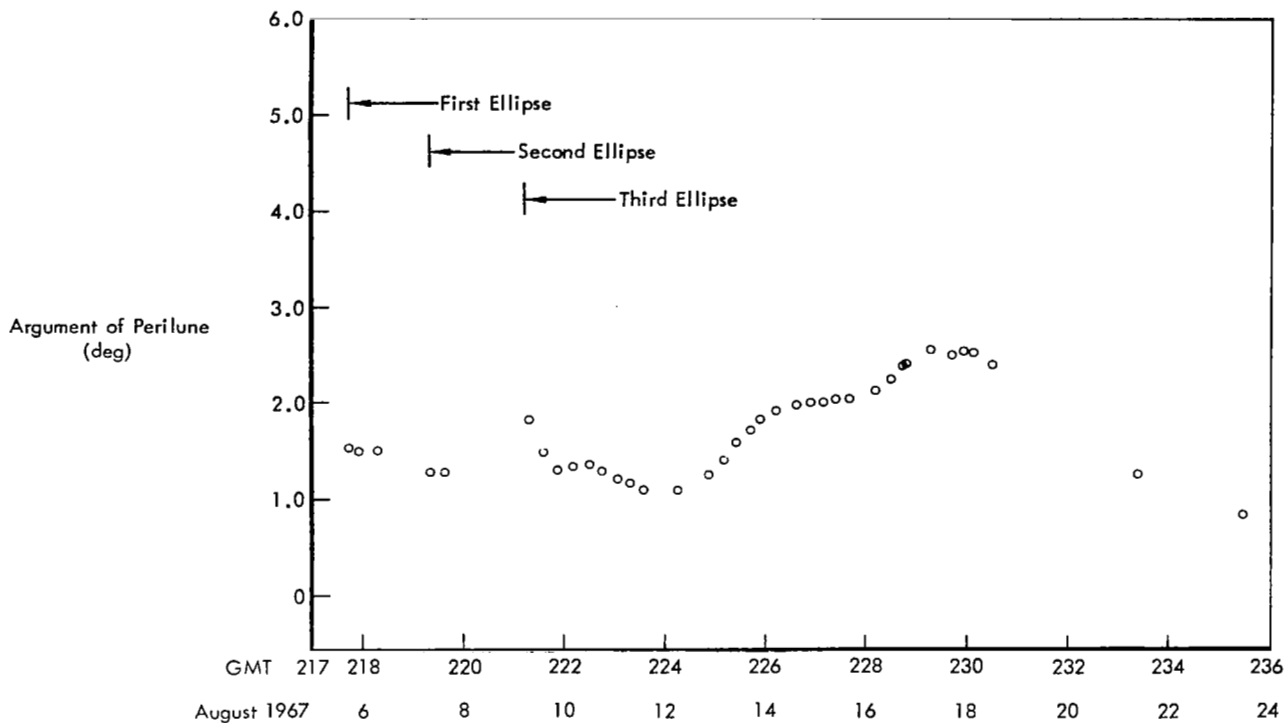

Figure 3-10: Orbit Inclination History

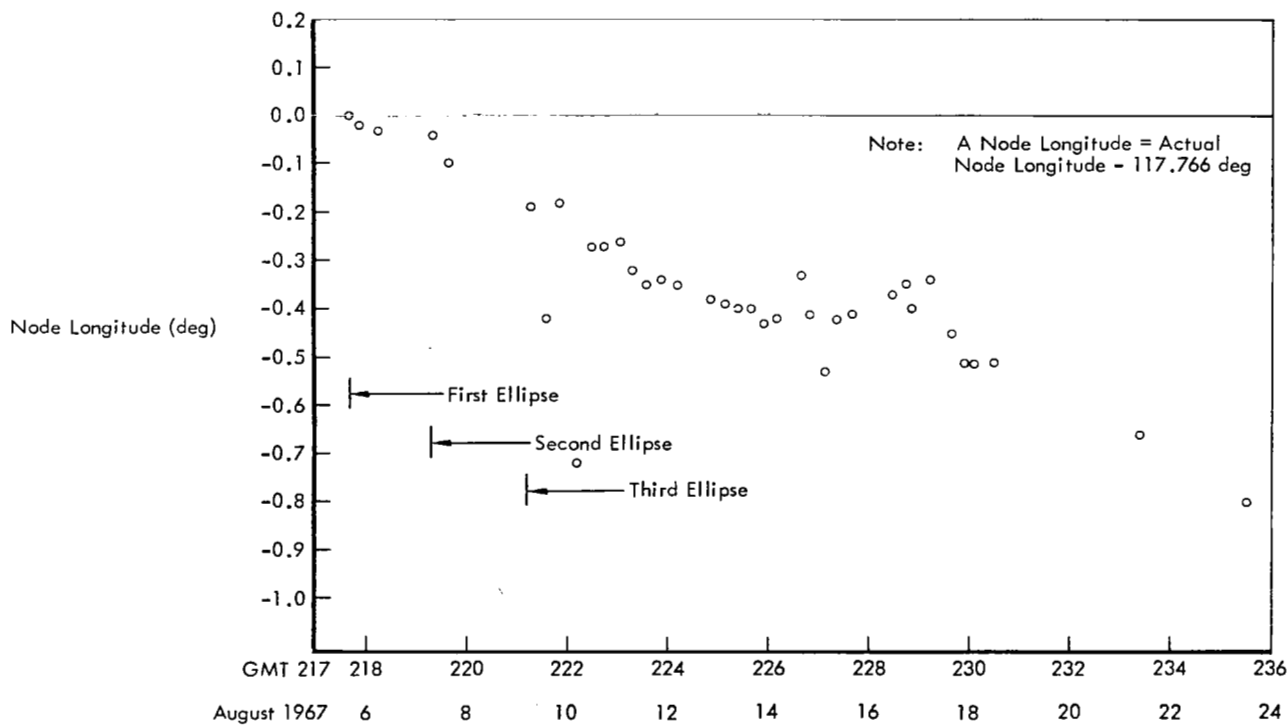**Figure 3-11: Argument of Perilune History**

Figure 3-12: Inertial Node Longitude History

A dual Mode 2 configuration (two complete computer strings online and operating in parallel) was used to support all critical phases and, due to the tight mission constraints, throughout most of the mission.

Computer String	Total Hours	Mode 2 (hours)
X String	355	350
Y String	366	306
W String	261	94
V String	18	18
Total	1,000	768

During the first 6 hours, the DSN was responsible for both orbit determination and data quality determination. For the entire mission the DSN was responsible for the history of data quality and analysis. Jet Propulsion Laboratory personnel performed the first orbit determination after cislunar injection. The orbit was determined within the allowable time and showed a nominal injection that was subsequently verified by later orbit determination computations.

Changes were made in the SPAC computer programs to expand the capability of the thermal program status reporting and plotting. The 14 SPAC programs were executed a total of 2,009 times, of which 1968 were successfully completed. Of the 41 failures to execute, 25 were attributed to input errors and the remaining 16 contained software and hardware errors.

3.4.2 Deep Space Stations (DSS)
The Deep Space Stations (Goldstone, California; Woomera, Australia; and Madrid, Spain) supported the Lunar Orbiter V mission by:
- Receiving and processing telemetry and video data from the spacecraft;
- Transmitting commands to the spacecraft;
- Communicating and transmitting both raw and processed data to higher user facilities.

Real-time tracking and telemetry data were formatted for transmission to the SFOF via the ground communications system. Video data were recorded on video magnetic tapes and, by mission-dependent equipment, on 35-mm film. All physical material, such as processed films, video tapes, logs, and other reports, was sent to the appropriate destinations via air transportation. All commitments were met and the incidence of error was low. The DSN provided tracking data for a total of 752 hours, which represents nearly 95% of the maximum support committed for this mission.

To avoid communication interference between the three spacecraft orbiting the Moon, the procedure for multiple-spacecraft operation that was developed during Mission IV was employed. Tests were made to determine the best lock frequency for the transponder. This frequency was measured at various times during the mission. For most of the mission the ground station VCO was offset 330 Hz.

Station handover was accomplished in a routine manner in all but one case. In this instance, an improper sequence was used by DSS-12 and transponder lock was lost at handover. The spacecraft was reacquired when the proper reacquisition procedure was employed.

3.4.3 Ground Communications System (GCS)
Ground communications between the DSS and the SFOF consist of one high-speed-data line (HSDL), three full-duplex teletype (TTY) lines, and one voice link. Communication lines to overseas sites are routed through the Goddard Space Flight Center at Greenbelt, Maryland. Performance telemetry data were normally transmitted via the HSDL and TTY lines, while the tracking data were transmitted via TTY line only.

Telemetry performance data can be transmitted via teletype lines with a reduction in the amount of data transmitted in real time.

Overall performance of the ground communication system was excellent, again demonstrating its high degree of reliability. Essentially all data transmitted via the HSDL were received at the SFOF. Station 41, which exhibited the lowest performance, transmitted all but 0.68% of its data. Primary station TTY lines also exhibited excellent performance of better than 99% reliability. Few and intermittent outages of the voice circuits were experienced during the 27-day mission.

3.4.4 Photo Processing

Photo processing at Eastman Kodak included printing negative and positive transparencies by successive-generation contact printing from the original GRE 35-mm transparencies. There were no machine-reassembled 9.5-by 14.5-inch subframes made for this mission. All reassembled photos were made from manually reassembled GRE film by the Army Map Service and NASA Langley Research Center using film copied at Eastman Kodak or produced from video tape playbacks through the Langley Research Center facilities.

GRE 35-mm film was printed on Type 5234 Eastman Fine-Grain Duplicating Film. Processing goals were to have a density (D) of 0.50 to reproduce on the copy at a value of 2.00 and a density of 2.00 to reproduce at a value of 0.50 (where a density of 0.50 corresponds to white and 2.00 corresponds to black). The inverse of densities is the normal result of the film transparency copy process in which white areas on the original produce black areas on the copy. These densities were within ± 0.10 density of the received D-maximum and within ± 0.05 density of the received D-minimum.

Density measurements were made on the GRE film processed at the sites and actually used to make the GRE copies. Measurements were made of the test bar pattern in the edge data format, pre-exposed on the spacecraft film prior to flight. Results of these measurements are shown in Table 3-13, where D max and D min are the maximum and minimum densities, respectively.

A processing and priority schedule was developed for the 35-mm film to satisfy the urgent requirements for film copies within the daily output capacity (30,000 feet per day) of the assigned facilities. During the final readout period, the copying schedule was modified to process the long readout period (up to 830 feet) film rolls. Mission processing plans were based on a nominal two-frame readout period which produced about 400 feet of GRE film. All 35-mm copies were completed and shipped within the planned periods.

3.4.5 Langley Photo Data Assessment Facility

The primary functions accomplished at the Photo Data Assessment Facility at Langley Research Center were to make:
- An analog tape copy containing only the video data;
- One GRE film for each analog tape;
- Additional GRE films as priority permitted.

During Mission V, 459 master video tapes were received from all sites; five of these tapes were

Table 3-13: Measured GRE Film Density

Station	GRE	Average D Max	2σ	Average D Min	2σ
Goldstone	03	1.96	0.11	0.45	0.07
Woomera	05	2.00	0.19	0.44	0.07
	06	2.00	0.13	0.45	0.06
Madrid	07	1.96	0.07	0.48	0.04
	08	1.96	0.10	0.47	0.07
Overall Average		1.98	0.12	0.46	0.06

unplayable. Each tape has been duplicated at least once and from three to 15 GRE films, depending on the NASA requirements, have been made. There has been no evidence of noticeable degradation in photo data from the repeated runs.

The electronic equipment developed during Mission III (to modify the input signal to the GRE and thus compensate for spacecraft read-out density variations) was employed during the playback of Mission V video tapes. In addition, work was initiated to develop an external video processor which will permit control of density and contrast independent of the GRE. A prototype of the electronic equipment is nearing completion and will be incorporated into subsequent processing requirements.
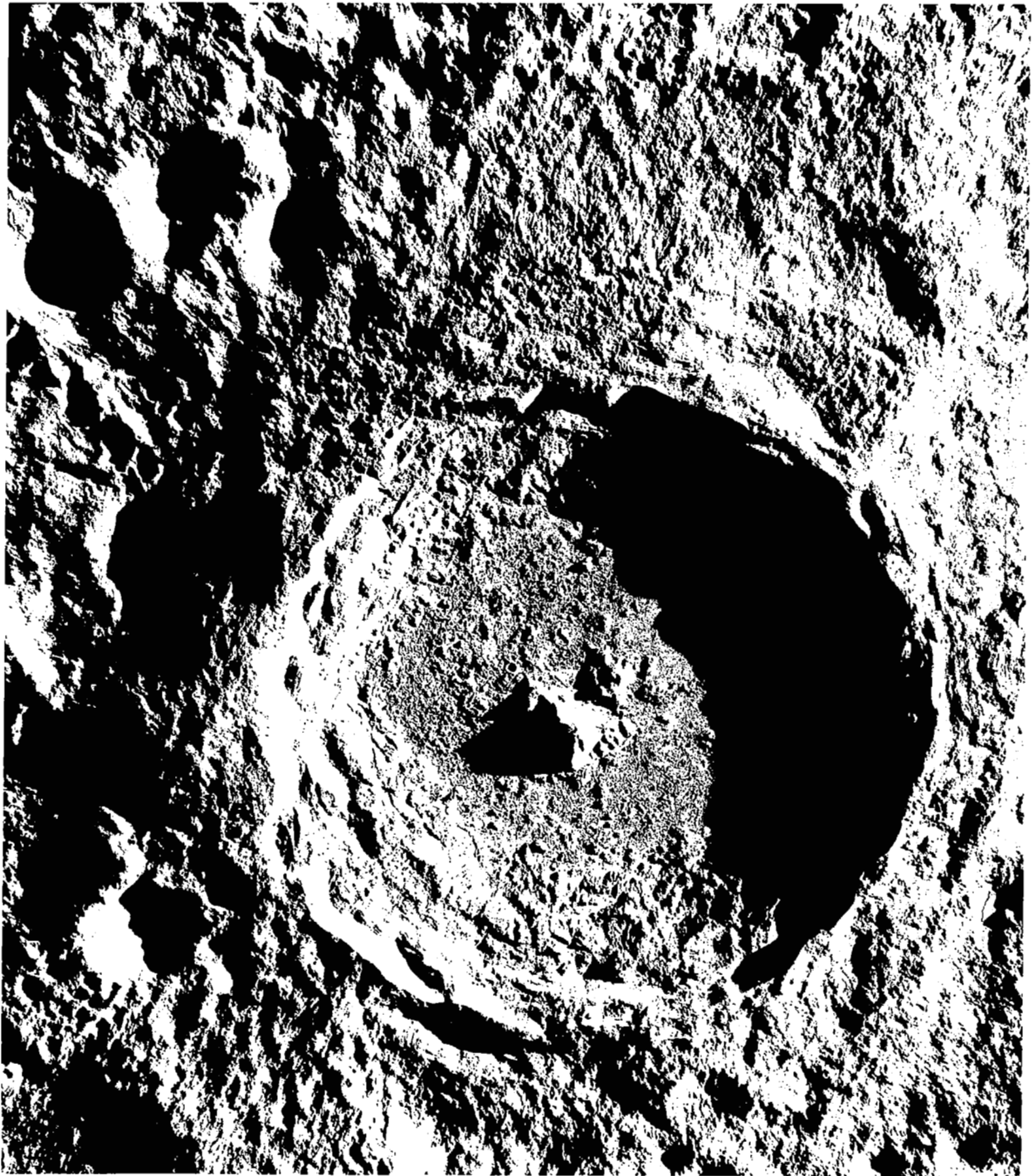
Wide-Angle Frame 125, Site V-30
Centered on the crater Tycho.

4.0 Mission Data

An objective of each Lunar Orbiter Mission has been to provide four types of data — photographic, lunar environmental, tracking, and spacecraft performance. The photographic data varied with the specific mission as defined in the NASA specifications and requirements. The Mission V objectives were completely fulfilled by the data obtained during the 27-day photographic mission.

Of the total of 213 dual-frame exposures, 174 were made of 41 sites located on the nearside and 37 of previously unphotographed areas on the farside. One frame was used to obtain the near full-Earth photo from near apolune of the intermediate ellipse, and one frame was used for film-set. The photo coverage of Mission V, when added to the previous data, shows that nearly the entire lunar surface has been photographed with resolution at least 10 times better than that obtainable from Earth-based observations.

The secondary objective of providing a spacecraft to be tracked by the Manned Space Flight Network (MSFN) to evaluate the Apollo Orbit Determination program will be accomplished during the extended mission.

Each type of data is discussed, in turn, in the following sections.

4.1 PHOTOGRAPHIC DATA
A total of 426 telephoto and wide-angle photographs (213 dual exposures) was taken during 50 sequences on the nearside and 25 sequences from near apolune, 23 of which obtained coverage of farside areas. The remaining two sequences were used for the Earth photo and a blank film-set exposure. Except for the addition of the Earth photo and slight relocation of some photo sites, the photography was conducted as planned. All of the photos taken, except for the last wide-angle exposure which was not processed before Bimat exhaustion, were read out and recorded at the Deep Space Stations during the final readout period.

Five basic photographic tasks were incorporated in the Mission V design requirements.

Each task includes the basic scientific interests; however, the site selection and photography employed were directed toward satisfying the further requirements of:
- Additional photography of specified candidate Apollo sites;
- Completion of a broad photographic survey of unphotographed farside areas;
- Photography of scientifically interesting Surveyor sites;
- Photography of scientifically interesting "landable" areas for the Apollo Applications Program (AAP);
- Photography of scientifically interesting areas.

Mission V photography was accomplished as shown in Table 4-1 to satisfy the above tasks.

Table 4-1: Exposure Allocations

Subject	Sites	Exposures	Sequences	Percent
Apollo	5	44	14	21
Science	36	130	36	61
Farside	23	37	23	17
Earth	1	1	1	} 1
Film set	1	1	1	

Three elliptical orbits were employed to satisfy the Mission V photographic requirements. An initial (6,000-kilometer apolune, 200-kilometer perilune) orbit was required to obtain telephoto coverage of the previously unphotographed farside areas beyond the western limb. Farside photography was continued during the intermediate orbit (6,000-kilometer apolune, 100-kilometer perilune) necessary for the safe transition to the final orbit (1,500-kilometer apolune, 100-kilometer perilune) required to support the nearside photography.

Photo sites on the nearside were located between 42°S latitude and 50°N latitude. The highly elliptical final orbit with perilune near

the equator produced significant changes in the photographic altitudes. Figure 4-1 shows the nominal variation of photographic altitude and static resolution as a function of latitude for a nominal final ellipse with a 100-kilometer perilune at the equator.

The Manned Spacecraft Center desires vertical, oblique, and convergent telephoto stereo photography for each of the candidate Apollo landing sites. Missions I, II, and III provided this data for the eight candidate sites selected after Mission III except:
- Convergent telephoto stereo: IIP-2, -6, -8, and IIIP-11;
- Oblique: IIP-2 and -6

In addition, Photo Site IP-1 showed promise of meeting the Apollo requirements for a candidate site; therefore, vertical, oblique, and conver-

gent telephoto photography of this area was included in Mission V photo requirements.

Apollo site photography was accomplished from altitudes of 96 to 103 kilometers, which provided approximately 2-meter resolution in the vertical photography. The wide variations in latitude of the science sites resulted in photo altitudes ranging between 96 and 273 kilometers.

A total of 86 priority readouts was completed prior to Bimat cut. The duration of priority readouts ranged from a minimum of 28 to a maximum of 440 framelets. Sixty-one final readout sequences were required to scan all of the photos taken. The longest final readout period contained 468 framelets. As the mission progressed, the number of video dropouts (discussed in detail in Section 3.2.1) increased. Each video dropout appeared as a thin white
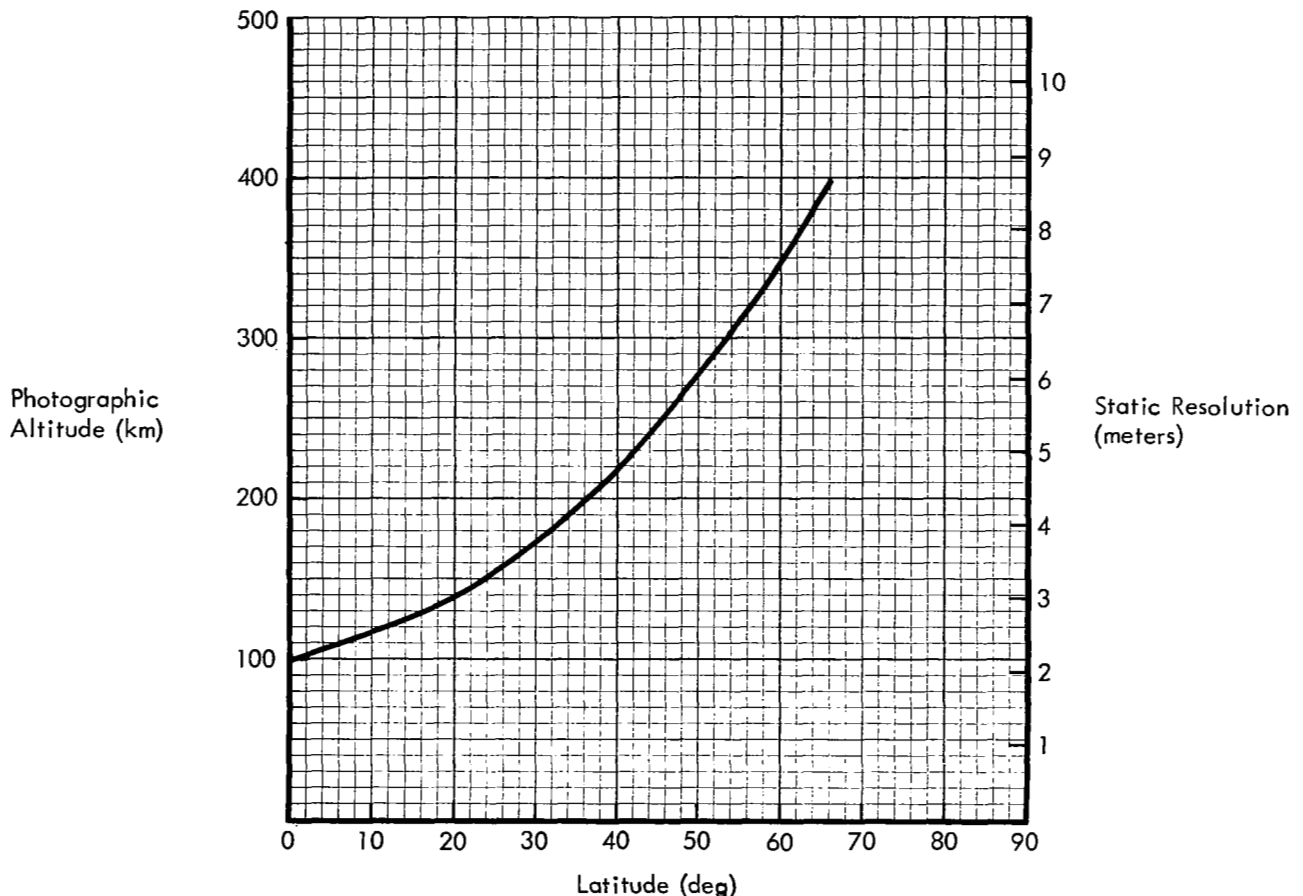

Figure 4-1: Altitude & Resolution Variation with Latitude

line 0.003 to 0.006 inch wide on the GRE film and therefore obscured very little of the photo data. Many of the exposures containing the drop-outs were read out in both priority and final readouts, which resulted in no actual loss in data.

To aid in the evaluation and detailed analysis of the Mission V photo data, reseau marks illustrated in Figure 4-2 were pre-exposed on the spacecraft film at the same time as the edge data. The fixed orientation, the same as that used on Missions III and IV, can help the photo analyst detect and compensate for distortions introduced after imaging by the camera lens.

4.1.1 Mission Photography
Analysis and assessment of Mission V photog-raphy were based on visual examination of second-generation GRE positive transparencies and paper prints made from manually reassemb-led GRE film using a 10 to 30X zoom macro-

scope and a quality-evaluation viewer. A samp-ling technique was employed for examination of the eight-frame sequences. Many of the sites were photographed by single exposures and four-frame sequences; therefore, each frame was evaluated because sampling was not practical.

Lunar orbital photography was made particu-larly difficult by uncertainties about the Moon's surface characteristics and its photometric function, both of which are critical to photog-raphy. The Moon has reflectance characteris-tics unlike any encountered in terrestrial photog-raphy. The wide range of reflectance can -- and did -- produce photographic images in adjacent areas having a density range that exceeded the capability of the spacecraft readout system (thus obliterating detail in areas of density ex-tremes) while exhibiting excellent detail in the surrounding areas. Experience gained during previous missions was used to refine the selec-tion of photographic parameters needed to
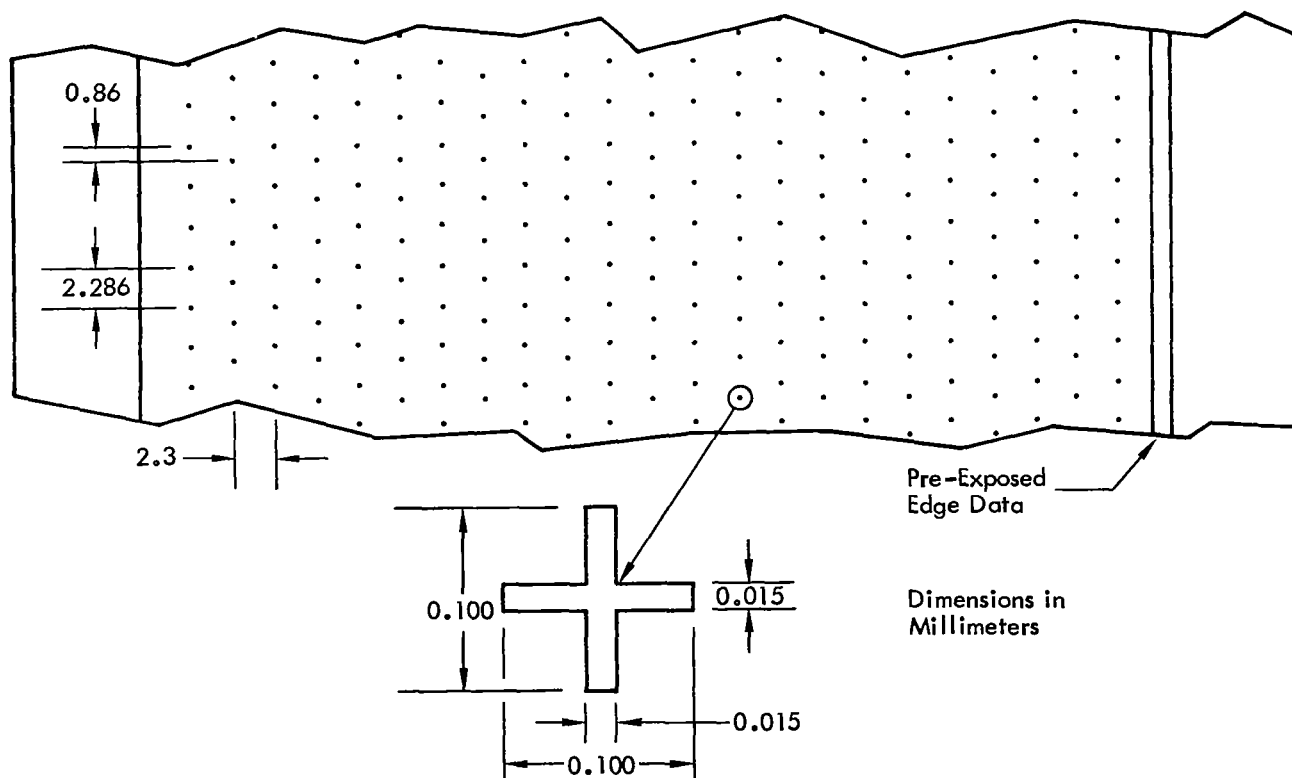

Figure 4-2: Pre-Exposed Reseau Mark Characteristics

65

determine the required exposure settings. Exposure of both the wide-angle and telephoto frames was satisfactory considering the wide range of photographic problems presented. Because of the topographic characteristics of the lunar terrain, the effects of the lunar photometric function, and photo subsystem limitations, almost all photographs include at least some areas of either under or over exposure where information was lost because of the extreme luminance range of the surface. Frequently, in areas of steep slopes, data can be lost, while adjacent areas of similar characteristics show excellent surface detail depending on the relative Sun angles.

Other photographic problems were encountered on Mission V as a direct result of the type of mission performed. Exposure control was selected using the predicted spacecraft film densities computed by the Photo Quality Prediction (QUAL) program. Factors in this computation included surface albedo and illumination geometry. The albedo charts provided by the U. S. Geological Survey were revised based on the experience gained on previous missions as well as the initial Mission V photo results. All apolune wide-angle photos cover an area that extends beyond the terminator at one extreme and tend to severe overexposure toward the bright limb at the other.

Image motion compensation was used on all nearside photography, except for Sites V-3.1 (westerly oblique of Site IP-1 to show the zero phase point), V-10 (oblique of Altai Scarp), and V-25 (oblique with long axis of telephoto frame aligned parallel to the Alpine Valley). These photos showed some evidence of image motion during exposure with an accompanying reduction in resolution.

To compensate for normal camera actuation delays, camera-on times were biased by a constant amount for all "V/H-off" photography and by the expression $-(0.1 + \dfrac{0.50}{V/H})$ for all "V/H-on" photography. A comparison of the photos from priority readout showed a downtrack error of about 6 kilometers on the lunar surface resulting from a systematic apparent pointing or positioning error. Beginning with Frame 102, therefore, the bias for "V/H-off" photos was increased from -0.9 to -1.0 second, and a -3.0-second bias was added to the above relationship for all "V/H-on" photos. Thereafter, the variations of actual and desired coverage included downrange as well as uprange displacement of considerably less magnitude. All deviations between actual and predicted median exposure time for the first photo of a sequence fell within the operating limits imposed by V/H sensor cycle times.

The Manned Spacecraft Center has defined the maximum useful crosstrack tilt to be approximately 30 degrees. This criterion was of prime consideration in selecting the 100-kilometer perilune for nearside photography. In addition, the 100-kilometer perilune increased the width of coverage by a factor of two for the Apollo sites near the equator, thus reducing the number of exposures required to obtain the desired coverage. This increased coverage permitted photography of additional sites, which would not have been possible from a 50-kilometer-perilune orbit. Although the telephoto resolution was increased from 1 to 2 meters, the change is not significant for the Mission V objectives. Evaluation of the photos showed that the expected resolution, as a function of photographic altitude, was obtained by both the wide-angle and telephoto exposures.

Processing marks resulting from the intermittent processing schedule employed during the mission were evident in many of the wide-angle photos. The resulting local degradation was expected because operational control procedures required placing these effects in the wide-angle rather than the telephoto exposure. Other characteristic processing defects were present in varying degrees on the spacecraft film. Examination of the photo processing data obtained during flight acceptance testing of the backup photo subsystem showed a "lace" or "bubble" effect similar to that observed on all flights. Although a complete explanation has not been found, it is believed to be associated with the process of lamination between the Bimat and film around the processing drum.

4.1.2 Photo Coverage

Mission V was a multi-site scientific mission with many photographic requirements. Exposures were made in four- or eight-frame fast-mode sequences (with 87% forward overlap of side-angle photos and contiguous telephoto coverage) as well as four-frame slow-mode sequences (with 50% forward overlap of side-angle photos and separated telephoto coverage). In addition, several sites were photographed by single-frame exposures to obtain coverage of the desired feature, area, or surface characteristics. In some instances, the shutter speed was set to obtain optimum exposure of a specific feature or area while accepting the resulting degradation of photo data in the surrounding areas.

A direct comparison of the coordinates of the photos with existing lunar charts cannot be made over the entire visible surface. Matching of individual photos with the most recent lunar charts indicates varying degrees of agreement. Some contributing factors are: the fact that the photo orbit did not pass directly over all sites, variations in lunar surface elevations, uncertainties in the mathematical model of the Moon, and uncertainties in spacecraft attitude based on cumulative effect of photo maneuvers without intervening celestial reorientation. In addition, a secondary objective of the Lunar Orbiter program is to obtain tracking data from which to refine the mathematical model of the Moon. To compute the photo supporting data and predicted photo locations, the best available estimates for these parameters must be used in the orbit determination routines. Therefore, some discrepancies can be expected in coordination of the computed photo location with the maps made from Earth-based observations.

Other errors in locating the photos stem from spacecraft attitude variations within the ±0.2-degree control deadband and lunar surface elevation changes.

It must also be remembered that considerable effort is required to transfer the data from the unrectified, nonorthographic projection photographs to the Mercator projection maps. In general, the lunar feature matching between the photos and lunar charts 'indicate that the pre-dicted photo locations are generally consistent with the chart "reliability diagram." Continued analysis and comparison of photos obtained from each photo mission will result in more accurate definition of the lunar surface, and reduction of the positioning error in subsequent lunar charts. In addition, the ability to discern surface features or formation detail from Earth-based observations falls off rapidly as the limbs and polar regions are approached. Prior to the Lunar Orbiter and Ranger photos, lunar mapping efforts were generally concentrated within ±10 degrees of the equator with limited and decreasing effort in the other regions.

Photo coverage of Mission V has been classified into four major categories to support the basic photo tasks. These categories are: Apollo sites, Apollo Applications Program sites, science sites, and farside sites. The single Surveyor site is identified in the science site tabulations. Supporting data for each category are presented in tabular form for each site located on a corresponding lunar mosaic.

Geometric parameters of photography are illustrated in Figure 4-3. The angle of incidence is defined as the angle between the Sun's rays and the normal to the lunar surface. The phase angle is the angle between the camera axis and the Sun's rays. The angle and altitude ranges are for the first and last frame of the group, respectively. The angle "alpha" is defined as the angle between the projection of the surface normal and the camera axis, measured in the phase angle (camera-Sun-principal point) plane. The slant distance is defined as the distance between the camera and the principal ground point (the intersection of the projected camera axis and the lunar surface). Tilt angle is defined as the true angle between the camera axis and the local vertical through the spacecraft. Tilt azimuth is the clockwise angle from lunar north to principal ground point measured from the vertical projection of the spacecraft on the lunar surface. Since the oblique photos were taken from different altitudes and involve use of cross-axis camera tilt, the lunar surface scale factor differs from one to another. These exposures are identified within each table.
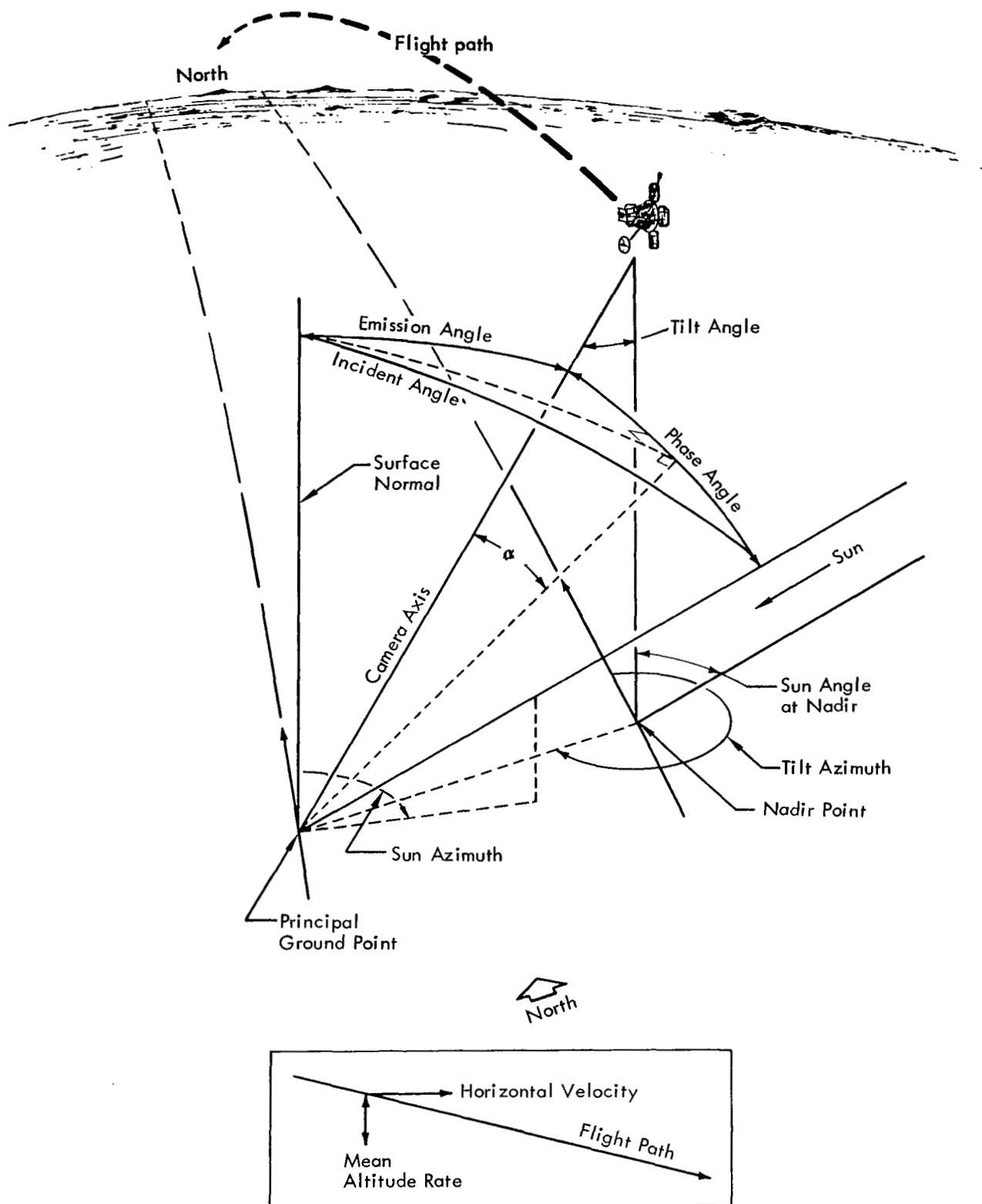
Figure 4-3: Geometrical Parameters of Photography

68

Apollo Sites -- The primary objective of Apollo site photography was to obtain selected coverage of specific sites, which completes the Manned Spacecraft Center basic requirements for each candidate site. Forty-four frames were exposed in 14 sequences of the five specified sites. The photography included convergent telephoto stereo (four-frame sequences on successive orbits) at each site and oblique photography of three of the five sites.

Examination of the photos showed that the photography of these sites was satisfactory and the desired coverage obtained. The Apollo sites are located within mare areas which have generally flat terrain and few large features, but a wide luminance range. Many craters contain hard shadow on one side where all detail is lost, and very bright slopes on the opposite side, where detail is lost in varying degrees depending on the brightness. Wide-angle and telephoto resolution appeared to be uniformly good, with few exceptions, and well within system specifications. Excellent detail of many craters, as well as of numerous surface features, is shown.

Oblique photography was taken in a westerly direction to provide a view of the landing approach as it would be seen by the Apollo astronaut. In this orientation, the wide-angle photos often contain the zero-phase point (the point in the field of view where the line of sight is along the sunline). This corresponds to full Moon illumination, and results in overexposure of the area within a few angular degrees of this line of sight. Where possible, the zero-phase point was placed closer to the frame edge to minimize the area of overexposure and still provide acceptable exposure along the camera axis.

Figure 4-4 shows the location of the candidate sites within the Apollo zone of interest ($\pm$ 5° latitude, $\pm$45° longitude) photographed during Mission V. Significant photo supporting data for each of the photo sequences covering these sites are given in Table 4-2.

Scientifically Interesting Sites -- Science sites for Mission V were selected to provide photographic data which might be expected to contribute to the scientific understanding of the Moon. Earlier Lunar Orbiter missions had shown that most lunar terrain had a subdued appearance and little more could be learned from the limited high-resolution coverage. Greater coverage of carefully selected areas at somewhat less resolution was considered to be more productive; therefore, Mission V sites were selected where geologically significant units were more likely to be exposed by fresh craters or other features. Mission IV photography was used extensively, in locating and making minor relocations of Mission V sites that met the criterion of freshness and, perhaps most importantly, in rejecting some previously selected sites.
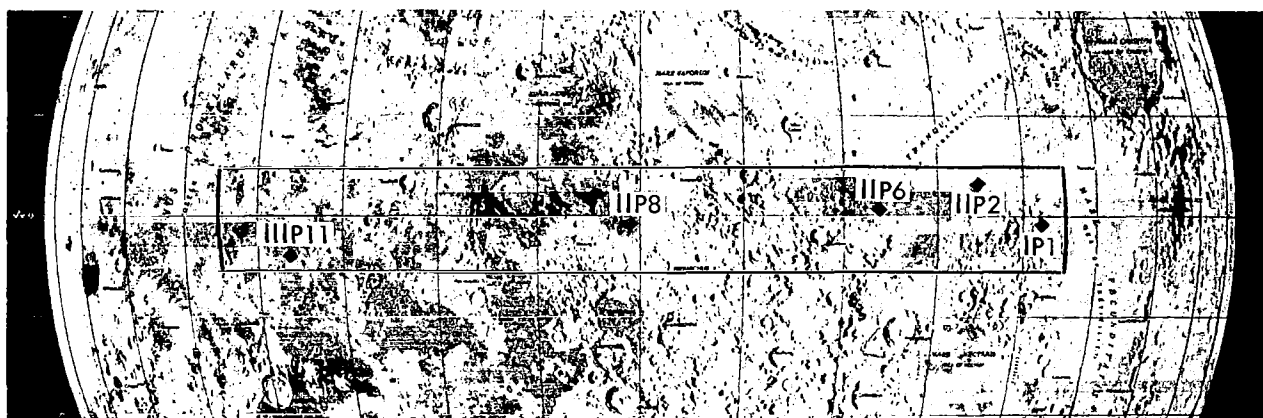

Figure 4-4: Selected Apollo Site Locations

Table 4-2: Supporting Data -- Candidate Apollo Site

Photo Site	Spacecraft Exposure No./Orbit	Shutter Speed (sec)	Location of Photo Center Long. (deg)	Location of Photo Center Lat. (deg)	Spacecraft Altitude (km)	Spacecraft Slant Distance (km)	Approximate Framelet Width Wide Angle (km)	Approximate Framelet Width Tele-photo (km)	Phase Angle (deg)	Alpha (deg)	Angle of Incidence (deg)	Camera Axis Tilt Angle (deg)	Camera Axis Tilt Azimuth (deg)
IP-1													
V-3.1	38/19	0.01	49.5°E	1.0° S	98	210	6.7*	0.87*	8.5	64.5	73.5	59.2	270
V-6	42/23	0.01	44.4°E	1.0° S	97	161	5.1*	0.67*	17.4	54.7	72.2	50.7	270
V-8a	44-47/26	0.02	42.9°E	1.1° S	97	97	3.1	0.40	64.0	4.7	68.7	4.5	267
V-8b	48-51/27	0.04	43.3°E	1.1° S	97	107	3.4*	0.45*	99.3	-26.3	67.1	24.9	96
IIP-2													
V-9.1	52/28	0.01	35.8°E	2.9°N	97	162	5.1*	0.67*	16.9	55.6	72.5	51.4	270
V-11a	55-58/31	0.02	34.2°E	2.6°N	96	97	3.1	0.40	60.8	8.5	69.2	8.1	278
V-11b	59-62/32	0.04	34.6°E	2.6°N	96	105	3.3*	0.44*	91.4	-23.8	67.6	22.6	96
IIP-6													
V-13	64/34	0.01	25.2°E	0.7°N	96	159	5.0*	0.66*	18.4	55.0	73.4	51.0	270
V-16a	71-74/37	0.02	23.8°E	0.7°N	96	96	3.0	0.40	66.4	3.5	69.9	3.3	267
V-16b	75-78/38	0.04	24.3°E	0.8°N	96	107	3.4*	0.45*	95.8	-27.5	68.3	26.1	96
IIP-8													
V-27a	108-111/51	0.02	1.2°W	0.3°N	97	99	3.1	0.41	61.5	10.7	72.2	10.1	273
V-27b	112-115/52	0.04	1.1°W	0.1°N	97	104	3.3*	0.43*	91.4	-20.9	70.6	19.8	96
IIIP-11													
V-42a	169-172/71	0.04	36.3°W	3.6° S	103	104	3.3	0.43	67.1	8.0	75.1	7.6	269
V-42b	173-176/72	0.04	36.2°W	3.5° S	103	109	3.5*	0.45*	92.6	-18.8	73.7	18.0	96

*Framelet width applies only at center

70

To support the Surveyor program, Mission V Site V-24 (Hipparchus) was photographed by a four-frame fast-mode sequence. A contiguous block of telephoto coverage of this potential Surveyor landing site will permit feature matching with Surveyor data. The comparison will uniquely locate the position of the Surveyor spacecraft. Although this was the only site identified for Surveyor landing, it is very likely that other science sites will prove to be satisfactory potential landing sites.

Evaluation of these photos showed that all of the desired surface features were within the field of view of the narrow telephoto lens. Excellent detail of all types of lunar surface features was obtained. Many characteristics were observed which can form the basis for typing or classifying lunar craters. Features covered include:
- Crater characteristics (central peak, floor cracks, shape, walls);
- Crater chains and rille structures;
- Thermal anomaly and high radar reflectivity areas;
- Details of both bright and dark crater rays;
- Surface characteristics (exposed strata, valley scarps, outcrops);
- Highland terrain surface texture;
- Evidence of past volcanic activity;
- Ejecta patterns and rolling rock paths;

Figure 4-5 shows the location of the scientifically interesting sites by site number on the lunar mosaic. Significant photo supporting data for each of these sites are shown in Table 4-3.

The selected science sites are located between 55°N and 45°S latitudes. As such, the photographic altitude varied between 96 and 248 kilometers from near-vertical attitude to 58 degrees camera axis tilt. Thus depending on the photo altitude and orientation, the on-axis telephoto photo resolution ranged from 2 to 7 meters. Spacecraft attitude control was sufficient to ensure that the desired feature or area was within the narrow field of view of the telephoto lens.

The 20 science sites and one Surveyor site were photographed with 68 exposures. Eight sites

were covered by single-frame exposures. Two eight-frame fast-mode sequences, four four-frame slow-mode sequences, and seven four-frame fast-mode sequences were initiated to obtain the desired coverage of the remaining 13 sites.

Each of the sites of interest to the Apollo Applications Program is included in the basic category of scientifically interesting sites because it satisfies all of the criteria established for a scientifically interesting site, as well as meeting the "landability" criteria. Thus, the discussion and tabulation of supporting data has been separated for reader convenience in the following.

Mission V photo sites were also selected to screen potential sites for the Apollo Applications Program in much the same manner as was done by Lunar Orbiters I and II for the Apollo program. A group of scientifically interesting sites was selected for Mission V on the basis of the far more detailed data obtained from Mission IV. Fifteen sites, located between 40°N and 25°S latitude, were photographed with 62 exposures. Except for two single-frame exposures and two eight-frame fast-mode sequences, all sites were photographed with four-frame fast-mode sequences.

A wide variety of terrain variations, topographic features, and surface characteristics was included in these sites. Spacecraft attitude control and camera pointing accuracy were sufficient to locate the critical target features within the narrow field of view of the telephoto lens. Photography of these sites was considered of high quality and the resolution was well within the system specifications. Some of the photos were exposed to obtain detailed information on a specific area or feature and it was expected that there could be some degradation in the surrounding areas.

Telephoto photography provided detailed information (resolution of 2 to 4 meters) on the following types of surface features within the 15 sites.
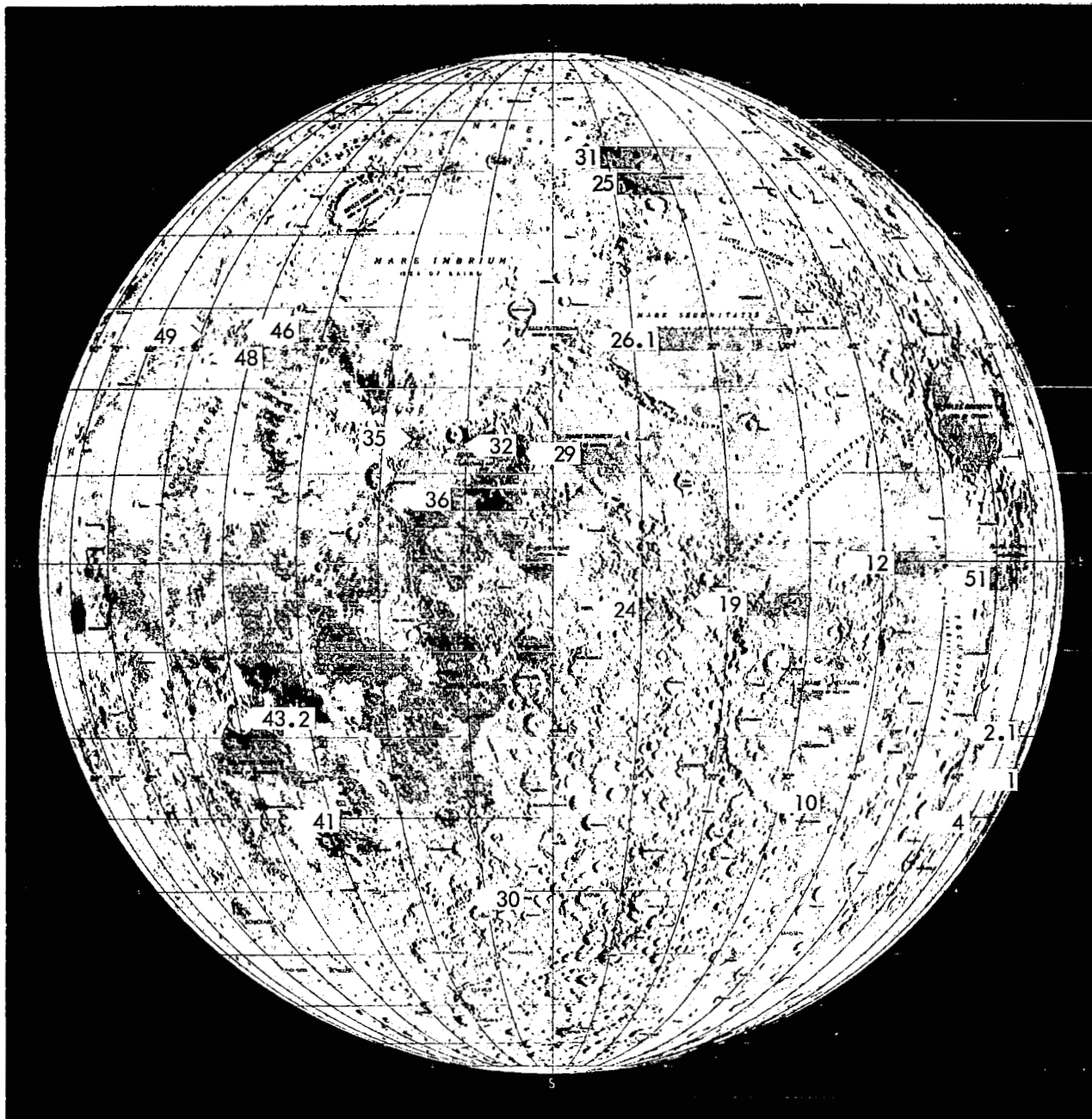- Rille structures and ray systems

Figure 4-5: Scientifically Interesting Site Locations

- Thermal anomaly craters
- Upland and mare terrain
- Crater chains
- Crater floors
- Dark-haloed and multiple-ringed craters
- Layered materials
- Domes

In addition to these specific features, the surrounding areas were covered with the same resolution. All of the desired photos and surface coverage were obtained as planned. These basic data provide excellent visibility of many sites at widely separated locations on the nearside for future lunar explorations.

72

Table 4-3: Supporting Data — Scientifically Interesting Sites

Photo Site	Spacecraft Exposure No./Orbit	Shutter Speed (sec)	Location of Photo Center Long. (deg)	Location of Photo Center Lat. (deg)	Spacecraft Altitude (km)	Spacecraft Slant Distance (km)	Approximate Framelet Width Wide Angle (km)	Approximate Framelet Width Tele photo (km)	Phase Angle (deg)	Alpha (deg)	Angle of Incidence (deg)	Camera Axis Tilt Angle (deg)	Camera Axis Tilt Azimuth (deg)
V-1	33-36/15	0.02	61.2°E	25.5°S	143-140	144-141	4.6-4.5	0.60-0.59	75.4	-3.7	71.7	5.5	129
-2.1	37/17	0.02	57.1°E	19.1°S	123	123	3.9	0.51	67.3	3.6	70.8	3.5	246
-4	40/20	0.02	52.0°E	31.3°S	162	165	5.2	0.69	83.3	-10.1	73.3	10.7	111
-5.1	41/21	0.01	47.2°E	2.0°S	98	175	5.6	0.73	15.9	55.2	72.6	53.5	275
-10	54/30	0.01	27.9°E	27.7°S	131	273	8.7	1.14	33.8	35.2	79.5	57.6	228
-12	63/33	0.02	32.8°E	0.4°S	96	111	3.5	0.46	98.5	-30.9	67.5	29.3	95
-19	84/42	0.02	13.9°E	15.0°S	113	113	3.6	0.47	71.2	1.6	72.8	2.2	219
-24	98-101/48	0.02	4.0°E	4.7°S	99	100	3.2	0.42	66.8	5.3	72.1	5.1	268
-25	102/49	0.02	1.0°E·	48.3°N	248	310	9.8	1.29	53.2	22.1	77.8	34.1	242
26.1	104-107/50	0.04	2.9°E	25.8°N	125-137	126-138	4.0-4.4	0.52-0.57	66.0	5.0	71.0	4.6-6.3	276-318
-29	120-123/54	0.04	3.8°W	12.8°N	104	107	3.4	0.45	83.1	-12.8	70.4	12.0	88
-30	125-128/55	0.04	11.8°W	42.0°S	218-210	219-210	7.0-6.7	0.91-0.87	79.8	1.2	80.9	4.2	183
-31	129-132/56	0.04	1.6°W	52.3°N	230-240	232-243	7.4-7.7	0.97-1.01	78.9	-5.7	73.1	7.3	60
-32	133-136/57	0.02	10.7°W	13.3°N	103-108	105-110	3.3-3.5	0.44-0.46	60.4	11.7	72.1	11.3	279
-35	142-145/61	0.04	16.1°W	14.4°N	105-111	107-112	3.4-3.6	0.45-0.47	80.5	-9.1	71.3	8.7	99-77
-36	146-149/62	0.04	18.0°W	6.8°N	100	105	3.3	0.44	87.9	-16.5	71.5	15.5	93
-41	168/70	0.04	37.6°W	30.6°S	167	170	5.4	0.71	69.9	10.5	80.4	9.6	255
-43.2	177-180/73	0.04	39.9°W	17.1°S	129-120	130-120	4.1-3.8	0.54-0.50	82.2	-5.6	76.6	6.2	130-96
-46	186-193/77	0.04	43.6°W	26.9°N	134-142	134-142	4.3-4.5	0.56-0.59	73.5	0.3	73.9	0.9-3.3	351-360
-48	194-201/79	0.02	47.4°W	23.2°N	125-131	125-131	4.0-4.2	0.52-0.55	74.6	-0.7	74.0	2.1	22
-49	202-205/80	0.04	49.6°W	25.4°N	132-135	133-136	4.2-4.3	0.55-0.57	68.5	6.1	74.6	6.2	298

Figure 4-6 shows the location of the scientifically interesting "landable" areas (of interest to the Apollo Applications Program) on a lunar mosaic. The numbers shown correspond to the Mission V site number. Significant photo supporting and orientation data for each photo sequence are shown in Table 4-4. Where two numbers are shown, they correspond to the first and last photo of the sequence.

Photographic altitudes ranged from 96 to 181 kilometers. Camera axis tilt varied between 0.5 and 18.9 degrees. The maximum variation between photo altitude and slant range was 6
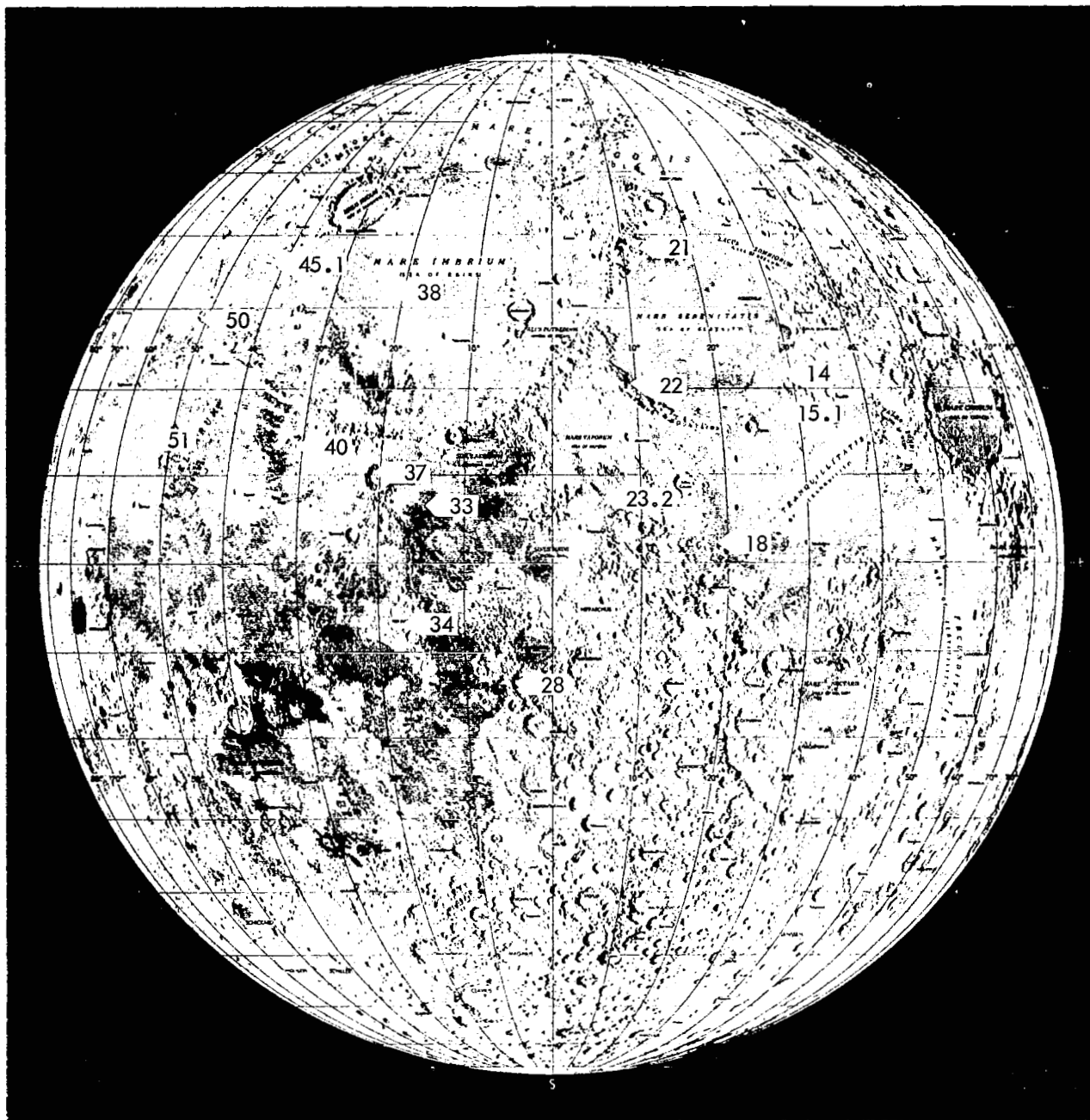
Figure 4-6: Scientifically Interesting "Landable" Site Locations

Table 4-4: Supporting Data -- Scientifically Interesting "Landable" Sites

Photo Site	Spacecraft Exposure No./Orbit	Shutter Speed (sec)	Location of Photo Center		Spacecraft		Approximate Framelet Width		Phase Angle (deg)	Alpha (deg)	Angle of Incidence (deg)	Camera Axis Tilt	
			Long. (deg)	Lat. (deg)	Altitude (km)	Slant Distance (km)	Wide Angle (km)	Telephoto (km)				Angle (deg)	Azimuth (deg)
V-14	66-69/35	0.02	29.3°E	22.0°N	120-123	120-123	3.8-3.9	0.50-0.51	68.4	0.4	68.8	1.4-2.3	354
V-15.1	70/36	0.02	26.4°E	17.2°N	111	113	3.6	0.47*	57.1	12.4	69.5	11.8	283
V-18	80-83/41	0.02	18.1°E	2.7°N	96	99	3.1	0.41*	83.9	−14.6	69.2	13.9	94
V-21	86-89/45	0.02	13.5°E	38.7°N	176-181	176-182	5.6-5.8	0.73-0.76	70.5	0.9	71.5	3.5	359
V-22	90-93/46	0.04	9.1°E	20.7°N	117-119	119-121	3.8	0.50	61.0	9.6	70.7	9.1	285
V-23.2	94-97/47	0.02	5.7°E	7.7°N	99	105	3.3	0.44*	51.7	19.9	71.6	18.9	275
V-28	116-119/53	0.04	3.9°W	14.1° S	113-111	117-115	3.7	0.49-0.48*	87.7	−14.8	73.0	14.5	102
V-33	137/59	0.04	14.7°W	6.5°N	99	102	3.2	0.42*	59.0	13.9	72.8	13.2	277
V-34	138-141/60	0.04	16.7°W	7.2° S	104	104	3.3	0.43	74.2	− 0.6	73.6	1.0	140
V-37	150-157/63	0.02	20.2°W	10.1°N	102-104	103-105	3.3	0.43	77.8	− 5.8	72.0	5.6	78
V-38	159-162/65	0.04	21.9°W	32.5°N	153-157	153-157	4.9-5.0	0.64-0.65	77.6	0.2	72.8	2.5	5.2
V-40	164-167/69	0.04	30.9°W	12.9°N	108	108	3.4	0.45	72.8	0.3	73.0	0.5	342
V-45.1	182-185/76	0.04	41.6°W	35.6°N	165-170	166-171	5.3-5.4	0.69-0.71	68.7	5.9	74.6	5.8	305
V-50	206-209/82	0.04	52.8°W	27.9°N	140-143	140-143	4.4-4.5	0.58-0.60	68.9	6.0	74.9	6.0	299
V-51	210-217/83	0.04	56.1°W	13.7°N	108-111	110-113	3.5-3.6	0.46-0.47	65.3	10.1	75.5	9.7	282

*Framelet width applies only at center

kilometers, which occurred while photographing site V-23.2 from an altitude of 99 kilometers and a tilt angle of 18.9 degrees.

Farside Photo Sites — Photographic coverage of the farside for Mission V was to provide visibility of areas poorly illuminated or not photographed on the previous four missions. The resolution of the photos was to be comparable to that obtained on previous missions. To complete the equatorial coverage of the Moon beyond the western limb, Lunar Orbiter V had to be launched during the first day for the August opportunity. Subsequent launch windows would have resulted in only partial coverage of the area.

Farside photography was taken near apolune on each of the three elliptical orbits. Photography during the initial and intermediate ellipses was taken from altitudes between 2,550 and 5,750 kilometers and between 1,180 and 1,400 kilometers during the final orbit. Initial orbit photo coverage was based on telephoto coverage that provided approximately 150 meters (on-axis) resolution. Final orbit photography provided isolated telephoto but continuous wide-angle coverage with a resolution (on-axis) of about 250 meters. Thus, the Mission V farside photos provided resolution comparable to, or better than, that obtained on the previous missions.

Farside coverage obtained during the Lunar Orbiter program is illustrated in Figure 4-7. The shaded area represents the cumulative coverage of Lunar Orbiters I through IV. Mission V telephoto coverage from the initial and intermediate orbits is outlined by the dashed line. Wide-angle coverage from the final orbit is outlined by the solid line. The figure indicates a small area of the north polar region that was not covered. However, the wide-angle photos from the initial orbits provide visibility of this area, although with less resolution. An additional region near the South Pole was photographed from the initial orbit. The Moon's libration and the location of the terminator in the photo resulted in a failure to recover detail of all of the area photographed. Initial orbit farside photos, near the western limb, provided visibility with less resolution of the northwest sections on the

nearside that were not obtained during Mission IV. With the exception of about 0.5% of the farside surface near the South Pole, the Mission V farside photos completed the coverage of the hemisphere and provided nearside coverage that completed the photographic coverage of the entire nearside lunar surface. Significant supporting data for the farside photos are provided in Table 4-5.

The following photographs, Figures 4-8 through -55, are representative of Mission V photography. Samples were selected to illustrate the many terrain features included in the scientifically interesting sites. In most cases, the photos illustrate a selected area within the complete telephoto or wide-angle photograph. Examples are included of wide-angle photos, with areas or detail of particular interest also shown from the telephoto photographs. Each photograph contains an appropriate descriptive caption.

Figures 4-24 through -27 illustrate the many types of terrain features on the floor, walls, and center rim of the crater Tycho. In addition, the landing site of Surveyor VII is shown in Figure 4-27. The terrain features identified in both Surveyor and Lunar Orbiter photos and used in the triangulation process are indicated.

A study of the crater Copernicus, using a Mission II oblique photo and Mission V vertical coverage, is shown in Figures 4-32 through -37. Areas were selected on the crater floor, inner walls, and the outer rim and are clearly shown on both types of photos.

Figures 4-44 through -49 present a series of photographs illustrating different characteristics of the walls of the crater Aristarchus. The wide-angle photo indicates the areas illustrated by the telephoto photography.

Figure 4-55 is a photo mosaic of the Surveyor VI Sinus Medii landing site and shows the location of the aiming points and actual landing site. This area was also photographed during Mission V vertical photography on Frames 109 and 110.
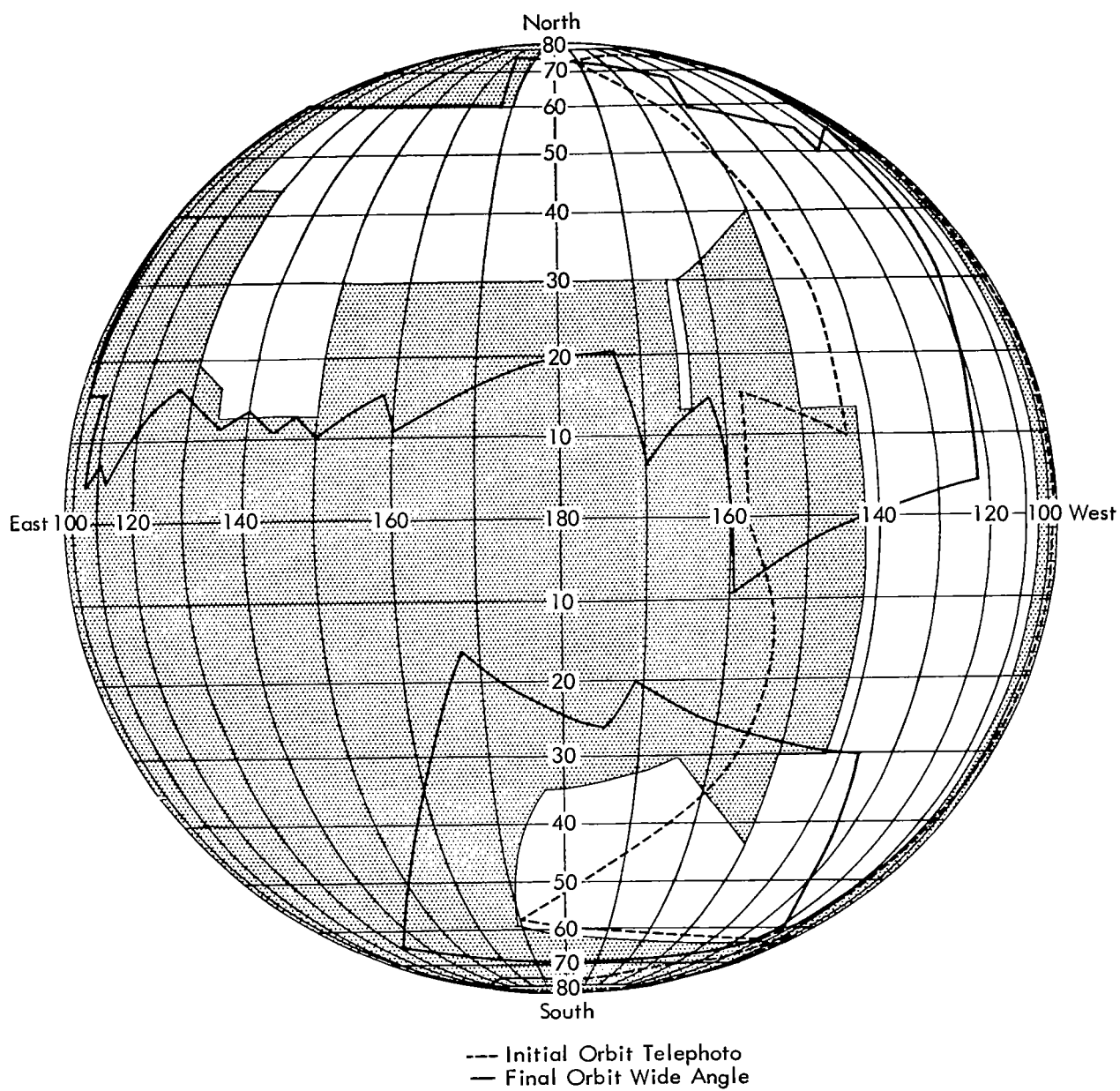
Figure 4-7: Farside Photo Coverage

Table 4-5: Supporting Data -- Farside

Photo Site	Spacecraft Exposure No./Orbit	Shutter Speed (sec)	Location of Photo Center		Spacecraft		Approximate Framelet Width		Phase Angle (deg)	Alpha (deg)	Angle of Incidence (deg)	Camera Axis Tilt	
			Long. (deg)	Lat. (deg)	Altitude (km)	Slant Distance (km)	Wide Angle (km)	Telephoto (km)				Angle (deg)	Azimuth (deg)
VA-1	5-12/2	0.04	110.1°W	60.0°N	2,642-2,745	2,733-2,745	86.9	11	106.8	−23.8	83.0	9.1	287
VA-2	13-20/2	0.04	103.1°W	13.0°N	5,752-5,755	6,006-6,009	191	25	122.0	−35.4	86.6	7.7	277
VA-3	21/3	0.04	178.6°W	83.9°S	3,393	3,955	126	16	119.8	−36.8	85.5	17.0	189
VA-4	22/4	0.04	114.8°W	27.2°S	5,107	5,480	174	23	126.1	−43.6	82.5	10.1	259
VA-6	24/5	0.04	118.6°W	26.3°N	5,006	5,246	167	22	118.7	−35.0	83.8	8.5	281
VA-7.1	25/6	0.04	127.5°W	59.4°N	2,549	2,635	83.7	11	106.3	−23.4	82.8	9.3	284
VA-8	26/7	0.04	127.1°W	27.3°S	5,067	5,417	172	23	125.2	−42.2	83.0	9.9	259
VA-10	28/8	0.04	132.2°W	26.2°N	5,010	5,247	167	22	117.7	−34.8	82.9	8.4	281
VA-11.2	29/9	0.04	145.0°W	59.3°N	2,546	2,656	84.3	11	106.8	−26.4	80.4	10.4	284
VA-12	30/10	0.04	140.4°W	26.6°S	5,067	5,410	172	23	124.2	−41.8	82.4	9.8	260
VA-13	31/11	0.04	135.3°W	28.0°N	1,361	1,570	49.8	6.5	129.7	−41.0	88.7	21.6	280
VA-14	32/13	0.04	137.6°W	24.8°N	1,395	1,597	50.7	6.6	129.8	−40.1	89.7	21.0	280
VA-15	39/19	0.04	158.4°W	38.4°N	1,250	1,550	49.2	6.5	130.1	−49.5	80.6	26.2	282

Table 4-5 (Continued)

Photo Site	Spacecraft Exposure No./Orbit	Shutter Speed (sec)	Location of Photo Center Long. (deg)	Location of Photo Center Lat. (deg)	Spacecraft Altitude (km)	Spacecraft Slant Distance (km)	Approximate Framelet Width Wide Angle (km)	Approximate Framelet Width Telephoto (km)	Phase Angle (deg)	Alpha (deg)	Angle of Incidence (deg)	Camera Axis Tilt Angle (deg)	Camera Axis Tilt Azimuth (deg)
VA-16.1	43/25	0.04	151.4°W	47.7°S	1,189	1,333	42.3	5.6	129.9	−35.6	94.3	20.2	252
VA-17.1	53/29	0.04	175.0°W	48.7°N	1,188	1,430	45.3	6.0	125.3	−44.0	81.5	25.0	297
VA-18.1	65/35	0.04	170.2°W	47.2°S	1,190	1,347	42.8	5.6	129.6	−37.0	92.6	20.9	253
VA-19	79/39	0.04	168.1°E	38.7°N	1,242	1,515	48.1	6.3	127.2	−47.4	79.8	25.4	281
VA-20	85/44	0.04	159.9°E	38.7°N	1,237	1,503	47.7	6.3	126.6	−46.9	79.8	25.2	281
VA-21	103/49	0.04	151.8°E	38.7°N	1,234	1,488	47.2	6.2	125.7	−45.9	79.8	24.8	281
VA-22	124/54	0.04	143.8°E	38.6°N	1,234	1,477	46.9	6.1	124.8	−45.0	79.8	24.4	280
VA-23	158/64	0.04	127.7°E	38.4°N	1,230	1,453	46.1	6.0	123.1	−43.2	79.9	23.6	279
VA-24	163/67	0.04	122.4°E	38.2°N	1,228	1,451	46.1	6.0	122.8	−43.3	79.5	23.7	279
VA-25	181/74	0.04	110.2°E	41.6°N	1,179	1,372	43.6	5.7	120.0	−40.9	79.2	23.0	278
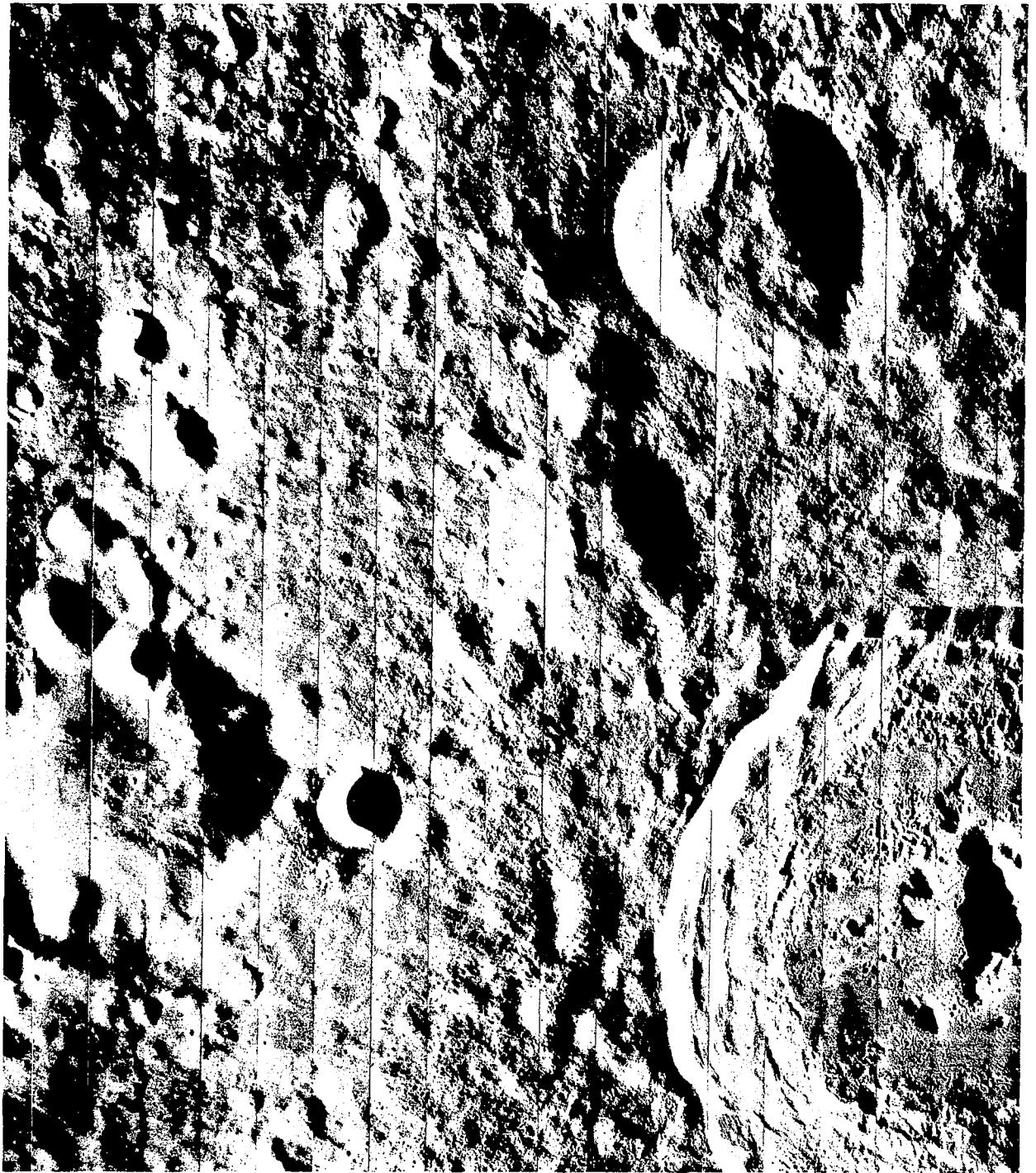
Crater Stevinus A and vicinity; framelet width 5.2 kilometers.

Figure 4-8: Wide-Angle Frame 40, Site V-4

Centered on crater Messier; framelet width 730 meters.

Figure 4-9: Section of Telephoto Frame 41, Site V-5.1

Centered on crater Messier A; framelet width 730 meters.

Figure 4-10: Section of Telephoto Frame 41, Site V-5.1

82
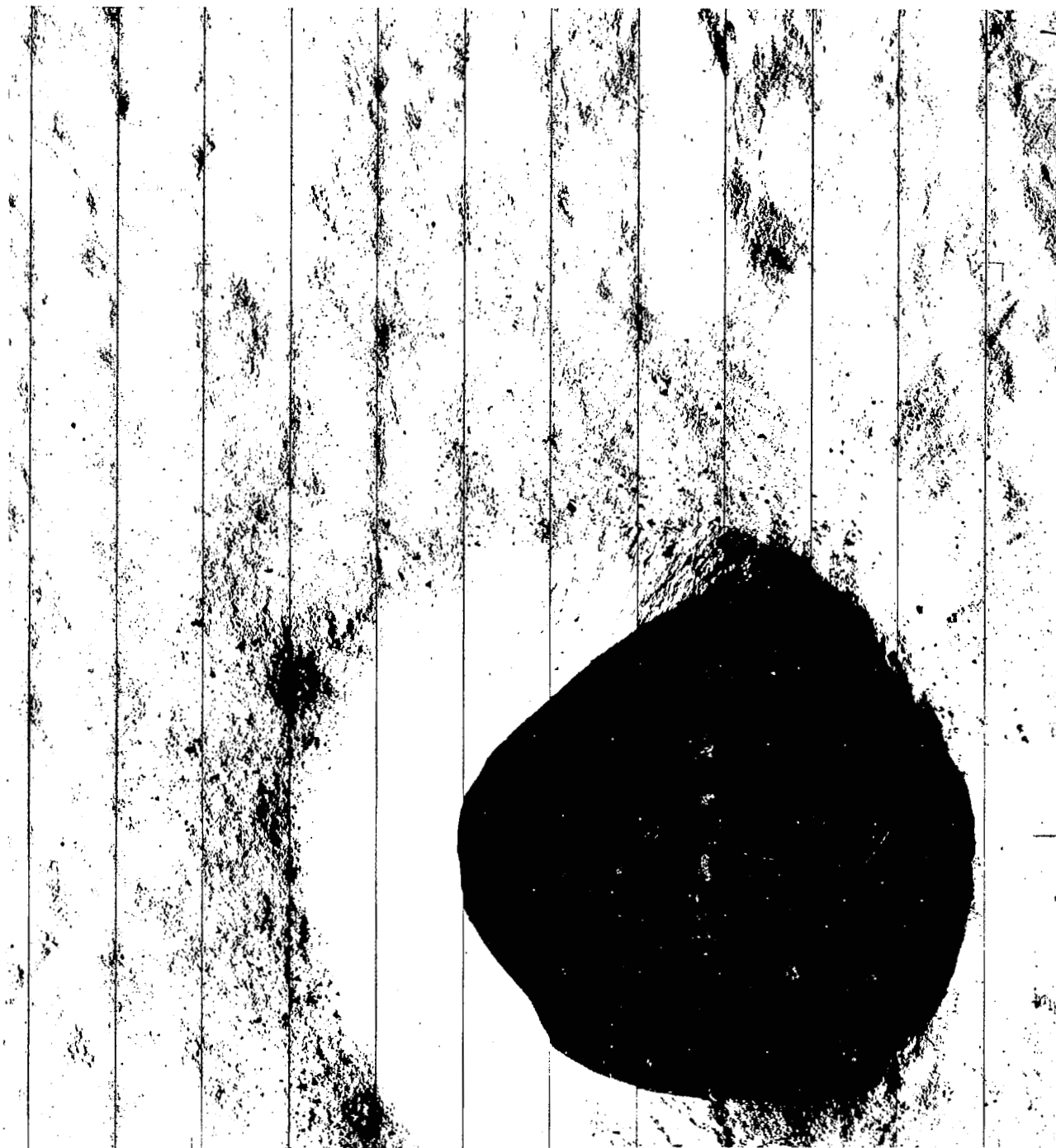
Centered on crater Censorinus; framelet width 460 meters.

Figure 4-11: Section of Telephoto Frame 63, Site V-12
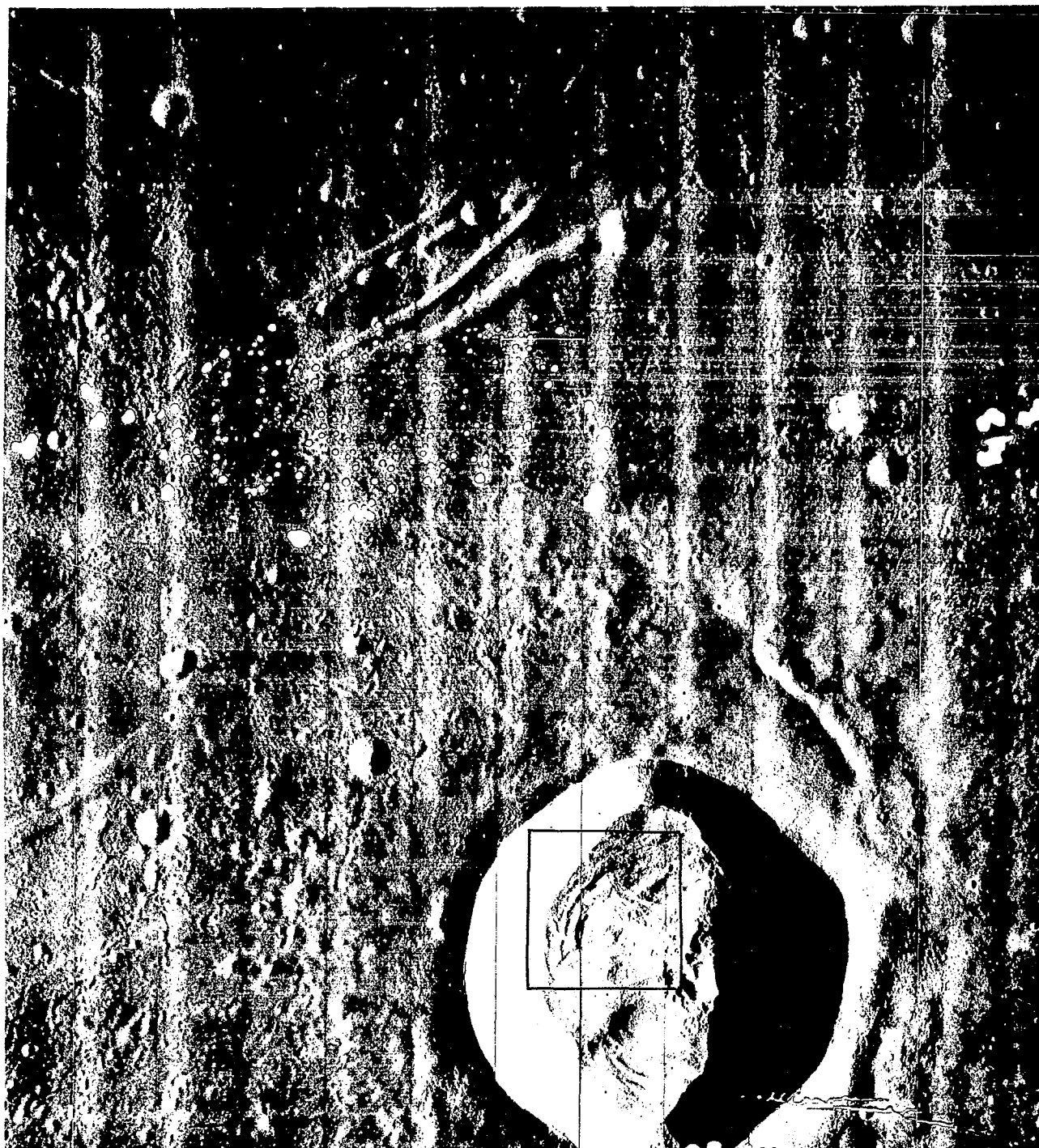
Centered on crater Dawes (outlined area covered by Figure 4-13); framelet width 3.6 kilometers.

Figure 4-12: Section of Wide-Angle Frame 70, Site V-15.1

Shows crater floor, northwest crater wall, and some processing (lace) defects; framelet width 470 meters.

Figure 4-13: Section of Telephoto Frame 70, Site V-15.1

85
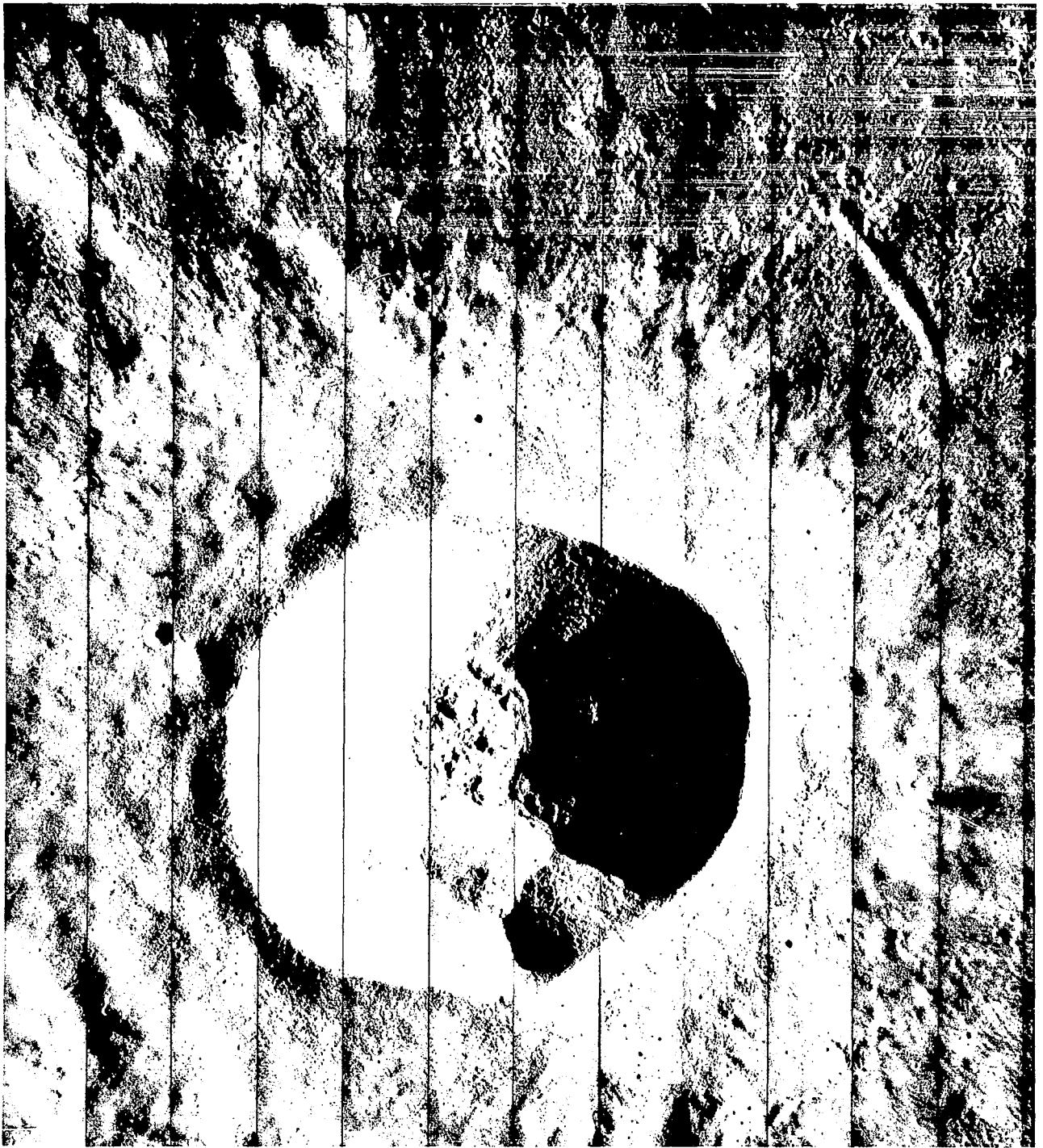
Centered on crater Dionysius; framelet width 3.1 kilometers.

Figure 4-14: Section of Wide-Angle Frame 81, Site V-18

Centered on Sulpicius Gallus Rille; framelet width 3.8 kilometers.

Figure 4-15: Section of Wide-Angle Frame 91, Site V-22
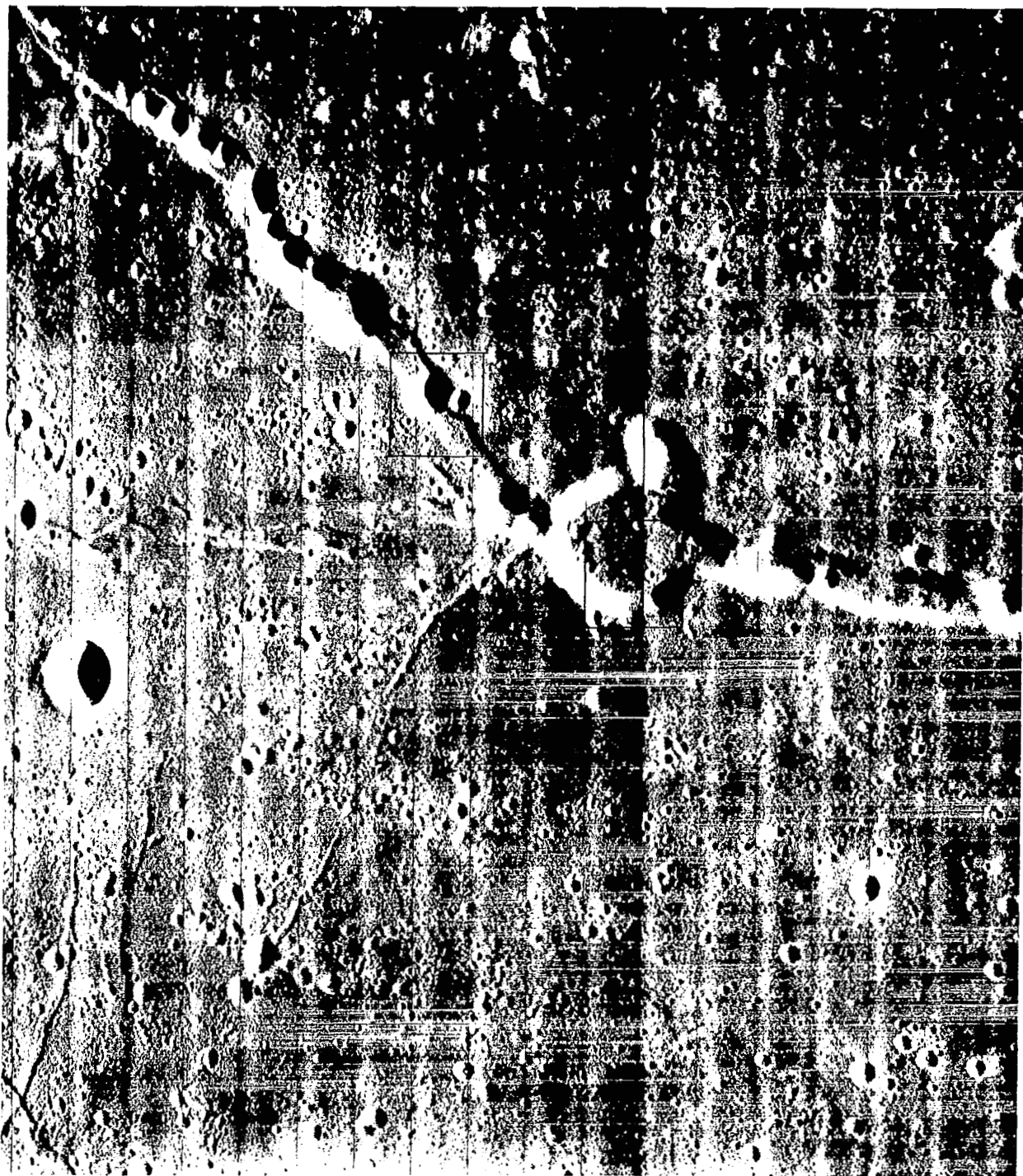
Hyginus Rille and vicinity (indicated areas covered by Figures 4-17, -18, and -19); framelet width 3.3 kilometers.

Figure 4-16: Wide-Angle Frame 95, Site V-23.1

Craters along rille structure; framelet width 440 meters.

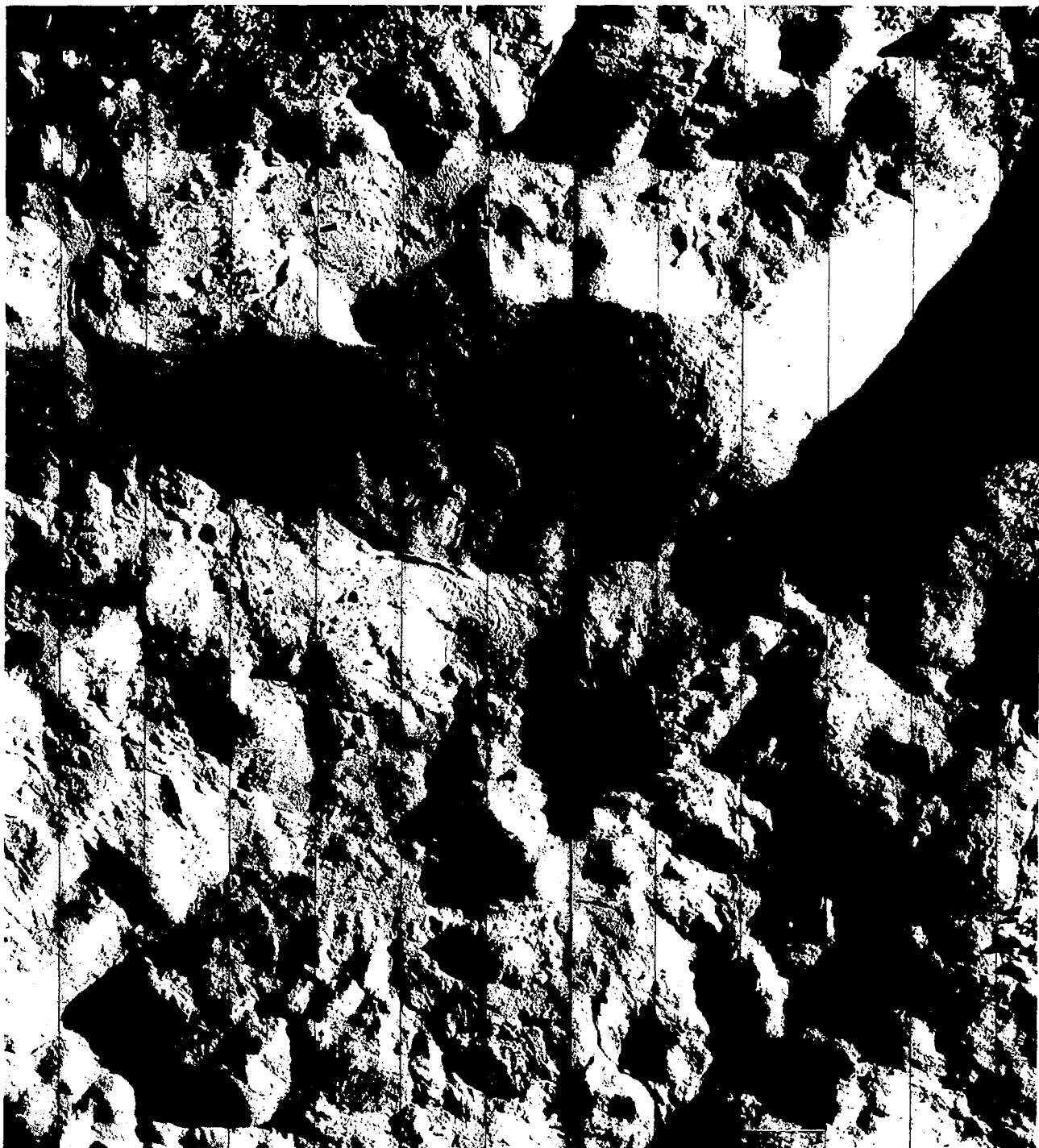Figure 4-17: Section of Telephoto Frame 96, Site V-23.1
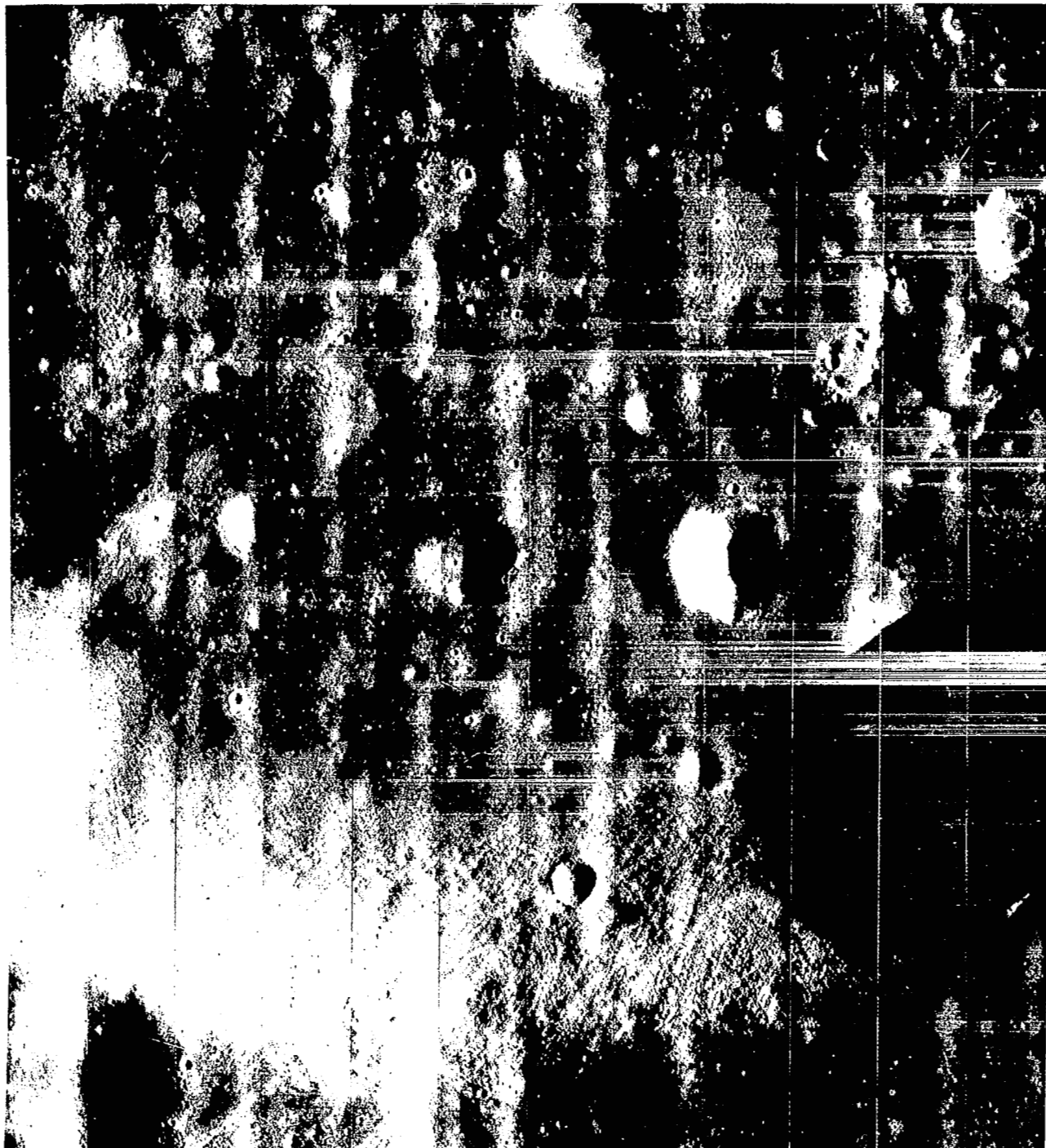
South wall of main crater; framelet width 440 meters.

Figure 4-18: Section of Telephoto Frame 95, Site V-23.1
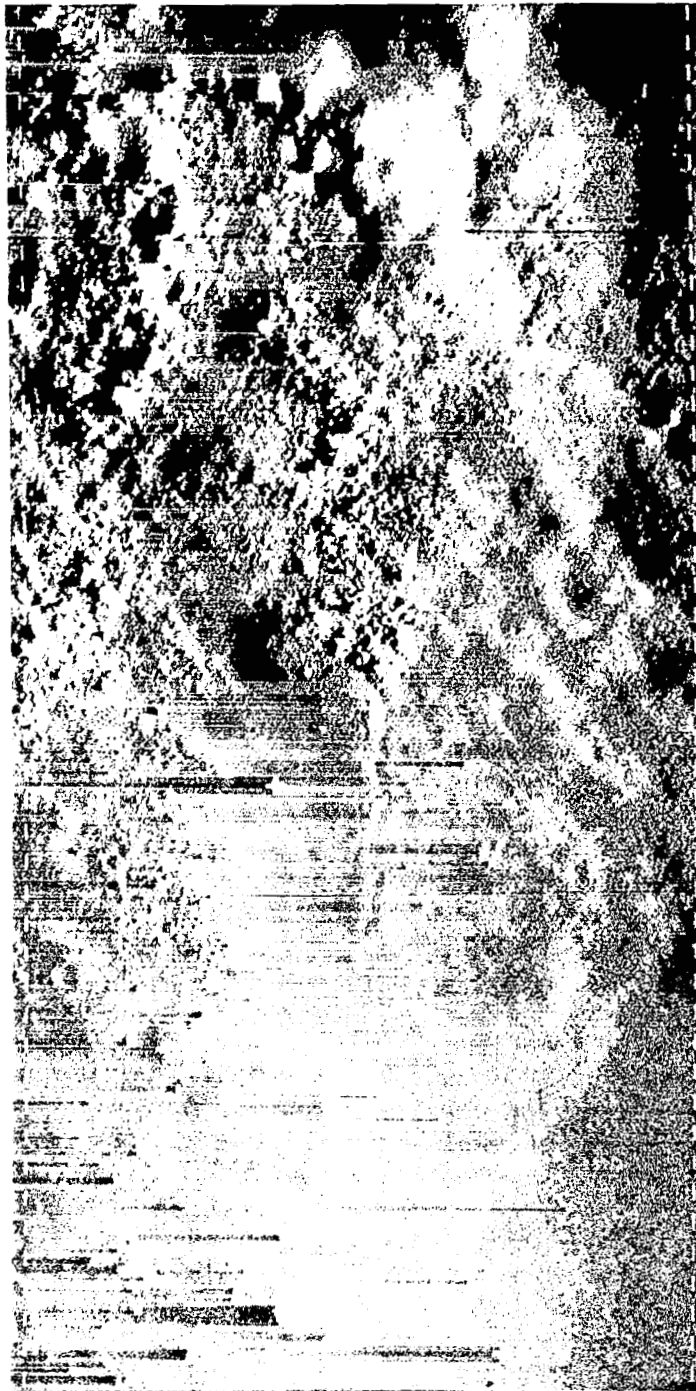
Enlargement of rolling stone; framelet width 440 meters.

Figure 4-19: Section of Telephoto Frame 95, Site V-23.1.
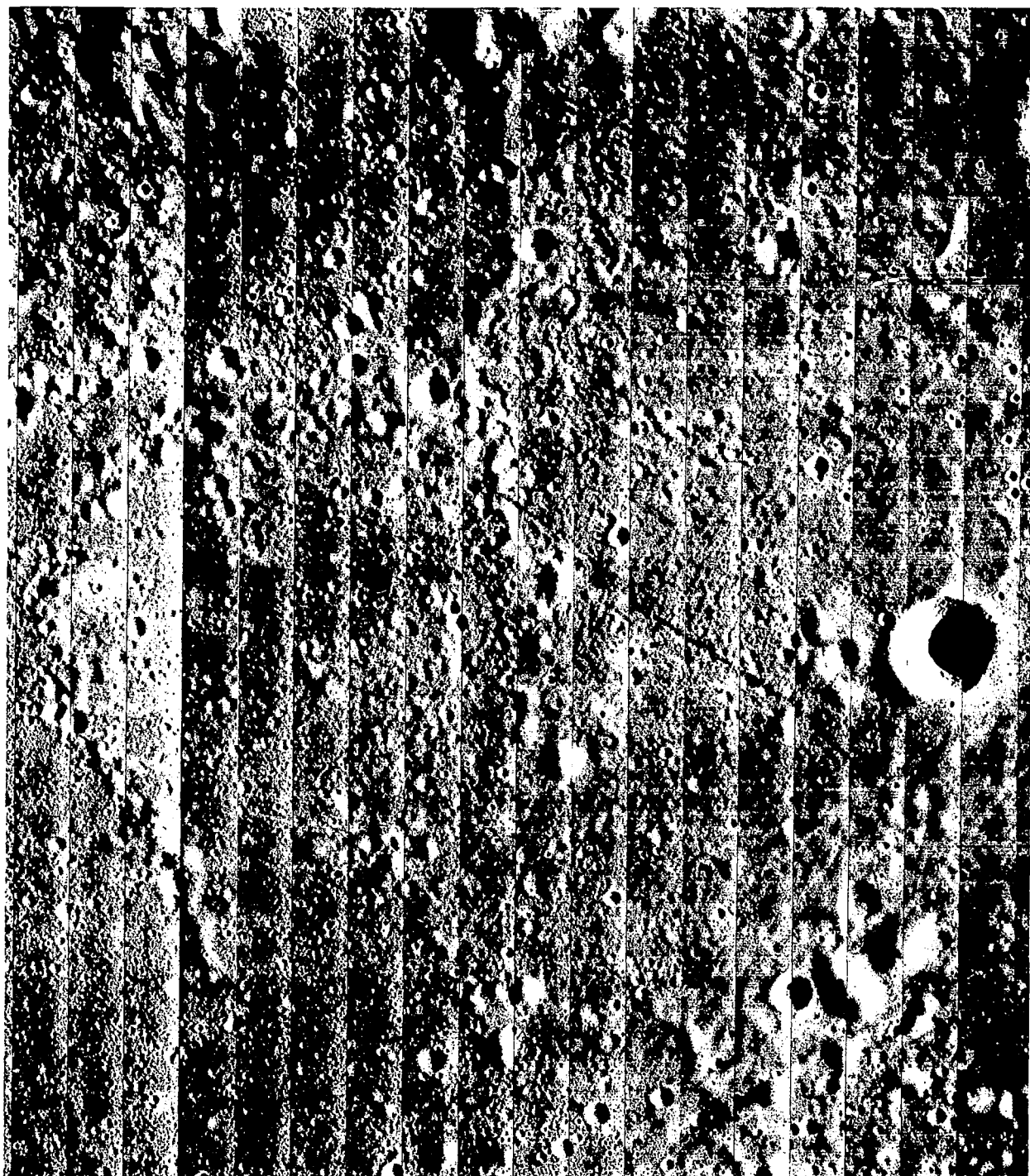
Potential Surveyor landing area on floor of crater Hipparchus; framelet width 3.2 kilometers.

Figure 4-20: Wide-Angle Frame 99, Site V-24

Rille area of Rima Bode II; framelet width 450 meters.

Figure 4-21: Section of Telephoto Frames 121 and 122, Site V-29

Hadley Rille and vicinity (outlined area covered by Figure 4-23); framelet width 4.1 kilometers.
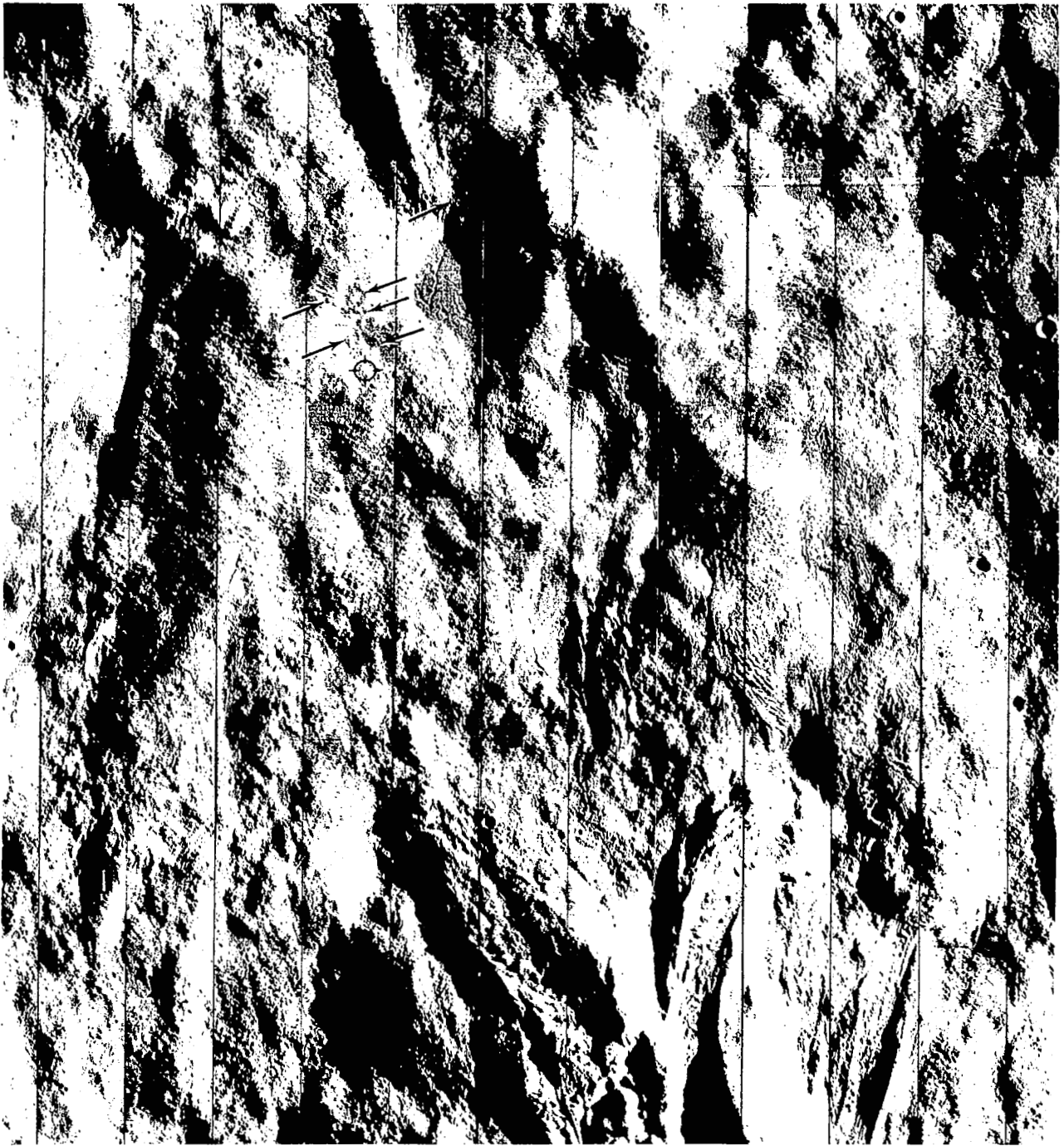
Figure 4-22: Wide-Angle Frame 105, Site V-26.1
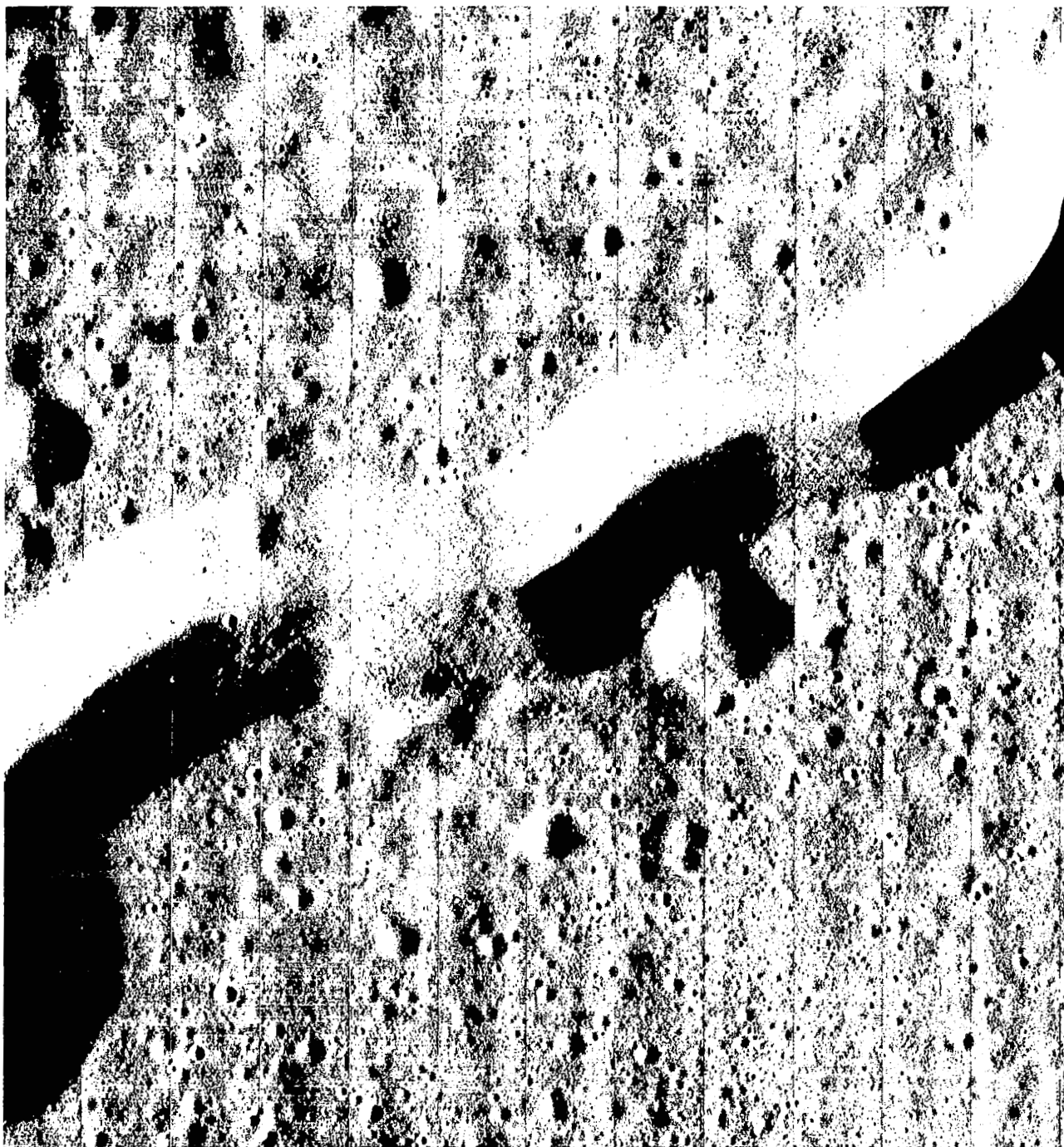
Section of rille structure; framelet width 540 meters.

Figure 4-23: Section of Telephoto Frame 105, Site V-26.1
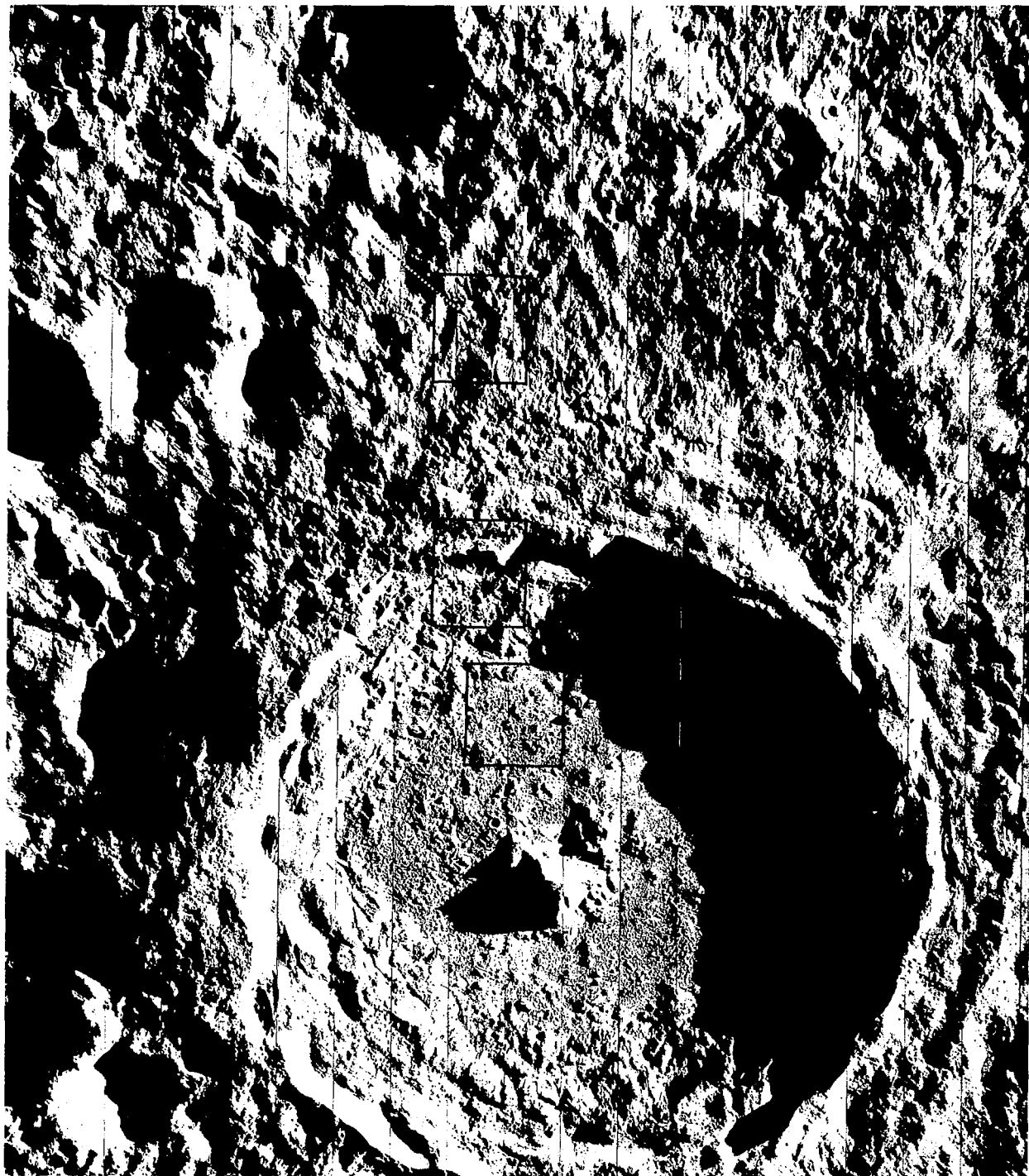
Crater Tycho and vicinity (outlined areas covered by Figures 4-25, -26, and -27); framelet width 6.9 kilometers.

Figure 4-24: Wide-Angle Frame 126, Site V-30
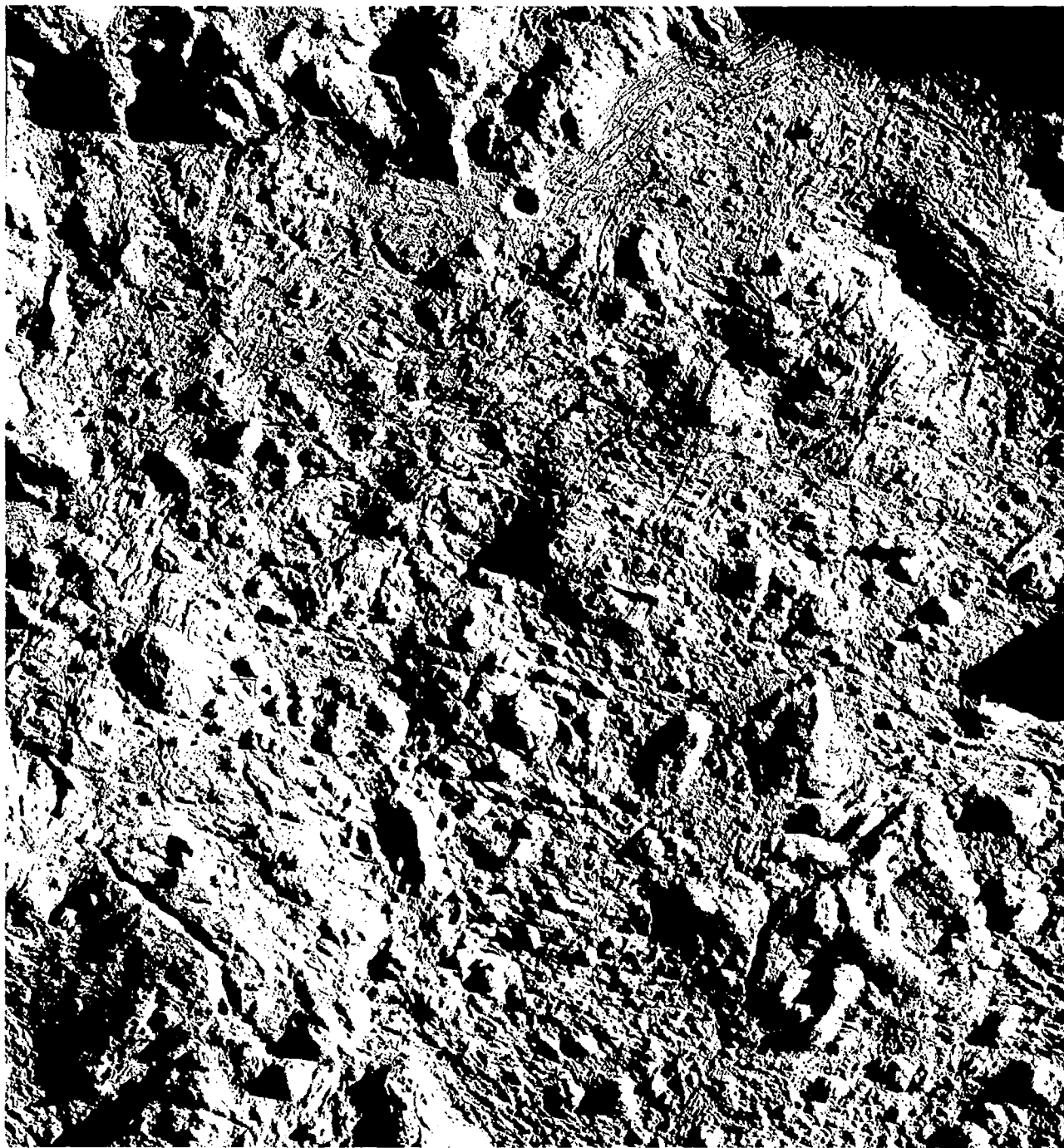
North area of crater floor; framelet width 910 meters.

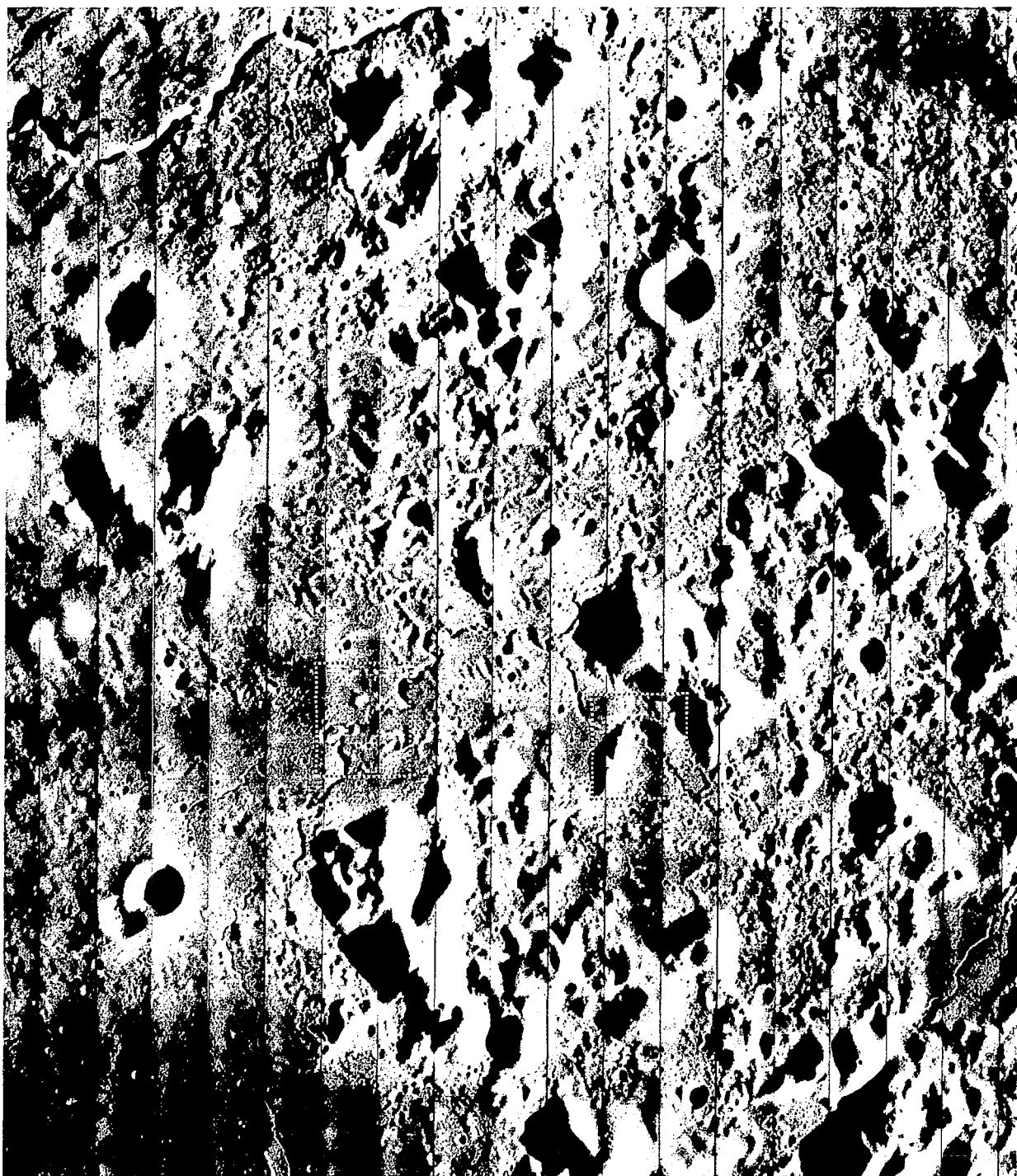Figure 4-25: Section of Telephoto Frame 125, Site V-30

97

Crater wall — north side; framelet width 900 meters.

Figure 4-26: Section of Telephoto Frame 126, Site V-30

Outer rim — north side; framelet width 870 meters.

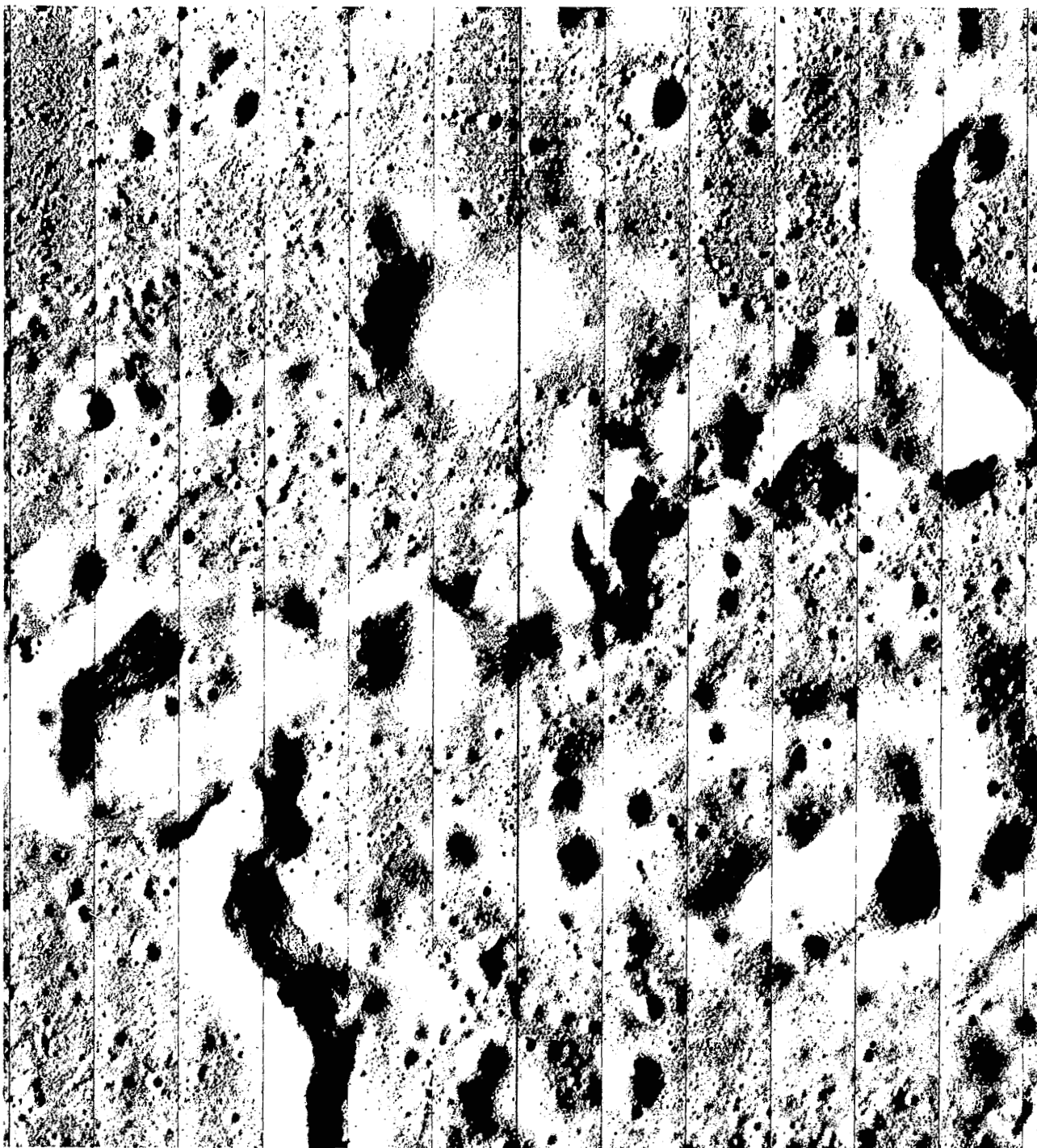Figure 4-27: Section of Telephoto Frame 128, Site V-30

Sinuous rille east of Plato and vicinity (outlined areas covered by Figures 4-29 and -30); framelet width 7.6 kilometers.

Figure 4-28: Wide-Angle Frame 131, Site V-31

100

Section of rille structures; framelet width 990 meters.

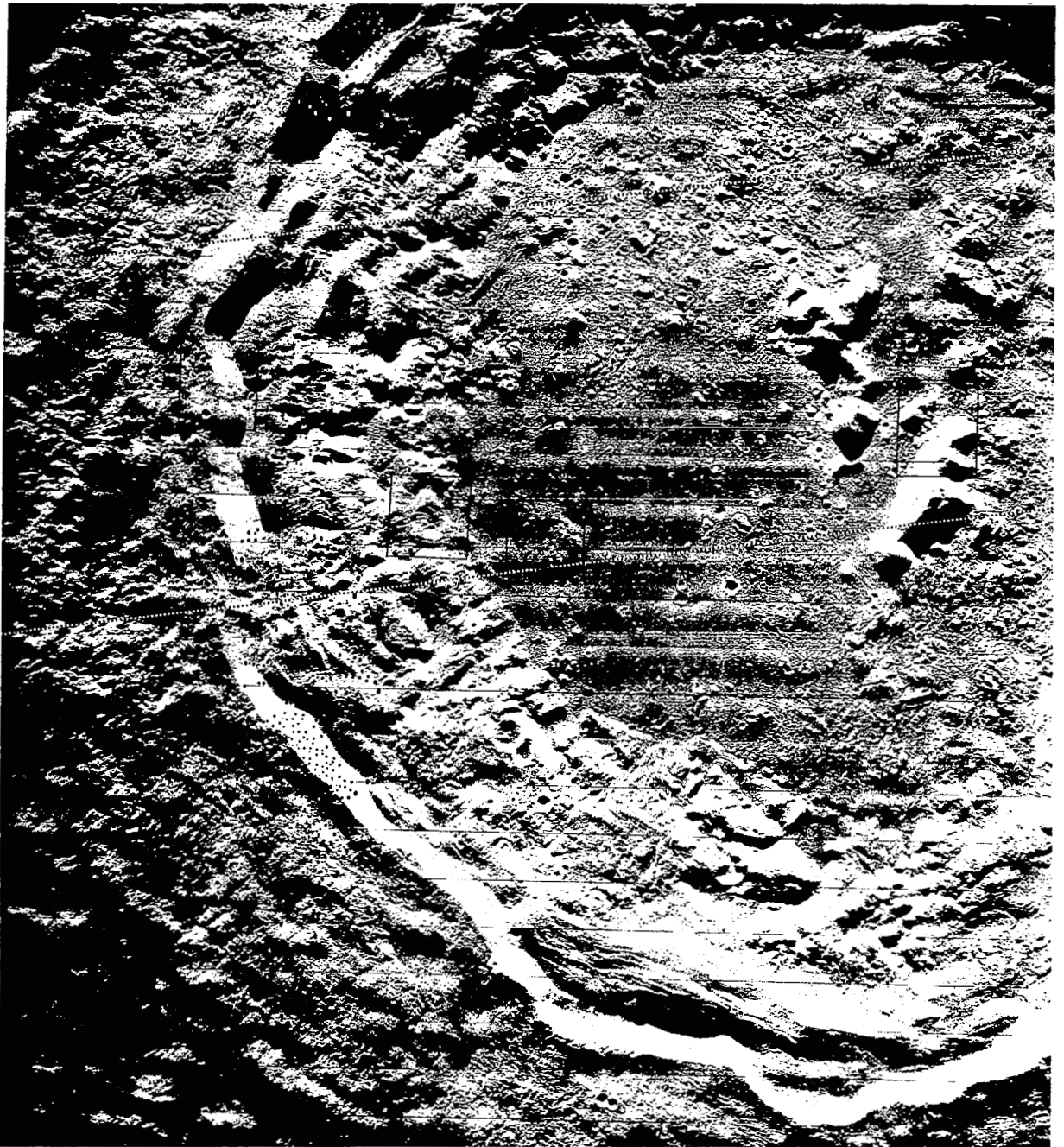Figure 4-29: Section of Telephoto Frame 130, Site V-31

Section of rille structure; framelet width 990 meters.

Figure 4-30: Section of Telephoto Frame 130, Site V-31

Crater Eratosthenes and vicinity; framelet width 3.5 kilometers.

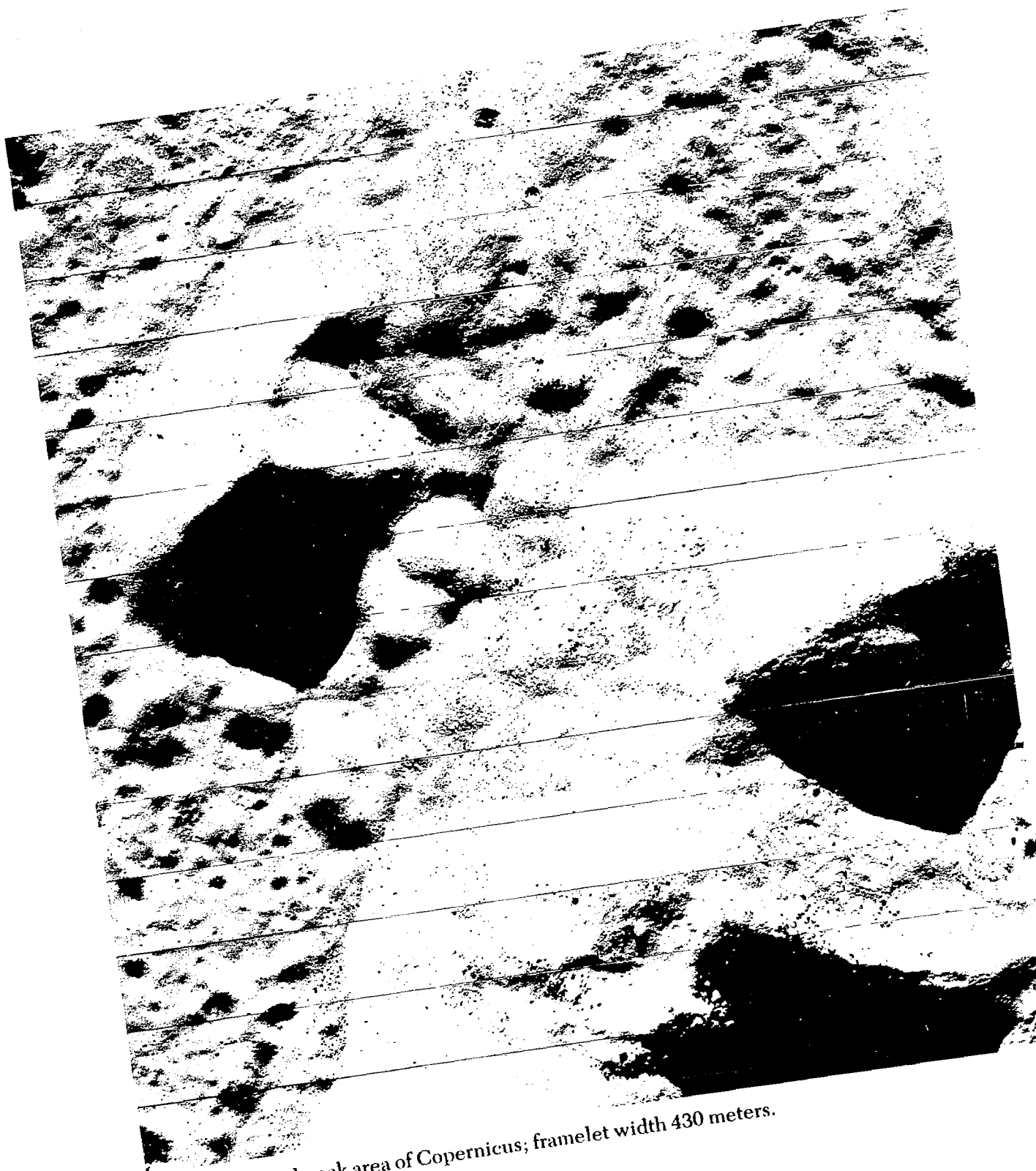**Figure 4-31: Wide-Angle Frame 136, Site V-32**

Northern portion of crater Copernicus (indicated areas covered by Figures 4-33 through -37); framelet width 3.2 kilometers.

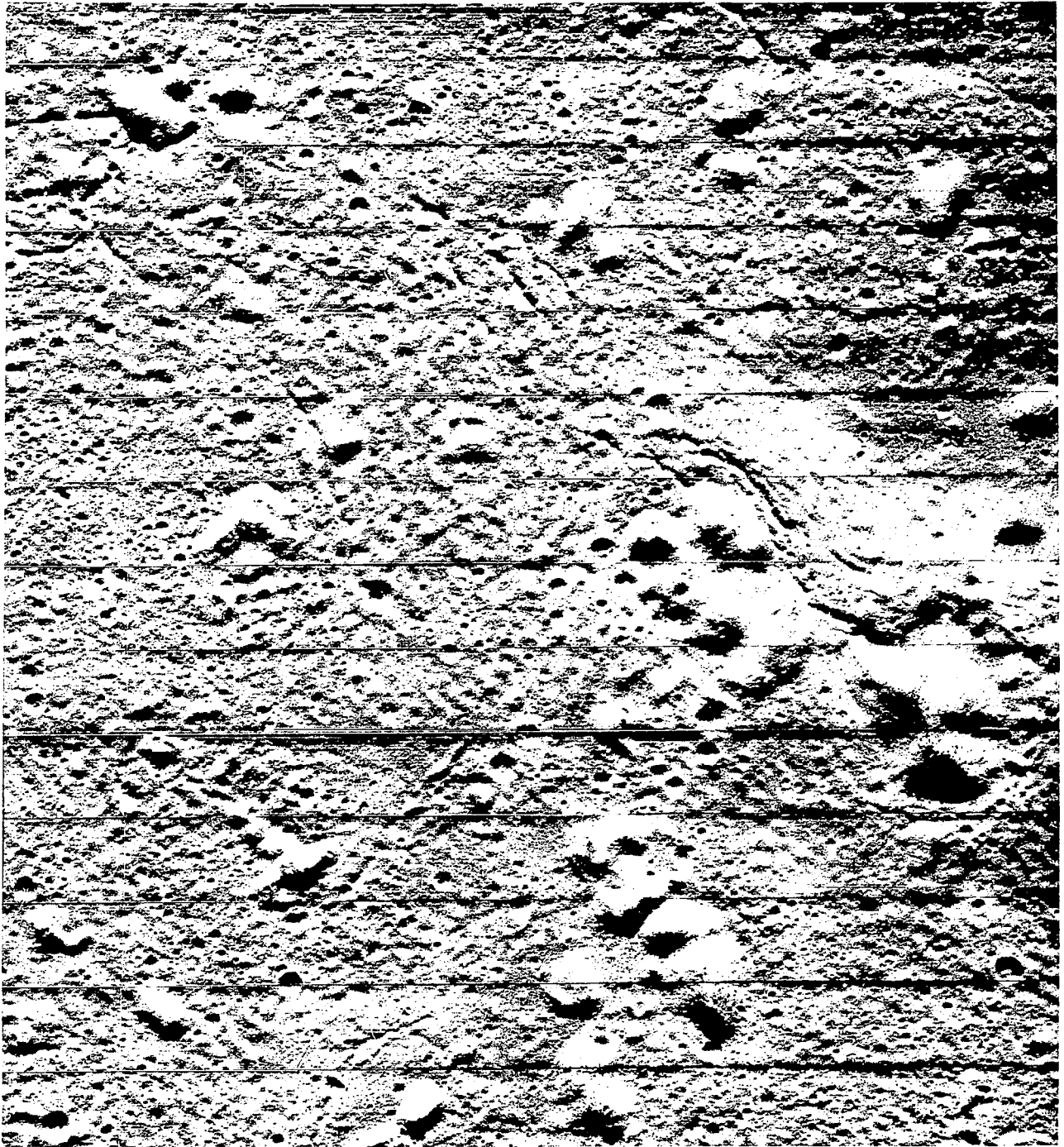**Figure 4-32: Wide-Angle Frame 154, Site V-37**

Oblique view of crater taken during Mission II (indicated areas covered by Figures 4-34 through -37).

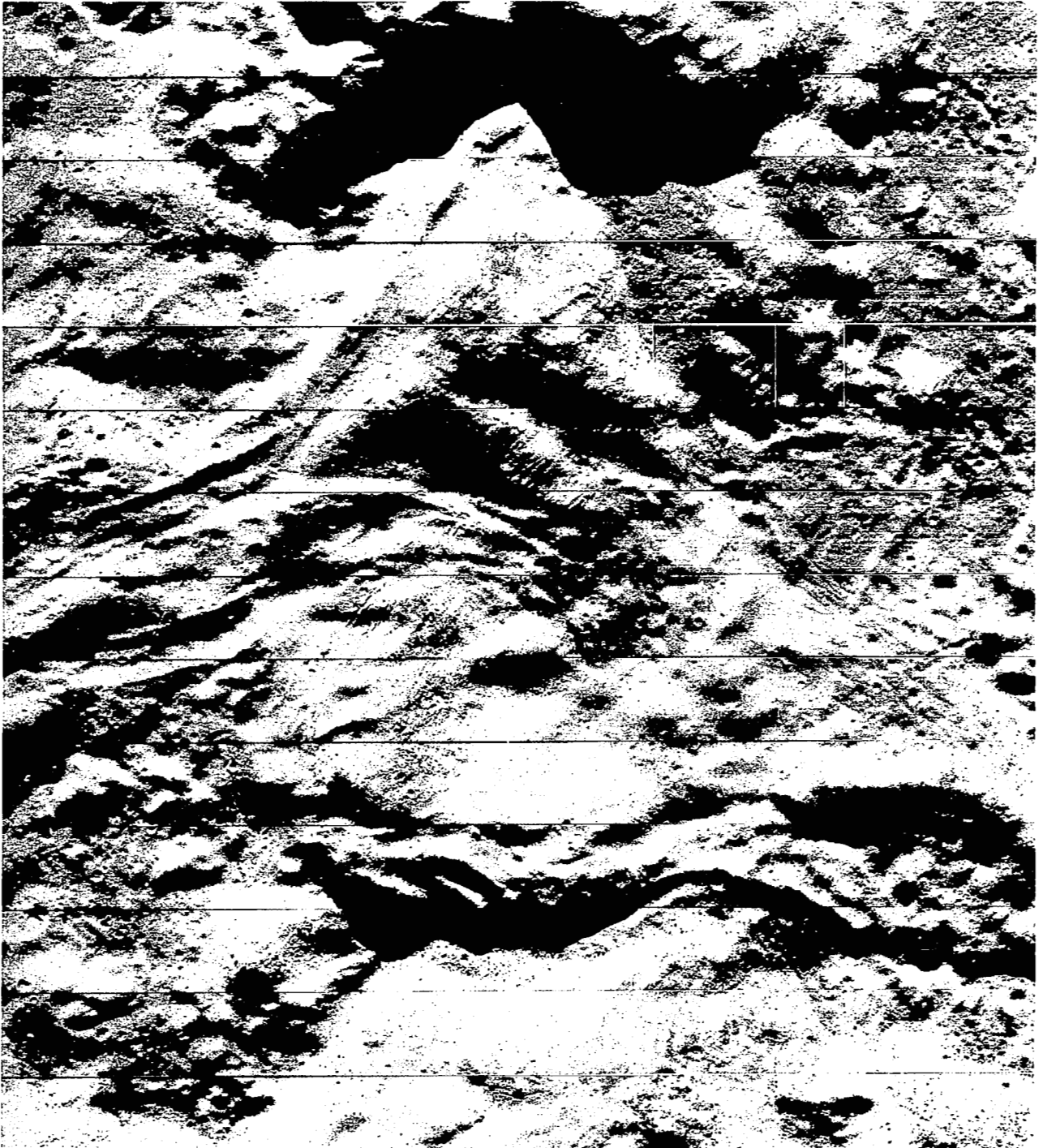**Figure 4-33: Section of Telephoto Frame 162, Site II S-12**

Central peak area of Copernicus; framelet width 430 meters.

Figure 4-34: Section of Telephoto Frame 151, Site V-37

106

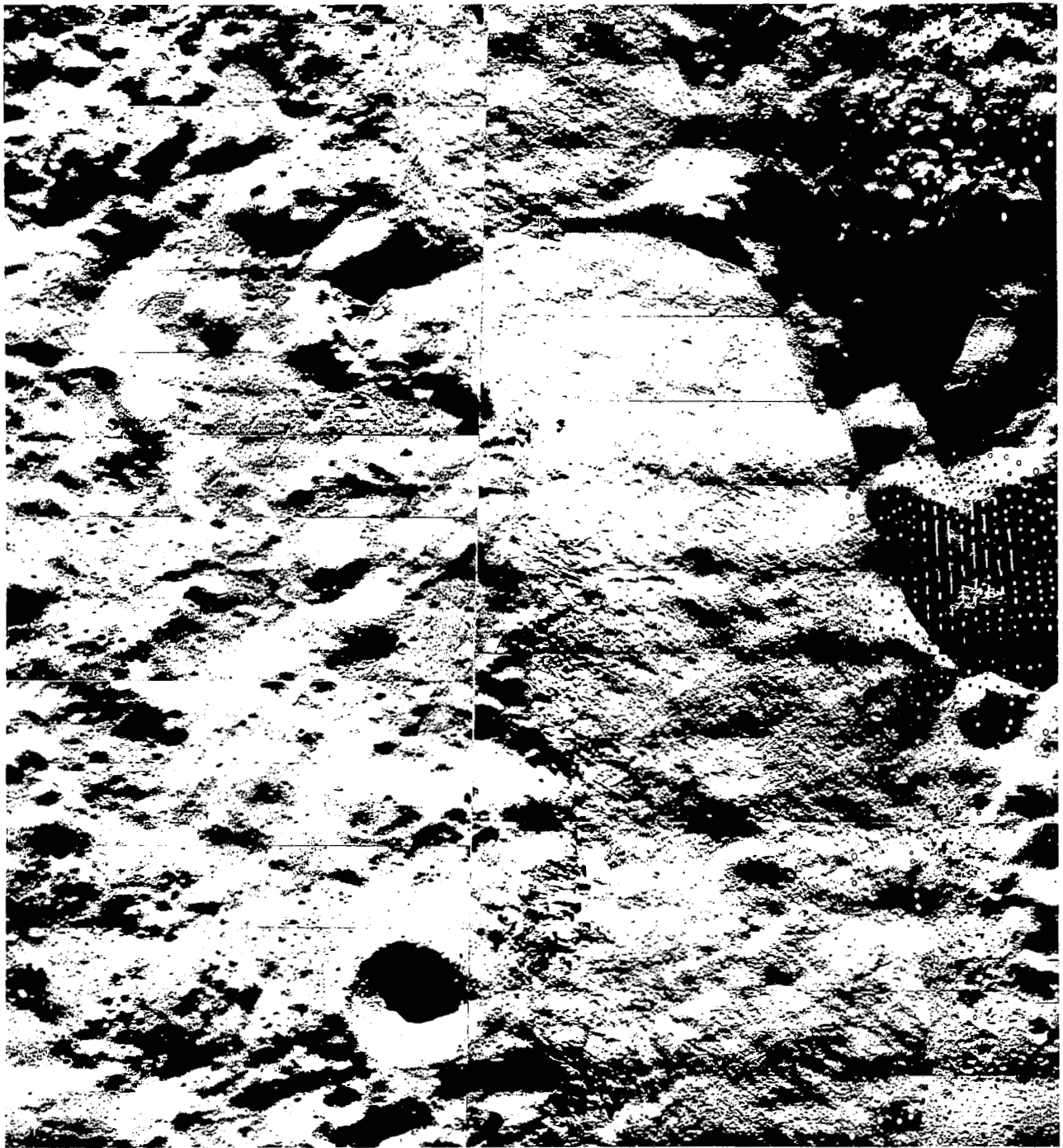Possible landing area in northwest area of crater floor; framelet width 430 meters.

Figure 4-35: Section of Telephoto Frame 154, Site V-37

Section of sinuous flow-like formation in northern inner slope; framelet width 430 meters.

Figure 4-36: Section of Telephoto Frame 155, Site V-37

Section of north crater wall; framelet width 430 meters.

Figure 4-37: Section of Telephoto Frames 156 and 157, Site V-37

Section of western crater floor area; framelet width 710 meters.

Figure 4-38: Section of Telephoto Frame 168, Site V-41

110
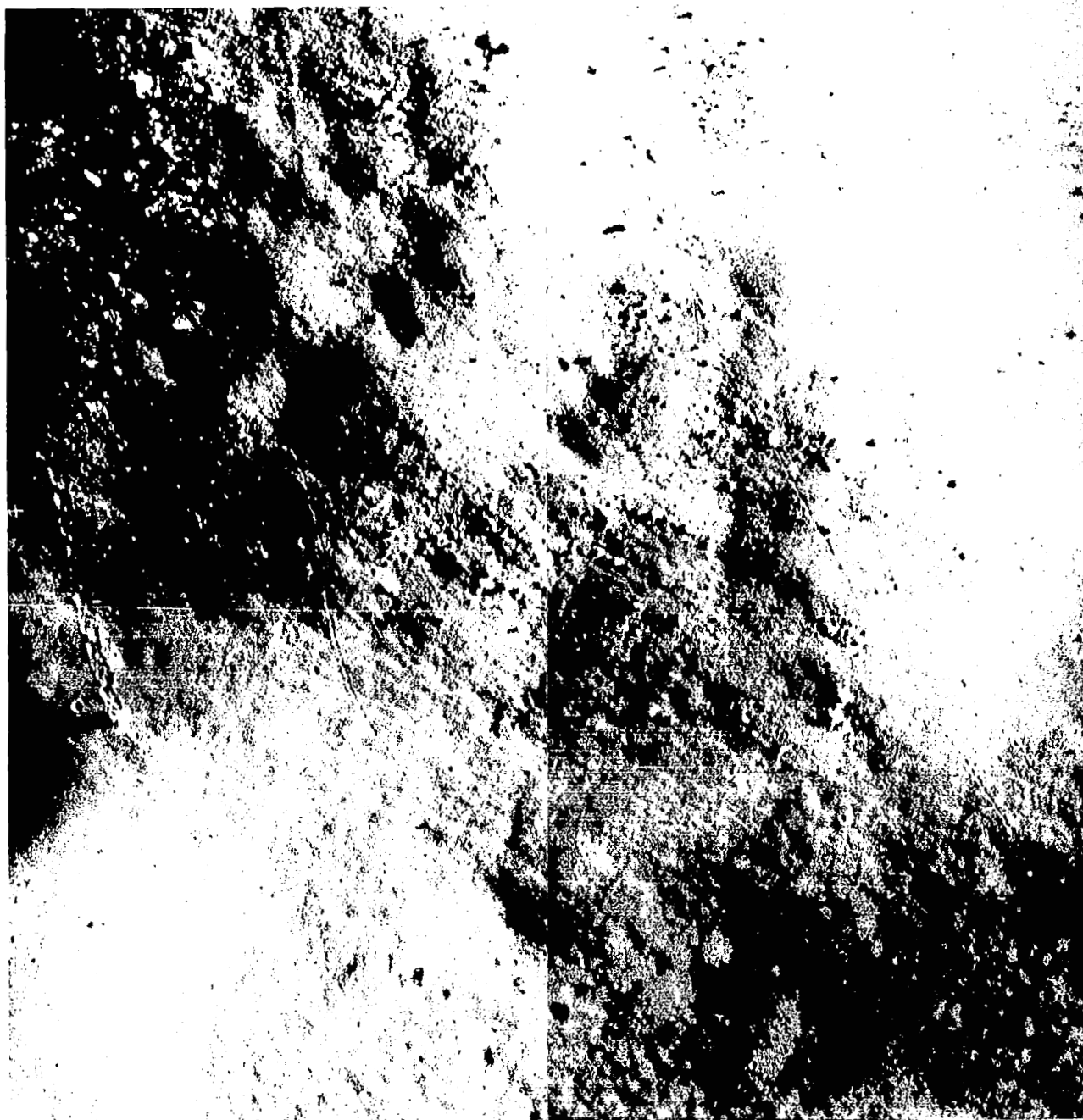
Enlargement of rolling stone tracks on crater floor; framelet width 710 meters.

Figure 4-39: Section of Telephoto Frame 168, Site V-41

Multiringed crater Gruithuisen K; framelet width 700 meters.

Figure 4-40: Section of Telephoto Frame 183, Site V-45.1
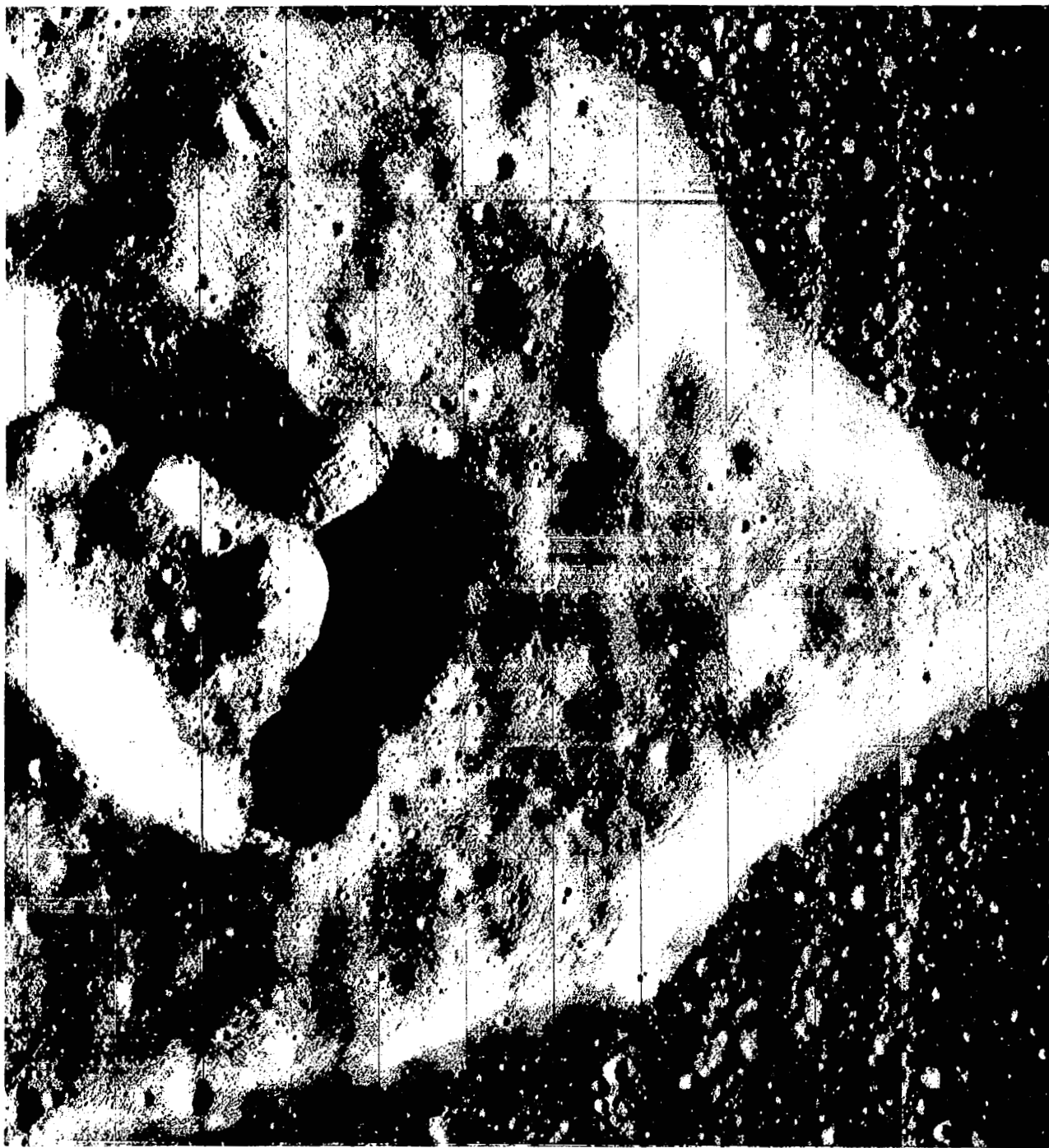
Domed area and crater near Gruithuisen K; framelet width 700 meters.

Figure 4-41: Section of Telephoto Frame 183, Site V-45.1
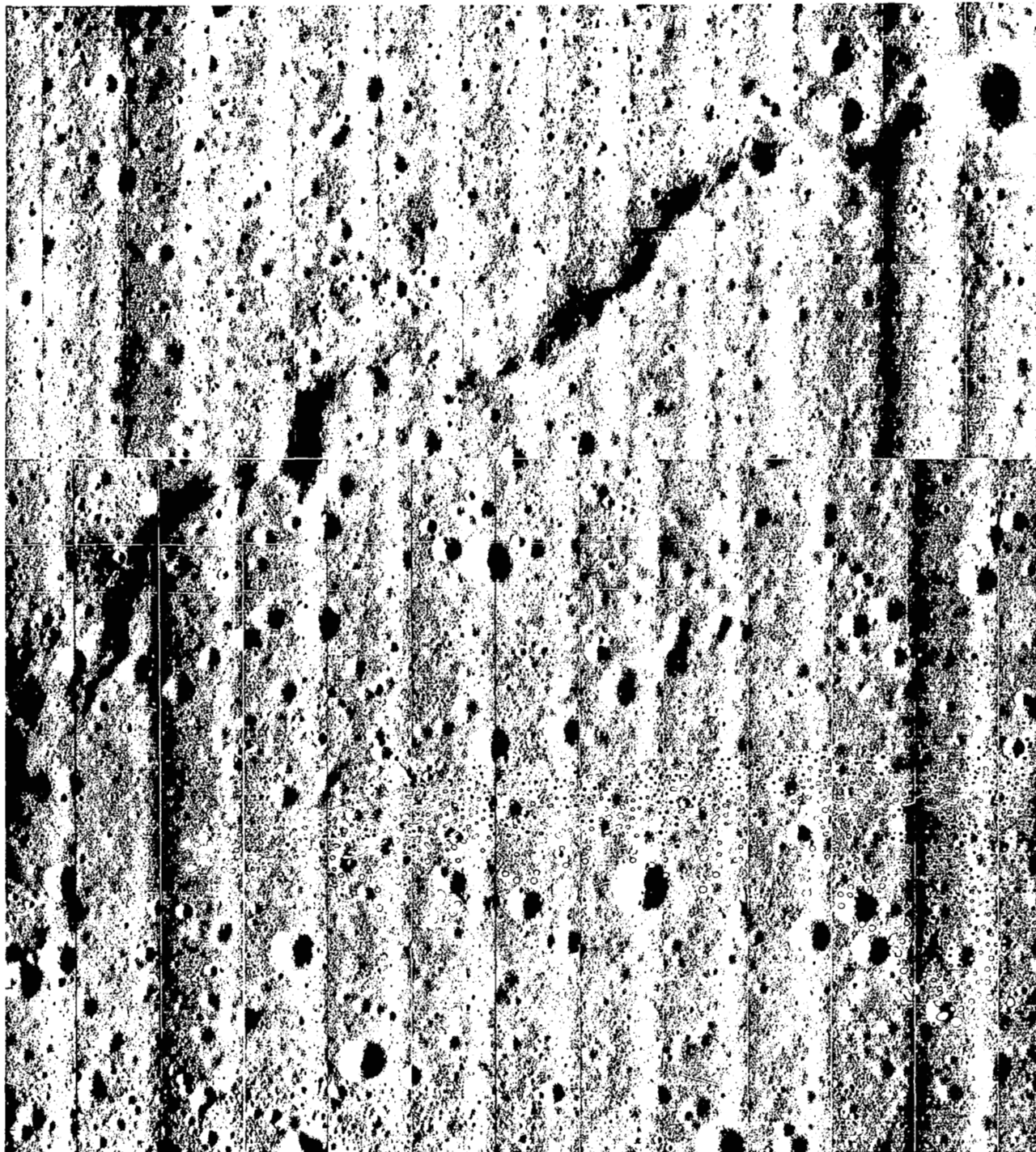
Section of Imbrium Flow edge; framelet width 640 meters.

Figure 4-42: Section of Telephoto Frames 160 and 161, Site V-38
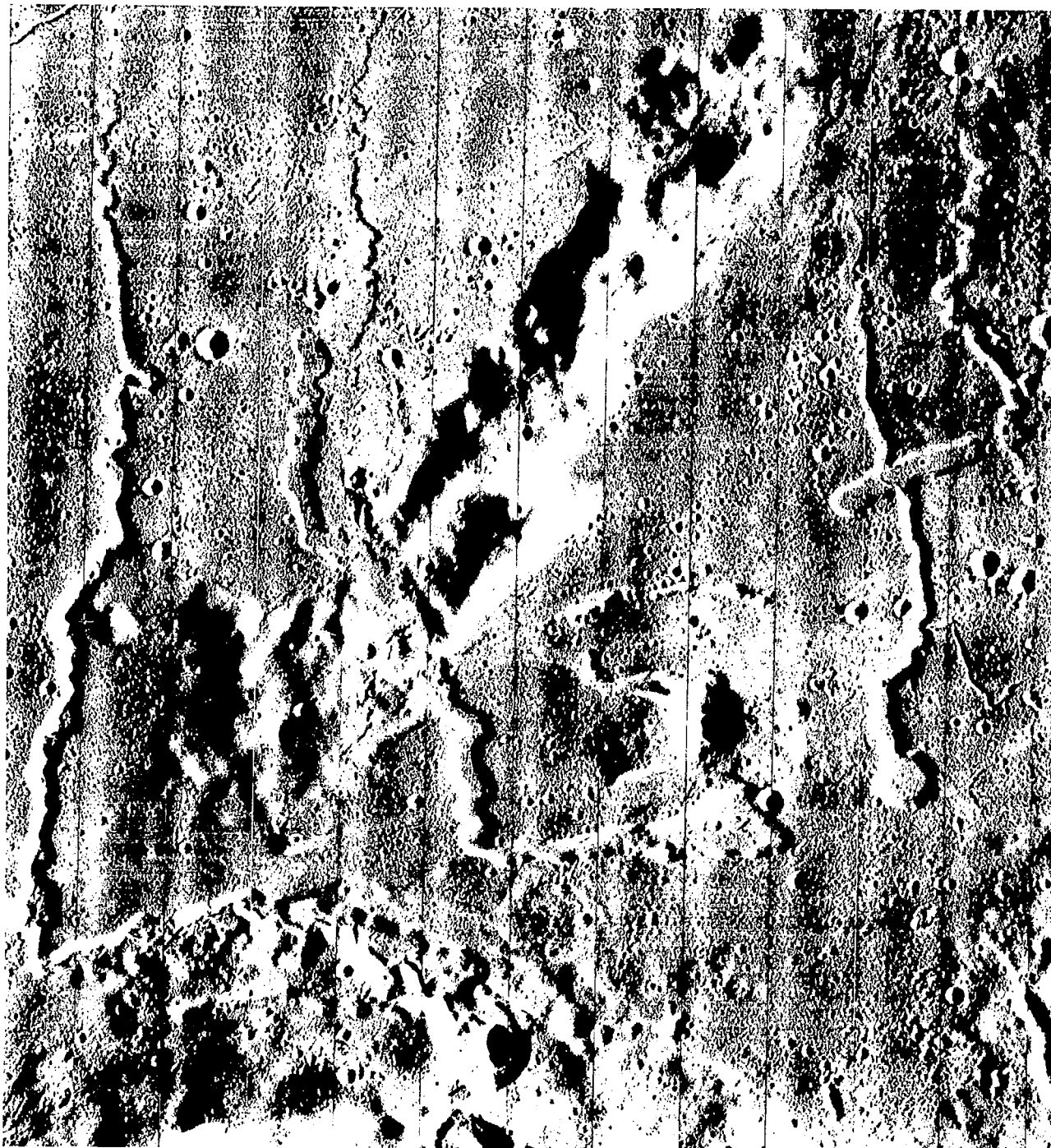
Centered on Harbinger Mountains and adjacent rille structure; framelet width 4.5 kilometers.

Figure 4-43: Section of Wide-Angle Frame 191, Site V-46
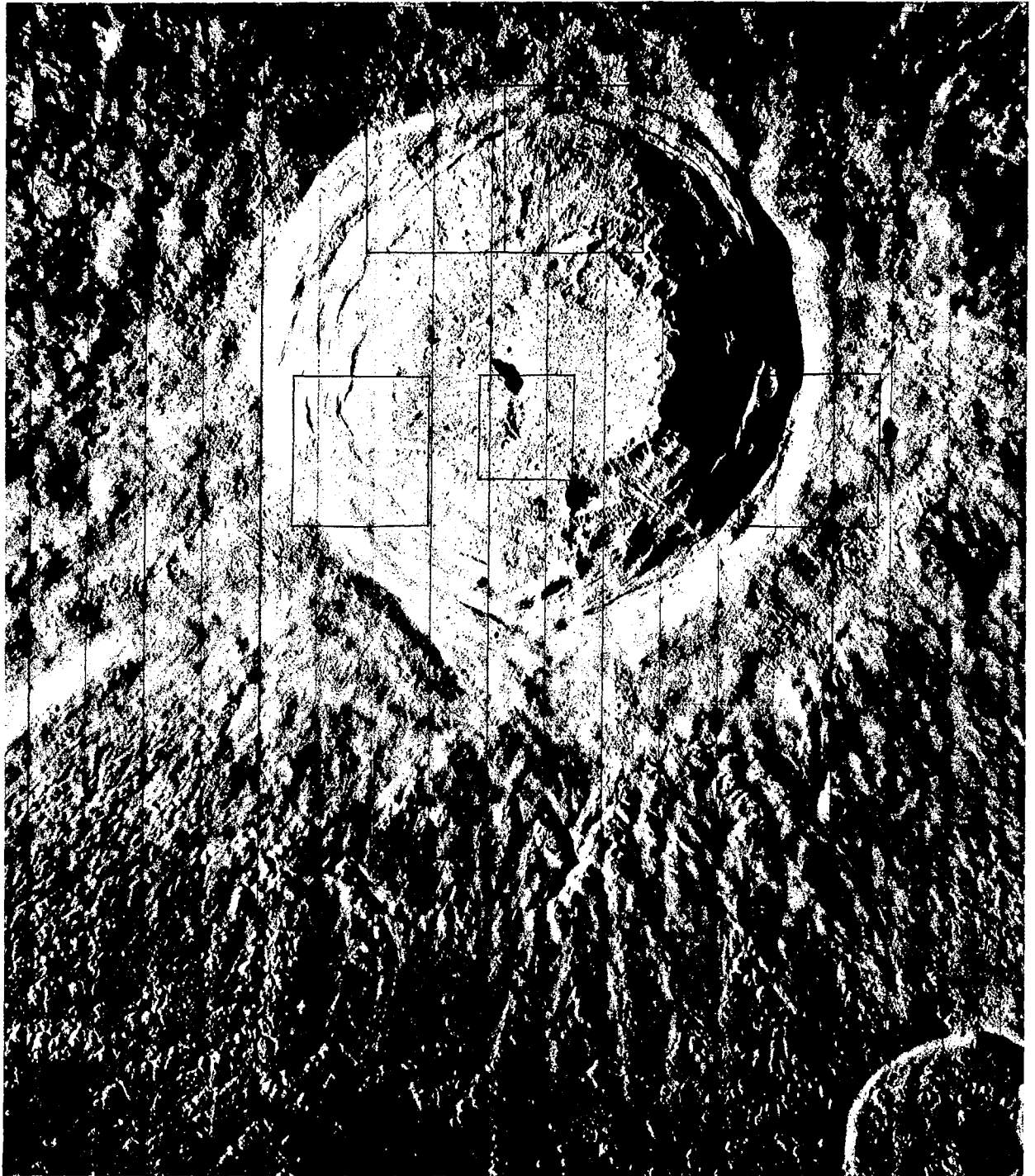
Crater Aristarchus (outlined areas covered by Figures 4-45 through -49); framelet width 4.1 kilometers.

Figure 4-44: Wide-Angle Frame 197, Site V-48

116
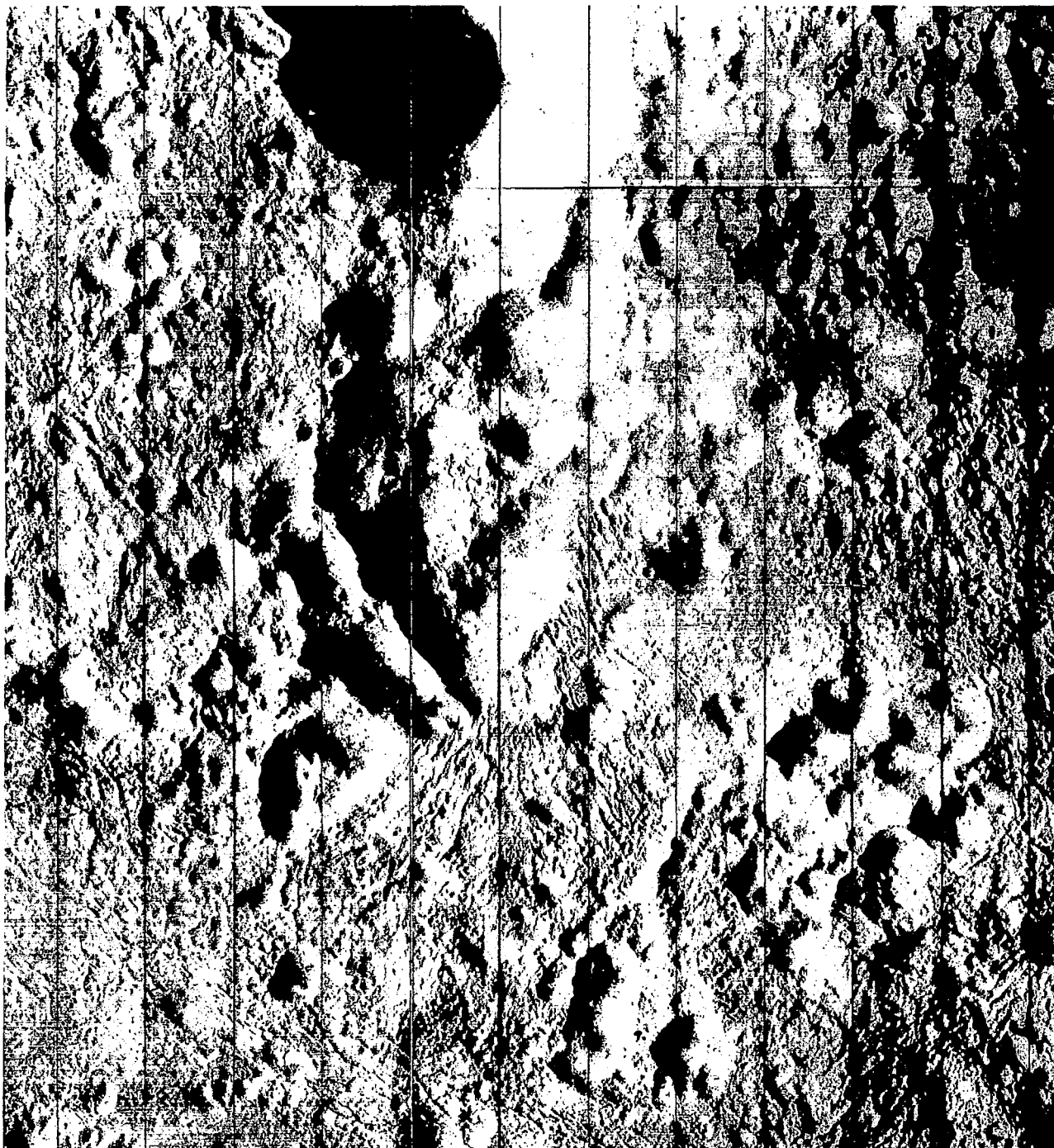
Central peak area; framelet width 530 meters.

Figure 4-45: Section of Telephoto Frame 198, Site V-48

117
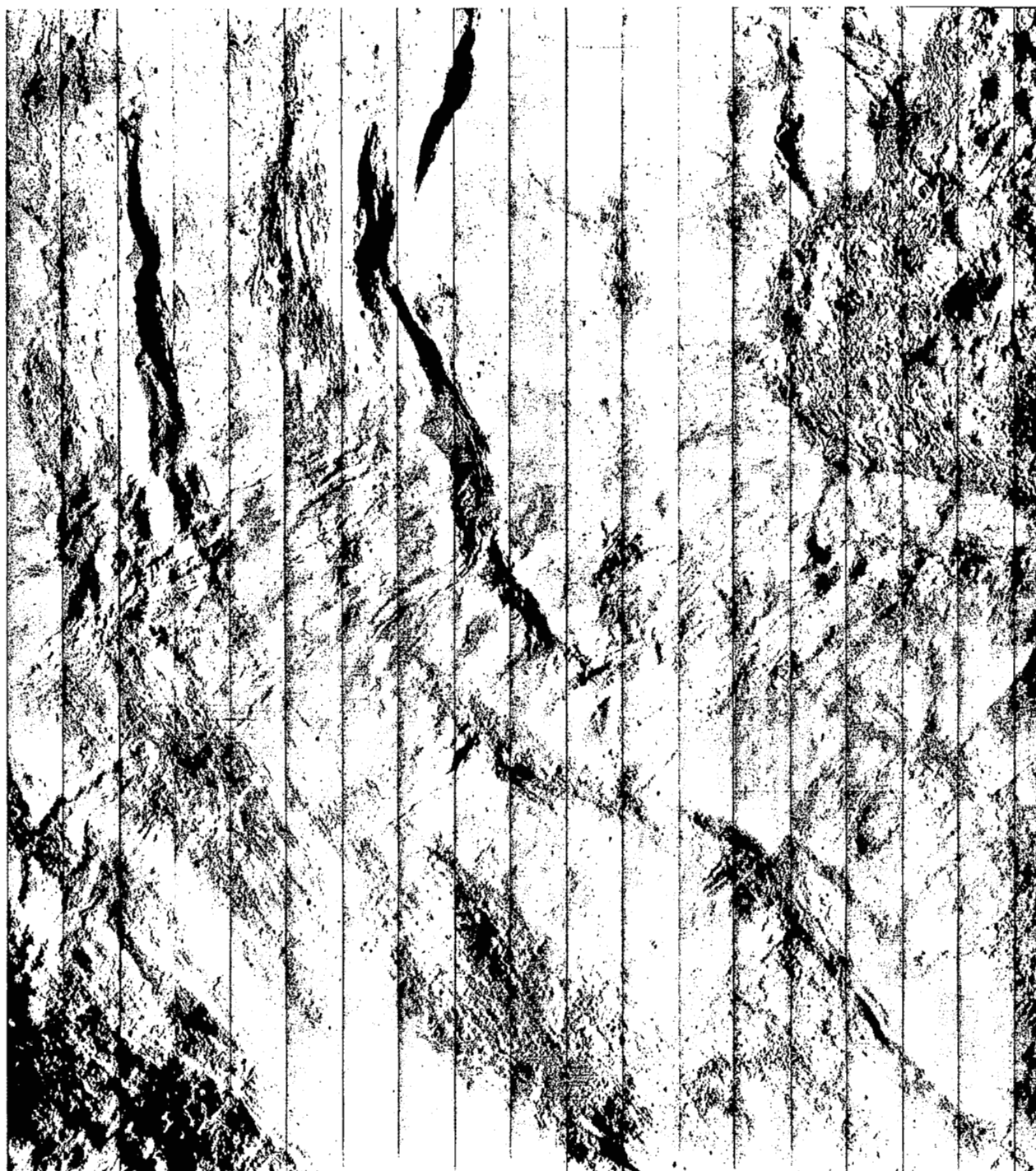
Southwest section of crater wall; framelet width 530 meters.

Figure 4-46: Section of Telephoto Frame 198, Site V-48

Section of southeast crater wall and outer rim; framelet width 540 meters.

Figure 4-47: Section of Telephoto Frame 198, Site V-48

119
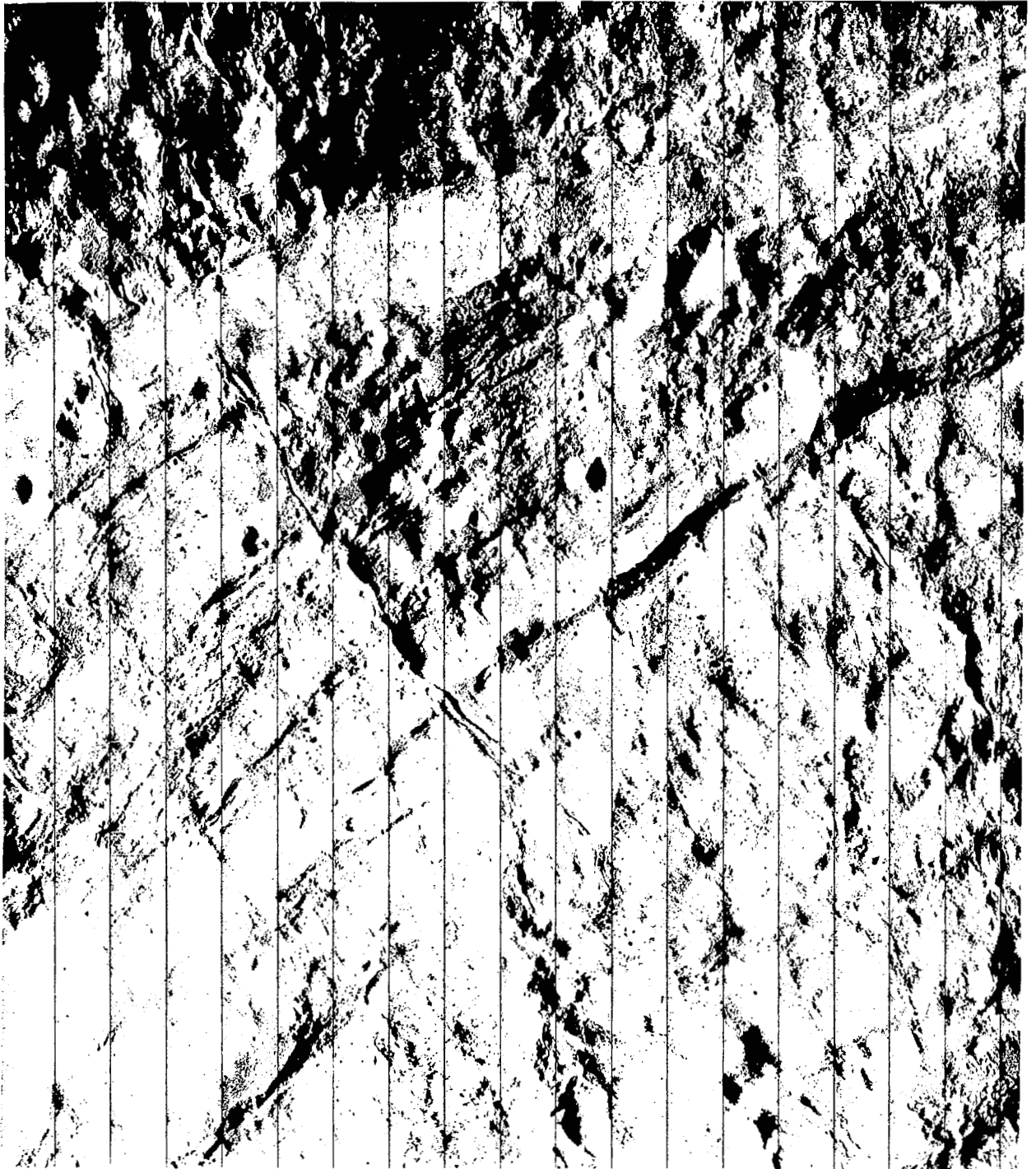
Northwest section of crater wall and floor; framelet width 550 meters.

Figure 4-48: Section of Telephoto Frame 200, Site V-48

120
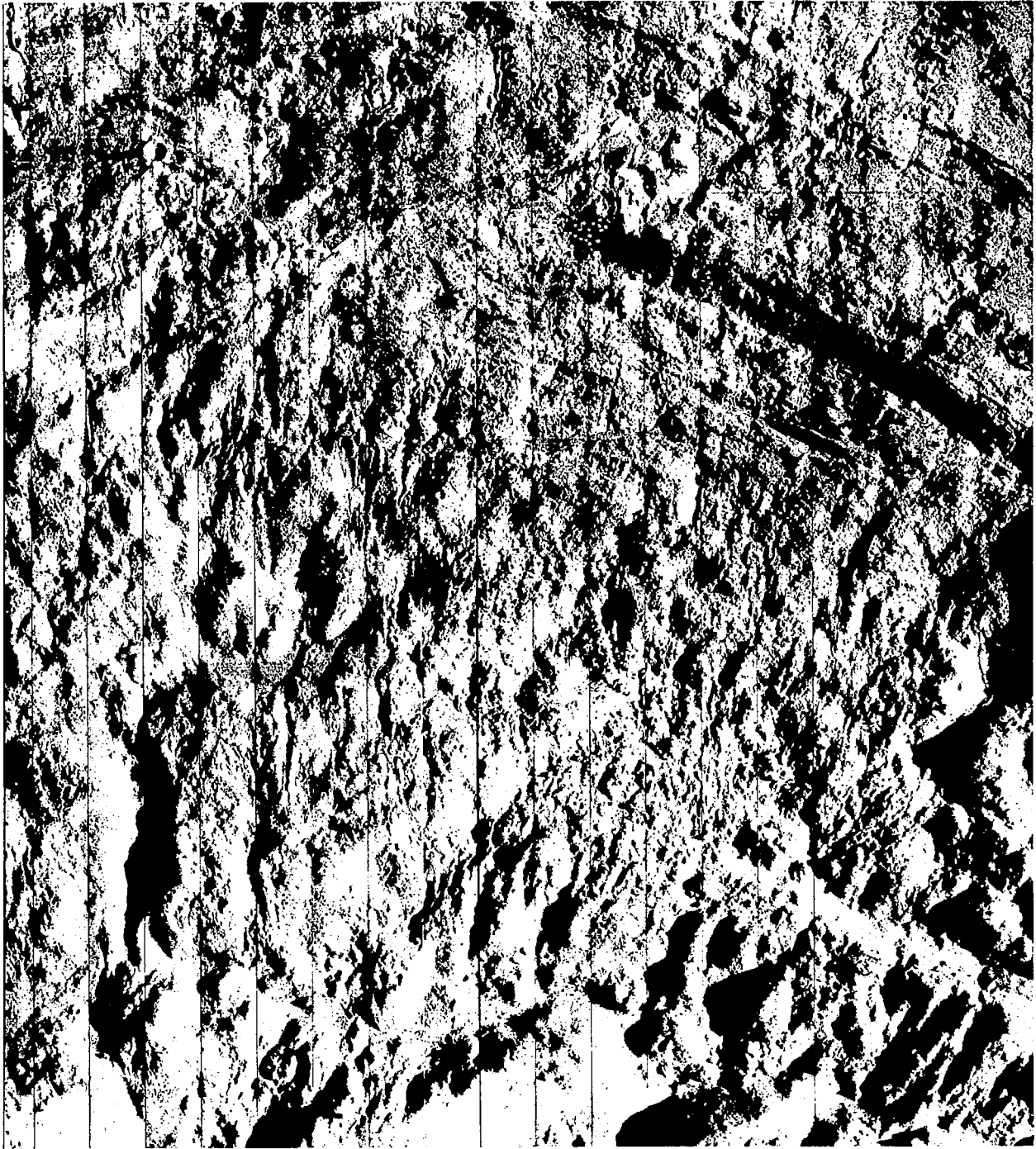
Northeast section of crater wall and floor (contiguous with Figure 4-48); framelet width 550 meters.

Figure 4-49: Section of Telephoto Frame 200, Site V-48
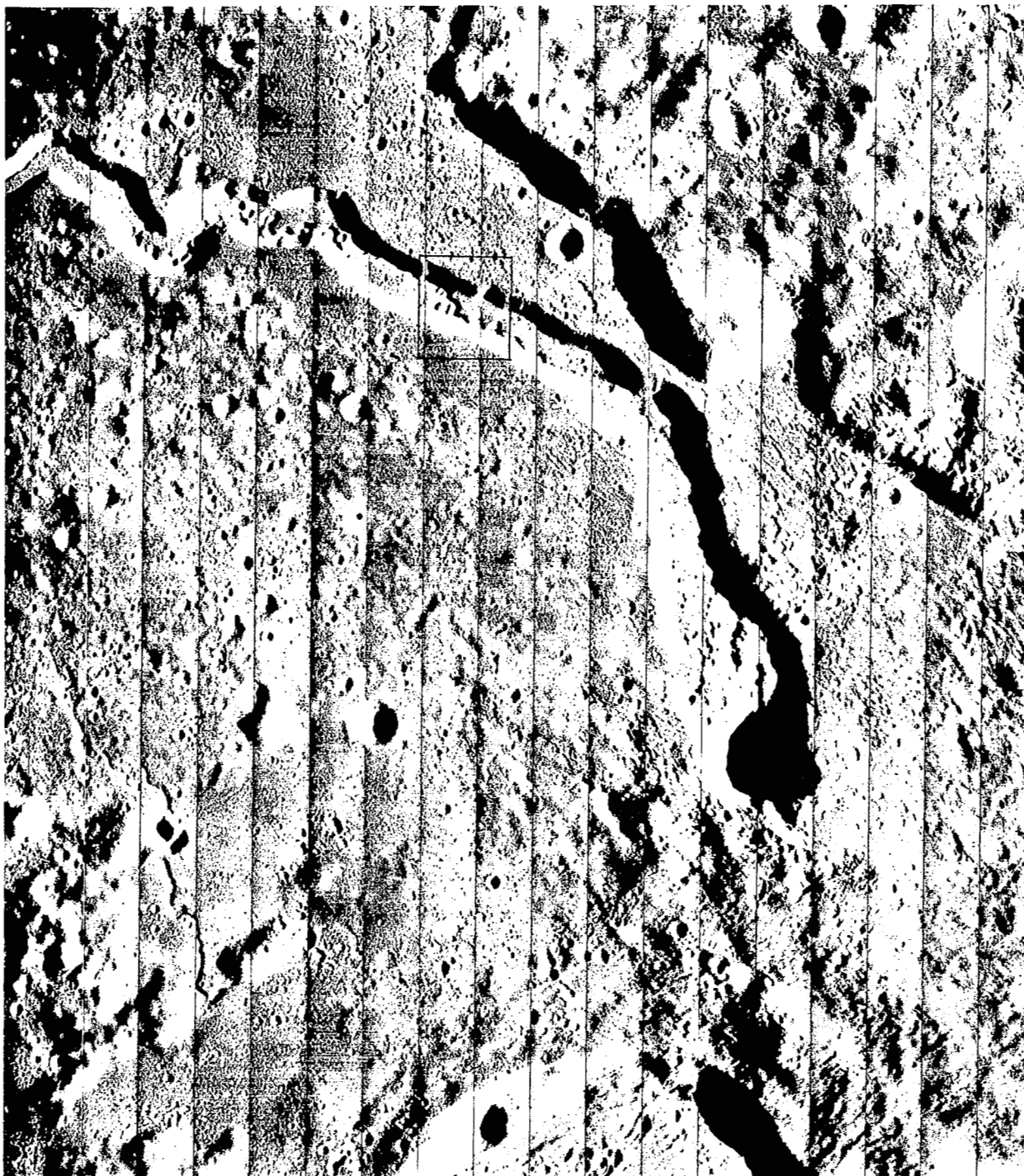
Cobra Head and vicinity (outlined area covered by Figure 4-51); framelet width 4.2 kilometers.

Figure 4-50: Wide-Angle Frame 202, Site V-49

Section of wall area; framelet width 570 meters.

Figure 4-51: Section of Telephoto Frame 204, Site V-49

123

Marius Hills area (outlined areas covered by Figures 4-53 and -54); framelet width 3.5 kilometers.

Figure 4-52: Wide-Angle Frame 212, Site V-51
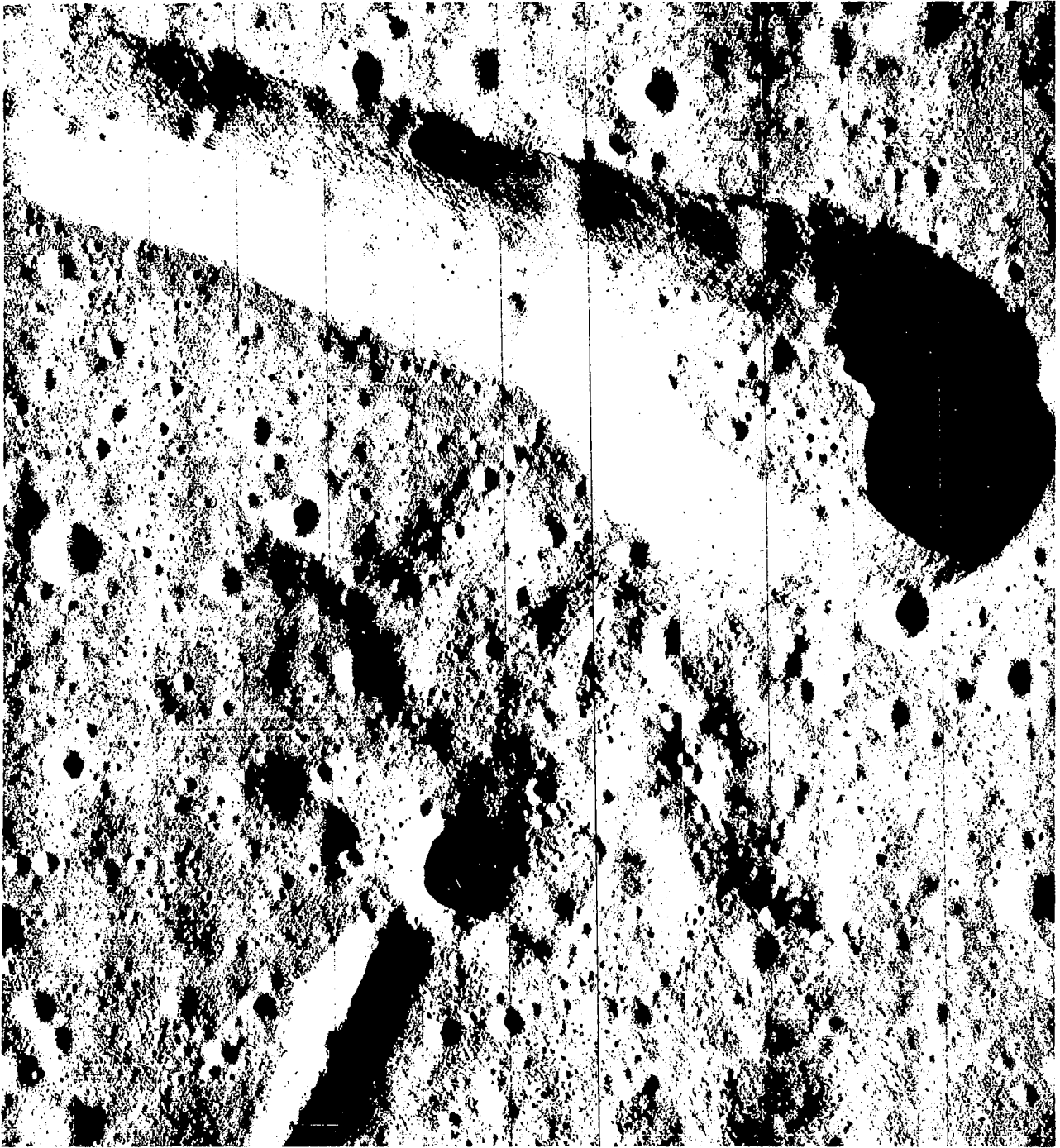
Rille structure; framelet width 460 meters.

Figure 4-53: Section of Telephoto Frame 213, Site V-51
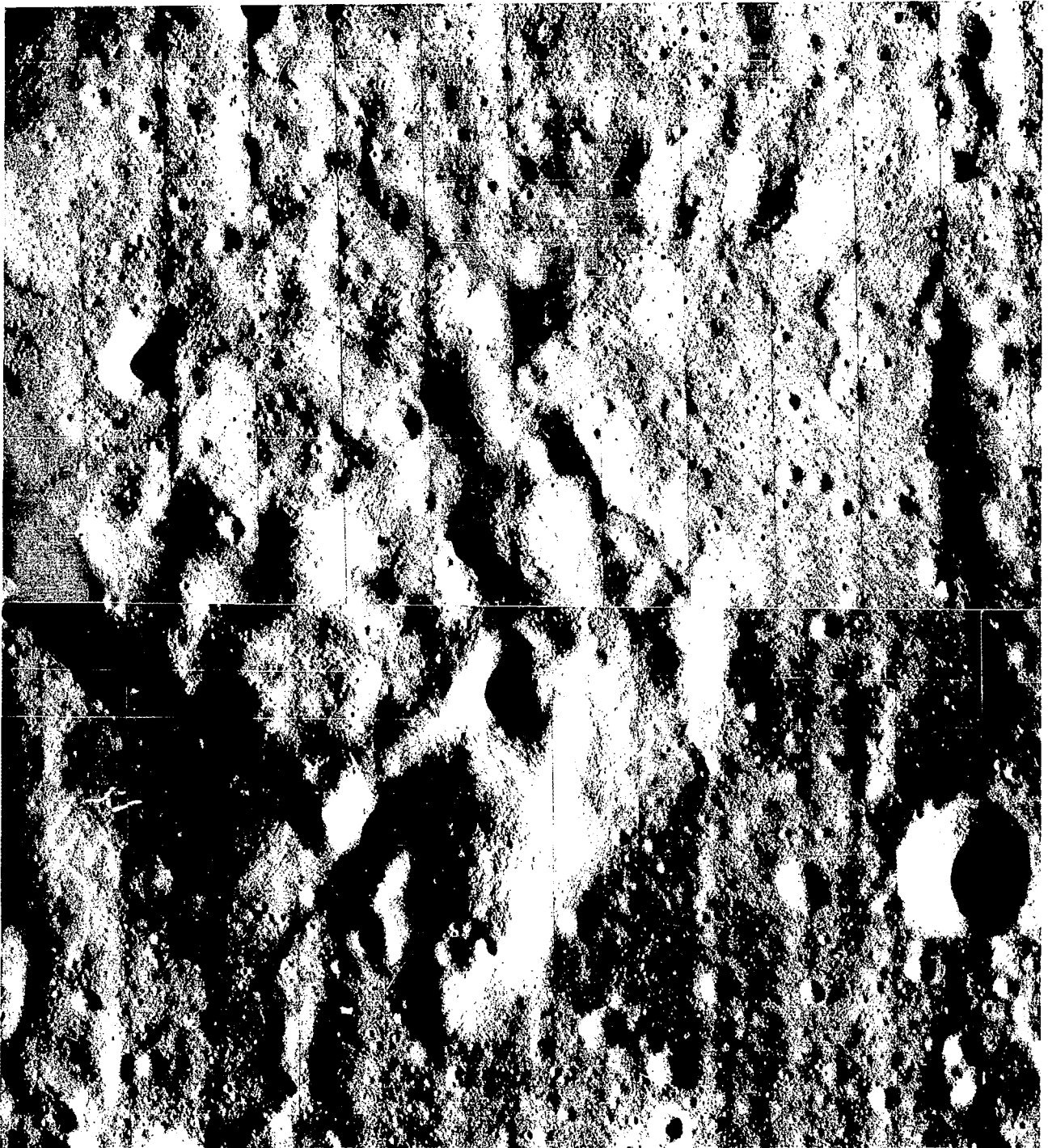
Hill area; framelet width 460 meters.

Figure 4-54: Section of Telephoto Frames 211 and 212, Site V-51

Sinus Medii (Photo courtesy Surveyor program)

Figure 4-55: Mission II Wide-Angle Mosaic

4.2 ENVIRONMENTAL DATA

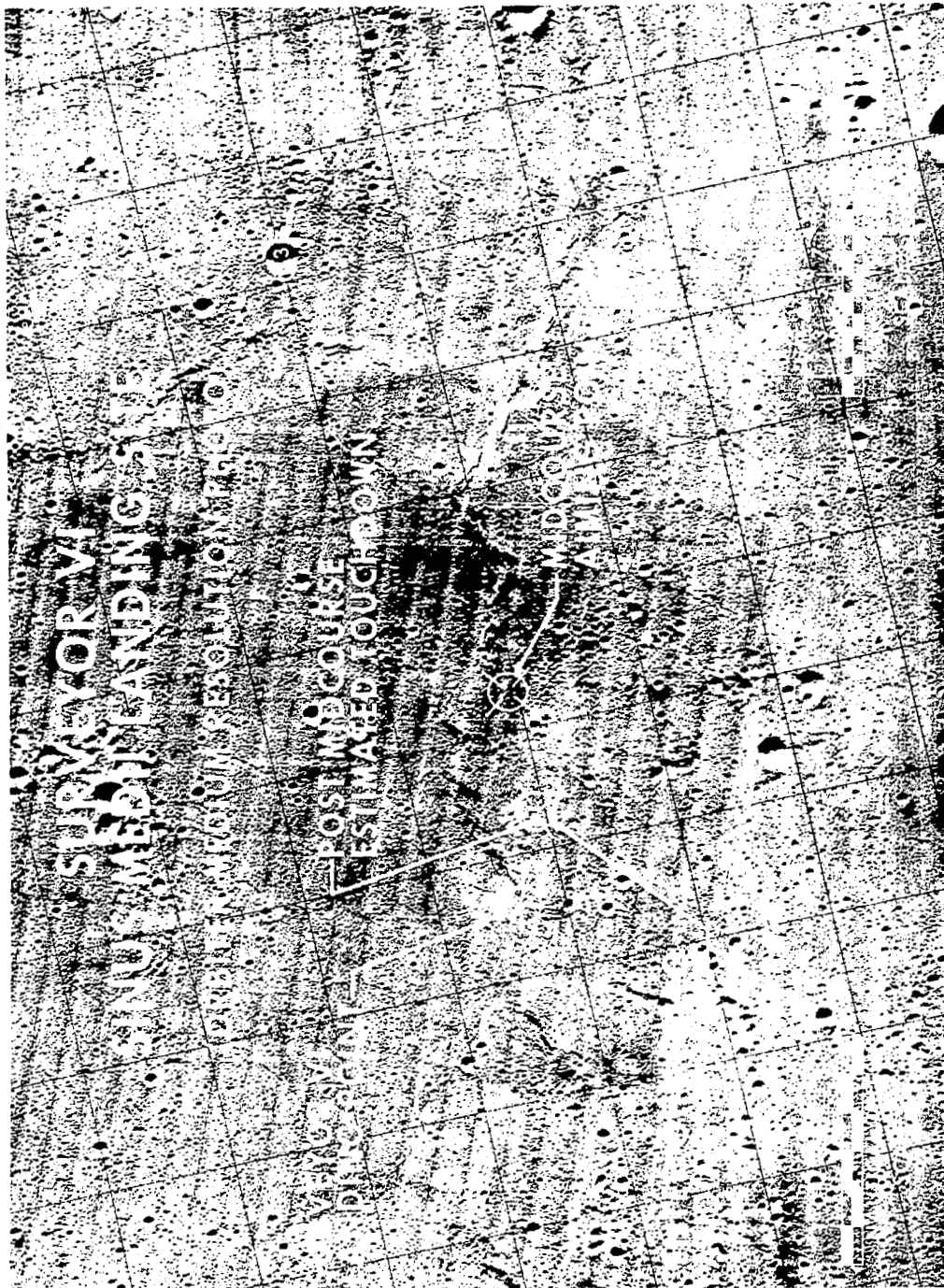Two types of telemetry instrumentation were installed on the Lunar Orbiter V spacecraft to monitor the lunar environmental conditions. Two radiation dosimeters were mounted adjacent to the photo subsystem. Twenty individual micrometeoroid detectors were circumferentially mounted on the tank deck.

4.2.1 Radiation Data

Dosimeter 1, located near the film cassette, had a sensitivity of 0.25 rad per count, with a capacity of 0 to 255 counts. Dosimeter 2, located near the camera looper, had a sensitivity of 0.50 rad per count and a similar capacity of 0 to 255 counts, and was turned on after passing through the Van Allen belts. Due to the inherent shielding of the spacecraft, the photo subsystem structure, and the 2-grams-per-square-centimeter aluminum shielding provided by the film supply cassette, it was estimated that solar flares of magnitude 2 or less would have negligible effect on the undeveloped film. Flares of magnitude 3 or greater would produce considerable fog on the film.

The radiation dosimeter measurement system (RDMS) functioned normally throughout the mission and provided data on the Earth's trapped radiation belts as well as the radiation environment encountered in transit to the Moon and in orbits about the Moon.

Data from Dosimeter 1 indicated that the film cassette was exposed to a total of 0.75 rad during transit through the Van Allen belts. This is considerably less than the 5.5 rads encountered during Mission IV during the same period. At the end of the photo mission, Dosimeter 1 had been exposed to 1.50 rads and Dosimeter 2 to 1.0 rad. This represents the normal combination of galactic cosmic ray background and dosimeter dark current.

State changes for each dosimeter during the mission are shown in Table 4-6.

4.2.2 Micrometeoroid Data

One micrometeoroid impact was detected during the period of the photo mission of Lunar Orbiter V. Detector 6 recorded a hit at 04:57:28

Table 4-6: Radiation Data Summary

GMT of Change				Radiation Reading	Counter (rads)
Day	Hour	Min	Sec	Dosimeter 1	Dosimeter 2
214	00	19	26	0.25	
214	00	33	15	0.50	
214	01	12	48	0.75	
218	11	44	30	1.00	
223	05	35	05		0.50
227	10	49	58	1.25	
236	13	53	31	1.50	
236	23	17	14		1.00

GMT on August 9. The spatial geometry and position of the spacecraft in orbit at the time of impact are shown in Figure 4-56. There was no detectable effect on spacecraft performance from the impact.

4.3 TRACKING DATA

Lunar Orbiter V provided lunar tracking data to augment the data obtained on the first four missions. The three elliptical orbits at 85 degrees inclination with transition maneuvers from a high apolune and intermediate perilune orbit to an orbit with an intermediate apolune and low perilune by Hohmann transfers provided new data for defining the lunar model coefficients. At the end of the photo mission on August 28, 752 station hours of doppler tracking data had been recorded. Over 48 hours of ranging data and 22 station time correlation checks were also obtained. All of this data has been furnished to NASA and will be further evaluated to refine the mathematical model of the Moon. The following discussions are pertinent to the quality of the tracking data obtained and the performance accuracy of the tracking system.

4.3.1 DSIF Tracking Data System

Lunar Orbiter V was one of three spacecraft orbiting the Moon and operating on the same frequency. To reliably track and communicate

128
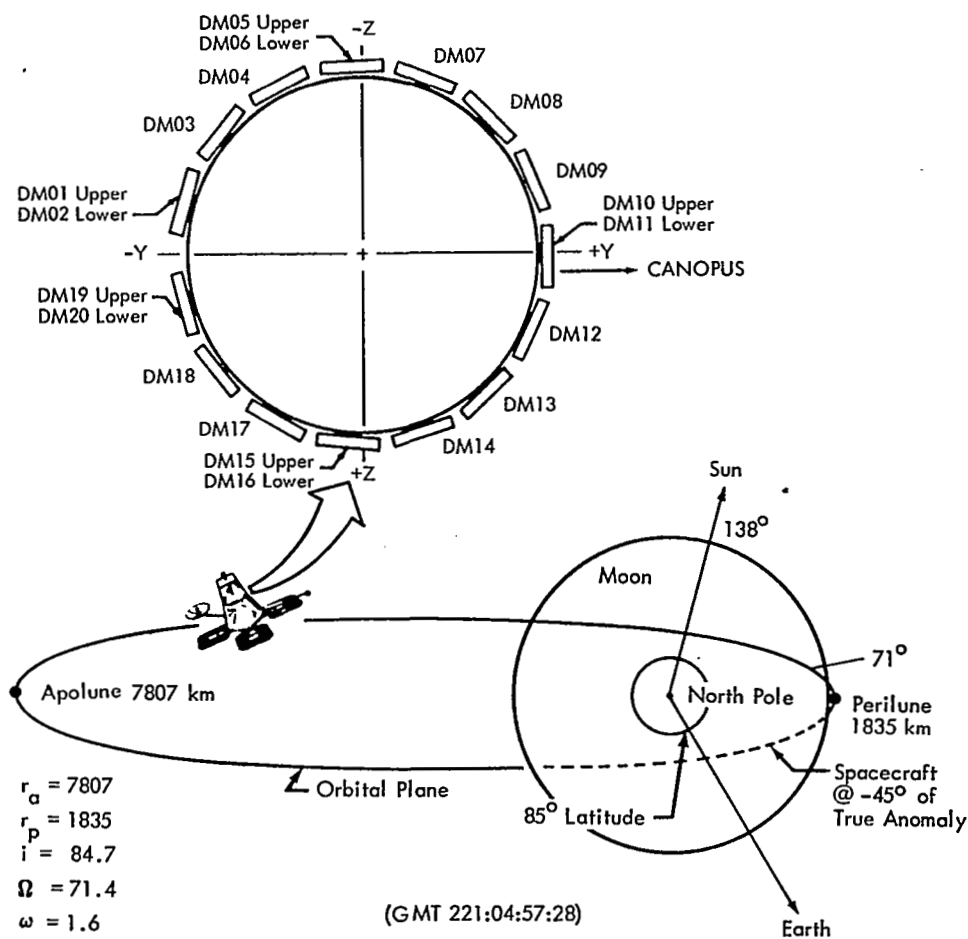
Figure 4-56: Micrometeoroid Impact Geometry

with Lunar Orbiter V, and avoid commanding the other spacecraft, an offset track synchronization frequency was employed based on the best lock frequency of the transponder. In general, the VCO offset value was 330 Hz. Station handover was accomplished at the offset frequency with no problems, except for one case where an incorrect ground procedure was employed. Ranging data was taken during the cislunar trajectory only. The complexity of activities during the photo mission precluded the scheduling of ranging data until the extended mission.

Tracking Data Validation -- The tracking data validation function was accomplished by back-feeding the tracking data to the Goldstone computer facility for processing by the Tracking Data Monitoring Program (TDM). This program compared the received data against a set of predictions and computed the residuals. It also calculated the standard deviation of the last five data points and provided an estimate of data noise. Program outputs were transmitted to the SFOF by teletype and printed in tabular form. The program outputs were also plotted on the Milgo 30 X 30 plotter through the IBM 7044 plot routine. During the cislunar phase the TDM generated its own predicted quantities by using an internal trajectory subprogram.

The internal trajectory subprogram of the TDM does not compute predictions for the lunar orbit phase. In this phase the JPL predictions are used and the residuals increased, which reflects inaccuracies of the lunar model in the prediction program. No deviations in the rf carrier were observed during Mission V. Noise

129

estimates of the TDM remained fairly accurate, indicating the overall good quality of the data. Spacecraft velocity changes were also monitored through the tracking data and showed good agreement with the other data.

Overall performance of the data validation system was very smooth and troublefree. Tracking data quality reports were made consistently throughout the active mission.

4.3.2 DSN

Tracking data were recorded at the Deep Space Stations and the Space Flight Operations Facility to satisfy requirements for the selenographic data. The Deep Space Station recording was five-level teletype paper tape. During the mission, the tracking data were transmitted to the SFOF via normal teletype messages. At the Space Flight Operations Facility, teletype data were received by communications terminal equipment and passed to the raw-data table on the 1301 disk by the IBM 7044 I/0 processor. These data were processed by the TTYX program to separate the telemetry data and tracking data in the messages received, and stored on the tracking raw-data file on disk. The tracking data processor (TDP) program generated the master tracking data table on the 1301 disk by smoothing and sorting the data from the tracking raw-data file by Deep Space Station identification. The output of this program was also recorded on magnetic tape and identified as the tracking data deliverable to NASA. An orbit data generator routine extracted selected master data file tracking data, smoothed it, sorted it according to time, and inserted it in the orbit determination program input file. Upon command from the FPAC area, orbit parameters were computed and predicted — based on selected data from the orbit determination program input file and the orbit determination program — and inserted into the data display for subsequent display by the user.

The raw tracking data paper tapes recorded at each Deep Space Station and the output of the tracking data processor at the Space Flight Operations Facility, recorded on magnetic tape, were collected and delivered to NASA for follow-up on selenodetic analysis purposes.

4.4 PERFORMANCE TELEMETRY

Spacecraft performance telemetry data were obtained by three different methods. Prior to spacecraft separation, the data were transmitted via assigned subcarriers of the VHF Agena telemetry link. These data were recorded at AFETR and, after real-time demodulation, transferred to DSS-71 (Cape Kennedy) for retransmission to the SFOF computers. In addition, the AFETR stations recorded the S-band signal directly from the spacecraft. After separation, the performance data were received directly from the spacecraft by the Deep Space Stations and reformatted for transmission to the SFOF. In all cases, the data were available for the subsystem analyst to continuously monitor the operational status of all spacecraft subsystems and environmental conditions.

Mission support by the DSN began 6 hours prior to liftoff on August 1, 1967, on a 24-hour-coverage basis, and terminated with the conclusion of photo readout on August 28, 1967.
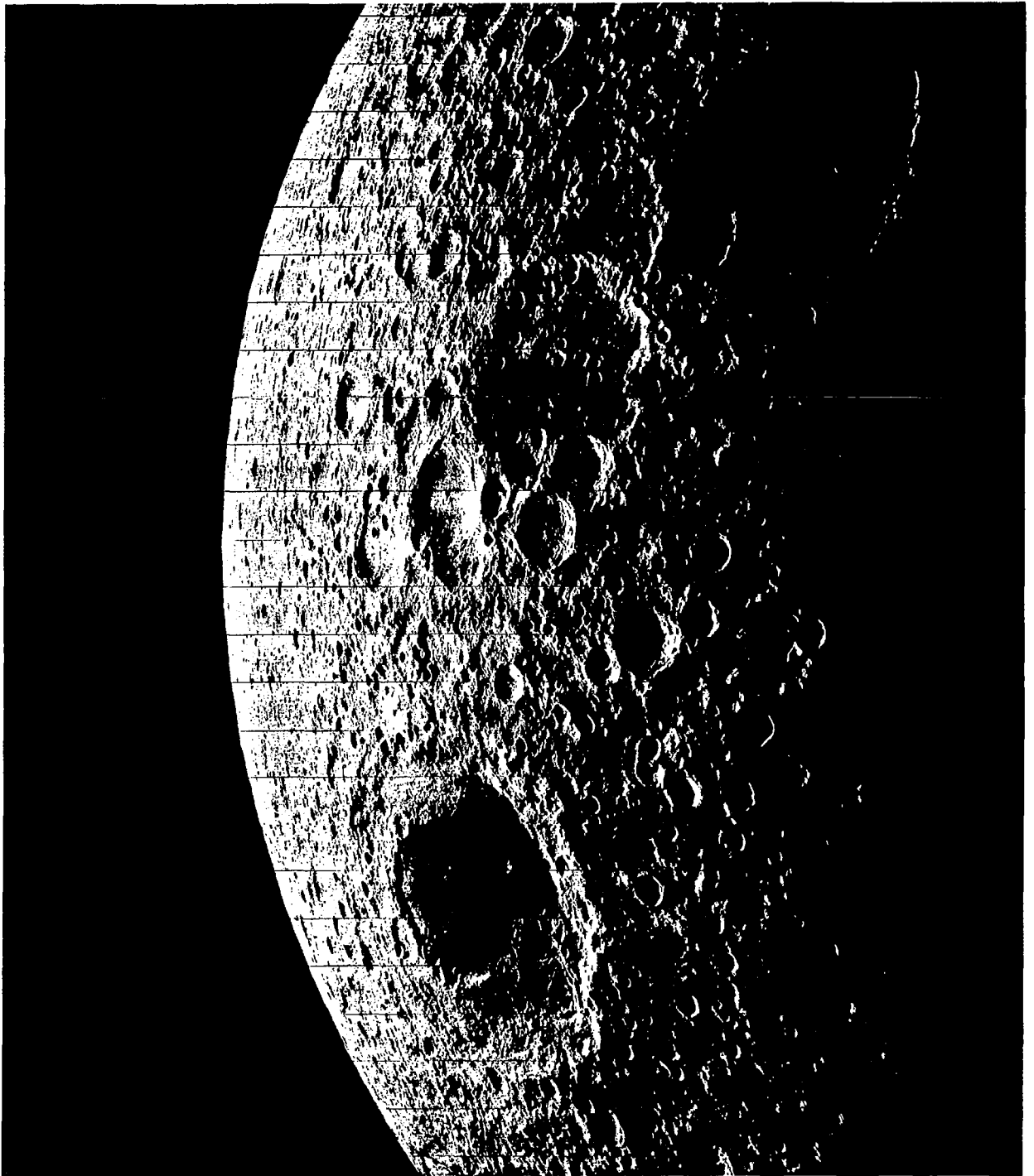
Wide-Angle Frame 103, Site VA-21
Covers north central area of farside.

5.0 Mission Evaluation

Lunar Orbiter V significantly increased the photographic data available for scientific investigation of numerous areas of particular interest widely distributed over the nearside. At least an order of magnitude improvement in resolution over the coverage of these sites during Mission IV was obtained. Farside photography provided coverage of essentially all of the areas not photographed during the preceding four missions with comparable resolution.

Significant accomplishments of Mission V include:

- Completed the photo requirement of vertical, oblique, and convergent telephoto stereo coverage for each of the eight candidate sites for the first Apollo landing.
- Provided photos of Apollo Application Program sites with resolution ranging between 2 and 10 meters.
- Provided near-vertical detailed photographs of specific areas and features selected as most significant for contributing to an understanding of the Moon and its geology.
- Provided detailed photos of approximately 40% of the farside which had not been previously photographed.
- Provided a near-full-Earth photo centered in the Indian Ocean and showing major land mass outlines.
- Performed attitude and velocity control maneuvers to reduce perilune and apolune altitudes by successive Hohmann type orbit transfers.
- Provided accurate tracking data for each of three elliptical orbits to improve the mathematical model of the Moon for 85-degree-inclination orbits.
- Demonstrated satisfactory operation of the power subsystem in providing adequate electrical power for photo subsystem operation when the solar panels were not illuminated.
- Demonstrated the capability to control cislunar trajectory, and orbit transfer maneuvers to place the spacecraft at specified location with respect to the lunar surface during a specified orbit.

Mission V was similar in many respects to Missions I, II, and III except that there were 45 photo sites on the nearside and 24 on the farside. Many of these sites were photographed with single-frame exposures. On several occasions, the spacecraft attitude was such that the solar panels were not illuminated. Experience gained during the preceding four missions enabled the satisfactory completion of this extremely complicated mission as outlined in premission planning. There were no significant spacecraft performance anomalies during the mission. The Bimat was exhausted during the processing of the next-to-last wide-angle exposure and the loss of only one wide-angle exposure (7% of the eight-frame sequence coverage).

The spacecraft properly responded to 472 (single-axis) commanded maneuvers and received, decoded, and executed 4,525 transmitted commands during the photo mission. The pointing accuracy was demonstrated by the Earth photo in which the center of the Earth was displaced about 0.13 degree from the planned center of the frame format.

Overall performance of the spacecraft was near-perfect during the mission and all objectives of this extremely complex mission were accomplished.
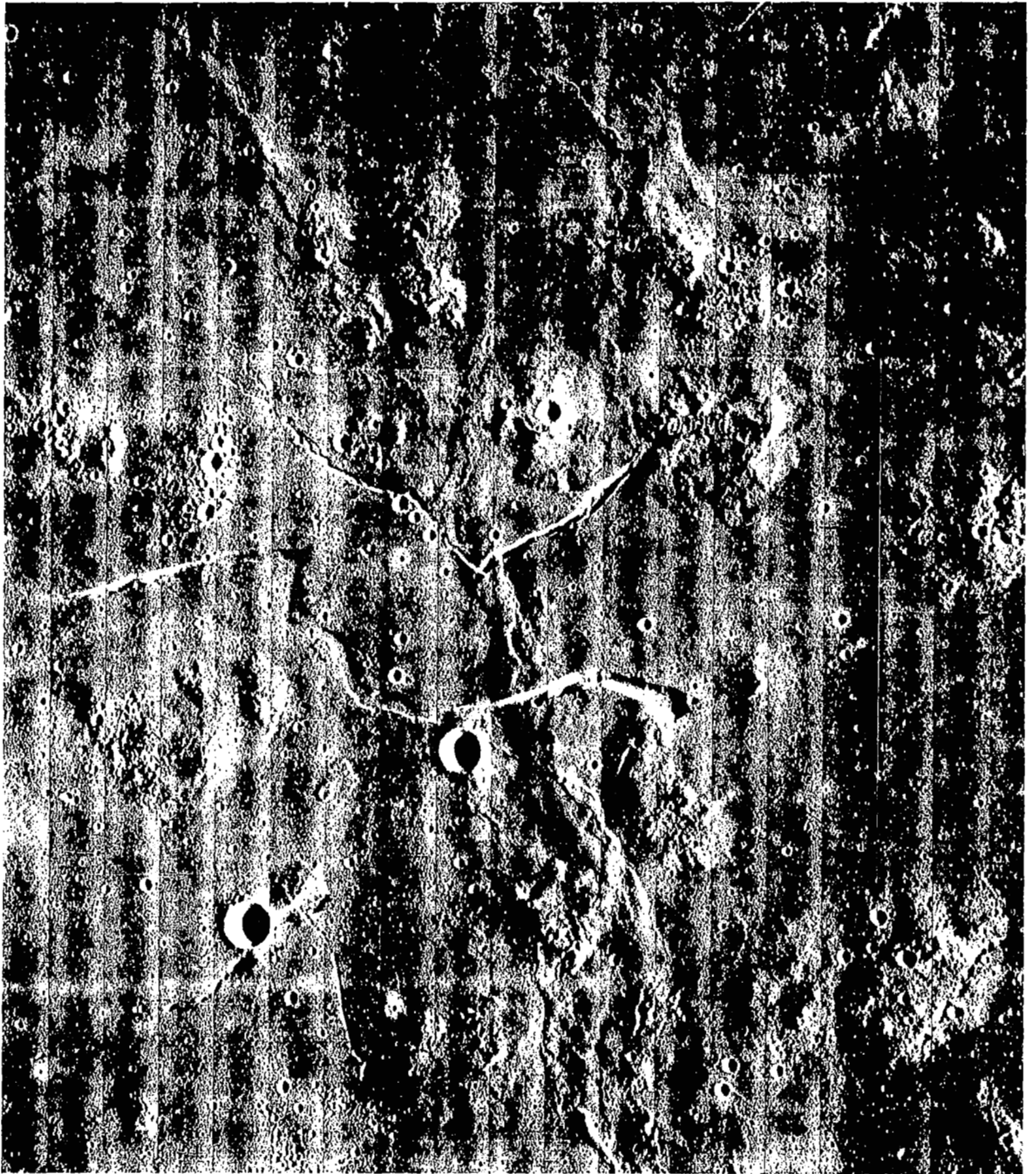
Wide-Angle Frame 212, Site V-51
Centered on the Marius Hills.

6.0 Program Summary

The following primary task was assigned to the Lunar Orbiter program as defined by Contract NAS 1-3800.

"To obtain, from lunar orbit, detailed photographic information of various lunar areas, to assess their suitability as landing sites for Apollo and Surveyor spacecraft, and to improve our knowledge of the Moon."

Results from the first three missions permitted concentration on scientific goals of the lunar exploration program during the last two missions. Members of the scientific community directly supporting the program were near-unanimous in their recommendation that remaining objectives of the program should consist of:

- Surveying the entire lunar surface at a resolution significantly better than that obtainable from Earth.
- Examining in detail various surface geological processes identified from this survey.

Other objectives of the program were:

- To provide trajectory information that will improve the definition of the lunar gravitational field.
- To provide measurements of micrometeoroid and radiation flux in the lunar environment for spacecraft performance analysis.
- To provide a spacecraft that can be tracked by the MSFN stations for the purpose of exercising and evaluating the tracking network and Apollo Orbit Determination program.

Primary Objectives — The primary task of the Lunar Orbiter program was essentially completed during the first three missions. Potential landing areas within the established Apollo zone of interest ($\pm 5°$ latitude and $\pm 45°$ longitude) had been selected based on Earth observations as augmented by Ranger and Surveyor program data. Landing sites are desired at a number of locations to fulfill the exploration and scientific objectives of the Apollo program and to provide an adequate launch window. The topography of an Apollo landing site must be smooth enough for an Apollo landing module (LM) landing. The approach terrain must be reasonably level to allow satisfactory LM landing radar performance. The surface resolution requirement to enable the selection of suitable sites for Apollo landings is approximately 1 meter.

Lunar Orbiters I and II accomplished photographic site-search missions of preselected areas grouped in southern and northern latitude bands, respectively. Lunar Orbiter III accomplished a comprehensive site-confirmation mission of the 12 most promising sites selected from Mission I and II photographs. Eight candidate site regions (shown in Figure 6-1) for early Apollo missions were selected by NASA after analysis of photographs from the three missions. The coordinates shown are the centroid of the areas photographed and may contain one or more site locations suitable for a manned Apollo landing site. It is anticipated that three primary sites will be chosen from this set of eight candidates, for the first manned landing on the Moon. Mission V provided additional coverage of selected sites to complete the vertical, oblique, and convergent telephoto coverage required for each site.

The additional tasks were assigned to Missions IV and V. A broad systematic photographic survey of the lunar surface features was conducted during Mission IV. The obtained telephoto photos provided approximately 99% areal coverage of the visible side of the Moon. With the exception of those eastern areas rephotographed from near apolune, the information and detail contained in these photos were at least 10 times better than Earth-based observations with resolutions of 60 to 90 meters, depending on the slant range to the surface and the location within the frame format. Resolution of the rephotographed eastern area telephoto photos was about 150 meters. Telephoto and wide-angle photography from Mission V provided additional visibility (at a reduction in resolution) of the areas not covered during Mission IV, to complete coverage of the visible hemisphere.

Each of the five missions contributed to farside coverage. Although photography was conducted
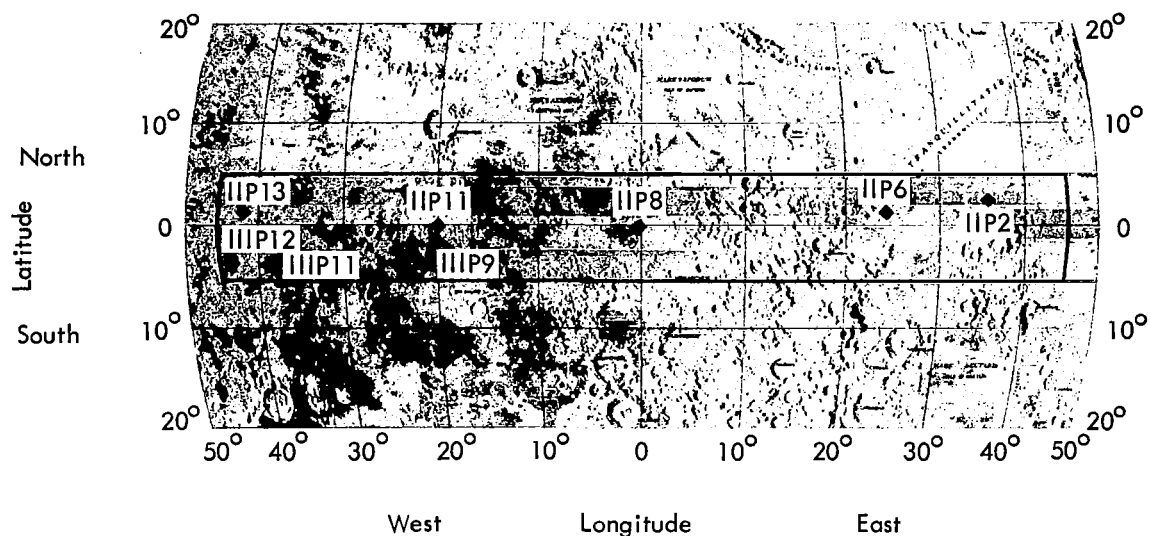
Site	Longitude	Latitude	Site	Longitude	Latitude
IIP-2	$34° 14'E$	$2° 40'N$	IIP-13	$42° 20'W$	$1° 30'N$
IIP-6	$23° 51'E$	$0° 45'N$	IIIP-9	$23° 15'W$	$3° 05'S$
IIP-8	$1° 06'W$	$0° 25'N$	IIIP-11	$36° 11'W$	$3° 30'S$
IIP-11	$19° 55'W$	$0° 05'S$	IIIP-12	$43° 48'W$	$2° 25'S$

Figure 6-1: Candidate Apollo Photo Site Locations

from 1,500 to 6,000 kilometers, the resolution of these photos was better than that obtainable from Earth on the nearside. Missions I through IV photographed about 60% of the farside. Mission V provided the remaining farside coverage by a combination of telephoto photography from the initial and intermediate orbits and the wide-angle photography from the final ellipse. With the exception of an area encompassing about 0.5% of the farside hemisphere near the South Pole, the five missions have provided photographs of the lunar farside topography. Figures 6-2 and 6-3 are photographic reductions of the Aeronautical Chart and Information Center Chart LFC-1, second edition, covering the lunar farside surface. This map was

prepared by evaluating the aerial coverage of the five Lunar Orbiter missions. It is significant to note that this farside coverage was integrated into the program planning and operational requirements during and subsequent to the first flight in August 1966.

Lunar Orbiter IV's mapping mission also provided early data of surface details and geological features to improve the site selections for the multi-site scientific mission planned for the last mission. Approximately 50% of the previously selected sites were revised based on Lunar Orbiter IV's data. Approximately 168 frames exposed during Mission V were taken to satisfy the scientific requirements for specific areas

and feature coverage and support the Apollo Applications Program.

The photo data obtained during the five missions provided coverage of the entire lunar surface and will stand for many years as the primary source of data on lunar surface features for scientific analysis and planning later explorations of the Moon.

Secondary Objectives – Data to satisfy the secondary objectives were obtained during each of the five missions. The selenodetic and environmental mission data objectives require the use of operational equipment and detectors on the spacecraft. Tracking data obtained throughout the mission produce the basic data required to satisfy selenodetic objectives. Micrometeoroid detectors mounted on the periphery of the spacecraft and radiation detectors mounted internally monitor the lunar environmental data on each flight for transmission to the ground stations.

In addition to the tracking data obtained during the photographic mission as shown in Table 6-5, other data was taken on a sampling basis during the extended-mission periods shown in Table 6-1.

Analysis of the tracking data has resulted in a more accurate determination of the mathematical model of the Moon for 12-, 21-, and 85-degree orbit inclinations. The Langley Research Center has determined and released

Lunar harmonics which are defined as the LRC 11/11 (fourth order) and the LRC 7/28B (seventh order) based on the Lunar Orbiter tracking data. .

Lunar environmental data, including radiation dosage and micrometeoroid impacts, obtained during the photo missions are summarized in Table 6-3 for each flight spacecraft.

Support of the Manned Space Flight Network (MSFN) was an assigned objective of the extended mission. The data from these tests will be reported in the extended-mission reports for the applicable spacecraft.

Program Accomplishments -- Accomplishment of these objectives began with the Lunar Orbiter I flight 28 months, 15 days after the start of the program, and subsequent flights at the prescribed intervals. Except for a 1-month delay in the delivery and flight of the first spacecraft, all spacecraft were delivered on schedule. The spacecraft were launched on the scheduled launch date, except for a single 1-day delay required to correct an erratic output signal from the launch vehicle instrumentation detected late in the initial launch countdown.

The Lunar Orbiter-developed on-board digital programmer, with its 128-word magnetic core memory, controls 120 separate spacecraft functions and provides the inherent high degree of operational flexibility. It has the capability of accepting up to 16 hours of stored information

Table 6-1: Time in Orbit Summary

	LO I	LO II	LO III	LO IV	LO V
Injection Date	8-14-66 15:43	11-10-66 22:58	2-8-67 22:03	5-8-67 15:17	8-5-67 16:49
Impact Date	10-29-66 13:29	10-11-67 07:17	10-9-67 10:27	7-17-67* 06:30	1-31-68 07:58
Total Orbits	547	2,289	1,843	225	1,201
Total Days	76	335	243	70	179

*Last communication with spacecraft

137
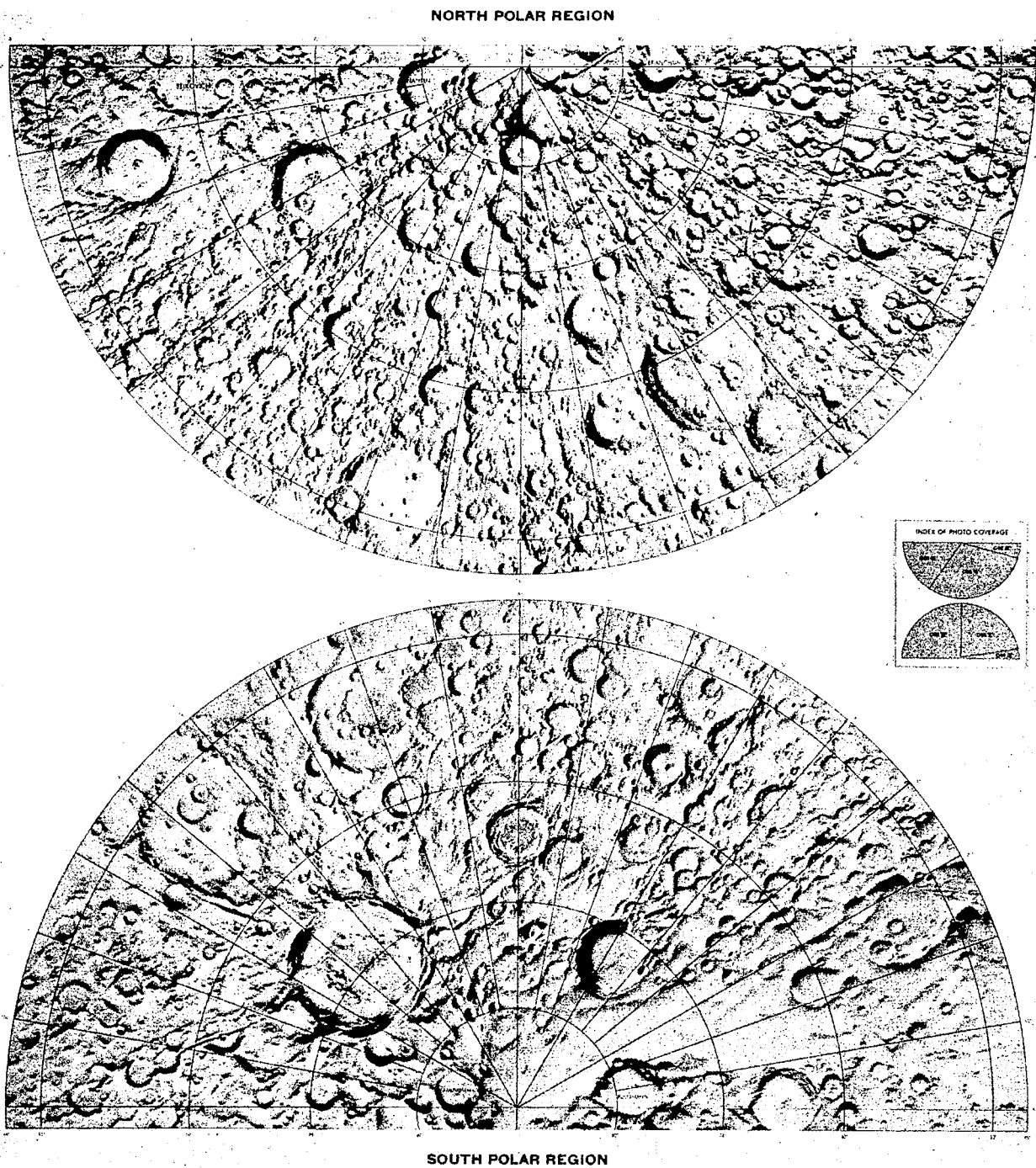
Figure 6-2: Lunar Farside Map (Polar Regions)

138

MARE MOSCOVIENSE

MARE MARGINIS

MARE SMYTHII
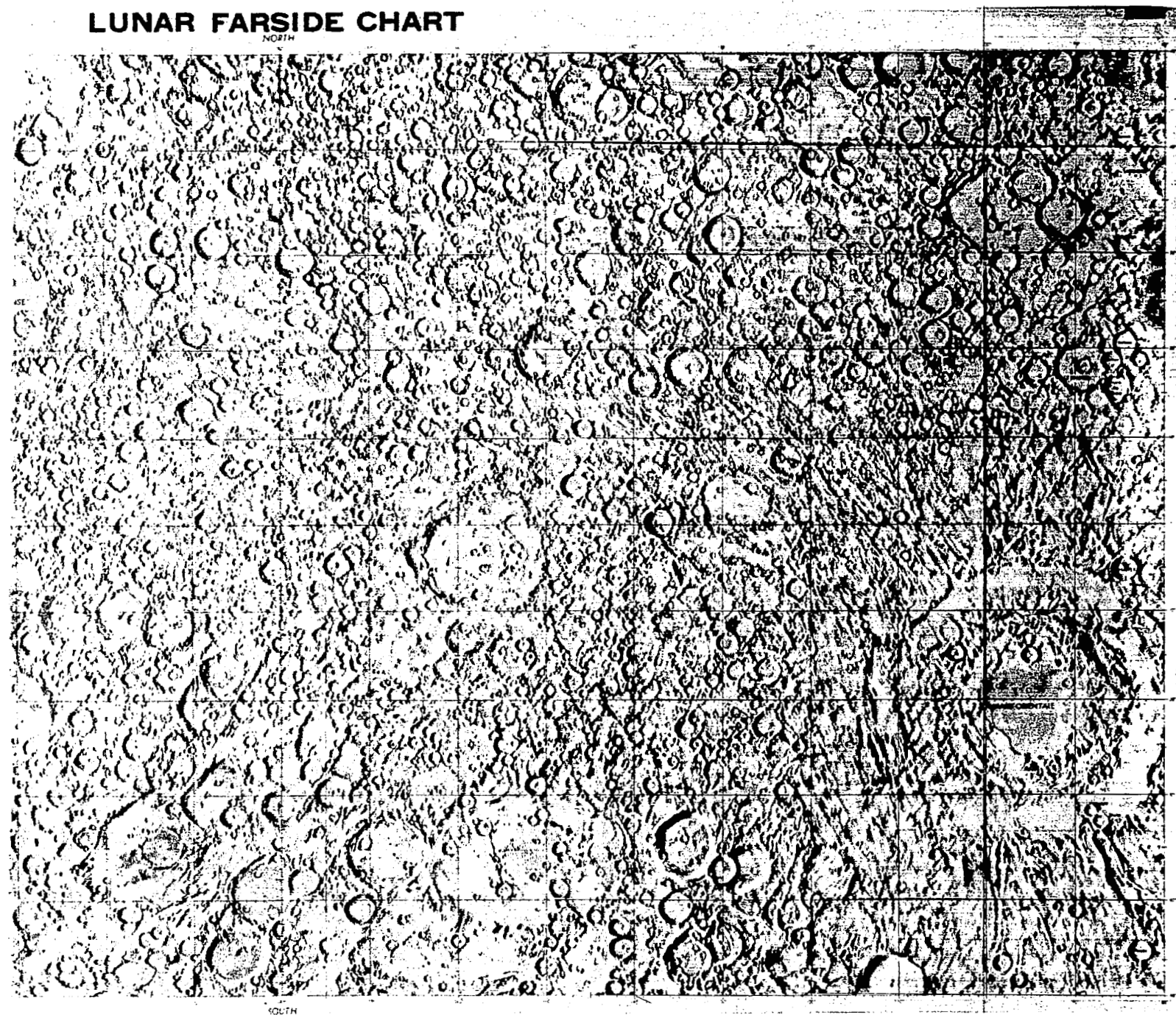
HUMBOLDT

MARE AUSTRALE
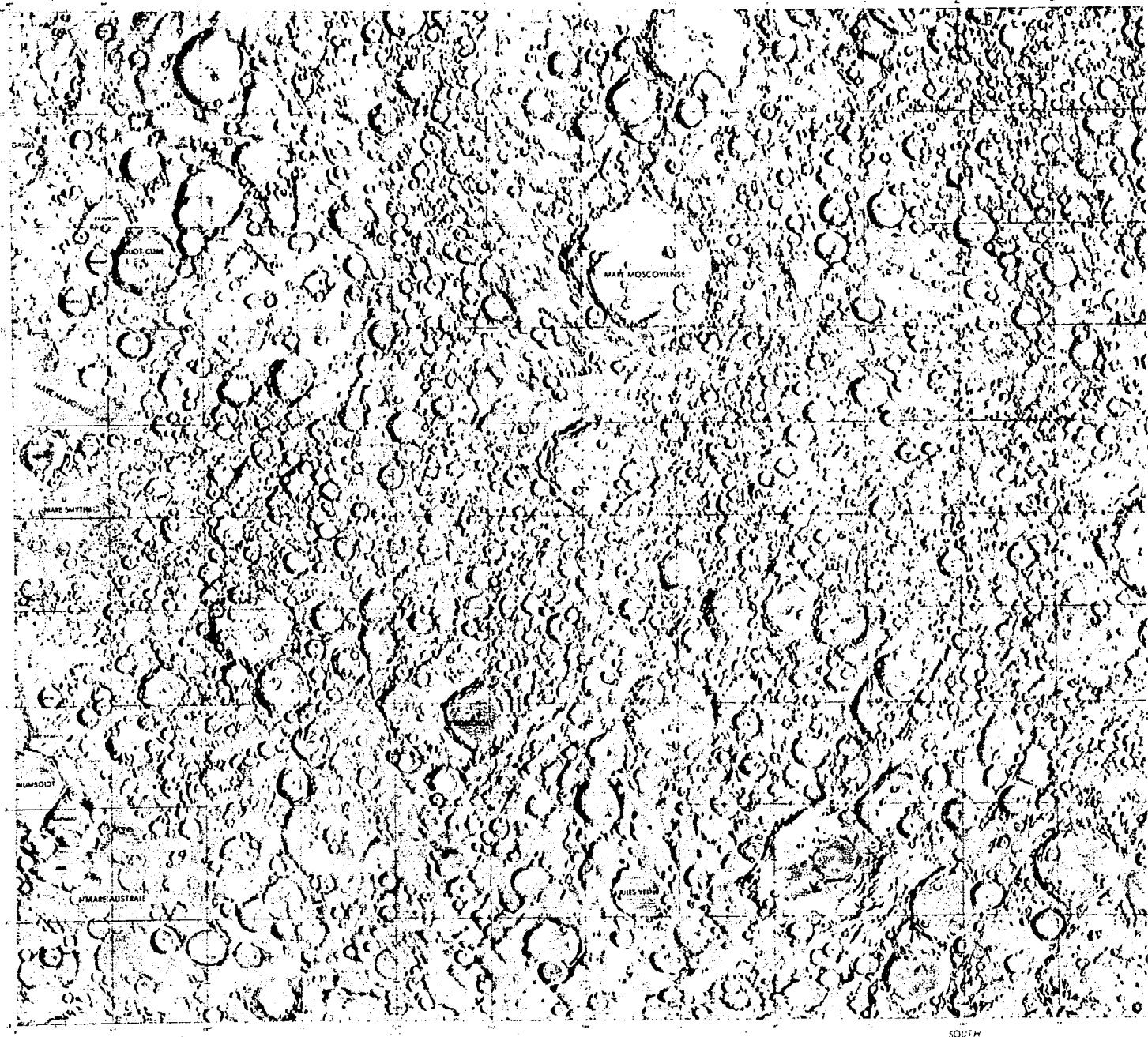
LUNAR FARSIDE CHART

Figure 6-3: Lunar Farside Map (Midlatitudes)

and instructions that can be changed by command at virtually any time during radio communication to update the stored sequences or introduce new real-time commands. The designed flexibility of the operational command and control concept and the adaptability of the supporting computer programs and software were exercised to greater limits on each successive mission. As operating experience was gained, the ability to perform extremely complicated photographic missions, including real-time changes in photo site locations and the reaction to nonstandard events, was routinely implemented.

This capability proved extremely important and was employed on a number of occasions to initiate special test sequences to support real-time analysis of operational problems and to implement corrective action that allowed completion of the mission with a minimum loss of data.

During the Mission I preflight design period, there was no plan considered originally for the photo subsystem operational constraint (film-set) exposures to be used to photograph any specific additional lunar sites other than the primary-site coverage which was limited to vertical photography. As the Mission I flight plan developed, the film-set frames (required to move film through the photo subsystem to prevent film handling problems) were considered for use to obtain additional information on potential sites for subsequent missions, as well as other lunar terrain features from Apollo considerations and scientific interests. Changes in site location during conduct of the mission and procedures were ultimately developed during the early flight period for accurately orienting the camera axis and timing the exposure to obtain the peculiar photo coverage. Spectacular photos of this type were the Earth as viewed from just beyond the Moon's limb and the oblique photo of the crater Copernicus.

The outstanding quality and detail of the Moon's topography, evident in the Earth-Moon photo, led to the development and employment of more off-vertical photography for succeeding missions. A Mission II experiment in converging telephoto stereo photography was a complete success. Based on the results obtained, all of the candidate Apollo landing sites have been photographed by a comprehensive series of vertical, oblique, forward, side overlap (wide-angle vertical coverage) and convergent telephoto stereo photography. The combined use of these photos provides an enormous source of detailed topographic and geological data to support any analysis of the lunar surface.

As each operational mission became more complex, it was necessary to augment the corresponding operation of the space flight operations system. The flight operations team (composed of NASA, Boeing, JPL, and other supporting government agencies) personnel developed improved and simplified operating procedures, data displays, communications, and computer routines based upon the experience gained on successive missions and intermission training exercises. Changes were also made in the organization of the flight operations team to change or eliminate the manning of operational positions for succeeding missions. An off-line planning and analysis group was added to work in parallel with the on-line team to handle the planning and command preparation necessitated by nonstandard events and other deviations to the basic mission plan. A detailed flight operations plan was developed prior to each mission based on the specific objective and photo sites defined. The flexibility of the flight operations team, supported by the inherent capability of the spacecraft command and control system and the operational software, made it possible to react quickly and effectively to changes in mission requirements, abnormal spacecraft performance, and problem diagnosis. These efforts resulted in real-time changes or adjustments to the basic mission plan or operating procedures to ensure the maximum possibility of satisfactorily completing the assigned mission.

Processing and evaluation of the reconstructed GRE film at the sites and the Space Flight Operations Facility proved to be a valuable tool in successful completion of program objectives. This procedure was invaluable in resolving the operating problems encountered

with the photo subsystem. In addition, the near-real-time evaluation resulted in direct feed-back for operational control of mission photography by indicating desirable adjustment of coverage and exposure. A modification of albedo values obtained from Earth-based observation was derived by experience to improve exposure predictions. Systematic errors in timing of the exposures were detected and corrections to activation times were applied to the computed predictions.

Lunar Orbiter photography has been used to accurately locate the landing sites of the Surveyor and Ranger spacecraft. The impact crater of Ranger VIII and the actual Surveyor I space-craft were identified in the Mission III photography. Surveyors III, VI, and VII were flown after Lunar Orbiter had photographed the planned landing regions. Analysis of terrain features in the Surveyor photos with the Lunar Orbiter photos of the same area have resulted in locating the position of Surveyors I, VI, and VII to within 1 to 2 meters on the lunar surface. This team concept of using overlapping information and data from the two programs will add materially to the overall scientific goal of understanding the Moon as an entity.

The following locations have been determined from the analysis of Lunar Orbiter and Surveyor data.

- Surveyor I   43.32°W   2.59°S
- Surveyor III   23.34°W   2.94°S
- Surveyor VI   1.40°W   0.49°N
- Surveyor VII   40.89°S   11.44°W

The photo data assessment facility at Langley Research Center has made a significant improvement in the reconstruction of Lunar Orbiter photos that enhances photo quality and the amount of information contained in the photographic prints. This has been accomplished by employing electronic equipment, developed subsequent to the first flight, between the FR-900 video tape playback equipment and the ground reconstruction equipment.

These improvements included the development of circuits to automatically compensate for variations in film density attributed to the characteristics of the spacecraft readout system. This technique reduces the characteristic "tiger stripes" evident on the original recordings. Other equipment was developed to electronically vary the density and contrast, independent of the GRE, thereby producing more uniform photos.

A procedure was also incorporated which may increase the video signal gain above the limits of the GRE equipment. This method shifted the entire gray scale of the photo and thereby enabled the recovery of surface details in many areas of high luminance which were overexposed in the original recordings. In addition, by making supplementary GRE reconstructions, detail was also enhanced in photos where underexposure was not severe. During Mission IV and many farside photos, this technique also enabled the recovery of additional detail near the edges of the acceptable illumination band.

The following tables (Tables 6-2 through 6-6) compare specific parameters of all the five missions and compare the predicted and actual performance when significant. Lunar Orbiters I through V have completed the extended-mission phase. Missions I, II, III, and V were terminated by command from the SFOF. The velocity control engine on each spacecraft was re-ignited to alter the orbit characteristics so that impact would occur during the commanded orbit. All communications with Lunar Orbiter IV were lost on July 17. Analysis of the Mission IV orbit data predicted that the spacecraft would impact the Moon during October 1967. Lunar Orbiter V impacted the lunar surface January 31, 1968. The data presented herein is limited to the period from launch to the end of the photographic mission. A program summary of the extended-mission experiments and operations will be included in the Mission V extended-mission final report. The data has been arranged in separate tables where related data are presented and include launch and boost, velocity control, trajectory, operational, environmental, and photographic parameters.

142

Table 6-2: Launch and Boost Parameters

Function	LO I Predict	LO I Actual	LO II Predict	LO II Actual	LO III Predict	LO III Actual	LO IV Predict	LO IV Actual	LO V Predict	LO V Actual
Launch Date (GMT)		8-10-66 19:26:01		11-6-66 23:21:00		2-5-67 01:17:01		5-4-67 22:25:01		8-1-67 22:33:00
Launch Azimuth (deg)		99.9		93.8		81.6		100.8		105.6
Spacecraft Launch Weight (lb)		852.84		855.22		856.71		859.84		864.50
Earth Orbit Coast Period (sec)		1,671.4		677.1		578.1		1,243.0		1,355.8
Velocity Imparted by Atlas (ft/sec)		18,520		18,509		18,534		18,518		18,534
Cislunar Injection Time (sec)		2,282.2		1,287.0		1,194.4		1,848.7		1,967.6
Cislunar Injection Parameters										
$\overline{B} \cdot \overline{T}$ (km) Prior to	6,630	15,643	6120	10,426	5,590	5,077	5,178	9,005	380	6,888
$\overline{B} \cdot \overline{R}$ (km) Midcourse	−1,135	−1,686	−410	−1,475	−2,460	−1,801	2,360	2,709	5,700	3,478
$\overline{B}$ (km) Maneuver	6,431	15,734	6134	10,529	6,107	5,387	5,482	9,404	5,713	7,716
Time of Closest Approach (GMT)	8-14-66 14:05:54	8-14-66 15:55:58	11-10-66 20:39:00	11-10-66 21:21:07	2-8-67 22:06	2-8-67 21:47	5-8-67 16:34	5-8-67 15:36	8-5-67 17:10	8-5-67 18:28

Table 6-3: Operational Parameters

Function	LO I	LO II	LO III	LO IV	LO V
Spacecraft Control					
Velocity Change Maneuvers	16	12	12	8	16
Photography Maneuvers	92	216	280	504	395
Attitude Update Maneuvers	144	30	11	14	27
Thermal Pitch-Off Maneuvers	77	9	67	41	23
Star Map, Canopus, and Other Maneuvers	45	17	13	19	11
Total	374	284	383	586	472
Real-Time Commands Transmitted (words)	1,988	1,289	1,266	3,666	1,703
Stored-Program Commands Transmitted (words)	2,522	2,282	2,349	3,445	2,822
TWTA Operation Hours	211.1	198	155	516	469.6
TWTA On-Off Cycles	148	129	114	15	6
Film Cassette Radiation Dosage					
Van Allen Belt	1.0	0.75	0.75	5.50	0.75
Cislunar Period	0.0	0.00	0.25	0.25	0.00
Lunar Orbits	1.0	1.00	1.50	0.50	0.75
Solar Flares	8.5	0.00	0.00	1.50	0.00
Total	10.5	1.75	2.50	7.75	1.50
Camera Looper Radiation Dosage					
Van Allen Belt	turned off	turned off	turned off	turned off	turned off
Cislunar Period	0.5	0.0	2.0	0.5	0.0
Lunar Orbits	2.5	1.0	1.0	11.0	1.0
Solar Flares	135.0	0.0	0.0	54.0	0.0
Total	138.0	1.0	3.0	65.5	1.0
Micrometeoroid Impacts	0	3 known 1 possible	0	2	1

Table 6-4: Velocity Control Parameters

Function	LO I Predicted	LO I Actual	LO II Predicted	LO II Actual	LO III Predicted	LO III Actual	LO IV Predicted	LO IV Actual	LO V Predicted	LO V Actual
Midcourse Maneuver										
Time From Launch		28h34m		44h33m		37h43m		18h20m		31h27m
Δ V Imparted (meters/sec)	37.8	37.8	21.1	21.1	5.1	5.1		60.85		29.76
Burn Duration (sec)	32.7	32.1	18.4±0.6	18.1	4.5+0.5	4.3	53.8±1.6	52.7	264±0.8	26.1
Specific Impulse lb-sec/lb	275.2	276.0	276.0	276.5	273.2	276	276	276	276	276
Thrust Developed (lb)	99.8	101.6	100.0	100.5	99.6	102.5	98	100	99	99.9
Deboost Maneuver										
Time From Launch		92h8m		93h6m		92h37m		90h15m		88h44m
Δ V Imparted	790.0	789.7	829.7	829.7	704.3	704.3	659.62	659.62	643.04	643.04
Burn Duration	588±10	578.7	618±10	611.6	541±10	542.5	501.4±8.5	501.7	501.1±8.5	498.1
Specific Impulse	274.7	276.0	276.0	276.0	276	277	276	276	276	276
Thrust Developed	99.8	101.3	100.0	101.0	100	99.9	100	100	99.5	100
Orbit Transfer Date (GMT)		8-21-66 09:50		11-15-66 22:58					Perilune	Change 8-7-67 08:28
Δ V Imparted	40.2	40.2	28.1	28.1	50.7	50.7			15.97	15.97
Burn Duration	2.7±1.6	22.4	17.5±0.9	17.4	33.4±1.6	33.7			10.95±0.6	10.78
Specific Impulse	274.5	276	276	276	277	277			276	276
Thrust Developed	112.6	113.6	101.5	102.3	101.3	100.3			100	101.6
Orbit Transfer Date	Perilune	Adjustment 8-25-66							Apolune	Change 8-9-67 05:08
Δ V Imparted	5.4	5.4							233.67	233.66
Burn Duration	3.0±1	3.0							151.1±4	152.9
Specific Impulse									276	276
Thrust Developed	114	113.6							100	99.9

Function	LO I		LO II		LO III		LO IV		LO V	
	Predicted	Actual	Predicted	Actual	Predicted	Actual	Predicted	Actual	Predicted	Actual
Lunar Encounter Parameters										
$\overline{B}{\cdot}\overline{T}$ (km)	6,402	6,458	6,010	6,044	5,605	5,607	723	726	351	352
$\overline{B}{\cdot}\overline{R}$ (km)	−1,171	−1,120	391	−373	−2,465	−2,479	9,811	9,808	5,701	5,696
$\overline{B}$ (km)	6,509	6,555	6,023	6,055	6,123	6,131	9,836	9,835	5,712	5,707
Time of Closest Approach	8-14-66	8-14-66	11-10-66	11-10-66	2-8-67	2-8-67	5-8-67	5-8-67	8-6-67	8-6-67
(GMT)	15:50:01	15:50:34	20:39:00	20:39:00	22:06:00	22:06:05	15:36:01.1	15:36:03.8	17:10:17.1	17:10:12.6
Initial Orbit Kepler Elements										
Perilune Altitude (km)	199	189	202	196	213	210	2,701	2,706	202	195
Apolune Altitude (km)	1,850	1,866	1,850	1,871	1,850	1,802	6,111	6,114	6,050	6,028
Orbit Inclination (day)*	12.04	12.16	11.99	11.97	21.05	20.94	85.48	85.48	85.05	85.01
Ascending-Node Longitude (deg)*	325.3	325.9	341.8	341.7	311.7	310.3	131.0	131.0	117.9	117.8
Argument of Perilune (deg)*	180.8	180.3	162.1	161.6	176.2	177.3	1.49	1.17	1.35	1.55
Eccentricity		0.303		0.302		0.289		0.277		0.600
Orbit Period (hours:min)	3:37	3:37		3:37				12:01		8:26.9
Number of Orbits		43		33		26		48		4
Orbit Transfer Kepler Elements									Perilune	Change
Perilune Altitude	57.9	56.0	50.2	49.7	54.8	54.8			101	100
Apolune Altitude	1,855	1,853	1,858	1,853	1,846	1,847			6,066	6,067
Orbit Inclination*	12.04	12.05	11.91	11.89	20.87	20.91			85.62	85.61
Ascending-Node Longitude*	234.1	234.0	272.8	273.3	258.6	257.9			95.9	95.9
Argument of Perilune*	181.5	181.2	163.3	162.8	178.3	178.9			1.32	1.34
Eccentricity		0.333		0.335		0.334				0.619
Orbit Period		3:29		3:28		3:28				8:20.7
Number of Orbits		30		146		123				6

Table 6-5: Trajectory Parameters

* Selenographic-of-date coordinates.

Function	LO I		LO II		LO III		LO IV		LO V	
	Predicted	Actual	Predicted	Actual	Predicted	Actual	Predicted	Actual	Predicted	Actual
Orbit Adjustment Kepler Elements									Apolune	Change
Perilune Altitude	40.0	40.5		N.A.		N.A.			99	99
Apolune Altitude	1,824	1,817							1,502	1,500
Orbit Inclination*	12.03	12.0							84.76	71.4
Ascending-Node Longitude*	176.7	177.0							1.61	1.88
Argument of Perilune*	186.0	185.3								0.276
Eccentricity		0.333								3:11.9
Orbit Period		3:26								136
Number of Orbits		135								
Tracking Data Recorded										
Doppler (hours)				819		942+		783		752
Ranging (hours)				200		168+		79		48
Station Time Correlations				36		35+		15		22
+DSN Data through 3-11-67										

Table 6-5 (Continued)

Table 6-6: Photographic Parameters

Function	LO I		LO II		LO III		LO IV		LO V	
	Plan	Actual	Plan	Actual	Plan	Actual	Plan	Actual	Plan	Actual
Dual Frames Exposed	212	211	211	211	212	211	212	199	213	213
First Photo Date		8-18-66		11-18-66		2-15-67		5-11-67		8-6-67
Last Photo Date		8-29-66		11-25-66		2-23-67		5-26-67		8-18-67
Telephoto Frames Read Out	212	211+	211	209□		170□		180		213
Wide-Angle Frames Read Out	212	211	211	208□		157□		179		212
Final Readout Started		8-29-66		11-26-66		2-23-67		5-29-67		8-19-67
Last Readout Completed		9-14-66		12-7-66		3-2-67		6-1-67		8-27-67
Primary Sites Photographed	10	10	13	13	12	12	176	147	41	41
Frames Exposed	180	156	184	184	156	156	191	160	174	174
Photo Sequences	11	11	22	22	19	20	176	147	50	50
Altitude Range (km)		45-54		44-57		45-62		2670-5790		96-248
Secondary Sites Photographed (Nearside)		41	13	13	31	30		N.A.		N.A.
Frames Exposed	42	44	23	23	55	54				
Photo Sequences	42	41	14	14	31	30				
Altitude Range (km)		46-239		41-51		44-63				
Farside Sites Photographed		7	4	4	1	1		8		23
Frames Exposed	0	11	4	4	1	1		9		37
Photo Sequences	0	7	4	4	1	1		8		23
Altitude Range (km)	0	1295-1454		1450-1517		1460		6110-6150		1180-5755

Table 6-6   (Continued)

Function	LO I		LO II		LO III		LO IV		LO V	
	Plan	Actual	Plan	Actual	Plan	Actual	Plan	Actual	Plan	Actual
Readout Sequences										
Priority Readout		45		53		53		122*		86
Final Readout		93		73		56		29		61
Total		138		126		109		151		147
Types of Site Photography										
(Frames)										
Vertical	212	209	196	196		79		190		50
Near Vertical		0	11	11		80		9		77
High Obliques		2	4	4		52		0		46
Convergent Telephoto Stereo		0	8	8		36		0		40

+ Telephoto photos smeared by camera abnormality.

☐ Contains some partial frames.

* Includes many short readouts during film advance irregularities

"*The aeronautical and space activities of the United States shall be
conducted so as to contribute . . . to the expansion of human knowl-
edge of phenomena in the atmosphere and space. The Administration
shall provide for the widest practicable and appropriate dissemination
of information concerning its activities and the results thereof.*"

— NATIONAL AERONAUTICS AND SPACE ACT OF 1958

NASA SCIENTIFIC AND TECHNICAL PUBLICATIONS

TECHNICAL REPORTS: Scientific and
technical information considered important,
complete, and a lasting contribution to existing
knowledge.

TECHNICAL NOTES: Information less broad
in scope but nevertheless of importance as a
contribution to existing knowledge.

TECHNICAL MEMORANDUMS:
Information receiving limited distribution
because of preliminary data, security classifica-
tion, or other reasons.

CONTRACTOR REPORTS: Scientific and
technical information generated under a NASA
contract or grant and considered an important
contribution to existing knowledge.

TECHNICAL TRANSLATIONS: Information
published in a foreign language considered
to merit NASA distribution in English.

SPECIAL PUBLICATIONS: Information
derived from or of value to NASA activities.
Publications include conference proceedings,
monographs, data compilations, handbooks,
sourcebooks, and special bibliographies.

**TECHNOLOGY UTILIZATION
PUBLICATIONS:** Information on technology
used by NASA that may be of particular
interest in commercial and other non-aerospace
applications. Publications include Tech Briefs,
Technology Utilization Reports and Notes,
and Technology Surveys.

Details on the availability of these publications may be obtained from:

SCIENTIFIC AND TECHNICAL INFORMATION DIVISION

NATIONAL AERONAUTICS AND SPACE ADMINISTRATION
Washington, D.C. 20546